Chemical modification of polysaccharides with hydrophilic polymers for CaCO3 crystal growth modification and filler retention, for paper applications

by

Howard Matahwa

Dissertation presented for the degree of

PhD (Polymer Science)
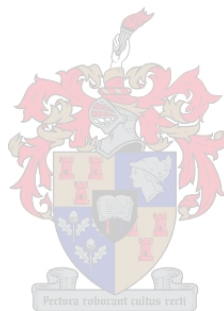
Promoter: Prof. R.D. Sanderson

Stellenbosch University

December 2008

Declaration

By submitting this dissertation electronically, I declare that the entirety of the work contained therein is my own, original work, that I am the owner of the copyright thereof (unless to the extent explicitly otherwise stated) and that I have not previously in its entirety or in part submitted it for obtaining any qualification.

Date: 19 November 2008

Abstract

Polysaccharides were modified with selected polymers via the grafting technique. Both anionic and cationic polysaccharides were prepared. Random and crosslinked graft copolymers were also prepared. The percentage grafting was determined by gravimetric analysis and results were confirmed by cross-polarization magic angle spinning carbon-13 nuclear magnetic resonance microscopy (CP/MAS ^{13}C NMR). These modified biodegradable polymers were then used to flocculate precipitated calcium carbonate (PCC). The effects of pH, percentage grafting, crosslinker concentration and polysaccharide concentration on PCC flocculation were evaluated. Furthermore, the effects of anionic and cationic starch, either added to PCC sequentially or simultaneously, on PCC flocculation were also investigated. Generally, anionically modified starch showed excellent flocculation properties, which are desirable for the end application of PCC retention.

The effect of polyacrylic acid (PAA) and polyacrylamide (PAM) modified cellulose fibers on calcium carbonate crystal nucleation and growth modification was investigated. When the heterogeneous crystallization of $CaCO_3$ was carried out in the presence of modified cellulose fibers the $CaCO_3$ crystals were found to be residing on the surface of the fibers. The morphologies of the crystallized $CaCO_3$, polymorph and fiber surface coverage were different for cellulose materials grafted with polymers of different functionalities, meaning that there is interaction between the crystal growth modifier and the growing nuclei.

The effect of the modified starch on the crystallization of calcium carbonate gave useful insight into designing $CaCO_3$ filler morphologies. It was found that the filler size, morphology and surface properties of fillers can be tailor-made by choosing suitable $CaCO_3$ crystallization conditions as well as a suitable crystal growth modifier. The crystallized $CaCO_3$ had a negatively charged surface. Results of fluorescence studies showed that the PAA modified starch (polymeric additive used) resided on the surface of the crystals. Thus the presence of the polysaccharide on the surface of a filler could be advantageous for strengthening fiber–filler bonding in paper applications.

Anionic starch materials were also used to prepare anionic-starch-coated starch particles. Both the anionic starch and anionic-starch-coated starch particles were evaluated for PCC retention and other properties of hand sheets. When anionic-starch-coated starch particles were used there was generally an improvement in the PCC retention, while the other paper properties remained desirable. The success achieved with the use of anionic-starch-coated starch particles now opens the way for the further preparation and testing of various modified starch particles, for optimization of filler retention.

Opsomming

Wysiging van polisakkariede met 'n verskeidenheid polimere is uitgevoer deur gebruik te maak van die entkopolimerisasietegniek. Beide kationiese en anioniese polisakkariede is berei, sowel as willekeurige kopolimere en gekruisbinde kopolimere. 'Cross-polarization magic angle spinning carbon-13 nuclear magnetic resonance' (CP/MAS ^{13}C NMR) is gebruik om die persentasie enting, bepaal deur gravimetriese analise, te bevestig. Hierdie gewysigde afbreekbare polimere is gebruik om neergeslaande kalsiumkarbonaat (NKK) uit te vlok. Die invloed van pH, persentasie enting, kruisbinderkonsentrasie en polisakkariedkonsentrasie is ondersoek. Die invloed van opeenvolgend en gelyktydige kationiese en anioniese styseladdisie op NKK is ook ondersoek. Oor die algemeen is bevind dat anioniese stysel die beste uitvlokking van NKK tot gevolg het, wat voordelig is.

Die effek van poliakrielsuur (PAA) en poliakrielamied (PAM) gewysgde sellulosevesel op CaCO$_3$ kernvorming en groei modifikasie is ondersoek. Die heterogene kristallisering van CaCO$_3$ wat uitgevoer is in die teenwoordigheid van gemodifiseerde sellulose vesel het tot gevolg gehad dat die CaCO$_3$ kristalle op die oppervlak van die vesels te vinde was. Die morfologie, polimorf en vesel oppervlakbedekking is verskillend vir elke tipe entpolimeer wat aan die polisakkariede geheg is. Dit dui aan dat daar 'n interaksie plaasvind tussen die betrokke entpolimeer en die groeiende vulstofkern.

Die invloed van die natuurlike wateroplosbare gemodifiseerde polisakkariede op die kristallisasie van CaCO$_3$ het insig gebied op die wyse waarop die vulstof ontwerp moet word. Die vulstof kristalgrootte, morfologie en die oppervlakeienskappe kan voorspel word deur 'n keuse van die reaksie kondisies sowel as die tipe kristalgroeimodifiseerder. Die gekristalliseerde CaCO$_3$ toon 'n negatiewe oppervlakte lading. Fluoressensie studies het getoon dat PAA-gewysgde stysel (polimeriese bymiddel gebuik) op die oppervlak van die kristalle teenwoordig is. Derhalwe kan die teenwoordigheid van polisakkariede op die oppervlak van die vulstof voordelig wees om die vesel–vulstof komponent in papieraanweding te versterk.

Anioniese stysel is ook gebruik om anioniese styselbedekte styselpartikels te berei en beide die gewone anioniese stysel sowel as die anioniese styselbedekte styselpartikels is gebruik om die invloed daarvan op vulstofretensie en ander eienskappe in papier handblaaie te ondersoek. Daar is oor die algemeen gevind dat die byvoeging van anioniese styselbedekte styselpartikels die NKK retensie verbeter het sonder 'n negatiewe impak op ander papiereienskappe. Die sukses wat hier behaal is baan die weg vir verdere toetse wat uitgevoer kan word op anioniese styselpartikels onder verskeie toestande met die oog op optimisering van vulstofretensie.

I dedicate this work to my family, friends and my wife Blessing.

List of contents

AA	Acrylic acid
ACC	Amorphous calcium carbonate
AM	Acrylamide
AP	Anionic polymer
APS	Ammonium persulfate
ASD	Apparent sheet density
ASt	Anionic starch
BI	Burst index
BS	Bending stiffness
BTS	Bendtsen smoothness
CAN	Cerium ammonium nitrate
α-CE	Alpha cellulose
CMC	Carboxyl methyl cellulose
CP	Cationic polymer
CP/MAS	Cross polarized/magic angle spinning
CSF	Canadian standard freeness
CSt	Cationic starch
DADMAC	Diallyldimethyl ammonium chloride
FD	Fully dissolved
FSC-A	Forward scatter
FT-IR	Fourier transform infrared
GAR	Gurley air resistance
GCC	Ground calcium carbonate
KPS	Potassium persulfate
LCST	Lowest critical solution temperature
MA	Methyl acrylate
MAPTAC	Methacrylamido-propyl-trimethyl ammonium chloride
MBAM	Methylene bisacrylamide
MWP	Microwave power
NaA	Sodium acrylate
NIPAM	N-isopropyl acrylamide
NMR	Nuclear magnetic resonance
PAA	Polyacrylic acid

PAANa	Polyacrylic acid sodium salt
PAM	Polyacrylamide
PCC	Precipitated calcium carbonate
PD	Partially dissolved
PDASt	Partially dissolved anionic starch
PEO	Polyethylene oxide
PVA	Poly(vinyl alcohol)
RBA	Relative bonded area
SSC-A	Side scatter
SEM	Scanning electron microscopy
SKL	Sulfonated kraft lignin
T.E.A	Tensile energy absorption
TEMED	N,N,N',N'-tetramethylethylenediamine
TGA	Thermogravimetric analysis
TI	Tensile index
TS	Tensile stiffness
UV	Ultraviolet
XRD	X-ray diffraction

Scientific contributions emanating from this study

Journal articles

1) <u>*Matahwa H., Ramiah V., Jarrett W.L., McLeary J.B., Sanderson R.D.*</u> Microwave assisted graft copolymerization of N-isopropyl acrylamide and methyl acrylate on cellulose: Solid state NMR analysis and $CaCO_3$ crystallization. Macromolecular symposia 2007, 255, 50–56.

2) <u>*Matahwa H., Ramiah V., Sanderson.*</u> $CaCO_3$ crystallization in the presence of modified polysaccharides and linear polymeric additives. Journal of Crystal Growth 2008, 310, 4561-4569

3) <u>*Matahwa H., Sanderson R.D.*</u> Surface and statistical analysis of $CaCO_3$ crystals synthesized in the presence of florescein tagged starch grafted with polyacrylic acid Journal of Crystal Growth 2008 (accepted)

Oral Presentation

1) Grafting of Polysaccharides with acrylamide and polyacrylic acid for $CaCO_3$ crystal growth. Presented at United Nations Education, Scientific and Cultural Organization (UNESCO) conference 2006, Stellenbosch.

2) $CaCO_3$ crystallization in the presence of modified polysaccharides and linear polymeric additives. Presented at the 42nd IUPAC World Polymer Congress, Macro 2008, Taipei, Taiwan.

Poster Presentations

1) <u>*H. Matahwa, V. Ramiah, W.L. Jarrett*, J.B. McLeary, R.D. Sanderson,*</u> Graft copolymerization of NIPAM and MA on α-cellulose by the ceric ion redox initiating system under microwave irradiation. Presented at The 4th IUPAC Sponsored International Symposium on Free Radical Polymerization: Kinetics and Mechanism, Lucca (Italy); 3-8 September 2006

2) <u>*H. Matahwa, R.D. Sanderson,*</u> Synthesis of $CaCO_3$ crystals in the presence of a fluorescein tagged crystal growth modifier. Poster to be presented at The 10th Annual UNESCO/IUPAC Conference on Macromolecules & Materials Berg-en-Dal, Kruger National Park, Mpumalanga, South Africa 7-11 September 2008

Chapter 1: Introduction and objectives

1.1: Introduction

Polymeric raw materials can be classified as synthetic polymers and natural polymers. In the early days, natural polymers were used to fulfill technological needs.[1] As the depletion of natural materials became inevitable, research moved towards synthetic polymers. Today polymeric materials are well known for their diversity and usefulness in modern technology. Polymer products are found in almost all aspects of technology, from simple household utilities to advanced polymeric composites in high-tech engineering such as computers, space ships, etc.

Synthetic polymers gained momentum over natural polymers because they can be easily tailored to offer properties superior to those of natural materials. Such properties enable synthetic materials to be easily processed and thereby readily transformed into products. Notwithstanding this advantage of synthetic polymers, the disadvantages include the fact that they are expensive and non-biodegradable, and some are considered 'toxic' when compared to natural polymers. Natural polymers are limited in their applications mainly because they are difficult to process and the products have poor properties. Therefore, modification of natural polymers is used to obtain materials with better properties and that are easier to process. Thus, in modern research, incorporating natural polymers to improve the performance of synthetic materials in their required applications will be cost effective. Moreover, the products will be biodegradable and safer to the environment.

1.2: Natural polymers

Natural polymers play critical roles in all animals and plants. Natural polymers include the following materials, mostly derived from plants: cellulose, starch and natural rubber and biological polymers derived from animals: chitin, DNA/RNA and proteins. Plant derived natural polymers (e.g. natural rubber, polysaccharides) are mostly found in abundance and are readily available, and therefore they are used in many industrial applications.

In this study, the focus is also on the modification of naturally occurring plant or cereal derived polysaccharides, and other related materials, for applications in $CaCO_3$ crystal growth modification and the paper industry.

1.3: Modification of polysaccharides

Various methods are used to modify polysaccharides in order to obtain useful products. The viscose process is a widely used method for the modification of polysaccharides, especially cellulose, to make them processable.[2] Other methods include esterification and etherification of polysaccharides by simple organic molecules,[3-5] and grafting of polysaccharides with polymers.[6,7] In most cases the nature of the etherifying/esterifying reagent or grafted polymer determines the final properties of the modified polysaccharide. Ultimately polymer design will come into effect to predict the properties of the final material with respect to the intended application.

1.4: Crystal growth modification

Biominerization is a process by which organisms synthesize minerals. In the process of biominerization, biological systems provide a chemical environment that controls the nucleation and growth of unique mineral phases.[8,9] Often these minerals exhibit hierarchical structural order, leading to superior physical properties, not found either in their inorganic counterparts or in synthetic materials. One particular aspect of interest to the material chemist is the means by which these biological organisms use organic constituents to mediate the growth of the mineral phases. Biominerals are grown under environmentally friendly conditions and have potential industrial and biomedical applications.[10] Thus, the controlled synthesis of inorganic materials with specific size and morphology can contribute to the development of new materials in various fields such as catalysis,[11-13] medicine,[14] electronics,[12] cosmetics,[12] etc. The biomimetics of $CaCO_3$ is currently being studied intensively due to its wide applications in industries such as rubber,[15] paper,[16] plastics[17] and paint.[18] $CaCO_3$ fillers are one of the most abundant minerals and, like most filler materials, its size, structure, specific surface area and morphology are of paramount importance.

1.5: The paper industry

The paper industry uses natural polysaccharides to produce all types of paper materials, mostly cellulose fiber and starch based materials. In order to reduce the cost of raw materials, and therefore increasing profits, low cost fillers, such as precipitated calcium carbonate (PCC) and ground calcium carbonate (GCC), are added to more expensive pulped cellulose fiber during the production of paper.[19]

1.6: Fillers

Fillers improve paper properties such as opacity, brightness and printability, and decrease the drainage time. However, there is a limit in terms of the filler loading to which fillers can be added. An excess of filler leads to deterioration of paper properties such as stiffness and strength. Introduction of filler (above a certain level) in paper thus requires additives to promote paper strength. Starch based materials are suitable for this purpose. Research is now underway to increase filler loadings in paper without compromising the properties of paper.[19-22] The use of materials that promote fiber-fiber bonding, fiber-filler bonding and filler-filler bonding is a key factor in increasing filler loadings in paper.

1.7: Objectives

The main aim of this study was to increase the PCC loading in paper without causing detrimental effects to the properties of the paper. Since polysaccharides form hydrogen bonds with pulp cellulose, they can be used as PCC retention aids when modification with polymers that can bind to PCC. Towards this aim, several aspects of polysaccharide modification and the effects of their use for paper application were investigated. The effects of the modified polysaccharides on the following were investigated: calcium carbonate crystal growth modification during crystallization; surface properties of the crystallized calcium carbonate, which is critical to fiber–filler bonding strength; and filler retention in paper.

The objectives of the study are as follows:
1. Study the graft copolymerization of cellulose using a double initiator system (Ce^{+4}– KPS) under microwave irradiation so as to shorten the grafting reaction times and carry out conventional grafting of polysaccharides using different initiator systems and monomers.
2. Study the PCC flocculation properties of the grafted polysaccharides. This study involved determining the effects of different modified polysaccharides, polymer concentration and pH on the size of the PCC flocculants.
3. Study the effect of the modified polysaccharides on the crystallization of calcium carbonate in terms of crystal morphology and size. This study included investigating the possibility of using an alternative route for filler addition (alternate to adding already formed PCC filler to pulp during papermaking), namely in-situ crystallization of calcium

carbonate (filler) in the presence of modified pulp or a starch-derived polymeric additive.

4. Test the performance of the modified polysaccharides on paper. The work involved preparation of hand sheets and evaluating the resulting properties such as the bending stiffness, tensile strength, including the determination of the filler retention in the hand sheets.

1.8: Layout of the thesis

The document is composed of seven chapters. Four chapters describe the experimental work done on the grafting of polysaccharides, crystallization of calcium carbonate, determination of surface properties and statistical analysis of crystallized calcium carbonate, and the use of modified starch as PCC retention aid in papermaking.

Chapter 1: Introduction and objectives

Chapter 2: Historical and Theoretical background

Chapter 3: Grafting of polysaccharides with vinyl monomers using various initiator systems

The chapter describes the use of microwave in conjunction with cerium (IV)-potassium persulfate double initiation for graft copolymerization. It describes the conventional grafting of polysaccharides with both anionic and cationic monomers, and results on PCC flocculation using modified polysaccharides are also discussed.

Chapter 4: Crystallization of $CaCO_3$ in the presence of polymer template

This chapter describes the effect of the polymer template on size, polymorph and morphology of $CaCO_3$ crystals. The study evaluates the interactions between calcium carbonate and the modified polysaccharides.

Chapter 5: Surface studies of the crystallized $CaCO_3$

This chapter describes the surface properties of crystallized calcium carbonate. Fluorescent tagged crystal growth modifiers and the measurement of particle zeta potentials was carried out. The work also included coating of crystallized calcium carbonate with cationic and fluorescent tagged starch.

Chapter 6: Polymer testing in paper application

Synthesized polysaccharides graft copolymers were used in papermaking and the results discussed. The work involved the use of modified starch and modified starch particles in hand sheet making in order to increase PCC filler retention and improved the other properties, such as the tensile strength and the bending stiffness. Thus, a comparison of the effect of different polymers and modified starch particles on their performance in paper in terms of PCC filler retention and properties of the hand sheets is reported.

Chapter 7: Conclusions and recommendations for future work.

1.9: References

(1)   Guyoy, A., Tauer K. *Reactions and Synthesis in Surfactant Systems,* **2001**, New York.

(2)   Engström, A. C., Ek M., Henriksson G. *Biomacromolecules* **2006**, *7(6)*, 2027-2031.

(3)   Antova, G., Vasvasova P., Zlatanov M. *Carbohydrate Polymers* **2004**, *57*, 131-134.

(4)   Satge, C., Veneuil B., Branland P., Granet R., Krausz P., Rozier J., Petit C. *Carbohydrate Polymers* **2002**, *49*, 373-376.

(5)   Wu, J., Zhang J., Zhang H., He J., Ren Q., Guo M. *Biomacromolecules* **2004**, *5*, 266-268.

(6)   Gupta, K. C., Khandekar K. *Biomacromolecules* **2003**, *4*, 758-765.

(7)   Sinn, C. G., Dimora R., Huin C., Sel O., Antonietti M. *Macromolecules* **2006** *39(18)*, 6310-6312. .

(8)   Colfen, H., Qi L. *Chemistry - A Euroupian Journal* **2001**, *7*, 106-116.

(9)   Yu, H., Lei M., Cheng B., Zhao X. *Journal of Solid State Chemistry* **2004**, *177*, 681-689.

(10)   Murphy, W. L., Mooney D.J. *Journal of the American Chemical Society* **2002**, *124(9)*, 1910-1917.

(11)   Piccolo, A., Conte P., Tagliatesta P. *Biomacromolecules* **2005**, *6(1)*, 351-358.

(12)   Corma, A., Moliner M., Diaz-Cabanas M. J., Serna P., Femenia B., Primo J., Garcia H. *New Journal of Chemistry* **2008**, *32(8)*, 1338-1345.

(13)   Coelfen, H., Antonietti M. *Metal Ions in Life Sciences* **2008**, *4* 607-643.

(14)   Venkatesh, S., Byrne M. E., Peppas N. A., Hilt J. Z. *Expert Opinion on Drug Delivery* **2005**, *2(6)*, 1085-1096.

(15)   Skelhorn, D. A. *Rubber World* **1997**, *216(1)*, 32-34.

(16)   Dougherty, M. J., Neogi A. N., Park D. W. *US Patent* **2005**, no. 20050247421.

(17)   Krysztafkiewicz, A., Grodzka J., Jesionowski T., Rager B. *Composite Interfaces* **2001**, *8(3-4)*, 227-232.

(18)   Luedecke, W., Aumann G. *European Coatings Journal* **2005**, *9*, 70-71.

(19)   Klungness, J. H., Pianta F., Stroika M. L., Sykes M., Tan F., AbuBakr S. *AIChE Symposium Series* **1999**, *95(322)*, 99-102.

(20)   Scallan, A. M., Middleton S.R. *Papermaking Raw Materials* **1985**, Oxford

(21)   Green, H. V., Scallan A.M. *Pulp and Paper Canada* **1982**, *83(7)*, 203-207.

(22)   Allen, G. G., Negri A.R., Ritzenthaler P. *Tappi Journal* **1992**, *75(3)*, 239-244.

Chapter 2: Historical and theoretical background

2.1: Introduction

2.1.1: Polysaccharides

Polysaccharides are relatively complex carbohydrates, with the general formula $(C_6H_{10}O_5)_n$ where n is usually between 40 and 3000. The polymer chains are made up of monosaccharide units linked together by glycosidic bonds. The class includes linear and branched, as well as semi-crystalline and amorphous, types of polysaccharides, which are often insoluble in water at ambient temperatures. Some polysaccharides contain the same type of polysaccharides (homopolysaccharides), e.g. starch, and some contain different types of polysaccharides (heteropolysaccharides), e.g. lignin. In nature, polysaccharides such as starch and glycogen serve as energy storage whereas cellulose and chitin are responsible for structural integrity.

2.1.2: Cellulose

Cellulose is the most abundant biopolymer and also the most abundant polysaccharide. It is made up of anhydroglucose units (AGUs) joined through 1,4-β-linkages,[1-4] see Fig. 2.1. Cellulose is the predominant material in plants which are renewable energy sources and can be utilized to produce vast quantities of cellulose.[4-8] The anhydroglucose units have three free hydroxyl (OH) groups which serve as reactive centers for chemical modification.[3] Some chemical modification results in cellulose having certain new properties, making it suitable for various applications, depending on the level of modification as well as the modifying polymer/reagent.
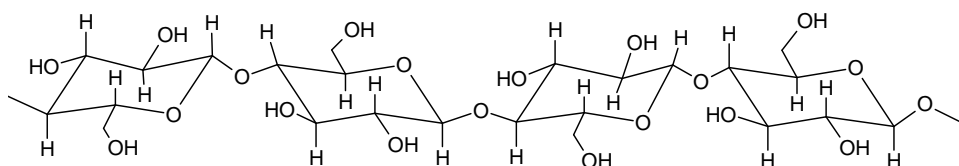
Fig. 2.1: The structure of cellulose.

Cellulose fiber consists of crystalline domains with amorphous domains between these crystalline sections. The amorphous regions are capable of holding relatively large amounts of water by capillary action, however, water cannot penetrate or swell crystalline cellulose.[9] The amorphous areas of cellulose can be easily etched away to give highly crystalline cellulose, although it results in the reduction of fiber length. Bonding in fibers is primarily via intra- and intermolecular hydrogen bonding between anhydroglucose (or other anhydropyranose) units. The intermolecular bonds principally extend from the primary hydroxyl groups on the sixth carbon atom, to the hydroxyls groups on the third carbon atom on an adjacent cellulose molecule.[10]

Natural cellulose (referred as cellulose I) is a metastable type of cellulose whose crystal structure consists of parallel cellulose strands with no inter-sheet hydrogen bonding. Cellulose I exists in two phases, namely cellulose Iα (triclinic) and cellulose Iβ (monoclinic). However, the proportions of each phase are different, and depend on the origin of cellulose I. Cellulose Iα is more predominately found in algae whilst Iβ is the major form in higher plants. The fiber repeat distance (1.043 nm for the repeat dimer interior to the crystal, 1.029 nm on the surface[11]) are the same for the two types of cellulose I but the displacements of their sheets relative to one another are different.[12]

The structure of cellulose fibers is best represented by a fibrillar network model.[12] The model considers the cellulose fibers as a network of elementary fibrils with random aggregation into micro and macro-fibrils. Important structural characteristic of these cellulose fibers include:

      i) the size of the crystallites

      ii) the degree of crystallinity

      iii) the molecular length of the polymer chains

      iv) the degree of orientation of the fibrils and fibrillar aggregation along the fiber axis

Other types of cellulose allomorphs are cellulose II and cellulose III. Cellulose II can be obtained by mercerization of cellulose I or regeneration from solubilized cellulose I. The structure of cellulose II has been reported to consist of a two chain unit cell and a P21 space group where, the two chains are in parallel arrangement and are cryptographically independent.[13,14] Regeneration of cellulose I gives the thermodynamically more stable cellulose II structure, with some inter-sheet hydrogen-bonding. Cellulose II contains two different types of anhydroglucose units (A and B) with different backbone structures and the chains consist of -A-A- or -B-B- repeat units[15]. Cellulose III is formed from cellulose mercerized in ammonia and is similar to cellulose II but with the chains parallel, as in cellulose Iα and cellulose Iβ.[16]

2.1.3: Starch

Starch consists of two major polymeric components, amylose and amylopectin, and is mainly obtained from cereal grains, root crops, leaves, etc. Amylose is a linear polymer with glucose units joined together by α(1–4) linkages.[17] Physical characteristics important to functionality are starch granule shape and size. The overall properties of starch are also a function of the amylose/amylopectin ratio.[18,19] The two polymers are very different structurally, amylose is linear and amylopectin is highly branched, and each plays a critical role in the ultimate functionality of the native starch.[17] Some of the properties affected by the amylose/amylopectin ratio include solubility, viscosity, gelatinization, shear resistance, texture, tackiness, gel stability and cold swelling.

2.1.3.1: The structure of amylopectin

Amylopectin is a branched polymer with glucose units linked together by α(1–4) glycosidic bonds with branching taking place after every 24 to 30 glucose units, see Fig. 2.2. The branching occurs through α(1–6) linkages and each amylopectin molecule contains up to two million glucose residues in a compact structure.[20]
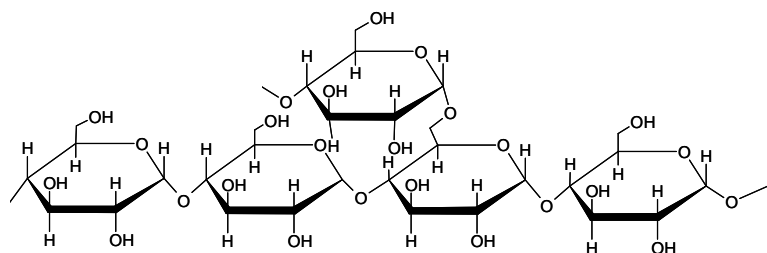
Fig. 2.2: The structure of amylopectin (amylose is linear).

The molecules are oriented radially in the starch granule and as the radius increases so does the number of branches. This results in the formation of concentric regions of alternating amorphous and crystalline structures, which contribute to growth rings. The Fig. 2.3A shows the organization of the amorphous and crystalline domains of the structure.
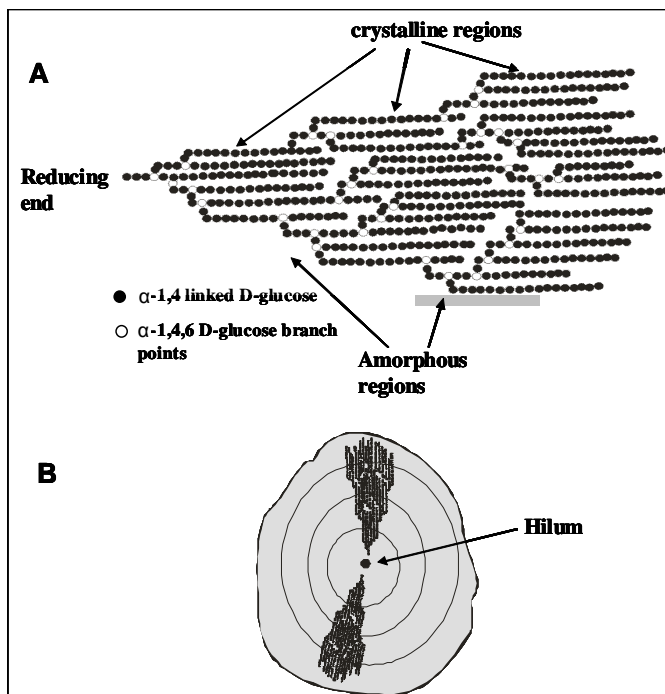
Fig. 2.3: A) Schematic representation of the branching nature of amylopectin in a starch granule. B) Orientation of amylopectin molecules in an ideal granule.[21]

2.1.3.2: Starch applications

Starch is widely used in different applications, some of which are tabulated in Table 2.1.

Table 2.1: Applications of starch in various industries[22]

Adhesives	Metal Industry
hot-melt glues	foundry core binder
stamps, bookbinding, envelopes	sintered metal additive
labels (regular and waterproof)	sand casting binder
wood adhesives, laminations	**Textiles Industry**
automotive, engineering	warp sizing
pressure sensitive adhesives	fabric finishing
corrugation	printing
paper sacks	**Cosmetic and Pharmaceutical Industry**
Explosives Industry	dusting powder
wide range binding agent	make-up
match-head binder	soap filler/extender
Paper Industry	face creams
internal sizing	pill coating, dusting agent
filler retention	tablet binder/dispersing agent
surface sizing	**Mining Industry**
paper coating (regular and color)	ore flotation
carbonless paper stilt material	ore sedimentation
disposable diapers, feminine products	oil well drilling muds
Construction Industry	**Miscellaneous**
concrete block binder	biodegradable plastic film
asbestos, clay/limestone binder	dry cell batteries
fire-resistant wallboard	printed circuit boards
plywood/chipboard adhesive	leather finishing
gypsum board binder	

The primary use of starch in papermaking is to enhance the surface properties for improved printability and writing. The introduction of a variety of cost reducing materials in paper, such as fillers and recycled fibers, and chemicals for improving the papermaking process has resulted in the wide use of modified starch to avoid a drop in paper quality. Starch is now being used in the wet-end together with pulp, to enhance paper properties such as the dry strength. During papermaking, different types of starch are introduced to the paper at different stages. The addition of starch depends on the effect of that particular type of starch on the pulp and other additives. Scheme 2.1 shows the contributions of starch in the papermaking process.
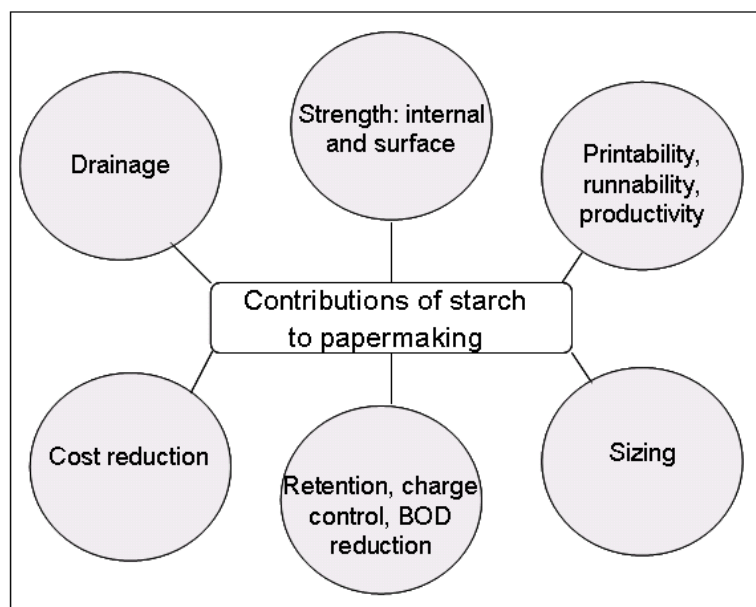
Scheme 2.1: The contributions of starch in the papermaking process

2.2: Grafting of polysaccharides

Grafting is one of the most widely used methods for chemically modifying polysaccharides.[23-28] The availability of a number of monomers that can be grafted onto polysaccharides results in polysaccharide materials with a wide range of properties. The extent of grafting dictates the ultimate properties of the grafted polysaccharides. The functionality of the grafted polysaccharides depends on the nature of the polymer grafted. Cationic and anionic polysaccharides can be synthesized by graft polymerizing cationic or anionic monomers respectively. Grafting reactions can be done in homogeneous or heterogeneous systems.

2.2.1: Grafting using vinyl monomers

A wide range of vinyl monomers can be grafted on polysaccharides to produce a wide range of biodegradable materials with different chemical and physical properties. The following methods are used to initiate free radical graft polymerization:

    i) Irradiation

        a) β, γ or X-ray irradiation

        b) visible or UV light usually in the presence of an activator, e.g. azo-compounds

        c) microwave irradiation

    ii) Treatment with metal ions with a high oxidation state such as Ce^{+4}, Cr^{+6} and Vn^{+5}

iii) Oxidation using reagents such as O_3, O_2 and H_2O_2

iv) Thermal, usually in the presence of free radical initiators such as potassium persulfate (KPS) and ammonium persulfate (APS)

Grafting of polysaccharides initiated by various transition metal ions via free radical initiation has been reported in literature.[24] Grafting of cellulose and its derivatives initiated by ceric (IV) ions has been widely studied.[6,23,25-32]
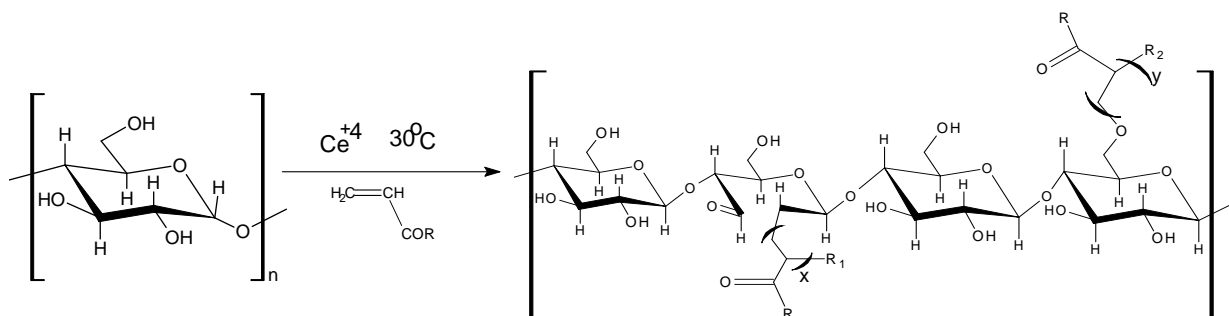
Scheme 2.3: Grafting points on polysaccharides for Ce^{4+} initiation (R1 and R2 are polymer chains with different degrees of polymerization)

The mechanism of initiation is through the formation of free radicals directly on the cellulose backbone, by cleaving of the C2–C3 bond,[33,34] as shown in Scheme 2.3, and oxidation of cellulosic chain ends containing hemiacetal linkages.[35] It has been suggested that the Ce^{4+} ions can also abstract protons from the hydroxyl groups of these polysaccharides thereby facilitating grafting reactions resulting in the formation of ether linkages.[34,36] The Ce[+4] can also form radicals on the monomer, which will result in homopolymer formation. Recently it has been shown that the addition of certain alcohols to Ce[+4] initiated grafting of cellulose resulted in a higher percentage grafting as well as improved grafting efficiency.[27]

A double initiating system termed Ce[+4]–KPS has been successfully used in the grafting copolymerization of diallyldimethyl ammonium chloride (DADMAC) and acrylamide on starch.[37] The inclusion of KPS in Ce[+4] initiated reactions was shown to improve the percentage grafting, by oxidation of Ce[+3] to Ce^{4+}, which is the active specie in grafting reactions, as shown in Scheme 2.4.

$$Ce^{4+} + RH \longrightarrow R^\bullet + Ce^{3+} + H^+$$

$$S_2O_8^{2-} + 2Ce^{3+} \longrightarrow 2SO_4^{2-} + 2Ce^{4+}$$
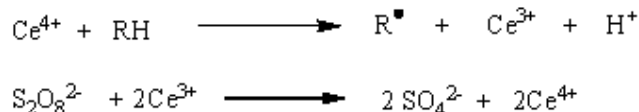
Scheme 2.4: The formation of radicals on polysaccharide and the regeneration of Ce^{4+} through the oxidation of Ce^{3+} by potassium persulfate

Grafting of itaconic acid on cellulose was also carried out using KPS as initiator and the mechanism of radical formation on the cellulose backbone was explained to be via proton abstraction by initiator radicals.[38] Microwave assisted grafting of chitosan[39] and guar gum[40] has been carried out with and without the redox system $AgNO_3$/KPS/ascorbic acid. Microwave activation was also used in the homogeneous esterification of cellulose.[41,42] The use of microwave in grafting reactions offers shorter reaction times compared to conventional methods.

In conventional free radical graft copolymerization, free radical sites are produced along the polysaccharide backbone either by chemical reactions or radiation.[36,37] Then the radicals formed initiate the graft polymerization of vinyl monomers. The major drawbacks of these methods include chain degradation of the polysaccharide backbone during the formation of free radical grafting sites,[43-45] the presence of a considerable amount of ungrafted material in the product, as well as little control over the grafting process in terms of yield and the molar mass of the graft copolymers.[43-45] The synthesis of grafted block copolymers is also not possible because the chain ends of the first block are not reactive. The living radical polymerization techniques permit the synthesis of well-defined cellulosic graft copolymers of predetermined molar mass, thus giving us the opportunity to tailor the surface properties of the cellulose for the required properties. Although living polymerization methods such as RAFT mediated polymerization[46] and ATRP[44,47] can be used to overcome some of the above-mentioned drawbacks of conventional free radical polymerization systems, the living processes requires multiple steps of modifying the polysaccharide with either a RAFT agent, macro initiator or vinyl monomer. Thus the graft density depends very much on the degree of substitution by these reactive modifiers. The method of choice for polysaccharides modification thus depends entirely on the end application intended for the material and practical considerations.

2.2.2: Other grafting techniques

Grafting processes that do not involve the use of vinyl monomers are classified in two groups: grafting by ring opening polymerization and grafting of a preformed polymer.

2.2.2.1: Grafting by ring opening polymerization

Cyclic monomers can be grafted onto polysaccharides via the ring opening polymerization technique.[48] Four classes of cyclic monomers that can undergo ring opening graft copolymerization include:

    i) epoxides

    ii) lactones

iii) α-amino acid N-carboxy anhydrides

iv) 2-alkyl oxazolines.

Some of the grafting reactions of the monomers above require a catalyst to initiate polymerization via a nonionic insertion mechanism. An example of a ring opening graft polymerization is given in Scheme 2.5.
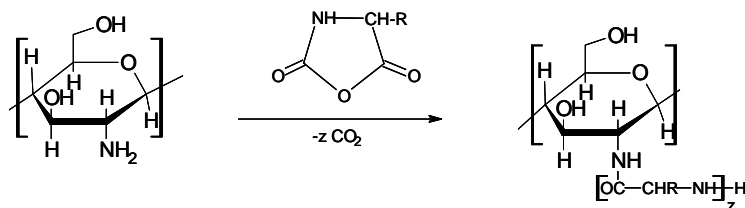
Scheme 2.5: Grafting of polysaccharides with α-amino acid N-carboxy anhydrides

2.2.2.2: Grafting of a preformed polymer

Polymer chains are prepared separately and then reacted with the polysaccharide substrate to form a graft copolymer. The preformed polymer should have a reactive end group to facilitate the reaction of the polymer chains with the hydroxyl groups of the polysaccharide. Such reactive end groups include the following: isocyanate, epoxide, amine, anhydride, chloroformyl, etc. Examples of this type of grafting include: i) grafting of polyurethane via the reaction of the isocyanate end group (polyurethane) and the hydroxyl group of the polysaccharide and ii) grafting of aliphatic polyamides onto partially acetylated cellulose via mesylation of the C6 hydroxyl group of the polysaccharide as shown Scheme 2.6.
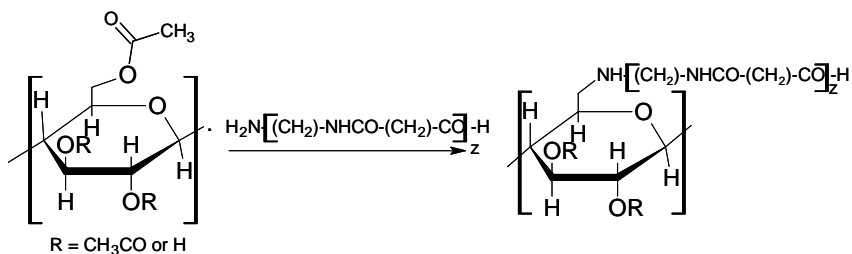
Scheme 2.6: Grafting of aliphatic polyamides onto partially acetylated cellulose via a mesylation reaction

One of the limiting factors of this type of grafting is the molecular weight of the polymer. The ease of grafting decreases with increasing molecular weight due to chain end groups being less accessible for reaction.

2.3: Biominerization: Crystal growth modification

2.3.1: Origin of biominerization

The literature on biominerization is interdisciplinary; it combines the research in microbiology, biotechnology, physics, geology, etc. Scientists and engineers have long been inspired by the beautiful structures and functional properties of the materials formed within living organisms. These minerals adopt complex and genetically determined shapes, often aligned to form arrays, and they fulfill many different functions. These include the mechanical functions of exo- and endo-skeletons, navigation in the earth's magnetic field, orientation in the gravity field, temporary storage, stiffening of soft tissues and much more.[49] In particular, the hard tissues of organisms (e.g. bone, teeth, mollusk shells) are composed of minerals that are typically in close association with an organic polymeric phase, and thus are biocomposites.[50,51] Examples include silicates in algae, carbonates in diatoms and invertebrates, and calcium phosphates and carbonates in vertebrates. These minerals often form structural features such as sea shells and the bone in mammals and birds. Other examples include copper, iron and gold deposits involving bacteria. The mineral crystals that are formed by the organisms, called biominerals, frequently have shapes that are very different from the crystals produced inorganically.

2.3.2: Nucleation and crystal growth mechanisms

During the nucleation stage of crystallization, a small, newly forming crystal is created. The nucleation process is relatively slow as the initial crystal components must interact in the correct orientation to allow them to adhere and form the crystal. Crystal nucleation can occur either homogeneously (without the aid of foreign particles) or heterogeneously (with the aid of foreign particles).[52] Generally, heterogeneous nucleation is faster because the foreign particles act as a template for crystal growth and thus help to stabilize the growing nuclei.[53] Thus, heterogeneous nucleation can take place by several methods, including small inclusions, or cuts, in the reaction vessel. This includes scratches on the sides and bottom of glassware, dust particles, polymeric additives, and other particles that can be voluntarily or involuntarily added to the system.

Crystal nucleation and growth each depend on a number of factors, including the solution's super saturation, temperature, volume and geometry, and the interfacial energy of the growing nuclei. The nucleation ability of additives is correlated to the nature and extent of interaction between the

additive and the crystallization precursors. From the classical nucleation theory, the steady state rate of nucleation is given by:[54,55]

$$J = J_{max} \exp\left[-\frac{4\beta_a^3 \gamma^3 v^2}{27\beta_v (k_B T)^3 (\ln S)^2}\right] = J_{max} \exp\left[-\frac{B}{T^3 (\ln S)^2}\right] \qquad 2.1$$

Where J is the number of nuclei formed per unit volume and unit time, J_{max} is the frequency factor, B represent a collection of variables characterizing the volume, geometry, and interfacial energy of the developing nuclei ($= 4\beta_a^3 \gamma^3 v^2 / 27\beta_v^2 K_B^3$), and S is the solution supersaturaton, where v is the specific volume, K_B is the Boltzmann constant, γ is the surface energy, T is the temperature, β_a is the shape factor and β_v is the volume factor.

For calcium carbonate $S = \gamma_{Ca^{2+}} C_{Ca^{2+}} \gamma_{CO_3^{2-}} C_{CO_3^{2-}} / K_{sp}$

where the numerator denotes the product of the activity coefficients and concentrations for the calcium and carbonate ions and K_{sp} is the solubility product for a particular $CaCO_3$ phase.

It should be noted that 1/J is the time required to form a nucleus per unit volume, and is known as the induction period.[56]

Crystal growth, which occurs after the nucleation stage, is the major stage of a crystallization process. It occurs via the addition of new atoms, ions or nucleates into the characteristic arrangement or lattice of a crystal nucleus.[57] The crystal growth is a faster process and spreads outwards from the nucleating site. Crystal growth can follow different pathways highlighted in Scheme 2.7, with a continuum of structures between A and C being possible.
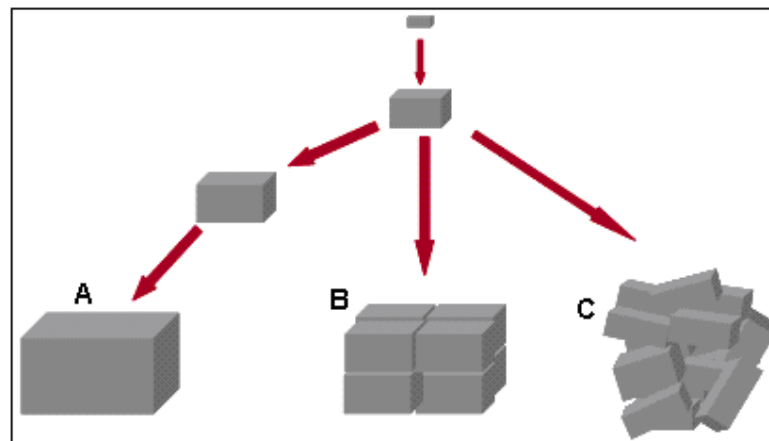
Scheme 2.7: Crystal growth mechanism (A) classical ion/molecule-mediated crystallization, and (B and C) non classical particle-based crystallization leading to mesocrystal (B) and polycrystal (C)[57]

Classical ion/molecule-mediated crystallization involves further growth of a critical nucleus to a single crystal, as shown in Scheme 2.7A. The non classical particle based crystallization involves

aggregation of preformed crystals to form a thermodynamic stable crystal either through uniform packing (Scheme 2.7B) or random packing of these crystals (Scheme 2.7C). The driving force for this packing is the reduction in the surface energy of the system. Kulak *et al.*[57] found that the polycrystals was favored by high solution super saturation, whereby rapid nucleation generates a large number of precursor nanoparticles. The nano precursors will then aggregate, forming polycrystalline structures held together by van der Waals forces. Reduction in super saturation allows the formation of mesocrystals due to slower aggregation effected by a smaller number of the nano precursor ions.

The presence of polymeric additives leads to modification of the size and shape of the primary nanoparticles as well as the number of particles produced. Thus, aggregation of different nano precursors gives crystals of different sizes and shapes. Moreover, polymorph selectivity can be effected by polymeric additives depending on the level of interaction of the additive and the calcium carbonate precursors.

2.3.3: Crystallization of calcium carbonate

The aim of biomimetics is to mimic the natural manner in which organisms produce minerals.[49] One particular area of interest is the molecular control mechanisms that biological systems use to form the well-defined inorganic solid state materials. Much of modern materials science is concerned with hybrid materials, which leads to some overlap in the techniques used in these fields. One property of biominerals must be that of low solubility under physiological conditions. Calcium carbonate deposition is generally controlled by an equilibrium shift due to the consumption of CO_2 but there are many processes with greater control for the formation of other biominerals.[58] Careful control of nucleation and crystal growth of these processes can be achieved via highly regulated active transport mechanisms and via specific modulation of surface reactivity.[59]

Calcium carbonate has various applications in the paper, textile, paint, rubber and adhesive industries. Therefore there is a growing interest in $CaCO_3$ crystallization using polymeric additives as crystal growth modifiers or nucleating agents.[60-66] Calcium carbonate exists in three polymorphs: vaterite, aragonite and calcite (in order of decreasing thermodynamic stability). The crystal type of calcite is trigonic, with three common modifications: rhombohedral (cubic), scalenohedral (columnar), and an intermediary prismatic (barrel-shaped) structure. The density of calcite is 2.72 kg/dm^3. The crystal type of aragonite is orthorhombic, needle-formed (acircular), forming rhombic double-pyramids, which are more dense (density 2.94 kg/dm^3) and harder than calcite. Both aragonite and calcite are bi-refringent, and the refractive index of aragonite is slightly higher than

that of calcite because of the higher density. Vaterite is an unstable hexagonal calcium carbonate, with a round particle shape.

The presence of polymers with functional groups during $CaCO_3$ crystallization directs nucleation and growth of $CaCO_3$ crystals.[51,67,68] Polymeric additives with polar groups influence $CaCO_3$ crystallization by an adsorption mechanism, through the interaction between the polar groups and the growing nuclei.[51,60,68] Studies carried out on the crystallization of $CaCO_3$ revealed that crystal growth and morphology are a function of a number of parameters, including the pH,[50,63,69] temperature,[50,63] reaction time,[50,63,70,71] stoichiometry of reactants,[57,70,72] concentration of the polymeric or organic additive,[50,59,64,69,70,73,74] and the nature of the polymeric additives.[57,59-61,64,66,71,73-76] In general, some polymeric additives such as polyacrylic acid, carboxymethylcellulose, and those containing the carboxylate group may act as inhibitors of $CaCO_3$ crystal growth.[77-80]

The use of polymeric or organic additives of different functionalities as crystal growth modifiers for $CaCO_3$ crystallization may result in $CaCO_3$ crystals of different sizes and morphologies, as well as polymorphs. In some cases, polymeric additives direct the synthesis of the less thermodynamic stable $CaCO_3$ polymorphs.[50,61-63,70,73,81,82] Takiguchi et al.[83] grew $CaCO_3$ crystals on the surface of a cation-exchange membrane and obtained mostly calcite crystals that self-assembled to form tubular agglomerates. Anionic dendrimers, e.g. poly(amidoamine), were also used by Naka et al.[80] to modify $CaCO_3$ crystals and predominantly calcite spherical crystals were obtained. Jada and Verraes[84] obtained spherical particles (1-5.5μm) when anionic polyelectrolytes were used to influence the growth of $CaCO_3$ and the polymorphs formed were a mixture of calcite and aragonite. Spherical particles were also synthesized in the presence of hyperbranched polyesters,[85] anionic surfactants,[73] modified carbon nanotubes,[86] and polyacrylic acid.[70] The effect of polyacrylamide polymers was studied by Yu et al;[63] aragonite nanorods were obtained after 12 hours at a crystallization temperature of 80 °C, and pH 7. At pH 10, the crystal morphology changed to hexagonal disks that were mostly vaterite, and to a lesser extent, aragonite. Kim et al.[74] also obtained aragonite nanorods when polyvinyl alcohol was used as crystal growth modifier. The nanorods were formed through the transformation of vaterite to aragonite after several days. Naka et al.[70] obtained spherical vaterite crystals when polyacrylic acid was used as polymeric additive. The synthesis of $CaCO_3$ was also carried out in microemulsions by Liu et al.[87] They used surfactants to stabilize the emulsions. Hexagonal vaterite crystals were obtained after a day and rod-shaped prismatic calcite crystals after six days. Biopolymers, xanthan, gellan, k-carrageenan, sodium alginate and pectin were also used as additives in $CaCO_3$ crystallization by Butler et al.,[59] and different crystal morphologies were obtained. Chitin, a nitrogen containing polysaccharide, was also used as a crystal growth modifier of $CaCO_3$ crystallization by Manoli et al.,[51] and calcite crystals

were obtained. The rates of crystallization of $CaCO_3$ in chitin were evaluated against collagen and styrene butadiene copolymer functionalized with sulfonic acid groups and was found to be faster in the chitin mediated crystallization reaction. Neira-Carrillo *et al.*[65] detected various $CaCO_3$ crystal morphologies when chitosan grafted with either polyacrylamide or polyacrylic acid was used. Studies on the deposition of $CaCO_3$ on cellulose were also carried out by Alince *et al.*[88] and Dalas *et al.*[89] The adsorption of $CaCO_3$ on cellulose was also investigated by Halab-Kessira and Ricard.[90] Thus, the addition of a polymeric additive to the crystallization solution can modify crystal growth and effect the following processes by:

i)   Complexing the ions and blocking or retarding the crystal growth via a single ion/molecule mechanism, making the non-classical crystallization mechanisms more significant than the classical crystal growth mechanism

ii) Lowering the interface energy of subcritical and critical nuclei, and increasing the number of primary nanoparticles

iii) Stabilizing of metastable intermediates such as amorphous precursor structures

iv) Altering the shape of primary nanoparticles by selective adsorption and/or enrichment onto the specific crystal faces, leading to growth inhibition of these crystal faces.

The paper industry uses $CaCO_3$ as a filler during paper production. The interaction between pulp fiber and calcium carbonate filler in the paper industry is of paramount importance as it influences the tear and tensile strength of the paper. Hence, in this study, modified polysaccharides (cellulose fibers and starches) were used in crystallization studies to evaluate their influence on $CaCO_3$ crystallization specifically their effect on the nucleation, growth, morphology and/or adsorption of $CaCO_3$ crystals on to the fiber.

2.4: Paper production

2.4.1: Pulp cellulose fiber

The cellulose is natively found in the forms cellulose I_α and I_β, but can be modified into cellulose II by precipitation or mercerization. Cellulose III_I and III_{II} are formed by recrystallization and have slight lattice dimensional differences. Heat treatment of cellulose under tension forms cellulose IV. The degree of polymerization (DP) for world pulp materials is typically in the 600-1200, range with the monomer units being 180 Da.

2.4.2: Bonding aspect of fibers

Bonding between untreated cellulosic fibers requires fiber-fiber contact. Since hydrogen bonding and other van der Waals forces are responsible for inter-fiber bonding, the fiber surface morphology becomes critical for fiber-fiber bonding strength. Generally cellulosic surfaces are rough on a scale of 0.01 to 10 μm,[91] hence surface modification is required to improve inter-fiber bonding strength. In the paper industry the fibers are fibrillated by mechanical means to form microfibrils on the fiber surface. The dimensions of primary microfibrils are reported to be in the range of 2-5 nm. Larger fibrils, resulting from partial delamination of outer layers of the cell wall, are also present.[92]

Fig. 2.4 illustrates the effect of fiber surface roughness on the fiber-fiber contact, which has a direct relationship with inter-fiber strength. Fig. 2.4A shows the conventional view of surface roughness in the wet state, where a series of indentations are observed on the surface of the fiber. Upon drying, little contact is formed and hence there is a weaker inter-fiber bonding. Fig. 2.4B shows the fibrillated surfaces of fibers in the wet state. On drying, stronger inter-fiber bonding is formed, as illustrated in Fig. 2.4C. In the wet state the molecular segments tend to mix with each other before the drying stage. The random orientation of the segments results in tangling and interpenetration, and as water is removed during drying the two surfaces are "welded" together.
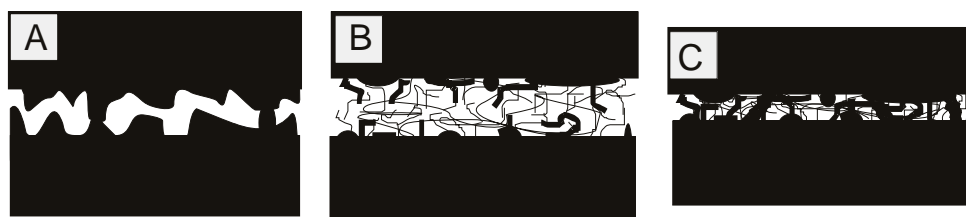
Fig. 2.4: The effect of fiber surface roughness on the fiber-fiber contact.[91]

The fibrillation increases the surface area for fiber-fiber interaction, and thus hydrogen bonding and van der Waals forces become more prevalent. Contrary to random molecular arrangement based on diffusional theory of bonding, Nanko and Oshawa[93] observed a lining up of microfibrils, flat against the adjacent fiber surfaces. Thus the micro-fibrils were tending to form fibrillar structures and this created regular structures within bonded regions of fibrillated surfaces. Generally inter-fiber bond strength increases as the fibers become highly swollen with water either as a result of chemical treatment or refining.

2.4.2.1: Capillary forces

Capillary forces were used to explain the development of paper strength during drying.[94,95] The ability of the wet paper to withstand significant tensile stress is due to capillary forces that tend to pull adjacent fibers together. The forces normal to the plane on the sheet lend strength within the plane of the sheet. Fig. 2.5 is an illustration showing a drop of water between two planes of paper and that the water perfectly wets the surfaces.
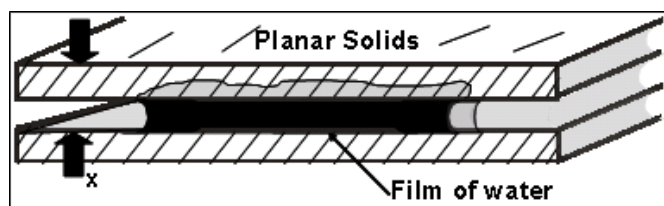
Fig. 2.5: Schematic representation of a drop of water between two planes of paper, wetting the surface completely.

Cambell[95] showed that the magnitude of the negative pressure (ΔP) within the meniscus can be estimated using the following equation:

$$\Delta P \approx \gamma/r \approx 2\gamma/x \qquad\qquad 2.2$$

where γ is the water-vapour interfacial tension, r is the smaller radius of curvature at the edge of the film of water, and x is the distance between the solids.

The capillary forces, including the one defined by the equation 2.2, were found to result in a reduction in the thickness of the wet paper as water is removed.[95] In general, fiber surface modification with surface active compounds results in weaker paper. There are two explanations for this: firstly, from equation 2.2, surface modification with surface active compounds results in a reduction of γ, thus decreasing the capillary forces that draw the paper together, and secondly, the presence of the surface modifiers on the fiber surface may hinder the formation of hydrogen bonds between surfaces.

2.4.2.2: Inter-fiber bond strength

The strength of the inter-fiber bonds is of paramount importance as it contributes to tensile failure. The tensile strength of paper can be related to the strengths of individual fibers as well as to the inter-fiber bonds. Light scattering techniques have been used to determine the relative bonded area (RBA) of paper.[96,97] The concept is based on the scattering of light as it passes through the paper

and thus, the scattering of light is directly proportional to the fiber surface area that is directly in contact with air. This is so because bonded areas do not contribute to light scattering.

The RBA is then given by the following equation:[96]

$$RBA = [S_{non-bonded} - S_{test-sample}]/S_{non-bonded} \qquad 2.3$$

where $S_{non-bonded}$ is the scattering coefficient of the paper sheet formed from butanol and $S_{test-sample}$ is the scattering coefficient of the test sample. The assumption is that the test sample has an identical composition to the non-bonded sample. The reference is formed from butanol because butanol does not swell cellulose and hence the paper formed is very weak due to lack of fiber-fiber bonding. Thus, one can assume that each fiber is surrounded by air giving maximum scattering of light as it passes through.

For the kraft pulps, the paper's tensile strength is determined using the following equation[97]:

$$1/T = 9/(8Z) + 12A\rho g/[bPL(RBA)] \qquad 2.4$$

where T is the maximum tensile force before failure (expressed as breaking length), Z is zero span breaking length (giving an indication of fiber strength), A is the average fiber cross-sectional area, ρ is the density of the fiber material, g is the gravitational acceleration, b is shear bond strength, P is the perimeter of the fiber, L is the length of the fiber and RBA is the relative bonded area (as a fraction). The first term in equation 2.4 involves the breaking of the individual fiber and the second term involves the separation of inter-fiber bonds. Thus, inter-fiber bond strength is the limiting factor.

2.4.2.3: Enhancement of inter-fiber bonds

Polymeric additives based on polysaccharides are normally used to enhance inter-fiber bonding strength. Since the inter-fiber bonding strength is the weakest link that contributes the most to tensile failures, improving the inter-fiber bonding strength will result in improved paper properties. As previously mentioned, the inter-fiber bonding strength can be improved by fiber refining, however, there is a limit to which fiber refining can be done. Although extreme fiber refining may result in improved inter-fiber bonding, it may also result in the loss in the strength of individual fibers and loss in bulkiness of the paper. Polyelectrolytes are widely used to improve the properties of paper. These polyelectrolytes are mainly based on starch, guar gum[98,99] and carboxymethylcellulose.[100-102] Cationic polyelectrolytes, anionic polyelectrolytes, polyelectrolyte complexes, and polyampholytes have been found to improve the dry strength of paper when added to paper.[91] However, cationic starch is by far the most widely used for improving the dry strength of paper in industry.[103-105] The charge density of the polyelectrolyte is of paramount importance in

order to achieve good dry strength of paper. When considering the addition of a cationic polyelectrolyte to a slurry of refined fiber, its interaction with fiber and orientation on the surface of the fiber are critical to the final dry strength of paper. The surface of a refined fiber is negatively charged and cationic polymers have a high affinity for the fiber surface. Fig. 2.6 illustrates the molecular orientation of the cationic polyelectrolytes of different charge density on the surface of paper.
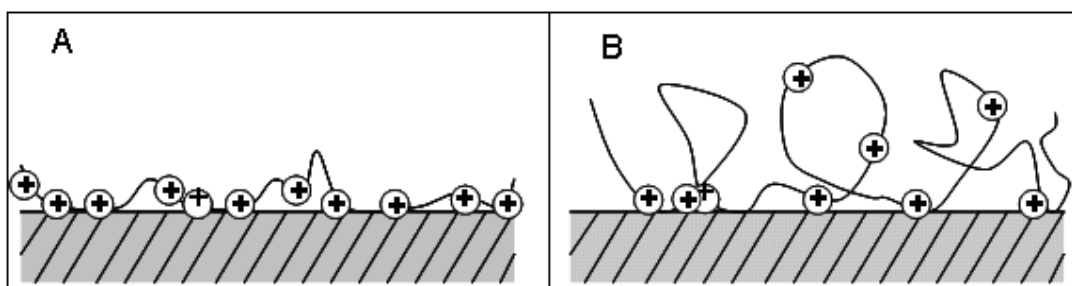
Fig. 2.6: Diagrammatic illustration of the adsorption of polyelectrolytes of different charge density on the surface of a fiber: A) a high cationic charge density polyelectrolyte giving the polymer a flat conformation on the surface of the fiber and B) a low cationic charge density polyelectrolyte giving the polymer a greater degree of molecular extension.

The high cationic charge density of the polyelectrolyte tends to reduce the amount of polyelectrolyte adsorbed on the fiber surface and forces the polymer to lie flat on the surface of the fiber. Low cationic charge density allows the polyelectrolyte to conform in a three dimensional manner on the surface of the fiber. Overcharging the system may result in the surface of the fibers having an excess of positive charges, which may result in lower inter-fiber bonding strength due to fiber-fiber repulsions.[91]

2.4.3: Fillers

The incorporation of fillers in various products has been a common practice for many years in different industries. Fillers are used to improve the performance of materials and may result in materials with better mechanical, chemical, electrical, physical properties, etc., depending on the nature of the filler. There is a wide range of materials that can be used as fillers with respect to their compatibility with the matrix and the ultimate application. Some of the filler types include alumina, calcium phosphate, carbon black, carbon, carbon fiber, ceramics, glass beads, glass fiber, graphite, metallic, molybdenum disulfide, silica, calcium carbonate, etc.

In the paper industry, inorganic materials are considered as essential components of different grades of paper.[106] The original purpose of adding filler to the paper matrix was to reduce furnish costs,

with the amount of filler limited only by strength considerations. Today the principal need for fillers is to impart specific quality improvements to the sheet. Depending on the performance characteristics of the fillers and the amount added to the paper, these products can improve the optical, physical, and aesthetic properties of the finished sheet. Moreover, the practice of utilizing fillers is based on choosing materials that will provide both cost and quality improvements.

2.4.3.1: Functions of fillers in paper

Fillers are added to paper in various percentages, typically 10-20%, to perform many different functions.[106,107] The choice of which filler or blend of fillers to use depends upon the specific properties desired.[108] While fillers are used in many different grades of paper they find their greatest utility in printing and writing paper grades. Fillers can contribute the following properties to paper:

- Reduce costs by replacing higher cost fibre with lower cost fillers
- Improve dimensional stability
- Provide a smoother surface
- Increase opacity and brightness
- Provide enhanced printability
- Improve sheet formation by filling in the void areas around fibre crossings.

The properties exhibited by fillers in paper are mainly dependent on two factors: i) the characteristics of the filler and ii) the way in which it is used. Filler characteristics of importance are their refractive index, particle morphology, particle size and distribution of size, specific surface area, brightness/whiteness, particle charge (zeta potential), and abrasiveness. The manner in which fillers are incorporated into paper varies considerably from machine to machine. The pulp species, type and amount of refining, wet-end furnish components (such as starch, retention aids, and sizing agents), and addition point of the fillers can cause the filler to behave quite differently depending on the furnish conditions. Certainly the amount of filler incorporated into the sheet will have a dramatic impact on sheet properties. More detailed information on the important characteristics of fillers is presented in Section 2.4.3.2 as well as the specific properties of the two widely used filler materials: precipitated calcium carbonate (PCC) and ground calcium carbonate (GCC).

2.4.3.2: Characteristics of fillers

Refractive index

The refractive index is a fundamental property of a filler, which is governed by its chemical composition and molecular structure. Atomic structure has a direct influence upon light scattering

(opacity), because light entering the filler is refracted from its principal path several times within the particle rather than transmitted through it. The greater the refractive index of a filler the greater the amount of reflected light, which increases the opacity of the paper.

Particle morphology

The morphology of filler particles has been shown to be a significant characteristic of fillers. The shape of the particles will influence the way light is scattered. This in turn will affect the optical performance of the filler in paper. It has been proven in studies by Gill,[109] Passaretti and Gill[110] and Fairchild[107] that different morphologies within PCC cause different behaviors, in their ability to scatter light. It is the size of the air microvoids that optimize light scattering, and not directly the size of the particle, hence there is a different optimum for light scattering based on particle size among the different morphologies.

The Mie theory[111] predicts that the maximum scattering of light is obtained by spherical particles that are one half the wavelength of light or 0.20–0.30 μm in diameter. Particles outside of this size range scatter light with less efficiency. However, the Mie theory only holds true for spherical particles such as plastic pigments, titanium dioxide, and certain types of 'spherical' calcium carbonates. Fillers of a non-spherical nature such as kaolin and talc, and some precipitated forms of calcium carbonates, do not behave in a way predicted by the classical Mie theory. Particle shape also dictates the packing nature of the filler particles and greatly affects the fiber structure of the sheet, influencing sheet bulk and porosity.[108,112]

Particle size and size distribution

The optical properties of all fillers are strongly influenced by the particle size, size distribution, and the degree of agglomeration of the filler particles. Studies have shown that a narrow particle size distribution promotes better light scattering efficiency, especially when the filler is uniformly distributed throughout the sheet. Koppelman[113] found that for plate-like particles like kaolin, the optimum opacity was obtained when particles were between 0.70–1.5 μm equivalent spherical diameters. Results of independent studies by Zeller[114] and Gill[109] showed that maximum opacity was obtained when the particle size for prismatic-PCC was 0.40–0.50μm equivalent spherical diameters and 0.9–1.5μm equivalent spherical diameters for scelenohedral-PCC. Furthermore, the more narrow the particle size distribution around the optimum particle size for these fillers the greater will be their contribution to paper opacity.

In the paper mill situation, the use of retention aids helps to retain fillers within the sheet, however, they also cause the fillers to agglomerate. Agglomeration has been shown to have a negative effect

on opacity. Filler agglomeration can be controlled by proper use of all wet-end chemicals, especially retention aids and starches, and optimizing the method and order of addition of the filler with the rest of the papermaking furnish. Some fillers have a greater tendency to agglomerate than others.

Specific surface area

The particle size, size distribution and shape of the filler have a direct impact on the specific surface area.[108,112] The filler's surface area affects light scattering and also influences the strength and printing characteristics of the paper. In general, high surface area fillers lend enhanced printability to the sheet but at the expense of strength and ease of sizing. The principle cause of this weakening effect is related to the filler interfering with fiber to fiber bonding within the matrix of the sheet.

Particle charge

The electrostatic charge, which surrounds a filler particle, plays an important role both in maintaining proper dispersion of the filler as it is fed to the paper machine and in retaining the filler within the paper.[115] The non-hydrodynamic forces, which affect the behavior of particles, are of three basic types: van der Waals (always attractive), electrostatic (requires unbalanced electrostatic charge–may be attractive or repulsive) and steric (between adsorbed molecules or polymers–usually repulsive if the molecules or polymers are water soluble). The balance between these forces (which varies with inter-particle distance) determines whether the particles will remain dispersed or flocculated. Zeta potential is a convenient measure of the electrostatic charge on the colloidal particle, which arises from the interaction of the particle surface with its solution environment.[115,116] It is important to point out here that the chemical nature of a particle surface is not given by knowledge of its bulk composition or is it necessarily consistent from one sample of a given material to the next. It is equally important to take into account the contribution of the solution environment around the particle to the zeta potential. Both specific ion concentrations and total ionic strength affect zeta potential and thereby the electrostatic contribution to colloidal behavior.

Abrasion

Abrasion is an important characteristic of all filler pigments. Highly abrasive pigments will cause excess wear of both paper machine wires and printing plates.[108] The abrasiveness of a filler is principally caused by the crystalline nature or hardness of the filler. The strength of the atomic bonds, spatial arrangements, impurities, etc., together with the filler's physical characteristics (size, particle size distribution, shape, surface area, etc.) are key factors.[113] Small quantities of impurities

such as silica and quartz can cause severe abrasion problems, and larger particles tend to be more abrasive than smaller particles of the same crystalline form.

2.4.3.3: The calcium carbonate filler

Calcium carbonates fall into two general classifications, the natural product made by grinding limestone (GCC) and the precipitated product made synthetically (PCC). The two types of calcium carbonate not only differ in their shapes but also, more importantly, in their surface properties. Ground calcium carbonate (GCC) is treated with a dispersant that imparts a negative charge to it, whilst precipitated calcium carbonate (PCC) is often used without treatment. As a result, their colloidal behaviors differ: GCC forms a stable suspension in water (no aggregation) whilst PCC is unstable and aggregates spontaneously. These properties may have a considerable effect on retention, when filtration is the main mechanism affecting filler retention during papermaking.[116]

Ground calcium carbonate (GCC)

GCC is a commonly used abbreviation referring to refined, ground grades of calcium carbonates obtained from chalk, limestone, and marble.[117,118] Chalk (whiting) is a sedimentary rock of soft texture, which consists almost exclusively of calcium carbonate in the form of calcite and aragonite. Typical properties for chalk are softness and porosity. The color varies from white to slightly grey.[117]

Limestone is a consolidated sedimentary calcium carbonate rock. The exertion of overlying earth layers has led to compression of the nano-fossils, resulting in reshaping, partly dissolving, and recrystallization of the mineral. Limestone is thus harder and less porous than chalk.[117]

Marble is a metamorphous rock. Owing to high pressure and temperature, the original calcite, aragonite, or dolomite re-crystallized, giving rise to dense, mainly coarse-grained, highly indurate masses of calcite or dolomite crystals. Impurities such as iron oxide and other substances cause frequent yellow to brownish red streaks in marbles.[117]

Precipitated calcium carbonate (PCC)

PCC is a fully synthetic product. The properties of PCC differ considerably from those of natural calcium carbonates, and PCC can often be used to improve paper quality by tailoring specific mineral properties (crystal form, size, shape, etc.).[118] In contrast to most other fillers used in papermaking, the surface of PCC can possess a cationic charge.

The starting material in the manufacture of PCC is normally crushed limestone. This is burned (calcined) in an oven at temperatures around 1000 °C, resulting in the formation of calcium oxide

("burnt lime", CaO). The calcium oxide is slaked with water to form a calcium hydroxide slurry into which carbon dioxide gas is introduced under controlled conditions (gas flow, temperature, concentration, time, additives, etc.) to yield precipitated crystals of calcium carbonate.[119]

The crystal forms of PCC are aragonite and calcite, depending upon manufacturing conditions. Typical aragonite morphology is needle-like and aggregates of needles, whereas calcite precipitates as scalenohedral or rhombohedral agglomerates, or prismatic particles.

2.4.3.4: Filler retention and flocculation

In many paper grades fillers are incorporated into the paper sheets to improve paper properties or reduce costs. It is essential for the filler to be well dispersed in the matrix to avoid zones of weaker cohesion, which may facilitate defects during stress conditions. The retention of fillers in the sheet requires retention aids, usually cationic polyelectrolytes. Usually when a suspension of fibres and filler is poured on a screen to form a sheet, the pigment particles may be too small to be captured mechanically and therefore pass into the effluent. To improve retention, the logical approach would be to introduce a polyelectrolyte. The absorption of the fillers to the fibres can either be by heteroflocculation or heterocoagulation. The former results in a bridging of the fibres and the fillers and the latter will result in a reduction in the electrical charges resulting in high deposits of the fillers on the fibres. Another solution would be to utilize a polymer that would flocculate only the filler and, owing to the increased sizes, the flocculants would be captured more efficiently. Anionic soluble and colloidal substances should be avoided in the system to prevent interactions with the cationic polymer, resulting in the greater availability of the cationic polymer to the filler.[116]

For systems that are heavily contaminated with anionic soluble and colloidal substances, non-ionic polyethylene oxide (PEO) can be used as a retention aid. Due to the non-ionic nature of PEO, it may act by either flocculating the pigment (homoflocculation), which is retained by filtration, or by forming a bridge between the fiber and the pigment (heteroflocculation). It was shown that GCC is not affected by PEO or sulfonated kraft lignin (SKL), indicating that absorption and bridging flocculation occur between GCC and the fibre. PCC is affected marginally by PEO but mainly by SKL, whereby SKL promotes its stability.[116]

With the increasing speeds of paper machines, the complexity of wet-end papermaking due to the large usage of additives and the high degree of water recirculation, retention aids that overcome these effects are required. This has resulted in dual and multi-component retention aid systems, one of which is the combination of a cationic polyelectrolyte and microparticles (colloidal silica, bentonite, aluminium hydroxide). The polyelectrolyte adsorbs onto the fiber and filler, resulting in

the formation of aggregates that may provide anchoring spots for the microparticles. The microparticles reflocculate the entire system and act as a bridge between all the components, thereby increasing the attachment of filler to fibre. It has been shown that at the optimum concentrations of bentonite increases the bond strength of cationic polyacrylamide, precipitated calcium carbonate and fibres. [88]

The flocculation performance of cationic starches on calcite pretreated with anionic sodium polyacrylate (NaPA) was investigated by measuring the mean particle size and the dynamic mobility of the calcite dispersion.[120] By varying the amount of NaPA (which has a strong affinity for calcium carbonate) one is able to anionically modify the particles and reverse the charge character of the originally cationic calcium carbonate. Via this mechanism, flocculation of cationic starch on calcite was shown to be highly efficient.[120] Similarly, cationic polyacrylamide was shown to have little effect on the flocculation of PCC in the absence of dextran sulphate (DS). The DS adsorbed on the surface of PCC reverses the particle net surface charge allowing much enhanced polyacrylamide (PAM) adsorption and bridging flocculation.[115] Another study investigated the effect of dextran on PAM–PCC flocculations when the mixtures were exposed to anionic colloidal substances that interfere with the cofactor (dextran)/PEO-induced PCC flocculations. Dextran was shown to enhance PAM-induced PCC flocculation and retention by increasing the calcium ion concentration near the PCC water interface, which in turn facilitates PAM adsorption.[121]

Another option for enhancing filler retention would be to introduce two oppositely charged polyelectrolytes which may be necessary for optimizing the filler flocculation and retention of calcium carbonate in the wet-end of paper machines. It was shown that the flocculation behavior of calcium carbonate was strongly influenced by mixtures of cationic starch and anionic NaPA.[122] Small quantities of added polyelectrolyte increased the flocculation and ionic strength, more specifically at lower NaPA to starch ratios. At higher concentrations of polyelectrolytes the increased amounts of deposited complexes at the particle surfaces overshadowed the effects of the properties of the individual complexes.[122]

The presence of other inorganic or organic surface-active agents, either as additives to the filler (slurry or dry) or to the papermaking system, will affect the colloidal behavior of the particles if they are absorbed on the particle surface. Such agents may modify the zeta potential and/or may contribute to steric repulsive forces. Low molecular weight polyelectrolytes (polyphosphates, polyacrylates) act as strong dispersants by both strong electrostatic and steric repulsion. Moderate to high molecular weight polymeric papermaking additives (starches, polyacrylamides) may act as dispersants or flocculants depending, on the exact methods of their use.

Although filler retention is important, the bonding between the fibers and fillers is critical. The introduction of fillers into paper results in the reduction of paper strength mainly due to disruption of fiber-fiber bonds. The effectiveness of intermolecular forces acting between fibers is reduced and a weaker paper is formed. Thus future additives that are created to promote filler retention should be purposefully designed to also promote filler-fiber bonding, to ensure that paper strength is maintained or improved.

2.5: References

(1)   Roman-Aguirre, M., Marquez-Lucero A., Zaragoza-Contreras E. *Carbohydrate Polymers* **2004**, *55*, 201-210.

(2)   Okeke, B., Obi S. *Bioresources Technology* **1995**, *51*, 23-27.

(3)   Klemm, D., Philipp B., Heinze T., Wagenknecht W. *Comprehensive Cellulose Chemistry.* **1998**, Wiley-vch, Germany.

(4)   Kiran, E., Pohler H. *Supercritical Fluids* **1998**, *13*, 135-147.

(5)   Lee, S., Koepsel R., Morley W., Matyjaszewski K., Russel A. *Biomacromolecules* **2004**, *5*, 877-882.

(6)   Gupta, K. C., Khandekar K. *Biomacromolecules* **2003**, *4*, 758-765.

(7)   Nishioka, N., Yamaguchi H., Kosai K. *Journal of Applied Polymer Science.* **1990**, *40*, 2007-2017.

(8)   Stenzel, M. H., Davis T. P., Fane A. G. *Journal of Materials Chemistry* **2003**, *13*, 2090-2097.

(9)   Princi, E., Vicini S., Pedemonte E., Arrighi V., McEwen I. *Journal of Thermal Analysis and Calorimetry* **2005**, *80(2)*, 369-373.

(10)   Nishiyama, Y., Langan P., Chanzy H. *Journal of the American Chemical Society* **2002**, *124(31)*, 9074-9082.

(11)   Andrievsky, G. V., Klochkov V. K., Karyakina E. L., Mchedlov-Petrossyan N. O. *Chemical Physics Letters* **1999**, *300*, 392-396.

(12)   Dumitriu, S. *Polysaccharides: Structural Diversity and Function Versatility.* **2004**, CRC Press, Germany.

(13)   Stipanovic, A. J., Sarko A. *Macromolecules* **1976**, *9*, 851-857.

(14)   Kolpak, F. J., Blackweel J. *Macromolecules* **1976**, *9*, 273-278.

(15)   Kono, H., Numata Y., Erata T., Takai M. *Polymer* **2004**, *45*, 2843-2852.

(16)   Wada, M., Chancy H., Nishiyama Y., Langan P. *Macromolecules*, 8548-8555.

(17)   Jane, J., Chen Y. Y., Lee L. F. , McPherson A. E. , Wong K. S., Radosavljevic M., Kasemsuwan T. *Cereal Chemistry* **1999**, *76*, 629–637.

(18)   Park, I. M., Ibanez A. M., Shoemaker C. F. *Starch* **2007**, *59*, 69-77.

(19)   Champagne, E. T. *Cereal Food World* **1996**, *41*, 833-838.

(20)   Parker, R. R. *Cereal Science* **2001**, *34*, 1-17.

(21)   Smith, A. M., Denyer K., Martin C. *Annual Review of Plant Physiology and Plant Molecular Biology* **1997**, *48*, 67-87.

(22)   Yuryev, V. P., Cesàro A., Bergthaller W. J. *Starch and starch containing origins - structure, properties and new technologies.* **2002**, Nova Science Publishers, New York.

(23)   Ali, F., Saikia C. N., Sen S. R. *Industrial Crops and Products* **1997**, *6*, 121-129.

(24)   Chauhan, G. S., Guleria L. Sharma R. *Cellulose* **2005**, *12*, 97-110.

(25)   Gupta, K. C., Sahoo S. *Biomacromolecules* **2001**, *2*, 239-247.

(26)   Halab-kessira, L., Ricard A. *European Polymer Journal* **1999**, *35*, 1065-1071.

(27)   Okieimen, F. E. *Journal of Applied Polymer Science* **2003**, *89*, 913-923.

(28)   Princi, E., Vicini S., Proietti N., Capitani D. *European Polymer Journal* **2005**, *41*, 1196-1203.

(29)   Zahran, M. K. *Journal of Polymer Research* **2006**, *13*, 65-71.

(30)   Gurdag, G., Yasar M., Gurkaynak M. A. *Journal of Applied Polymer Science* **1997**, *66*, 929-934.

(31)   Okiemen, F. E., Ogbeifun D. E. *Journal of Applied Polymer Science* **1996**, *59*, 981-986.

(32)   Majumdar, S., Dey J., Adhikari B. *Talanta* **2006**, *69*, 131–139.

(33)   Mino, G., Kaizeman S., Rasmussen E. *Jounal of Polymer Science* **1959**, *39*, 523-529.

(34)   Gaylord, N. *Journal of Polymer Science, Polymer Symposia* **1972**, *37*, 153-173.

(35)   Iwakura Y., K. T., Imai Y. *Journal of Polymer Science, Part A* **1965**, *3*, 1185-1193.

(36)   Mino, G., Kaizeman S. *Journal of Polymer Science* **1958**, *31*, 242-243.

(37)   Lu, S., Lin S., Yao K. *Starch* **2004**, *56*, 138-143.

(38)   Sabaa, M. W., Mokhtar S. M. *Polymer Testing* **2002**, *21*, 337-343.

(39)   Singh, V., Tiwari A., Tripathi D. N., Sanghi R. *Polymer* **2006**, *47*, 254-260.

(40)   Singh, V., Tiwari A., Tripathi D. N., Sanghi R. *Carbohydrate* **2004**, *58*, 1-6.

(41)   Satge, C., Verneuil B., Branland P., Granet R., Krausz P., Rozier J., Petit C. *Carbohydrate Polymers* **2002**, *49*, 373-376.

(42)   Antova G., V. P., Zlatanov M. *Carbohydrate Polymers* . **2004**, *57*, 131-134.

(43)   Koenig, H., Roberts W. *Journal of Polymer Science* **1974**, *18*, 651-666.

(44)   Carlmark, A., Malmström E. *Biomacromolecules* **2003**, *4*, 1740-1745.

(45)   Biermann, J., Chung B., Narayan R. *Macromolecules* **1987**, *20*, 954-957.

(46)   Roy, D., Guthrie, J. T., Perrier, S. *Macromolecules* **2005**, *38*, 10363-10372.

(47)   Vlcek, P., Janata M., Kriz J., Toman L. *Polymer* **2006**, *47*, 2587-2595.

(48)   Li C., Y. N., Xinchao B., Xueyu Q., Xiuli Z., Xuesi C., .Xiabin J. *Carbohydrate Polymers* **2005**, *60(1)*, 103-109.

(49)   Mann, S. *Biomimetic Materials Chemistry* **1995**, John Wiley and Sons.

(50)   Yu, H., Lei M., Cheng B., Zhao X. *Journal of Solid State Chemistry* **2004**, *177*, 681-689.

(51)   Manoli, F., Koutsopoulos S., Dalas E. *Journal of Crystal Growth* **1997**, *182*, 116-124.

(52)   Mercer, K. L., Lin Y., Singer P. C. *American Water Works Association* **2005**, *97(12)*, 116-125

(53)   Zhang, F., Hou Z., Sheng K., Deng B., Xie L. *Journal of Materials Chemistry* **2006**, *16*, 1215-1221.

(54)   Mulin, J. W. *Crystallization.* **2001**, Butterworth heinemann, Oxford.

(55)   Dirksen, J. A., Ring T. A. *Chemical Engineering Science* **1991**, *46*, 2389-2391.

(56)   Guo, J., Stevertson S. J. *Industrial and Engineering Chemistry Research* **2003**, *42*, 3480-3486.

(57)   Kulak, A. N., Iddon P., Li Y., Armes S. P., Colfen H., Paris O., Wilson R. M. Meldrum F. C. *Journal of the American Chemical Society* **2007**, *129*, 3729-3736.

(58)   Dickinson, S. R., Henderson G. E., McGrath K. M. *Journal of Crystal Growth* **2002**, *244*, 369-378.

(59)   Butler, M. F., Glaser N., Weaver A. C., Kirkland M., Heppenstall-Butler M. *Crystal Growth and Design* **2006**, *6*, 781-794.

(60)   Pai, R. K., Hild S., Ziegler A., Marti O. *Langmuir* **2004**, 3123-3128.

(61)   Wei, H., Shen Q., Wang H., Gao Y., Zhao Y., Xu D., Wang D. *Journal of Crystal Growth* **2007**, *303*, 537-545.

(62)   Pan, Y., Zhao X., Sheng Y., Wang C., Deng Y., Ma X., Liu X., Wang Z. *Colloids and Surfaces, A: Physicochemical Engineering Aspects* **2007**, *297*, 198-202.

(63)   Yu, Q., Ou H-D., Song R-Q., Xu A-W. *Journal of Crystal Growth* **2006**, *286*, 178-183.

(64)   Jayaraman, A., Subrambramyam G., Sindhu S., Ajikumar P. K., Valiyaveettil S. *Crystal Growth and Design* **2007**, *7*, 142-146.

(65)   Neira-Carrillo, A., Yazdani-Pedram M., Retuert J., Diaz-Dosque M., Gallois S., Arias J. L. *Journal of Colloid and Interface Science* **2005**, *286*, 134-141.

(66)   Colfen, H., Antonietti M. *Langmuir* **1998**, *14*, 582-589.

(67) Ueyama, N., Hosoi T., Yamada Y., Doi M., Okamura T., Nakamura A. *Macromolecules* **1998**, *91*, 7119-7126.

(68) Manoli, F., Dalas E. *Journal of Crystal Growth* **1999**, *204*, 369-375.

(69) Colfen, H., Qi L. *Chemistry - A European Journal* **2001**, *7*, 106-116.

(70) Naka, K., Huang S-C., Chuyo Y. *Langmuir* **2006**, *22*, 7760-7767.

(71) Sedlak, M., Colfen H. *Macromolecular Chemistry and Physics* **2001**, *202*, 587-597.

(72) Jung, T., Kim T., Choi C. K. *Crystal Growth Design.* **2004**, *4*, 491-495.

(73) Wei, H., Shen Q., Zhao Y., Zhou Y., Wang D., Xu D. *Journal of Crystal Growth* **2005**, *279*, 439-446.

(74) Kim, I. W., Robertson R. E., Zand R. *Crystal Growth and Design* **2005**, *5*, 513-522.

(75) Ajikumar, P. K., Lakshminarayanan R., Valiyaveettil S. *Crystal Growth and Design* **2004**, *4*, 331-335.

(76) Agarwal, P., Berglund K. A. *Crystal Growth and Design* **2003**, *3*, 941-946.

(77) Kato, T., Suzuki T., Amamiya Y,. Irie T. *Supramolecular Science* **1998**, *5*, 411-415.

(78) Zhang, S., Gonsalves K. E. *Langmuir* **1998**, *14*, 6761-6766.

(79) Boggavarapu, S., Chang J., Calvert P. *Material Science Engineering* **2000**, *11*, 47-49.

(80) Naka, K., Tanaka Y., Chujo Y., Ito Y. *Chemical Communication* **1999**, 1931-1932.

(81) Hosoda, N., Sugawara A., Kato T. *Macromolecules* **2003**, *36*, 6449-6452.

(82) Gopal, K., Lu Z., de Villiers M. M., Lvov Y. *Journal of Physical Chemistry* **2006**, *110*, 2471-2474.

(83) Takiguchi, M., Igarashi K., Azuma M., Ooshima H. *Crystal Growth and Design* **2006**, *6*, 1611-1614.

(84) Jada, A., Verraes A. *Colloids and Surfaces, A: Physicochemical Engineering Aspects* **2003**, *219(1-3)*, 7-15.

(85) Meng, Q., Chen D.,Yue L., Fang J., Zhao H., Wang L. *Macromolecular Chemistry and Physics* **2007**, *208*, 474-484.

(86) Li, W., Gao C. *Langmuir* **2007**, *23*, 4575-4582.

(87) Liu, D., Yates M. Z. *Langmuir* **2006**, *22*, 5566-5569.

(88) Alince, B., Bednar F., van de Ven T. G. M. *Colloids and Surfaces, A: Physicochemical Engineering Aspects* **2001**, *190*, 71-80.

(89) Dalas, E., Klepetsanis P. G., Koutsoukos P. G. *Journal of Colloid and Interface Science* **2000**, *224*, 56-62.

(90) Halab-Kessira, L., Ricard A. *Journal of Colloid and Interface Science* **1996**, *184*, 437-442.

(91) Hubbe, M. A. *Bioresources* **2006**, *1(2)*, 281-318.

(92) Hon, D. N. S., Shiraishi N. *Wood and Cellulosic Chemistry.* **2000**, Marcel Dekker, New York.

(93) Nanko, H., Ohsawa J. *Journal of Pulp Paper Science* **1989**, *15(1)*, J17-J23.

(94) Campbell, W. B. *Technical Association Papers* **1947**, *30(6)*, 177-180.

(95) Campbell, W. B. *TAPPI* **1959**, *42(12)*, 999-1001.

(96) Parsons, S. R. *Paper Trade Journal* **1942**, *115(25)*, 314-322.

(97) Page, D. H. *TAPPI* **1969**, *52(4)*, 674-681.

(98) Leech, H. J. *TAPPI* **1954**, *37(8)*, 343-349.

(99) Dugal, H. S., Swanson J. W. *TAPPI* **1972**, *55(9)*, 1362-1367.

(100) Watanabe, M., Gondo T., Kitao O. *TAPPI Journal* **2004**, *3(5)*, 15-19.

(101) Hubbe, M. A., Jackson T. L., Zhang M. *TAPPI Journal* **2003**, *2(11)*, 7-12.

(102) Lofton, M. C., Moore S. M., Hube M. A., Lee S. Y. *TAPPI Journal* **2005**, *4(9)*, 3-7.

(103) Marton, J., Marton T. *TAPPI* **1976**, *59(12)*, 121-124.

(104) Roberts, J. C., Au C. O., Clay G. A., Lough C. *TAPPI Journal* **1986**, *69(10)*, 88-93.

(105) Formento, J. C., Maximino M. G., Mina L. R., Srayh M. I., Martinez M. J. *Appita* **1994**, *47(4)*, 305-308.

(106) Xu, Y., Chen X., Pelton R. *Tappi Journal* **2005**, *4*, 8-12.

(107) Fairchild, G. H. *TAPPI Journal* **1992**, *75*, 85-90.

(108) Hagemayer, R. W. *TAPPI Journal* **1960**, *43*, 277-288.

(109) Gill, R. A. *Nordic Pulp and Paper Research Journal* **1989**, *4*, 120-127.

(110) Passaretti, J. D., Gill R. A. *TAPPI Papermakers Conference Proceedings* **1991**, 293-298.

(111) Maron, S. H., Lando J. B. *Fundamentals of Physical Chemistry.* **1974**, Macmillan, New York.

(112) Gill, R. A. *TAPPI International Paper Physics Conference Proceedings* **1991**, 211-218.

(113) Koppelman, M. H. *TAPPI Papermakers Conference Proceedings* **1981**, 197-199.

(114) Zeller, R. C. *TAPPI Coating Conference Proceedings* **1980**, 103-109.

(115) Smith-Palmer, T., Pelton R. *Colloids and Surfaces A: Physicochemical and Engineering Aspects* **2001**, *181*, 171-181.

(116) Cechova, M., Alince B., van de Ven T. G. M. *Colloids and Surfaces A: Physicochemical and Engineering Aspects* **1998**, *141*, 153-160.

(117) Bergandy, W. *Cement-Wapno-Gips* **1980**, *3*, 72-74.

(118) Dimmick, A. C. *Tappi Journal* **2007**, *6(11)*, 16-22.

(119) Cho, S. H., Park J. K., Lee S. K., Joo S. M., Kim I. H., Ahn, J. W., Kim H. *Materials Science Forum* **2007**, *8*, 881-884.

(120) Nyström, R., Backfolkc K., Rosenholm J. B., Nurmic K. *Journal of Colloid and Interface Science* **2003**, *262*, 48-54.

(121) Gibbs, A., Pelton R., Cong R. *Colloids and Surfaces A: Physicochemical and Engineering Aspects* **1999**, *159*, 31-45.

(122) Nyström, R., Hedström G., Gustafsson J., Rosenholm J. B. *Colloids and Surfaces A: Physicochemical and Engineering Aspects* **2004**, *234*, 85-93.

Chapter 3: Grafting of polysaccharides with hydrophilic vinyl monomers
using various initiator systems

3.1: Introduction and objectives

3.1.1: Microwave-assisted graft copolymerization

The use of microwave irradiation is viewed as one of the facile ways to make modified polysaccharides within reasonable time and yields, compared to conventional grafting methods.[1,2] Microwave irradiation result in radicals being formed on the backbone of the polysaccharide via O–H bond cleavage. Microwaves are also reported to lower the activation energy of reactions.[1-4] Microwave assisted grafting of chitosin[1] and guar gum[2] has been carried out with and without the redox system silver nitrate/potassium persulfate (KPS)/ascorbic acid. When a redox initiator was used the reaction times were shorter and the yields were higher compared to reactions that were carried out without a redox initiator.

3.1.2: Conventional free radical grafting techniques

Grafting of cellulose, starch and related materials can be done via free radical polymerization using various vinyl monomers as well as different initiator systems. The initators used are capable of creating radicals on the backbone by either C–C homolytic bond cleavage or hydrogen abstraction. The following redox initiators are widely used in the grafting of polysaccharides: Ce^{4+}–KPS (other metals such as Fe^{3+}, Cu^{2+}, V^{5+}, etc. can be used),[5] Ag^+–ascorbic acid[1,2] and APS–N,N,N',N'-tetramethylethylenediamine (TEMED). After grafting, it is necessary to remove homopolymers from the grafted materials by means of extraction. Acrylic acid has been used to prepare anionic polysaccharides,[6,7] whereas monomers such as diallyldimethyl ammonium chloride (DADMAC)[8] and methacrylamido-propyl-trimethyl ammonium chloride (MAPTAC)[9] were used to prepare cationic polysaccharides. Some anionic starches have been crosslinked during grafting using the free radical crosslinker N,N-methylene bisacrylamide (MBAM). Acrylamide monomer has also been used in the graft polymerization of acrylic acid and DADMAC. It has been found that the inclusion of acrylamide in the graft copolymerization of DADMAC using a modified batch process increases the grafting efficiency.[8] The most important parameter of the modified polysaccharides is the percentage grafting (% G). The parameter is mainly calculated from gravimetric analysis,[1,2,6,7,10] and in some cases, NMR.[11,12]

3.1.3: The choice of monomer

The choice of monomers to be grafted depends on the end use of the modified polysaccharide. Gupta and Khandekar[13] grafted N-isopropyl acrylamide (NIPAM) onto cellulose to form a temperature responsive gel. The poly(NIPAM) shows a thermally reversible soluble-insoluble

change in response at its lower critical solution temperature (LCST) of 32 ^{o}C in aqueous solution. The phase transition behavior has applications in drug delivery systems. Ethyl methacrylate has been used by Gupta and Sahoo[7] in the synthesis of cellulose based antimicrobial materials since polyethylmethacrylate has some antimicrobial properties. Yeng *et al.*[14] synthesized starch based coatings by grafting polyacrylamide (PAM) onto starch. The grafted PAM increased the viscosity as well as the stability of the coating. PAM was also used to synthesize guar gum based hydrogels for controlled drug release applications by Soppirmath and Aminabhavi.[15] Navarro *et al.*[16] grafted polyethyleneimine onto cellulose to produce chelating adsorbents for metal ions. Polyacrylic (PAA) grafted cellulose and other polysaccharide materials are widely used as super adsorbents (water retention).[6,17] Starch modified with polymers such as PAM, PAA and some cationic polymers can be used as dry-strength additives.[18,19]

3.1.4: Objectives

In this study, a new redox initiator system under microwave irradiation was studied. Graft copolymerization of N-isopropyl acrylamide and methyl acrylate on α-cellulose was carried out under microwave irradiation with cerium (IV) ammonium nitrate and KPS as the initiating system. The role of KPS was to oxidize Ce^{3+} to Ce^{4+}, which is the active species in radical formation. The monomers were chosen as they have characteristic ^{13}C NMR peaks that are easy to identify and this simplifies characterization. The redox system was chosen on the basis of the action of Ce^{+4} on polysaccharides during conventional grafting, whereby radicals are created on the backbone of the polysaccharide via C2–C3 bond cleavage. Thus, the grafted polymers are linked to the polysaccharide polymer backbone through strong C–C bonds in addition to ether linkages. Conventional grafting of polysaccharides using vinyl monomers was also carried out using different initiators and initiator systems. The materials were then tested for their ability to flocculate PCC. The PCC flocculation is important for paper applications, whereby the interaction of modified polysaccharides with PCC and pulp is essential for the retention of PCC. The focus of this chapter was also on the synthesis of grafted polysaccharides for calcium carbonate crystal growth modification and PCC retention in paper application.

3.2: Experimental

Materials

Methyl acrylate (MA) (Aldrich) was purified by first extracting stabilizers with aqueous sodium hydroxide (0.3 M), drying over magnesium sulfate, and then distilling under vacuum. The purified MA was stored below 5 ^{o}C until use. NIPAM (Sigma) was recrystallized from methanol and stored below 5 ^{o}C. Cerium (IV) ammonium nitrate (CAN) (Fluka), KPS (Aldrich), APS, TEMED (Aldrich) were used as received. Acrylic acid (AA, Acros) was purified by vacuum distillation at 30 ^{o}C, and stored below 5 ^{o}C. Acrylamide (AM) (Merck) was recrystallized from methanol and stored below 5 ^{o}C. MAPTAC (Aldrich), DADMAC (Aldrich), MBAM (Labchem) were used as received. α-Cellulose (α-CE) was washed with water and then ethanol and vacuum dried at 60 ^{o}C to a constant weight. Potato starch (Acros) was used as received. Nitric acid (55%, R & S Enterprises) was used as received. PCC and cationic starch (DS = 0.02) were provided by Mondi Business Paper.

3.2.1: Microwave-assisted grafting

Procedure. In a typical reaction, α-cellulose (0.5g, 3.08 x10^{-3} moles of anhydroglucose unit) was dispersed in 2.5 x 10^{-3} M HNO$_3$ (45 mL), CAN (0.025g, 9.5 x10^{-5} moles) was added and the mixture was stirred for 30 minutes. The two monomers (total moles 5.0 x 10^{-3}, mole ratio MA: NIPAM = 1) were then added whilst vigorously stirring. The microwave oven was set at the appropriate microwave power (MWP), temperature, and run time of 10 minutes and the reaction mixture was microwaved. After 10 minutes, the products were precipitated from a 1:4 mixture of water and methanol. The homopolymers were soxlet extracted using a 1:4 water/THF mixture until there was no weight loss, signaling complete removal of homopolymers. The resulting graft copolymer was then dried to constant weight and the percentage grafting was calculated gravimetrically and using solid state ^{13}C NMR data. The graft copolymers (α-CE-g-NIPAM-co-MA) are referred as G1, G2 and G3, in order of an increasing percentage grafting (% G).

3.2.2: Conventional grafting

3.2.2.1: APS-TEMED initiation

Procedure. The grafting reactions were carried out according to literature,[6,8,10,13,15,20] with some modifications. The starch was dissolved in deionized water at 80 ^{o}C until the solution became clear

under nitrogen purging. The starch solution was cooled to 60 ^{o}C and then the monomer(s), initiator (APS) and co-initiator (TEMED) were added. The reactions were carried out under nitrogen for 8 h. In the case of grafting starch/PVA blends, both starch and PVA were dissolved at 80 ^{o}C, simultaneously. For grafting reactions where crosslinking was done, the crosslinker (MBAM) was added together with the monomer(s). The grafted polysaccharides were precipitated out using suitable solvents and the homopolymers were soxlet extracted using suitable solvents (methanol/water or morpholine for PAANa and PAA) until there was no weight loss of the grafted material due to homopolymer removal. The quantities of reactants used and the % G are shown in Tables 3.2 and 3.3.

3.2.2.2: Ce^{4+} and Ce^{4+}-KPS initiation

Procedure. The grafting reactions were carried out according to literature,[6,8,10,13,15,20] with some modifications. These reactions were initiated using the Ce^{4+} and/or the Ce^{4+}-KPS initiator system for both cellulose and potato starch. Cellulose was swelled in an aqueous solution of 2.5 x 10^{-3} M HNO$_3$ at 50 ^{o}C whereas the starch was dissolved in deionized water at 80 ^{o}C. Both solutions were cooled to 30 ^{o}C before addition of the monomer and initiator. The reactions were carried out under nitrogen for 4 h. The graft copolymerization of AM and DADMAC was done using a modified batch process[8] to avoid copolymer composition drift due to different reactivity rations, r$_1$ = 5 and r$_2$ = 0.04 for AM and DADMAC, respectively. The grafted polysaccharides were precipitated out using suitable solvents and the homopolymers were soxlet extracted using suitable solvents (methanol/water for PAM, DADMAC and MAPTAC, and morpholine for PAA) until there was no weight loss in the grafted material due to homopolymer removal.

Grafting of partially dissolved starch (PDSt) was done using the procedure for grafting fully dissolved starch. The only difference was that the partially dissolved starch was prepared by swelling the starch at 75 ^{o}C for about 45 minutes (or until the viscosity began to increase). The quantity of reactants used and the % G are shown in Tables 3.4–3.7

3.2.3: Flocculation of precipitated calcium carbonate

The modified starch and other carboxylate polysaccharides/polymers were tested for their ability to flocculate PCC. The effect of modified starch and other carboxylated polysaccharides/polymers on the flocculation of calcium carbonate is of paramount important when it comes to paper application. Flocculation is required for the retention of PCC during papermaking. However, the size of the flocculants is critical and it should therefore be optimized. Too much flocculation may have a detrimental effect on the quality of paper. Thus, the distribution of PCC in paper should be uniform

and hence the PCC should be well dispersed. In this study, PCC flocculation is used as an indicative measure of the binding efficiency of modified polysaccharides on PCC, and does not necessarily mean that the larger the size of flocculants the better the polymeric additive in paper application.

Procedure. The grafted materials were used in flocculation experiments. Samples of different polymer content were prepared in distilled deionized water in order to investigate the effect of polymer concentration on the flocculant size. A solution of polymer sample of known mass was placed into glass bottles and then 20% PCC (10 mL) was added whilst stirring, using a magnetic stirrer. The final volume of the samples after pH adjustment was 20 mL. The mixture was then stirred for 48 h, after which flocculant sizes were measured.

3.3: Analysis

3.3.1: Gravimetric analysis

The weight of the grafted cellulose after homopolymer extraction was used to calculate the % G as well as the grafting efficiency (% GE), using the following equations:

$$(\%G) = \frac{W_1 - W_o}{W_o} \times 100 \tag{3.1}$$

$$(\%G.E) = \frac{W_1 - W_o}{W_2} \times 100 \tag{3.2}$$

Where W_o, W_1 and W_2 denote the weight of the original α-cellulose, grafted α-cellulose and monomer used respectively.

3.3.2: Cationic degree of graft copolymers

The degree was calculated from chlorine analysis. The chlorine content was determined by the titration method reported by Lu *et al.*[8] In a typical titration, a dry sample (0.2 g) was dissolved in distilled water then 1 mL of aqueous potassium chromate solution (0.5 M) was added. The latter was then titrated using 0.5 M silver nitrate solution until the color of solution turned brick red.
The cationic degree (DC) was then calculated from the following equation:

$$DC = M_{w,monomer} \times 0.05 \frac{V - V_o}{1000W} \times 100 \tag{3.3}$$

where $M_{w, monomer}$ is the molecular weight of the cationic monomer, V and V_o are the volumes of silver nitrate consumed for the sample and blank respectively, and W is the weight of the sample.

3.3.3: FT-IR spectroscopy

A Perkin Elmer FT-IR transmission spectrophotometer ranging from 400–4500 cm^{-1} was used. KBr was used to prepare the sample discs for analysis.

3.3.4: Thermogravimetric analysis

Thermogravimetric analysis (TGA) curves of all the samples were obtained using a Shimadzu analyzer, with a heating rate of 10 $^{\circ}$C per minute.

3.3.5: Cross polarization magic angle spinning ^{13}C NMR analysis

The anomeric and carbonyl ^{13}C NMR peak intensities were used to estimate the % G. The ^{13}C intensities from cross polarization magic angle spinning (CP/MAS) ^{13}C NMR spectra are not quantitative because the peak intensities depend on the rate of cross polarization, which is usually different for different carbon atoms.[12] Thus, direct integration of ^{13}C peaks of different carbon nuclei types may give misleading peak ratios. In order to quantify peaks using ^{13}C peak intensities, the following equations were used.[11]

$$\frac{S(\tau)}{S_o} = \frac{1}{\lambda}\left[1 - \exp\left(\frac{-\lambda\tau}{T_{IS}}\right)\right]\exp\left(\frac{-\tau}{T_{1\rho}\left(^1H\right)}\right), \tag{3.4}$$

$$\lambda = 1 + \frac{T_{IS}}{T_{1\rho}\left(^{13}C\right)} - \frac{T_{IS}}{T_{1\rho}\left(^1H\right)} \tag{3.5}$$

where S_o is the "true" area of resonance, $S(\tau)$ is the area of resonance, $T_{1\rho}\left(^1H\right)$ and $T_{1\rho}\left(^{13}C\right)$ are the proton and carbon spin lattice relaxation times in the rotating frame, T_{IS} is the cross relaxation time between protons and carbons and τ is the contact time. By fitting the experimental data obtained from a plot of the area of resonance of both the anomeric carbon and carbonyl carbon versus contact time (Fig. 3.2) to equation 3.4, S_o and $T_{1\rho}\left(^1H\right)$ for the three graft copolymers were calculated.

In the ^{13}C CP/MAS spectra there are two side bands [SB1 (A) and SB2 (C)], which are due to the carbonyl carbon. The two side bands were also used in the calculation, with an assumption that the carbonyl carbon relaxation data is the same for the side bands as for the main carbonyl peak. The % G was then calculated using equation 3.6.

$$\text{Corrected NMR \% G} = \frac{S_o(T)}{S_o(D)} \times 100 \qquad (3.6)$$

$$\text{and } S_o(T) = S_o(A) + S_o(B) + S_o(C) \qquad (3.7)$$

where $S_o(T)$ is the sum of the true area of resonance $S_o(A \rightarrow C)$, with B denoting the main peak of the carbonyl carbon, and A and C denoting the side bands SB1 and SB2, respectively, and $S_o(D)$ is the true area of resonance for the anomeric carbon.

However, besides using the corrected areas of resonance of the carbon peaks, direct integration of the ^{13}C peaks was done and the ratio of the carbonyl peaks (main peak and the side bands) to the anomeric carbon of α-cellulose was used to calculate % G. The results from NMR were compared with results from gravimetric analysis.

3.3.6: Flocculation

Flocculation of PCC was measured using a Saturn DigiSizer 5200 V1.10. The refractive index of PCC is used to evaluate the flocculant size.

3.4: Results and discussion

3.4.1: Microwave assisted grafting of polysaccharides

The use of microwave irradiation on Ce^{4+}–KPS initiated grafting of cellulose was carried out successfully; the reaction times were reduced to 10 minutes from at least 3 h for the conventional method. Fig. 3.1 shows the ^{13}C NMR spectra of three graft copolymers G1, G2 and G3 which synthesized at different microwave power. The carbonyl peaks (a, b and c) of grafted polymers and the anomeric carbon peak (d) of cellulose were used to calculate % G whilst the MA peak (f) and NIPAM peak (h) were used to estimate the percentage incorporation of each monomer in the graft copolymer. Carbon peaks (e) and (g) are from the cellulose and the grafted polymers, respectively.

In order to correlate the intensities of the anomeric carbon and carbonyl carbon peaks, the proton and carbon spin-lattice relaxation times were determined. A series of spectra were recorded with the contact time ranging from 0 to 12 ms and are shown in (Fig. 3.2). The proton relaxation times measured on the anomeric carbon and carbonyl carbon Fig. 3.2 were similar. Similar proton relaxation time means that the system can be treated as homogeneous.[11] The % G calculated by (i) direct integration of ^{13}C NMR peaks and by (ii) correction of the area of resonance of the ^{13}C

CP/MAS peaks gave results that were similar to those obtained from the gravimetric method. This showed that solid state NMR can be used to estimate % G of α-cellulose.
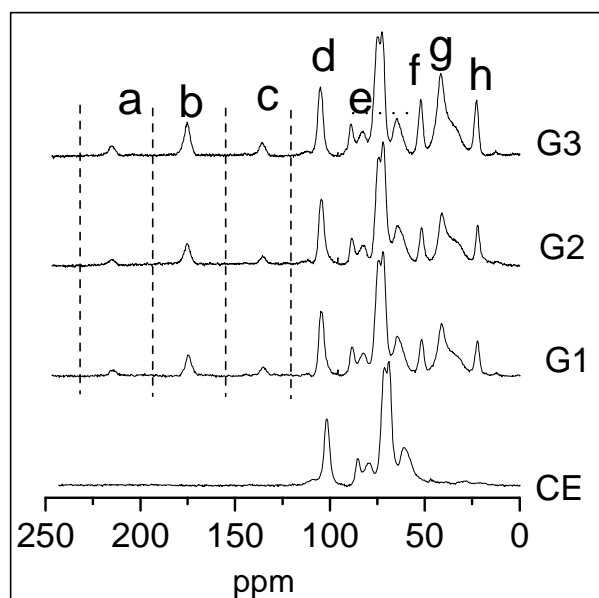
Fig. 3.1: ¹³C CP-MAS NMR spectra of α-CE and the graft copolymers G1, G2 and G3: a) and c) carbonyl side bands, b) carbonyl peak, d) anomeric carbon, e) C2-C6 of cellulose, f) CH₃ carbon peak of MA, g) the carbon peaks of the grafted copolymer (NIPAM-co-MA), h) 2x CH₃ carbons of NIPAM.
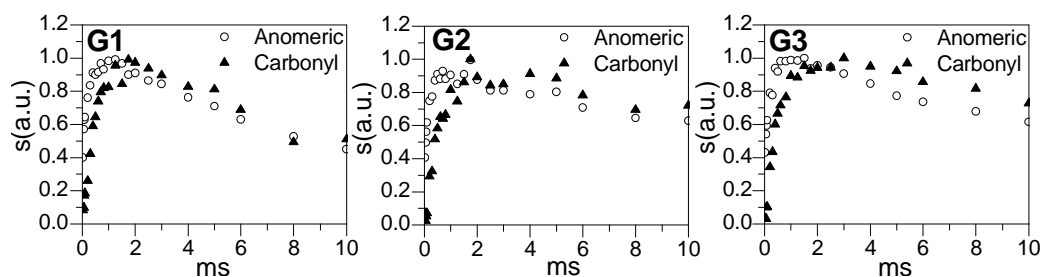
Fig. 3.2: Correlation between area of resonance C1 (Anomeric carbon) of α-cellulose and the area of resonance C* (NIPAM/MA) of the two monomers used and the contact time for the three graft copolymers G1, G2 and G3.

Table 3.1: A comparison of the percentage grafting of cellulose as calculated from three different methods, and the percentage incorporation of each monomer

Sample	MWP (W)	Carbonyl	SB1	SB2	Anomeric	% G CP/MAS	% G Calc.	% G (WG)	% MA	% NIPAM
G3	800	28.33	0.968	0.7113	50.86	52	49	55	66	34
G2	600	20.65	0.782	0.881	62.71	36	38	42	64	36
G1	400	20.65	0.725	0.82	63.9	34	37	38	67	33

The percentage incorporation of each monomer was also determined from CP/MAS spectra: MA incorporation was much higher than that of NIPAM (Table 3.1). This is expected, as MA has higher polymerization constant (kp) than NIPAM. The microwave power had no effect on the percentage incorporation of the monomers and only a small effect on % G. The FT-IR spectra of the graft copolymers (Fig. 3.3) show the MA and NIPAM carbonyl absorption peaks of the grafted copolymers polymers at 1736 and 1650 cm^{-1}, respectively. The peak at 2900 cm^{-1} is due to sp^3 C–H (stretch) of cellulose and grafted polymers. The peak at 1638 cm^{-1} for cellulose is due to C–O (bending) for adsorbed water. In the region 1300–1000 cm^{-1} is where the C–O (stretch) absorption peaks of cellulose and grafted the polymers.
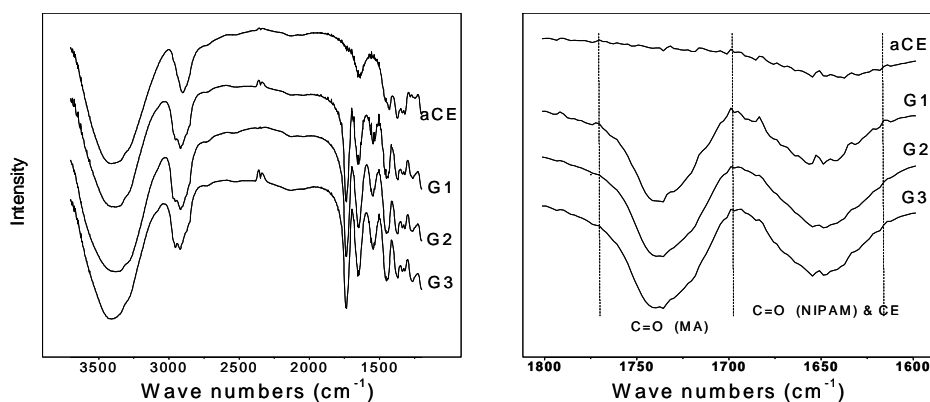
Fig. 3.3: A comparison of the FT-IR spectra of α-CE and the graft copolymers G1, G2 and G3, showing the carbonyl peaks due to the grafted polymers.

The TGA curves (Fig. 3.4) show an increase in thermal stability with an increase in percentage grafting.
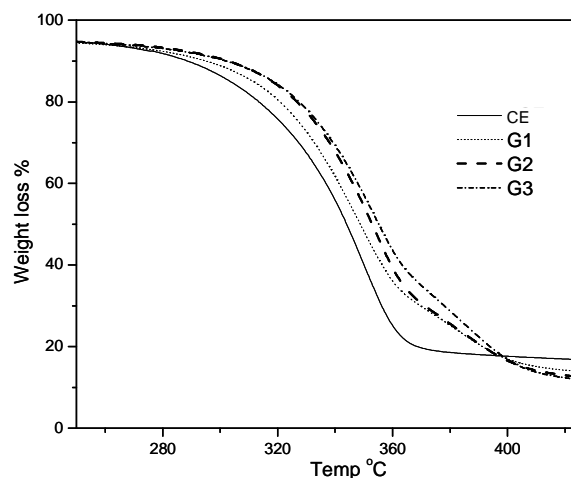
Fig. 3.4: TGA curves of α-CE and the graft copolymers G1, G2 and G3, showing an increase in thermal stability with an increase in % G.

Solid state NMR spectra (Fig. 3.5) for analogous reactions carried out at microwave reaction temperature set at 80 °C for grafting α-cellulose with monomers, NIPAM and MA, showed that there was no grafting. The NMR results were in conflict with the results from TGA, where there was an increase in thermal stability of the grafted materials (Fig. 3.5A), which is typical for grafted materials. However, the carbonyl peak of the polymers was also not observed in the ^{13}C NMR spectrum (Fig. 3.5B) as well as in FT-IR spectrum (spectrum not shown).
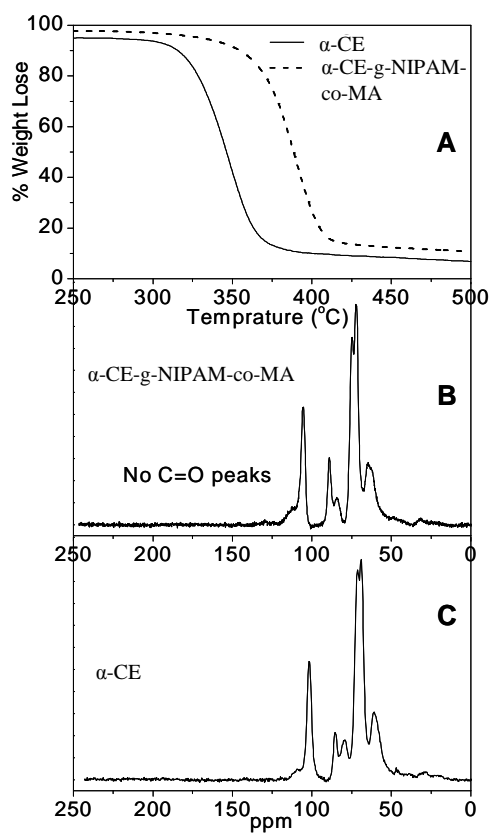
Fig. 3.5: A) TGA curves of α-CE and α-CE grafted with NIPAM showing the thermally more stable ungrafted material. C and B) ^{13}C NMR of α-CE and α-CE grafted with NIPAM and MA (α-CE-g-NIPAM-co-MA), respectively.

The reason for the increase in thermal stability of the cellulose grafted materials is suggested here to be due to the crosslinking of cellulose. Previous studies on conventional Ce^{4+} initiation, a decrease in % G and an increase in homopolymer formation as the temperature was increased to 60 °C, was observed.[6,13] It is, therefore, proposed here that the Ce^{4+}-KPS initiation system is not suitable for microwave reactions above 60 °C as only homopolymer was formed. The presence of a water soluble initiator, KPS, can also contribute to homopolymer formation rather than grafting at this high temperature.

3.4.2: Conventional grafting of polysaccharides

Conventional grafting of polysaccharides was done using various monomers to produce materials for $CaCO_3$ crystal growth modification and paper application as filler retention aids. A number of factors were observed to affect the % G of starch. Table 3.2 shows the effect monomer concentration as well as the effect of adding a free radical crosslinking agent on % G and % GE. It was shown (Table 3.2) that increasing the monomer concentration results in an increase in the % G. However, the grafting efficiency decreases with increasing monomer concentration. The increase in viscosity of the medium is prevalent at high monomer concentration, and negatively affects the diffusion of monomers to the active sites.[7] The % G values are related to the monomer conversion, and the presence of residual homopolymer may lead to high values. Thus, homopolymer removal is of paramount importance. It was also observed (Table 3.2) that addition of a crosslinking agent results in higher % G. Thus, crosslinking will result in improved grafting since growing homopolymer chains (polymeric radicals) have a possibility of adding to a grafted polymer via the double bond of a crosslinker, or vice versa. Moreover, crosslinked homopolymers will be difficult to remove using extraction methods due to their high molecular weight, which favors the formation of strong entanglements with grafted starch, in addition to hydrogen bonding. An increase in the crosslinking agent concentration resulted in an increase in the % G values.

Grafting of starch with monomers such as acrylic acid and sodium acrylate gives superabsorbent materials. The super absorption property is not required for some paper products because moisture absorption will be inevitable, and will compromise the strength of paper. The addition of small quantities of a free radical crosslinker will result in a decrease in the absorption of water, as shown in Appendix C, Fig. C1. The crosslinks prohibit the material from expanding during water absorption, thereby limiting the amount of water that can be absorbed. The more crosslinks there are the less water is absorbed, and vice versa.[15,21] However, the solubility of the crosslinked starch and the mobility of the chains are also reduced by the introduction of crosslinks.

Table 3.3 shows the effect of increasing the poly(vinyl alcohol) (PVA) concentration in the starch/PVA blend on the % G and % GE. When the blends (starch/PVA) were grafted, it was observed that decreasing the starch to PVA ratio resulted in a decrease in the value of % G, suggesting that it easier to abstract protons from the polysaccharide than from PVA (Table 3.3). A similar grafting reaction, with no PVA added, gave a higher % G. This means that it is easier to graft starch than polyvinyl alcohol.

Graft copolymerization of DADMAC and AM was done at various monomers feed ratios. Table 3.5 shows the influence of monomer ratios on the DC. Increasing the DADMAC concentration whilst

decreasing the AM concentration resulted in a decrease in the DC. This is because inclusion of AM in DADMAC polymerization results in an improvement of conversion of DADMAC to polymer, and a high molecular weight polymer. However, the author disagrees that an increase in DADMAC concentration will result in more inhibition of the polymerization by the chloride ions of the DADMAC.[8] The % G was found to increase with an increase in AM concentrations.

The cationic monomer MAPTAC was also grafted copolymerized with AM on starch and Table 3.5 shows the effect of the concentration of MAPTAC on DC. DC increased as the MAPTAC concentration increased. However, the % G did not change much with increasing MAPTAC concentration.

Table 3.2: Quantities of reactants and conditions used to graft potato starch at 60 ºC

Sample	Potato starch	Acrylic acid	Sodium acrylate	MBAM	APS	TEMED	Solids	Grafting	Grafting efficiency
	(mol AHGU)	(mol)	(mol)	(mol x10^{-5})	(mol x10^{-3})	(mol x10^{-4})	(%)	(%)	(%)
HM 1	0.06646	0.1102	0.1113	-	1.096	1.747	13.60	66	43
HM 2	0.06657	0.1111	0.1110	-	1.096	1.798	10.42	68	45
HM 3	0.06663	0.0690	0.0710	-	1.104	1.772	6.69	44	48
HM 4	0.06635	0.0282	0.0284	-	1.102	1.730	7.43	27	69
HM 5	0.06630	0.0141	0.0137	-	1.101	1.730	8.80	14	73
HM 6	0.06768	0.1121	0.1109	0	1.132	1.781	12.59	76	51
HM 7	0.06635	0.1107	0.1112	0.6492	1.127	1.764	9.84	117	77
HM 8	0.07033	0.1118	0.1111	1.4280	1.109	1.755	7.01	123	85
HM 9	0.06657	0.1124	0.1122	2.6620	1.127	1.773	8.15	133	87

APS: ammonium persulfate, TEMED: tetramethylethylene diamine, MBAM: methylenebisacrylamide, AHGU: anhydro-glucose unit, Solids–grafted starch solution's solid content. Grafting (%) and grafting efficiency (%) were determined gravimetrically.

Table 3.3: Quantities of reactants and conditions used to graft a blend of starch from potato and polyvinyl alcohol (viscosity of 62–72 cps) at 60 ºC

Sample	Potato starch (mol AHGU)	PVA (mol 'repeat unit')	AA (mol)	AANa (mol)	APS (mol x10^{-3})	TEMED (mol x10^{-4})	Solids (%)	Grafting (%)	Grafting efficiency (%)
HM 10	0.01506	0.00511	0.02785	0.02673	1.101	1.764	17.60	49	32
HM 11	0.01037	0.01093	0.02715	0.02701	1.108	1.746	9.63	39	21
HM 12	0.00514	0.01502	0.02698	0.02758	1.099	1.755	12.67	37	13
HM 13	0.06629	0	0.11150	0.11150	1.100	1.764	14.96	63	40
HM 14	0.13250	0	0.22220	0.22220	2.331	1.781	10.38	69	45

Table 3.4: Quantities of reactants and conditions used to graft starch from potato using cerium (IV) initiation at 30 ºC

Sample	Potato starch (mol AHGU)	AM (mol)	AA (mol)	AANa (mol)	Ce^{+4} (mol)	Solids (%)	Grafting (%)	Grafting efficiency (%)
HM 15	0.04458	0	0.16660	0	0.003332	12.30	65	44
HM 16	0.08292	0.07042	0.06944	0	0.006386	9.67	57	76
HM 17	0.08323	0	0.16890	0	0.003387	8.12	52	65
HM 18	0.04436	0	0.08333	0.08329	0.003831	15.01	71	41

PVA: polyvinyl alcohol, AA: acrylic acid, AANa: sodium acrylate, APS: ammonium persulfate, TEMED: tetramethylethylene diamine, AHGU: anhydro-glucose unit, AM: acrylamide, Solids–grafted starch solution's solid content. Grafting (%) and grafting efficiency (%) were determined gravimetrically.

Table 3.5: Quantities of reactants and conditions used to graft potato starch with cationic monomers using Ce^{4+}–KPS initiation at 60 ºC

Sample	Potato starch (mol AHGU)	AM (mol)	DADMAC (mol)	MAPTAC (mol)	Ce^{+4} (mol x10^{-4})	KPS (mol x10^{-4})	Solids (%)	Grafting (%)	Grafting efficiency (%)	CDS (%)
HM 19	0.06657	0.05835	0.03018	0	4.480	1.921	13.27	49	66	4
HM 20	0.06635	0.03841	0.05014	0	4.507	1.941	10.79	43	48	6
HM 21	0.06629	0.02307	0.06704	0	4.498	1.937	12.26	35	34	15
HM 22	0.06663	0	0.08851	0	4.496	1.929	8.76	15	13	11
HM 23	0.06646	0.03527	0	0.009185	4.496	1.931	3.95	34	58	8
HM 24	0.06679	0.02673	0	0.018140	4.482	1.927	6.65	38	54	13
HM 25	0.06650	0.00813	0	0.036240	4.469	1.957	4.35	41	59	23
HM 26	0.06646	0	0	0.044330	4.635	1.931	4.48	39	48	36

AM: acrylamide, DADMAC: diallyldimethylammonium chloride, KPS: potassium persulfate, AHGU: anhydro-glucose unit, CDS: cationic degree of substitution, MAPTAC: methacrylamido-propyl-trimethyl ammonium chloride. Grafting (%) and grafting efficiency (%) were determined gravimetrically.

Table 3.6: Quantities of reactants and conditions used to graft cellulose AA and AA/AM mixtures using Ce^{4+} initiation at 30 °C

Sample Code	Cellulose (mol AHGU)	AA (mol)	AM (mol)	Ce^{+4} (mol)	Grafting (%)	Grafting efficiency (%)
HM 27	0.02762	0.04166	0	0.002659	42	51
HM 28	0.02767	0.02083	0.02113	0.002746	61	82
HM 29	0.02769	0	0.04296	0.002737	49	81
HM 30	0.02773	0.1042	0	0.006387	90	61
HM 31	0.02765	0.05555	0	0.003649	59	74
HM 32	0.02767	0.02777	0.02817	0.003649	65	82

Table 3.7: Quantities of reactants and conditions used to graft cellulose and potato starch using Ce^{4+}–KPS initiation under microwave irradiation

Sample Code	Polysaccharide	Polysaccharide (mol AHGU)	AA (mol)	AM (mol)	Ce^{+4} (mol x10^{-3})	KPS (mol x10^{-4})	Grafting (%)	Grafting efficiency (%)
HM 33	CE	0.08834	0.16880	0	1.472	8.962	39	52
HM 34	CE	0.08978	0.08819	0.08464	1.474	9.032	44	58
HM 35 a	St	0.09149	0.16660	0	1.461	9.081	47	65
HM 35 b	St	0.08956	0.08486	0.08507	1.467	9.103	51	68

AM: acrylamide, AA: acrylic acid, KPS: potassium persulfate, AHGU: anhydro-glucose unit, CE: cellulose, St: starch. MW: microwave power 800W was used.
Grafting (%) and grafting efficiency (%) were determined gravimetrically.

3.4.3: PCC flocculation using modified starch

3.4.3.1: Flocculation using anionic starch and cationic starch

Polymeric additives that can flocculate or bind PCC can be used as retention aids in paper production. However, the fiber-filler interactions are also important for the paper strength and thus the use of polysaccharide based filler surface modifiers would enhance fiber-filler bond strength through hydrogen bonding. The flocculation process involves the binding of PCC particles together to form larger particles. Fig. 3.6 shows the effect of (A) anionic starch (HM $1^{3.2}$) concentration, (B) difference between cationic and anionic starch, (C) anionic and cationic starch complex (1:1 ratio) and (D) anionic and cationic starch complex (1:2 ratio) on the size of PCC flocculants. Increasing the polymer content resulted in larger PCC flocculant size, with a subsequent peak broadening, as shown in Fig. 3.6A. At high polymer content bimodal flocculant size distribution was observed. The bimodality and peak broadening was probably due to bridging of PCC flocculants.
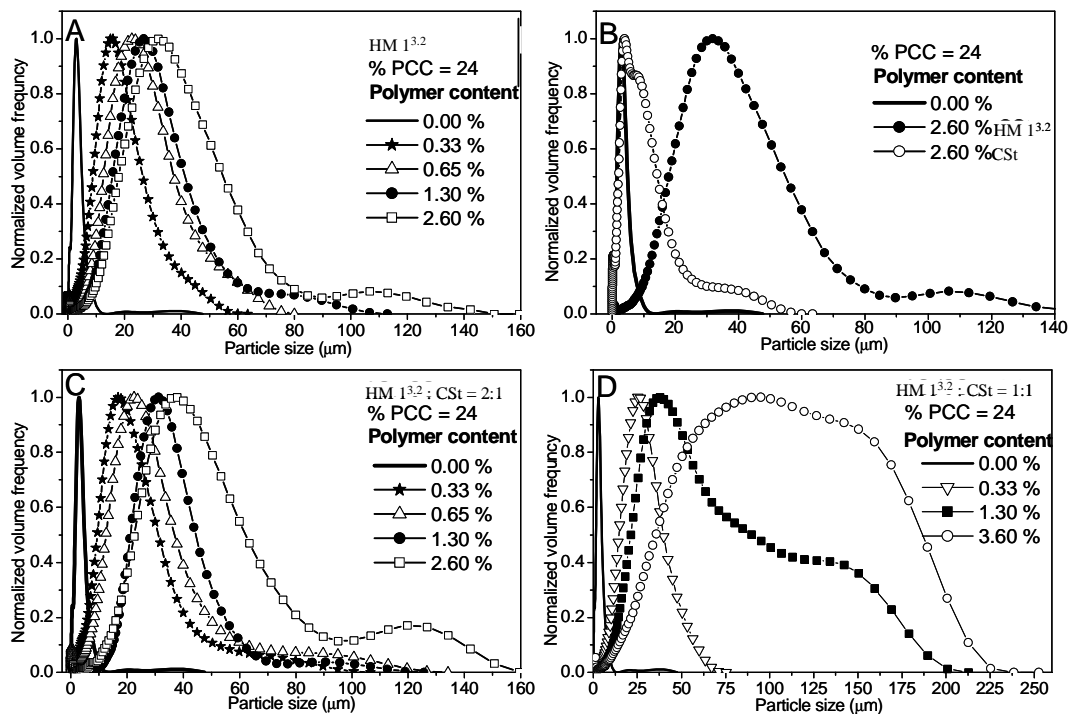
Fig. 3.6: PCC flocculation using different anionic starch contents and mixtures of anionic starch and cationic starch (Mondi Business Paper). (0.00 % is pure PCC).

55

A comparison of the effect of cationic starch (CSt) (Mondi Business Paper) and anionic starch on PCC flocculation, using the same polymer content, is shown in Fig. 3.6B. The results show that the cationic starch on its own does not cause much flocculation compared to the anionic starch.

A mixture of anionic starch and cationic starch (Mondi BP) in the ratio of 2:1 (w/w) was used to flocculate PCC. Samples of different percentage polymer content were prepared and the size of the flocculants was measured for each sample. Fig. 3.6C shows the same effect as seen in the case of anionic starch (Fig. 3.6A), where an increase in polymer content resulted in an increase in flocculant size. A bimodal distribution was also observed, especially for higher polymer content. When 2.6% of the anionic starch to cationic starch at a ratio of 1:1 was used (Fig. 3.6D), significant peak broadening was observed for the higher polymer content, with a substantial increase in the average size of flocculants. The peak broadening effect could be due to the bridging of flocculants via anionic-cationic interactions. Lower polymer content does not show this effect mainly because most of the anionic groups are involved in flocculation rather than in anionic-cationic interactions. These phenomena were then tested in hand sheets to determine their effects on the properties of the hand sheets.

Fig 3.7 shows a comparison on the average size of PCC flocculants at different concentration of the flocculating agents. The bar graph (Fig. 3.7) clearly shows that a mixture of HM $1^{3.2}$ and CSt gave higher average flocculant size than the corresponding HM $1^{3.2}$, at all polymer content levels. (It must be mentioned again that large PCC flocculants may cause detrimental effects on the paper properties although they may result in high filler retention.)
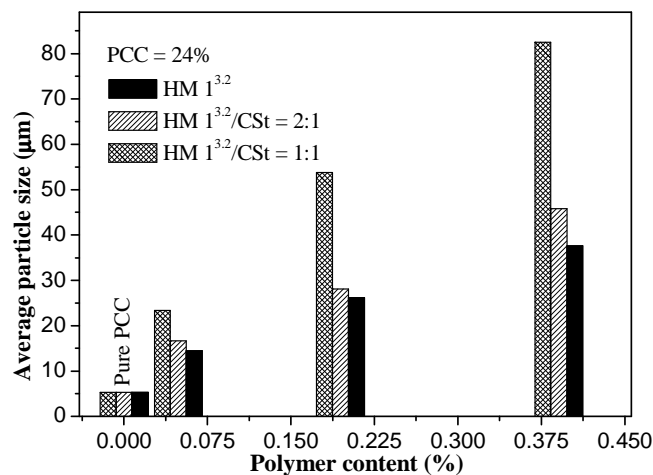
Fig. 3.7: The effect of HM $1^{3.2}$ and two HM $1^{3.2}$/CSt (Mondi Business Paper) blend ratios on the average particle size of PCC flocculants.

3.4.3.2: Effect of pH on Flocculation of PCC

The polymer content was kept constant and the pH was varied in this set of experiments. PCC dissolves at very low pH, thus adjusting the pH of the polymer system was done before adding PCC. Fig. 3.8, shows that as the pH of the polymer system was adjusted to higher values there was also an increase in the average flocculant size of PCC. This shows that the pH is of paramount importance in PCC flocculation. Under basic conditions (pH>8), the polymer's carboxylate groups fully dissociate, thereby enhancing the interactions of the polymer and PCC. Flocculation of PCC using a complex mixture of anionic and cationic starch was also sensitive to pH, as shown in Fig. 3.8B.
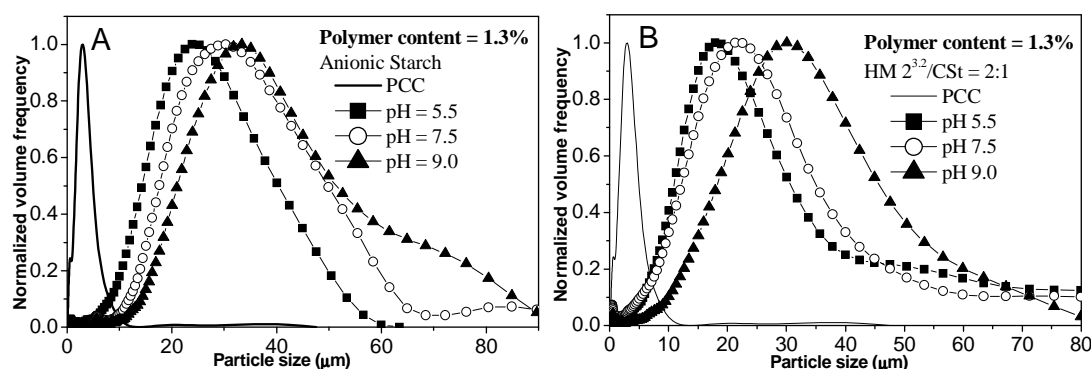
Fig. 3.8: The effect of pH on PCC flocculation using 1.3% total polymer content of (A) HM $2^{3.2}$ and (B) HM $2^{3.2}$ /CSt blend.

3.4.3.3: Partially dissolved grafted anionic starch

PCC flocculation using partially dissolved (PD) grafted anionic starch (Fig. 3.9) showed that an increase in polymer content had a significant effect on peak broadening, with the appearance of bimodal distribution. The peak at lower flocculant size did not change much with the increase in polymer content. The broadening of the peak with increasing polymer content could mean that the modified starch was bridging flocculants together to form much larger flocculants. Since the grafted starch material was partially dissolved, the combined effect of fully dissolved starch and particulate starch is causing the huge broadness of the peaks, especially at higher polymer content. Comparing the results obtained with fully dissolved starch (Fig. 3.6A), the partially dissolved starch gave a broader flocculant size distribution and larger average flocculant size. PCC flocculation using a partially dissolved anionic starch /cationic starch mixture (1:1 ratio (w/w)) (Fig. 3.9B) gave even higher average flocculant sizes and size distribution was broader. Thus not only does an increase in

polymer content and pH have an effect on the average flocculant size but also the ratio of anionic starch (ASt) to CSt. Tri-modality and peak broadening were more pronounced when partially dissolved modified starch/cationic starch mixtures were used.
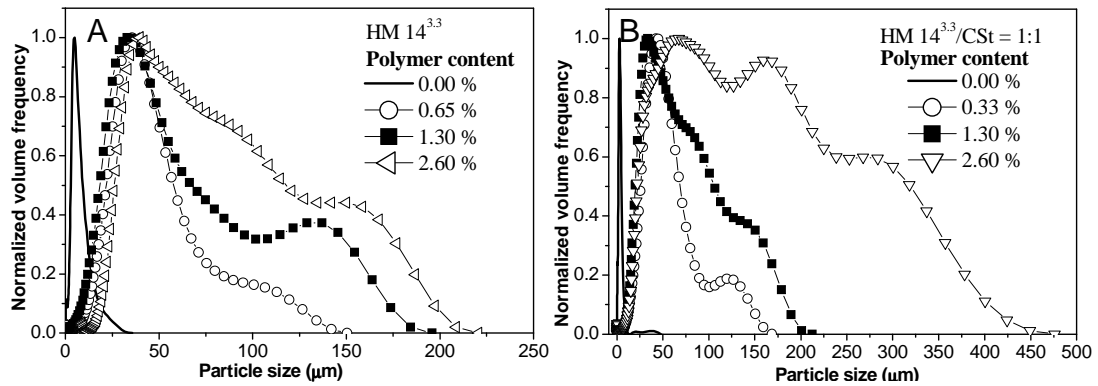
Fig. 3.9: PCC flocculation using different concentrations of (A) HM 14$^{3.3}$ and (B) HM14$^{3.3}$/CSt (Mondi business Paper) blends, in the ratio f 1:1 content, at different polymer content. (0.00 % is pure PCC).

Fig. 3.10 shows that a mixture of partially dissolved anionic starch gave the highest average flocculant sizes at all three polymer contents. It should be noted that the % G values of these materials were comparable. It is also important that any application of these materials in papermaking should also take into account the effect that these polymeric additives will have on the flocculant size of the PCC flocculants. Although flocculation tests were used as an indirect way to check whether the additives are active towards PCC, it does not follow that (during application of these materials) the better the flocculation the better the performance of the additives in paper. Thus, there is every need to determine the optimum size of flocculants to produce the best paper properties.
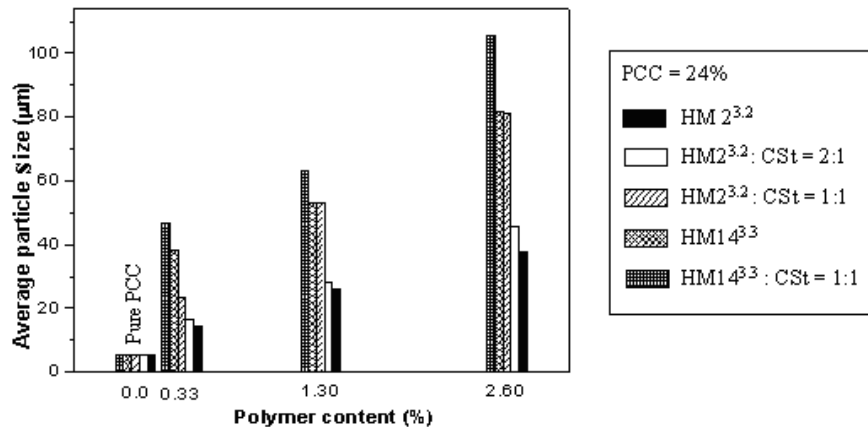
Fig. 3.10: A comparison of PCC flocculation using fully and partially dissolved anionic starches, HM 2$^{3.2}$ and HM 14$^{3.3}$, and their blends with cationic starch (Mondi Business Paper).

58

3.4.3.4: Effect of order of addition of oppositely charged starch and percentage grafting

Additives are added at different stages during papermaking depending on their intended function. It was, therefore, important to study the effect of two oppositely charged polymeric additives on the size of PCC flocculants. A sequential addition of polymeric additives, starting with the anionic additives to PCC followed by the cationic additive, resulted in higher average PCC flocculant sizes, as shown in Fig. 3.11A. Fig. 3.11B shows that an increase in the % G of anionic starch resulted in an increase in the sizes of PCC flocculants. Thus, the effect of % G is similar to increasing the concentration of anionic starch, as is seen in Fig. 3.6A.
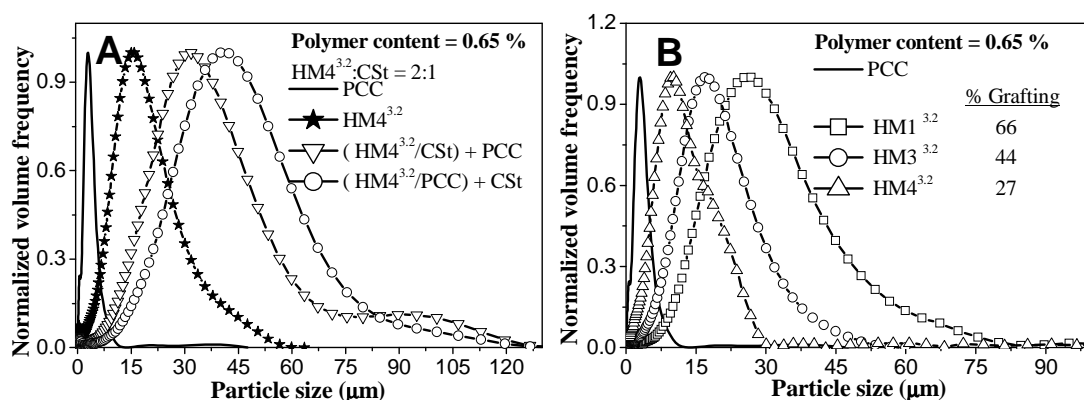
Fig. 3.11: The effect of; (A) the order of addition of cationic and anionic polymers to PCC and B) the % G of starch on the size of PCC flocculants.

3.4.3.5: Flocculation of PCC using carboxylmethyl cellulose

Carboxylmethyl cellulose (CMC) is a water soluble anionic polysaccharide that is already on the market and it was therefore necessary to compare the flocculation efficiency of grafted starch synthesized in this study with CMC. CMC sodium salt (Aldrich, degree of substitution 0.6-0.9) was tested for its PCC flocculation properties. Samples of different CMC concentration were prepared including those of a mixture of CMC and cationic starch (Mondi Business Paper). The ratios used (CMC: CSt) were dictated by their application in the paper industry.

PCC flocculation using different CMC and CMC/CSt (w/w) blends (Fig. 3.12A and B) shows that neither CMC nor a blend of CMC/CSt had much effect on PCC flocculation. Thus, PCC flocculation depends on the number of the carboxylate groups on the polysaccharide, which was low for CMC. The resulting flocculant sizes were slightly higher than that of PCC without any flocculating polymer.
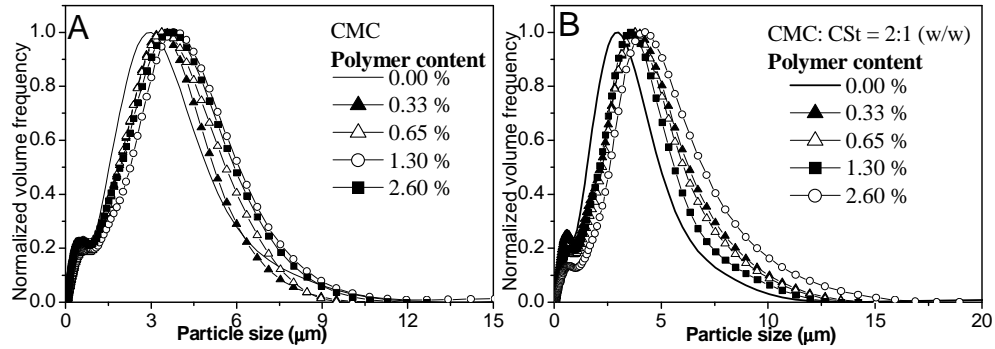
Fig. 3.12: PCC flocculation using different CMC and CMC/CSt (Mondi Business Paper) blends; 0.00% is pure PCC.

3.4.3.6: Flocculation of PCC using crosslinked PAA grafted starch

Fig. 3.13 shows the effect of the crosslinking reagent concentration on flocculation. The curves show that crosslinking resulted in bimodality and peak broadening. When 0.65×10^{-5} mole of crosslinking agent was used the size distribution broadened and there was a clear shift in the peak maxima to high flocculant size (Fig. 3.13A). The average flocculant size increased with increasing concentration of the crosslinking agent, as shown in Fig. 3.13B.
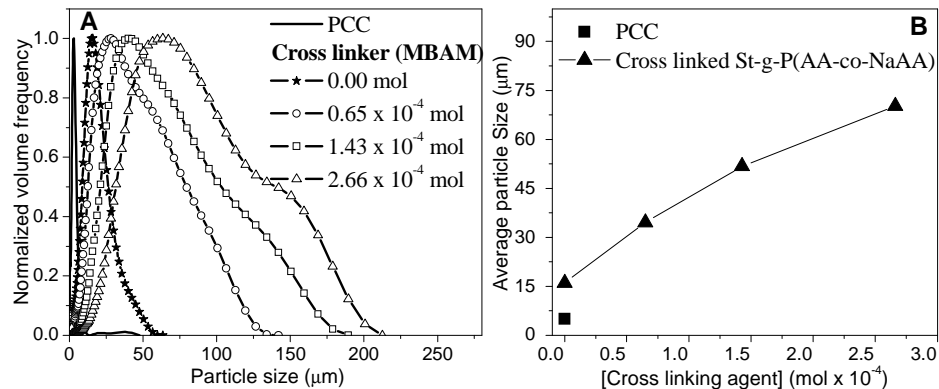
Fig. 3.13: The effect of crosslinking agent MBAM on flocculant size distribution (A) and the average flocculant size (B). (HM $6^{3.2}$–HM $9^{3.2}$ were used and polymer content in these experiments was 0.65%.

An increase in the concentration of the crosslinking agent resulted in an increase in the % G (Table 3.2 which affected the flocculant size. The bimodality observed when increasing the concentration of the crosslinking reagent could be due to the effect of inter-chain networks formed that can bridge flocculants. A broad distribution of molecular architectures, ranging from low molecular weight single chains to high molecular weight branched chains, results when a crosslinking agent is used. Thus, these molecular architectures have different effects on PCC flocculation. Hence, the use of

crosslinked materials for PCC flocculation showed a broad distribution of flocculant sizes even at low doses of the crosslinking reagent. The broad distribution in the size of flocculants may have a detrimental effect on paper properties such as the porosity, burst strength tensile strength, etc.

3.4.3.7: Flocculation properties of St/PVA blends and cationic starch

Grafting of a blend of starch and PVA was carried out and the resulting materials were tested for flocculation behavior. Fig. 3.14A shows that the materials were capable of flocculating PCC but, in comparison to the equivalent starch based material, the flocculation was low. The size of flocculants increased with decreasing PVA concentration because the % G also increased with decreasing PVA concentration. Fig. 3.14B shows that the prepared cationic starch materials were also capable of flocculating PCC. Although PCC is partially positive and the cationic starch positively charged, the cationic starch is still able to interact with PCC via an adsorption mechanism. The average surface charge of PCC is positive but the surface is amphoteric because of the presence of CO_3^{-3} and Ca^{2+}, therefore adsorption of cationic polymers is possible.
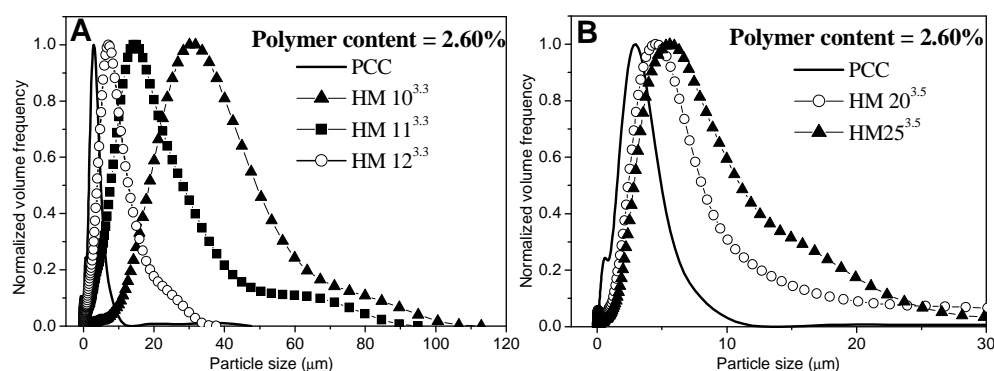
Fig. 3.14: Flocculation of PCC using (A) P(AA-co-NaAA) grafted starch/PVA blends and (B) cationic starches HM $20^{3.5}$ and HM $25.^{3.5}$

3.5: Conclusions

The grafting of polymers onto cellulose, after the homopolymer had been removed via soxlet extraction, was confirmed by solid state NMR, FT-IR as well as thermogravimetric analysis. The % G calculated from ^{13}C NMR correlated well with % G calculated from gravimetric analysis. It was found that microwave irradiation of cerium initiated grafting of cellulose is limited to temperatures lower than 60 °C. Higher temperatures resulted in crosslinking of the celluloses, as concluded from TGA curves and ^{13}C NMR spectra. The reaction times in microwave assisted grafting were reduced

significantly when compared to conventional grafting methods and the effect of microwave irradiation power on % G was less significant.

Anionic and cationic polysaccharides were synthesized successfully via conventional grafting of anionic and cationic monomers, respectively. All the initiation methods (Ce^{4+}, Ce^{4+}–KPS, and APS–TEMED) used yielded grafted materials with considerable % G. A comparison between the initiator systems is, however, not simple as the grafting efficiency depends on a number of factors, including the time of reaction, initiator and reactants concentrations, temperature and even the purity of the reactants such as the monomers and polysaccharides. Modified polysaccharides of different % G were obtained by varying the polysaccharide to monomer ratio. Inclusion of a crosslinking agent resulted in higher % G values. In general, any of the initiator systems used and described in this study can be used to modify polysaccharides via the grafting technique.

It was also shown that the prepared anionic starch materials were good flocculating agents for PCC. The average size of flocculants could be varied by varying the modified starch concentration and pH. The effect of % G on the size of PCC flocculants was equivalent to that of varying the concentration of the modified starch. Thus, the higher the % G of the modified starch and the concentration of anionic starch, the larger the average sizes of PCC flocculants.

Selected modified starch materials were used for $CaCO_3$ crystal growth modification (see Chapter 4). Some of the modified polysaccharides were also tested for PCC retention in paper and were also used in the preparation of anionic starch coated starch particles for filler-fiber bonding in paper application (see Chapter 6).

3.6: References

(1)   Singh, V., Tiwari A., Tripathi D. N., Sanghi R. *Polymer* **2006**, *47*, 254-260.

(2)   Singh, V., Tiwari A., Tripathi D. N., Sanghi R. *Carbohydrate* **2004**, *58*, 1-6.

(3)   Satge, C., Verneuil B., Branland P., Granet R., Krausz P., Rozier J., Petit C. *Carbohydrate Polymers* **2002**, *49*, 373-376.

(4)   Antova, G., Vasvasova P., Zlatanov M. *Carbohydrate Polymers* **2004**, *57*, 131-134.

(5)   Chauhan, G. S., Guleria L. Sharma R. *Cellulose* **2005**, *12*, 97-110.

(6)   Gurdag, G., Yasar M., Gurkaynak M. A. *Journal of Applied Polymer Science* **1997**, *66*, 929-934.

(7)   Gupta, K. C., Sahoo S. *Biomacromolecules* **2001**, *2*, 239-247.

(8)   Lu, S., Lin S., Yao K. *Starch* **2004**, *56*, 138-143.

(9)   Chen, T.-S. R., DeVito V. L., Frederick K. V. *US patent* **2006**, no. 7001953.

(10) Princi, E., Vicini S., Proietti N., Capitani D. *European Polymer Journal* **2005**, *41*, 1196-1203.

(11) Stejskal, E. O., Memory J. D. *High Resolution NMR in the Solid State Fundamentals of CP-MAS.* **1994**, NewYork: Oxford University Press.

(12) Haris, R. K., Granger P. H. *Multinuclear Magnetic Resonance in Liquids and Solids-Chemical Application.* **1990**, Kluwer Academic Publishers, Dordrecht.

(13) Gupta, K. C., Khandekar K. *Biomacromolecules* **2003**, *4*, 758-765.

(14) Yeng, W. S., Tahir P. M., Chiang L. K., Yunus W. M. Z. W. *Journal of Applied Polymer Science* **2004**, *94*, 154-158.

(15) Soppirnath, K. S., Aminabhavi T. M. *European Journal of Pharmaceutics and Biopharmaceutics* **2002**, *53*, 87-98.

(16) Navarro, R. R., Sumi K., Matsumura M. *Water Research* **1999**, *33(9)*, 2037-2044.

(17) Athawale, V. D., Lele V. *Starch* **2001**, *53*, 7-13.

(18) Marton, J., Marton T. *Tappi* **1976**, *59(12)*, 121-124.

(19) Roberts, J. C., Au C. O., Clay G. A., Lough C. *Tappi Journal* **1986**, *69(10)*, 88-93.

(20) Okieimen, F. E. *Journal of Applied Polymer Science* **2003**, *89*, 913-923.

(21) Soppirnath, K. S., Kulkarni A. R., Aminabhavi T. M. *Journal of Biomaterials Science, Polymer Edition* **2000**, *11*, 27-43.

Chapter 4: Crystallization of CaCO$_3$ in the presence of polymeric additives

4.1: Introduction

CaCO$_3$ is often used as filler in various industries, including the paper industry. The properties of the main crystal morphologies of CaCO$_3$ fillers have been highlighted in Chapter 2. Precipitated calcium carbonate (PCC) and ground calcium carbonate (GCC) are widely used in the paper industry. The papermaker can improve drainage by blending PCC with GCC, which can translate into increased machine speeds. Inclusion of GCC has less effect on the bulkiness of the paper but the paper stiffness and tensile strength are improved when compared to using a 100% PCC filler. PCC is a mixture of two CaCO$_3$ polymorphs, calcite and aragonite, which are more thermodynamically stable than vaterite. Calcite is the most thermodynamic stable polymorph and is abundant. The crystal morphologies of calcite and aragonite in PCC are different. Calcite crystals exist in two crystal shapes, scalenohedral and prismatic, whereas aragonite typically has an orthorhombic (needle-like) morphology. In general, fillers should be compatible with the matrix and, in the case of paper; filler-fiber bonding should be promoted.

The efficiency of a polymeric crystal growth modifier in nucleation is correlated to its binding capacity towards the Ca^{2+} and this is essential for the formation of sub-critical nuclei that will then grow to the required size for crystal growth. The presence of a polymeric additive may inhibit crystal growth during the nucleation stage, resulting in an induction period. The relationship between the induction period, surface energy and super saturation for calcite nuclei is given below:[1]

$$\log\tau \propto \left(\frac{\beta\vartheta^2\gamma_s^{\,2}}{\left(2.303k_BT\right)^3}\right)\frac{1}{\left(\log S\right)^2} \qquad\qquad 4.1$$

Where τ is the induction time, β is a shape factor for the calcite nuclei ($16\pi/3$ for spherical shapes), ϑ is the molar volume of calcite ($=1.89 \times 10^{-5}$ m^{-3}), γ is the surface energy of the nuclei, k_B is the Boltzmann's constant, T is the reaction temperature and S is the solution supersaturation.

The induction time depends mainly on the solution supersaturation and the surface energy of the growing nuclei. Thus, the induction time is correlated to the effect of the polymeric additive or any other contaminant present on nucleation and crystal growth.

In this study, crystallization experiments were carried out to investigate the effect of polymeric additives on the morphology of CaCO$_3$ and the extent of interaction between polymeric additives and CaCO$_3$. The effect of the crystallization temperature on the crystal morphology was also investigated. Thus, CaCO$_3$ crystallization was performed using different polymeric additives. The study explores the feasibility of performing *in situ* crystallization of calcium carbonate in the

presence of fibers in order to increase filler retention during papermaking. Further, filler size and morphology modification using soluble polymeric additives were of special interest, as well as the surface properties of the crystallized $CaCO_3$ (see Chapter 5).

4.2: Experimental

Materials

Materials synthesized as described in Section 3.2: Cellulose graft copolymerized with MA and NIPAM, acrylic acid (AA) grafted cellulose, acrylamide (AM) grafted cellulose and acrylic acid (AA)/sodium acrylate grafted starch were used as crystal growth modifiers in the crystallization experiments. $CaCl_2$, Na_2CO_3 and NaOH were used as received.

4.2.1: Crystallization of $CaCO_3$

The grafted materials and their corresponding homopolymers were used as crystal growth modifiers for $CaCO_3$ crystallization. The cellulosic materials were swollen in deionized water at 50 ^{o}C for 1 h. The starch based materials were dissolved at 80 ^{o}C to prepare a stock solution of 1.8 g/L. A stock solution (0.75 g/L, pH 7) was also prepared for PAM and PAA homopolymers. In a typical $CaCO_3$ crystallization reaction, modified polysaccharide (15 ml, 1.8 g/L) was dispersed/dissolved in de-ionized water, stirred under N_2, then a Na_2CO_3 solution (10 mL, 0.025 M) was added and the pH adjusted to pH 8.5. The latter was further stirred for 30 minutes at the required reaction temperature for equilibration, after which $CaCl_2$ (10 mL, 0.025 M) solution was added slowly whilst stirring. The reactions were carried out at 25 $\pm$ 2 ^{o}C and 80 $\pm$ 2 ^{o}C for 24 h. The products were filtered through a 0.22 micron membrane filter paper to collect the $CaCO_3$ micro particles and the crystal growth modifier (if insoluble), then rinsed three times using deionized water and dried.

4.2.2: Rates of crystallization

The rates of crystallization were obtained from following the turbidity of reaction solution during crystallization using a Lambda 20 UV/VIS spectrometer. The wavelength of light used was 500 nm. In a typical experiment, 2 ml of a solution of the polymeric crystal growth modifier (0.5 g/L) was added to a cuvette followed by $CaCl_2$ solution (1 ml, 0.002 M). Lastly, a solution of Na_2CO_3 (1 ml, 0.002 M) was added, and the absorbance of the solution measured against time.

4.2.3: Characterization of CaCO$_3$ crystals

Scanning electron microscopy (SEM) was used to determine the morphologies of CaCO$_3$ crystals. All samples were gold coated before analysis. The instrument was a Leo 1430VP scanning electron microscope fitted with a field emission source. An accelerating voltage of 15 kV was used.

The X-ray powder diffraction (XRD) measurements were done using a modified computer-controlled Philips 1410-diffractometer. The crystal structure was determined using Cu Kα radiation (40 kV), 0.2^o step and 2θ range of 15–60°. XRD was not used for quantifying the polymorphs because the less thermodynamically stable polymorphs may not be detected by XRD due to high calcite content. The instability of the less thermodynamically stable polymorphs also result in quantification of the polymorphs being difficult because they can be converted to calcite with time making the quantification time dependant.

4.3: Results and discussion

4.3.1: Crystallization in the presence of PAM and PAA homopolymers

PAM and PAA were used in crystallization of CaCO$_3$ to obtain information that is crucial for comparison with results obtained using modified polysaccharides under similar conditions. Since identical crystal growth modifiers can give different rates of crystallization, morphologies and polymorphs depending on the conditions used, it was therefore necessary to study the effect of the homopolymers on crystallization of CaCO$_3$ in order to relate their effects to those of the grafted polymers.

The efficiency of a polymeric crystal growth modifier is correlated to its ability to reduce the interfacial energy of subcritical and critical nuclei, and increase the number of primary nanoparticles.[2] The rates of crystallization were obtained from following the turbidity of the solution during crystallization by measuring the absorption of the reaction solution with time. The concentration of the reactants was such that the maximum absorption was below 1 (to obey Beer-Lambert's law). The absorbance at time (t) = 0 was not zero (Fig. 4.1) because of the delay between injecting the second calcium carbonate precursor and the measurement. As was expected, Fig. 4.1 showed that the control reaction had no induction time. The introduction of polymeric additives PAA and PAM lead to two opposing effects, when considering equation 4.1, both affecting the induction time. Firstly, the surface energy of the subcritical nuclei decreases, favoring the reduction in the induction period and, secondly, the super saturation decreases, favoring an increase in the induction time.[1,2] The induction time for PAA mediated crystallization is longer than that of the

control and PAM mediated crystallization (Fig. 4.1). This can be explained by considering the strong interactions of PAA with the metal ions before formation of sub-critical crystals, resulting in reduction in the super saturation leading to an increase in induction time.
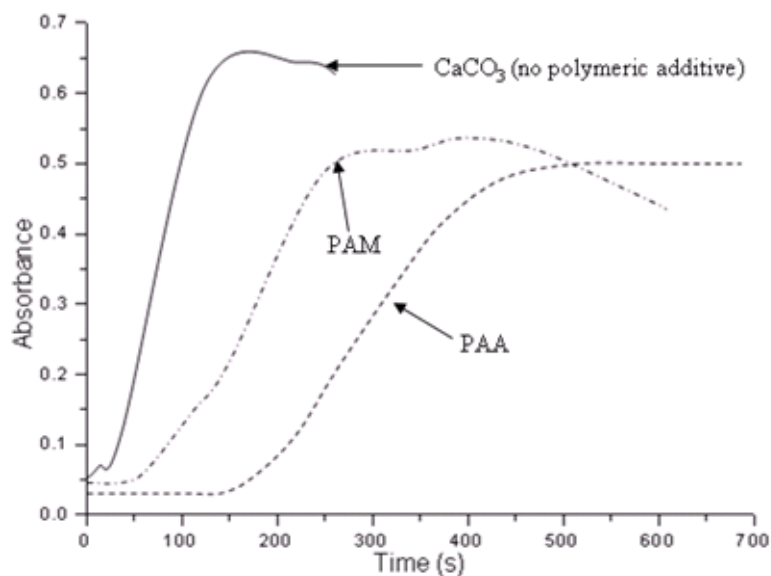
Fig. 4.1: Rate of CaCO₃ crystallization in the presence of PAA and PAM.

The functional group on the polyacrylamide polymer does interact with the metal ions but to a much lesser extent (less effect on super saturation) when compared to the functional group on PAA, hence a shorter induction time was observed. The solution absorbance increased with time as crystal growth occurred with more crystals being formed. The absorbance reached a plateau, signaling the completion of the inorganic reactants and the particles formed were colloidally stable. However, particle growth continues via Ostwald ripening, resulting in unstable colloids that tend to sediment, and resulting in a decrease in the absorbance of the solution. The driving force behind Ostwald ripening is the decrease in the surface energy of the colloids. The control reaction showed an immediate decrease in the absorbance soon after the plateau compared to the case of PAM and PAA, indicating that the polymeric additives stabilized the colloids with PAA giving more stability to crystals. Similar experiments were not done for the modified polymers due to the particulate nature of cellulose and the high flocculation of modified starch. The modified cellulose does not form a stable suspension and tends to drop to the bottom of the cuvette, distorting the UV signal. On the other hand, modified starch flocculates the CaCO₃ crystals resulting in large particles that are colloidally unstable and thus the UV signal is distorted as well. However, the effect of the grafted polymers (PAA and PAM) on CaCO₃ crystallization was expected to be similar to the one effected by the homopolymers since the functionality polymers that controls the crystallization

process is the same. It was expected that PAA grafted polysaccharides will give longer inhibition periods than PAM grafted polysaccharides. However, this is subject to the solution super saturation and the concentration of the polymeric additive. A combination of high solution super saturation and low concentration of polymeric additive (or low metal ion binding efficiency polymeric additive) may lead to masking of the induction period.

Fig 4.2 shows the SEM images of $CaCO_3$ crystals synthesized in the absence of polymeric additive and in the presence of PAM and PAA at 25 ^{o}C and 80 ^{o}C. The calcium carbonate crystals synthesized in the absence of any polymeric additive (blank) at 25 ^{o}C were rhombohedral in shape Fig. 4.2(A1) and were mostly calcite, as seen in the XRD spectrum in Fig. 4.3 (labeled blank).
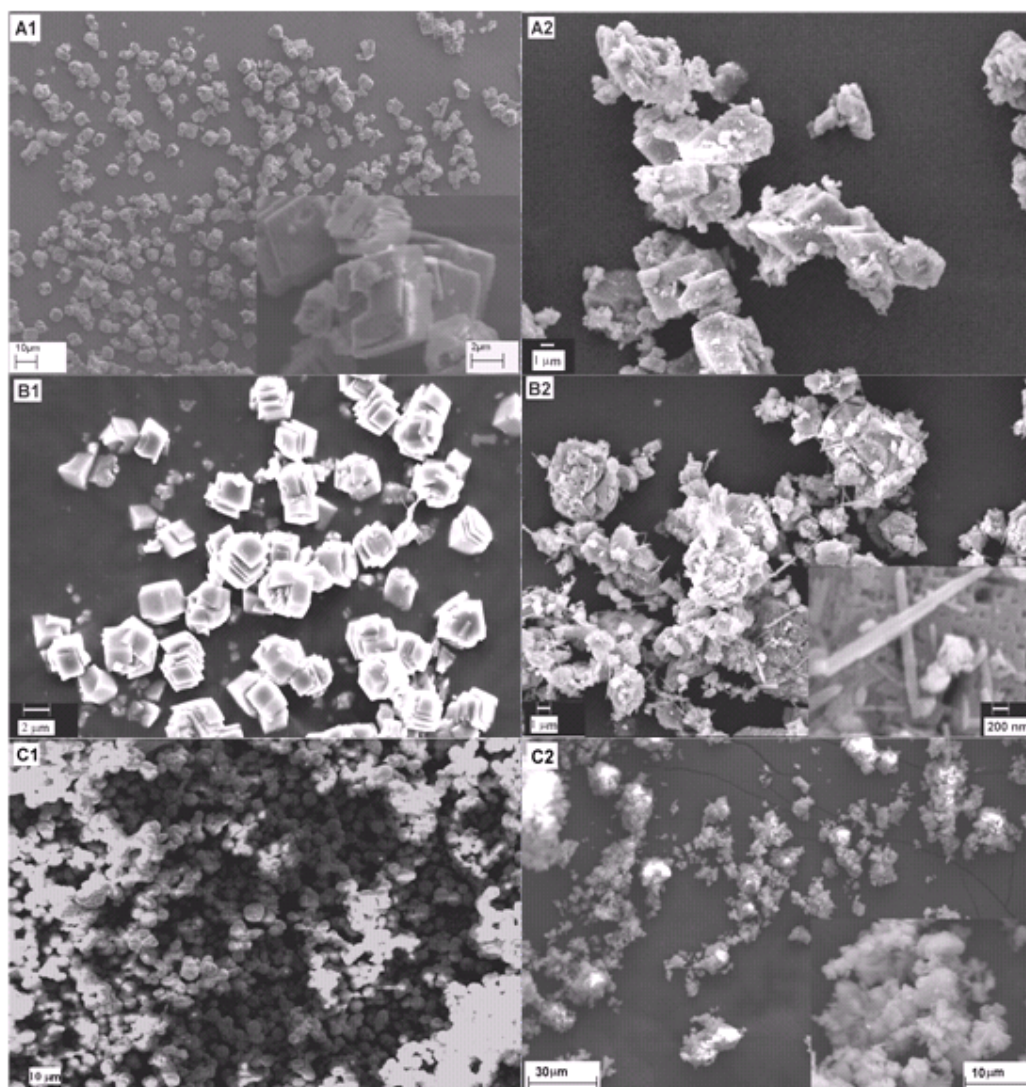
Fig. 4.2: SEM images of (A) CaCO$_3$ crystals, (B) PAM modified CaCO$_3$ and (C) PAA modified CaCO$_3$ crystals. (polymeric additive concentration 0.32g/L, pH 8.5.)

When the reaction temperature of the blank reaction was raised to 80 ^{o}C the CaCO$_3$ crystal were also calcite (XRD spectrum not shown) but with a less defined rhombohedral shape and with secondary crystals on the surface (Fig. 4.2(A2)).

The crystal morphology obtained in the presence of PAM at 25 ^{o}C was a mixture of flat rhombohedra which appeared to be stacked together and single cubical crystals (Fig. 4.2(B1)). The XRD spectrum of CaCO$_3$ crystals synthesized in the presence of PAM, Fig. 4.3 (PAM, 25 ^{o}C), shows that only calcite was formed. Earlier studies suggested that functional groups such as C=O and >N-H effect the nucleation of CaCO$_3$ crystals through their interactions with Ca^{2+} ions.[3,4] However, it has been found that the addition of polymeric additives has a stabilization effect on the amorphous calcium carbonate (ACC) that is initially formed.[2,5-7] The ACC is then transformed into thermodynamically more stable polymorphs through a re-crystallization process that takes place in the presence of moisture.[5] The formation of flat crystals (Fig. 4.2(B1)) occurred due to the influence of PAM on crystal growth through selective adsorption of the PAM on the crystal faces of CaCO$_3$, forcing the crystals to grow in two dimension. The platelets aggregated to form mesocrystals to reduce their surface energy.
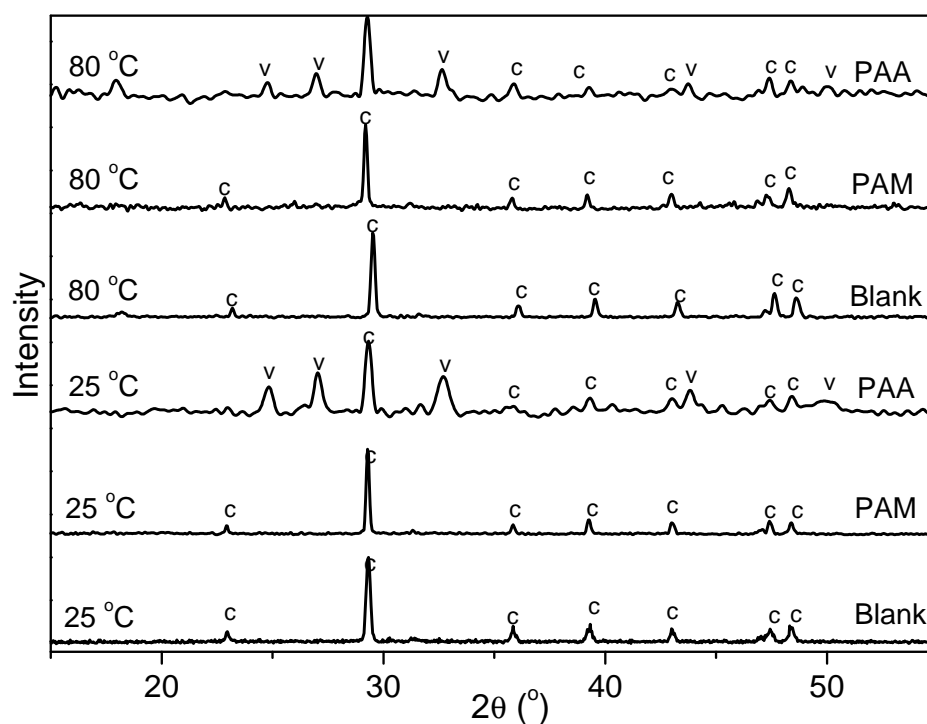
Fig. 4.3: XRD spectra of CaCO$_3$ crystals obtained in the absence and presence of polymeric additives (c and v represent calcite and vaterite polymorphs, respectively.)

The single cubes observed in Fig. 4.2(B1) therefore grew under no influence of the polymeric additive, and thus followed the non-classical crystal growth mechanism.[8] When the terpolymer

poly(acrylamide-co-2-acrylamido-2-methyl-1-propane sodium sulfonate-co-N-vinyl pyrrolidone) was used as crystal growth modifier by Pai et al.,[4] stacks of plate-like crystals were also formed. When crystallization was done at 80 ^oC in the presence of PAM the crystal shapes were a mixture of rhombohedra and nano-rods (Fig. 4.2(B2)) and only calcite crystals were formed, as shown in Fig. 4.3 (PAM, 80 ^oC).

It was found that a change in the crystal morphology does not necessarily mean that the polymorphism changes as well.[9] Nanorods have been previously obtained when polyvinyl alcohol (PVA)[10] and PAM[11] were used as crystal growth modifiers in $CaCO_3$ crystallization. The formation of the $CaCO_3$ nano-rods in the presence of PVA as crystal growth modifier occurred through vaterite to aragonite phase transformation over several days.[10] In this study, the size and number of the rod-like crystals is small compared to the rhombohedra cubes co-existing with them. The surface of the rhombohedra crystals have concaves which may be due to dissolution of $CaCO_3$ which then re-crystallizes to form secondary crystals[12] (nano-rods in this case) on the surface of the crystals, as observed in Fig. 4.2(B2). This phenomenon has been reported by Wei et al.,[13] who suggested that the less thermodynamically stable polymorphs can dissolve from the surface of the crystals, creating concaves. Dissolution of $CaCO_3$ from the surface may then be followed by re-crystallization, leading to the formation of a more thermodynamic stable polymorph.[10] Secondary crystallization can also result in a mixture of crystal morphologies and generally smaller crystals compared to the primary crystals observed.[14]

The crystals obtained in the presence of PAA at 25 ^oC were monodispersed spherical crystals (Fig. 4.2(C1)). The presence of PAA stabilizes the ACC, resulting in the formation of the ACC-PAA gel that will then crystallize spherulitically into stable crystalline polymorphs.[5] The homogeneous size and morphology of $CaCO_3$ crystals shown in Fig. 2(A1) was attributed to better control of nucleation and crystal growth by PAA. It has been suggested that monodispersed crystals are favored if the inorganic reactants (Ca^{2+} and CO_3^{2-}) are consumed during the early stage of reaction.[14,15] This will allow the crystals to grow via Oswald ripening[15] and thus no secondary nucleation will take place during crystal growth. The overall effect is elimination of secondary crystal formation and ultimately monodispersed crystals are formed. The polymorphs formed were calcite and vaterite, as can be seen in the XRD spectrum in Fig. 4.3 (PAA, 25 ^oC). The presence of vaterite in $CaCO_3$ crystals synthesized in the presence of PAA is due to the strong interaction of the carboxylic acid group with the vaterite surfaces.[12] The adsorption of negatively charged polymers on vaterite surfaces is aided by Ca^{2+} ions that are present on the (100), (101) and (110) planes of vaterite.[16] Thus, the phase transformation of vaterite to form a more thermodynamically stable polymorph is suppressed by the adsorbed PAA.[12] Morphology and polymorph transformation was

observed when the $CaCO_3$ crystals synthesized in the presence of PAA at 25 ^{o}C were stirred for six days. The spherical particles obtained after 24 hrs of reaction were fused together forming 3D net works (Fig. D2(A), Appendix D). The transformation can be attributed to a further decrease in the surface energy by the system through the formation of stable structures and one polymorph (since calcite only was observed). The crystal morphology obtained at 80 ^{o}C for PAA mediated crystallization was a mixture of large spherical-like crystals and smaller regular-shaped crystals that were on the surface of the large spherical crystals, as shown in Fig. 4.2(C2). A deviation in crystal morphology may be due to the shift in the kinetic/thermodynamic balance and not necessarily due to the binding of the polymer on the crystal face as postulated by Dickinson *et al.*[17] The stabilization effect of the –COOH group was also effective at higher temperature as vaterite crystals, present at 25 ^{o}C, were also present at 80 ^{o}C, as shown in Fig. 4.3 (PAA, 80 ^{o}C). Vaterite is a meta-stable phase of calcium carbonate and is the less thermodynamically stable polymorph, with a higher solubility than calcite and aragonite.[18] Generally, once vaterite is exposed to water it converts to either calcite at low temperature or aragonite at high temperature. However, the dissolution of vaterite may also depend on the extent of stabilization effected by the polymeric additive.[12] Pan *et al.*[19] obtained a mixture of calcite and aragonite crystals when PAA was used as crystal growth modifier in the temperature range 75–95 ^{o}C. Moreover, they showed that the fraction of aragonite gradually increased with increasing temperature, indicating that aragonite is favored at high temperature.[19] Some factors known to influence polymorph selectivity include the $[COOH]/[Ca^{2+}]$ ratio, which affects phase transformation of the polymorphs, and an increase in the ratio resulted in no transformation of vaterite to calcite at low temperature.[12] The $[Ca^{2+}]$ and $[CO_3^{2-}]$ were also found to influence polymorph selectivity, with an excess of $[Ca^{2+}]$ favoring the formation of vaterite.[20] Since vaterite is present at 80 ^{o}C, the stabilization of PAA was effective in suppressing the formation of aragonite which is favored at high temperatures. Thus, the existence of vaterite at high temperature is likely to be due to a combination of both thermodynamic and kinetic effects.

4.3.2: Crystallization of $CaCO_3$ in the presence of cellulose and cellulose graft copolymerized with MA and NIPAM

When cellulose was used as a crystal growth modifier in $CaCO_3$ crystallization at 25 ^{o}C, the single crystals formed were rhombohedral in shape and were observed on the surface of the cellulose fibers (Fig. 4.4). XRD analysis showed that the crystals were calcite, as shown in Fig. 4.9A (ii). Results for the crystallization of calcium carbonate showed that the cellulose grafted with PMA-co-NIPAM can nucleate $CaCO_3$ crystal formation much better than ungrafted cellulose can, as shown

in Fig. 4.4B. Crystals formed in the presence of cellulose were rhombohedral single crystals, whereas platelet like crystals that stacked together and cubical single crystals were formed in the presence of MA and NIPAM graft copolymerized on cellulose.
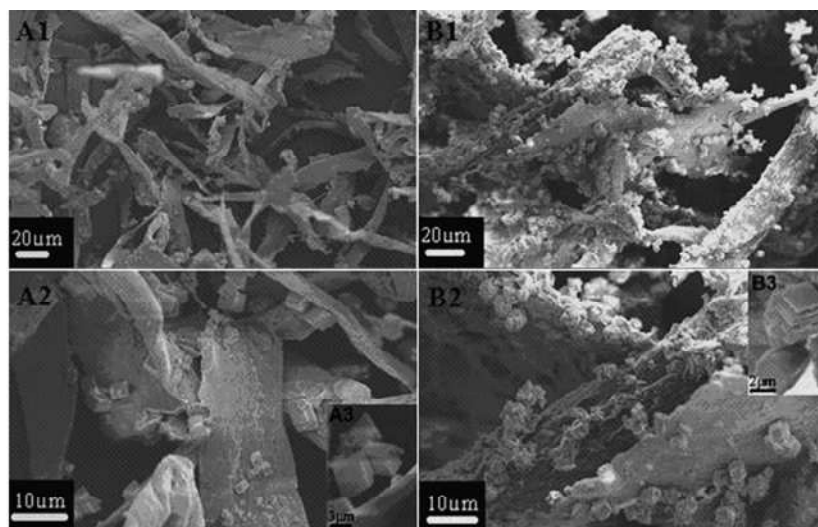
Crystals were synthesized at 25 °C, $[Ca^{2+}] = [CO_3^{2-}] = 0.025$ M, pH 8.5 and [polymeric additives] =0.77 g/L and A2 and B2 are enlargements whereas inserts A3 and B3 in A2 and B2 respectively are further enlargements

Fig. 4.4: SEM images of CaCO$_3$ crystals obtained in the presence of (A) cellulose at different magnifications (A1-A3).and (B) NIPAM & MA graft copolymerized on CE (G2).

Grafting can also enhance the adsorption of CaCO$_3$ crystals on the surface of the fiber as many particles were adsorbed on the surface of the grafted fibers. However, there was no observed effect of % G on the morphology of crystals of CaCO$_3$. This could be because the % G values of the grafted celluloses were close to one another (see Table 3.1). Calcium carbonate exists as three polymorphs: vaterite, aragonite and calcite, in order of their thermodynamic stability and phase transformation possible. Fig 4.5 shows that the calcite polymorph was obtained for crystals synthesized in the presence of cellulose and cellulose graft copolymerized with NIPAM and MA. The peaks at 876 cm^{-1} and 711 cm^{-1} (Fig. 4.5) are due the calcite.[21] The absence of the aragonite and vaterite polymorphs' characteristic peaks at 1057 and 1082 cm^{-1},[22] and 745 cm^{-1},[21] respectively, means that the synthesized CaCO$_3$ consisted of mainly the calcite polymorph. These characteristic peaks are due to the C–O (stretch) of the different polymorphs.
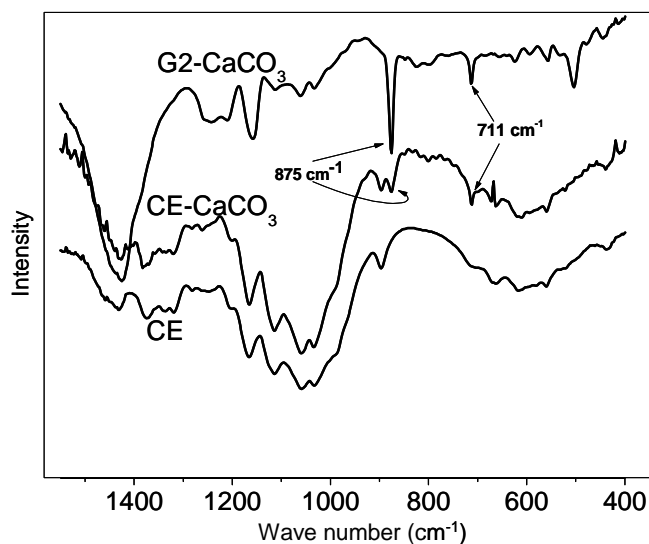
Fig. 4.5: FT-IR spectra of α-CE, α-CE-CaCO$_3$ and the graft copolymer G2-CaCO$_3$, showing the peaks due to the calcite.

4.3.3: Crystallization in the presence of PAA and PAM grafted cellulose

The CaCO$_3$ crystals synthesized in the presence of PAM grafted cellulose at 25 ^{o}C were rhombohedral platelets that aggregated to form 'spherical' particles as shown in Fig. 4.6(A1 & A2) and from the XRD spectrum Fig. 4.9A(iii), only the calcite polymorph was present. The CaCO$_3$ crystals formed in the presence of PAA grafted cellulose at 25 ^{o}C were spherical in shape (Fig. 4.6(B1 & B2)). However, the XRD spectrum CaCO$_3$ crystals synthesized in the presence of PAA grafted cellulose (Fig. 4.9A (iv)) shows that a mixture of calcite and vaterite were present. PAM and PAA grafted cellulose had more CaCO$_3$ crystals on the surface of the fiber compared to ungrafted cellulose and cellulose graft copolymerized with NIPAM and MA (comparison of Fig. 4.4A to Fig. 4.4B and Fig. 4.6).

The effect of the concentration of the reactants (Ca^{+2} and CO$_3^{2-}$) on the crystal morphology and polymorphism was also studied using PAA grafted cellulose, at 25 ^{o}C. When the concentration of Ca^{+2} was reduced from 0.025 M to 0.0125 M the crystal morphology was still the spherical type (Fig. 6.7 A) and, calcite crystals and vaterite crystals were formed, as was observed for the [Ca^{+2}] of 0.025 M. However, fewer crystals were observed on the surface of the fiber (comparison of Fig. 4.6 B and Fig. 4.7A).
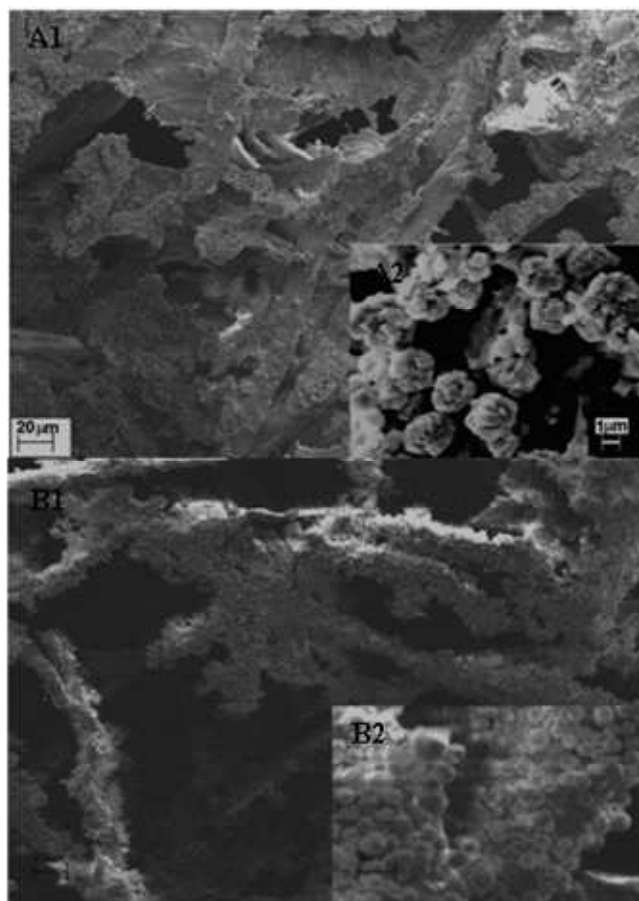
Crystals were synthesized at 25 °C, $[Ca^{2+}] = [CO_3^{2-}] = 0.025$ M, pH 8.5 and [polymeric additives] = 0.77 g/L

Fig. 4.6: SEM images of CaCO$_3$ crystals obtained in the presence of (A) PAM grafted cellulose (HM 29$^{3.6}$) and (B) PAA grafted cellulose (HM31$^{3.6}$).

As the concentration of $[Ca^{+2}]$ was increased to 0.05 M the crystal morphology changed to rhombohedra and more crystals were formed (Fig. 4.7 B(1 & 2)). The polymorph present was mostly calcite, with traces of vaterite. The evolution of the morphology in the manner described was expected as the effect of polymer on crystal nucleation and growth is overshadowed by the high concentration of reactants used. The net effect is a reduction in the interactions between the polymer and growing nuclei. Although nucleation may still be induced by the polymer, crystal growth will be independent of the polymer-growing nuclei interactions but dependent on the concentration of the reactants.
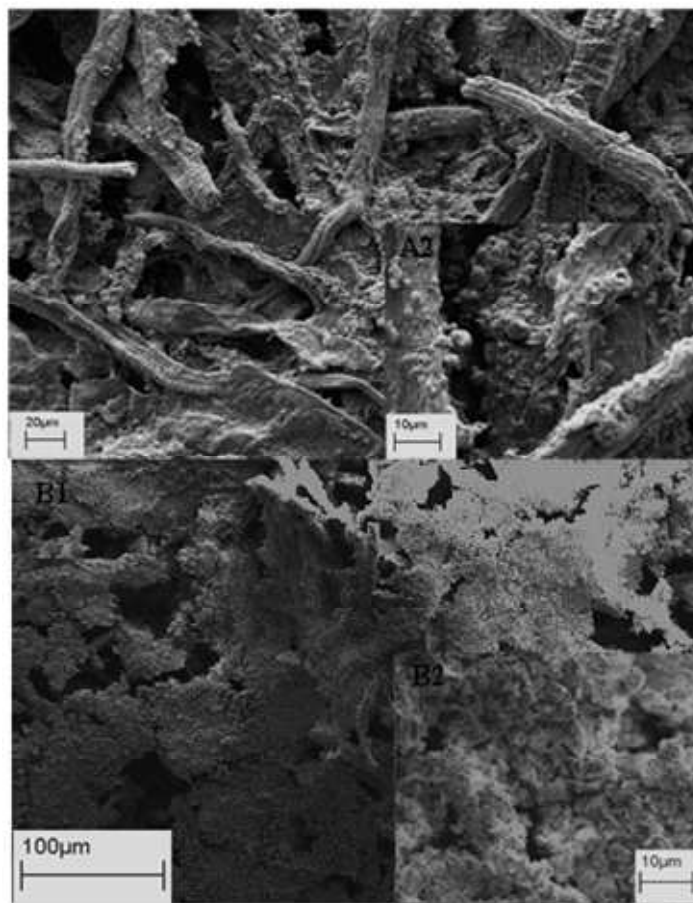
Crystals were synthesized at 25 °C, $[Ca^{2+}]$ = [CO_3^{2-}] = 0.025 M, pH 8.5 and [polymeric additives] =0.77 g/L

Fig. 4.7: SEM images of CaCO₃ crystals obtained in the presence of PAA grafted α-cellulose (HM 31³·⁶): (A) [Ca⁺²] = 0.0125 M and B) [Ca⁺²] = 0.0500 M.

When the reaction temperature was increased to 80 °C there was a significant change in crystal morphology for PAM grafted cellulose (polymeric additive) but the polymorph was still calcite. The shape of the crystals on the surface of the fiber was less defined (Fig. 4.8(A1)) than the crystals obtained at 25 °C (Fig. 4.6A1). However, Fig. 4.8(A2) shows that large cubical crystals with secondary crystallites were not located on the fiber surface. In the case of PAA grafted cellulose, a different morphology as well as polymorphs were found at 80 °C compared to those found at 25 °C. Fig. 4.8(B1) shows irregular shaped crystals on the surface of the fiber and Fig. 4.8(B2) shows the needle shaped crystals that were not on the surface of the fiber. The crystals on the surface of the fiber were smaller than those not on the fiber surface. The polymorphs formed were now calcite and aragonite. Very few crystals were cubical and the cubical crystals may have formed during the beginning of the reaction under no influence of the crystal growth modifier.

$[Ca^{2+}] = [CO_3^{2-}] = 0.025$ M, pH 8.5 and [polymeric additives] $=0.77$ g/L
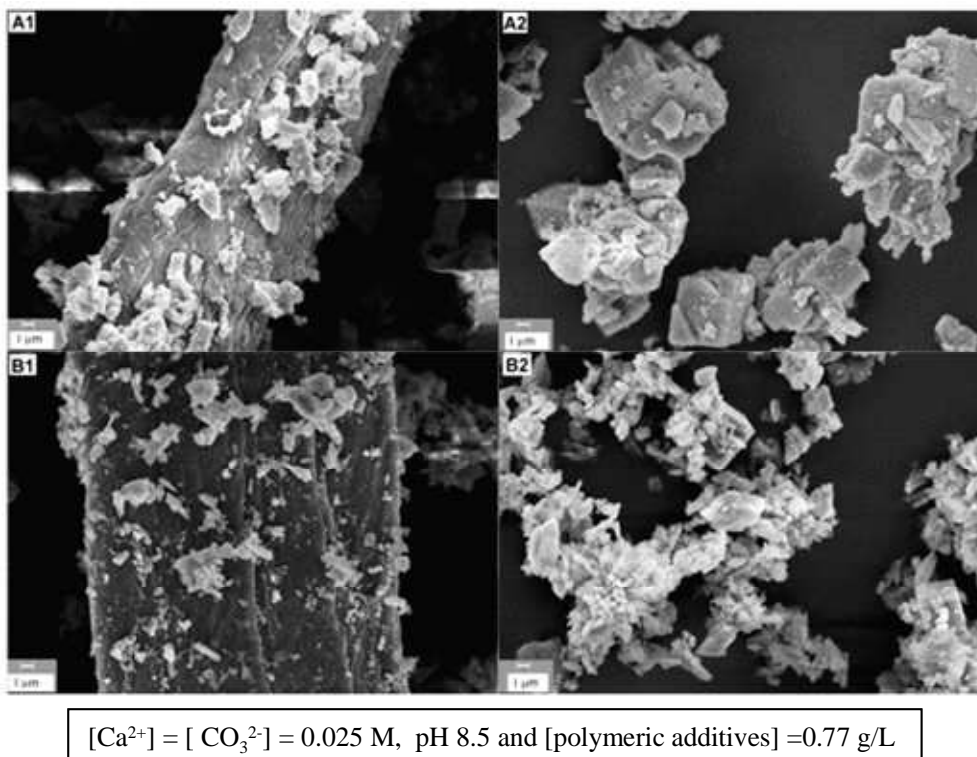
Fig. 4.8: SEM images of CaCO$_3$ crystals obtained in the presence of (A) PAM grafted cellulose (HM 29$^{3.6}$) and B) PAA grafted cellulose (HM 31$^{3.6}$) at 80 ^{o}C. A2 and B2 show CaCO$_3$ crystals that were not attached to the fiber surface

The grafted cellulosic materials showed better nucleation/adsorption of CaCO$_3$ crystals on the surface of the fiber at 25 ^{o}C than at 80 ^{o}C. The modified fiber surface played a stabilization role for both the nucleation and crystal growth of the CaCO$_3$. Stabilization is attributed to the interactions between the polymer functional groups (–NH$_2$ and –COOH) with the growing nanocrystals via an adsorption mechanism. The fact that the two different functional groups gave different morphologies as well as polymorphs shows that the type of functional groups on the polymer can critically affect crystal nucleation and growth.

The –COOH and –CONH$_2$ groups have different influences on the stability of the ACC as well as the nucleation of crystalline CaCO$_3$ and, as such, the resulting crystal morphologies are likely to be different. The initial stage of crystallization is the formation of ACC on the surface of the fiber stabilized by the grafted polymer chains. The transformation of ACC to crystalline polymorphs will then occur, to form different morphologies as directed by the grafted polymers via growth inhibition of some crystal faces. It has been shown that the –COOH group can also act as an inhibitor of crystal growth[9,23] and hence fewer crystals should have been observed here.
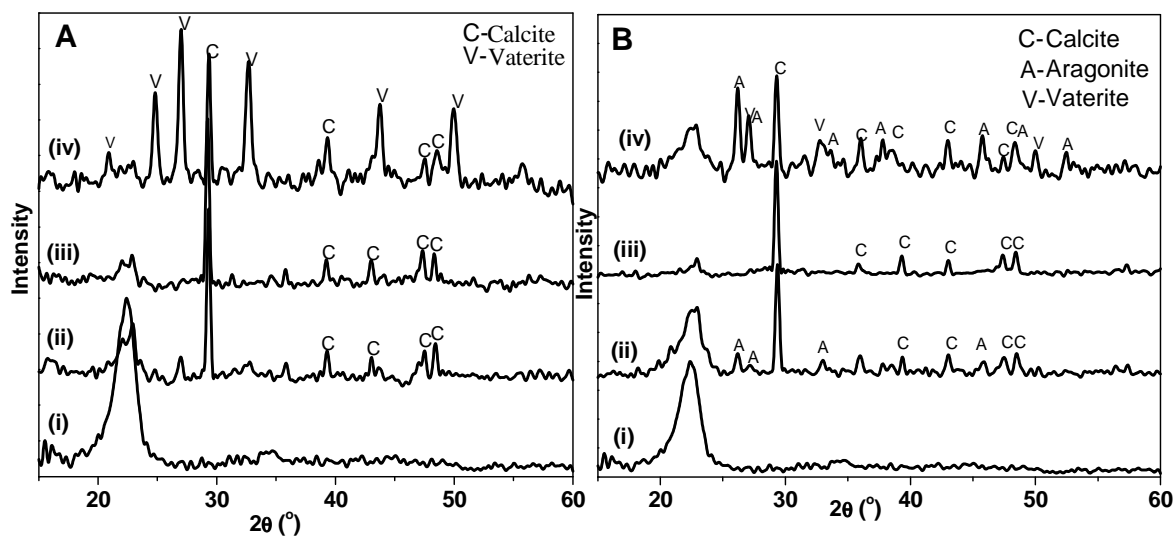
Fig. 4.9: XRD spectra of α-cellulose (i), and CaCO₃ crystals obtained in the presence of (ii) α-CE, (iii) PAM grafted cellulose (HM 29³·⁶) and (iv) PAA grafted cellulose (HM 31³·⁶) at A) 25 °C and B) 80 °C. ([Ca²⁺] = [CO₃²⁻], pH 8.5, [polymeric additives] = 0.77 g/L.)

The extent of inhibition is dependent on the number of –COOH groups on the fiber that can effectively cause inhibition relative to the concentrations of the inorganic reactants which determine the maximum amount of $CaCO_3$ that can be formed.[12] The presence of vaterite crystals shows that the PAA grafted cellulose surface stabilized the less thermodynamically stable $CaCO_3$ polymorph. Also, the PAA grafted cellulose surface may have better $CaCO_3$ adsorption properties than the PAM grafted cellulose surface. Hence more crystals were seen on the PAA grafted cellulose surface. In PAM grafted cellulose the fact that the flat rhombohedral crystals were aggregating to form spherical particles means that the interaction between the PAM grafted cellulose fiber and the $CaCO_3$ crystals was less favorable in comparison to the PAA grafted cellulose fiber. However, the 'spherically' aggregated rhombohedral $CaCO_3$ crystals are seen as being anchored on the surface of the fiber with better surface coverage compared to $CaCO_3$ formed in the presence of unmodified cellulose. Thus, primary crystal aggregation was favored on the surface of the already formed $CaCO_3$ crystals rather than on the surface of the fiber. The –$CONH_2$ and –COOH groups on the surface of the fiber influence the nucleation and the crystal growth, possibly via adsorption onto the surface of the growing crystal, thereby suppressing further growth. The amide and carboxylic acid groups were found to effect morphological variations in crystallization of $CaCO_3$[24] When crystallization of $CaCO_3$ was done at 80 °C in the presence of modified cellulose fiber most of the crystals were not on the surface of the fiber as previously found at 25 °C. It is highly possible that the grafted chains were being stripped off the surface of the fiber by partial solubilization of the

grafted cellulose chains at high temperature and under basic the conditions used. Ultimately the nucleation and growth will occur to a lesser extent on the surface of the fiber but more in solution. Furthermore, at high temperatures (80 ^{o}C), the polymer–CaCO$_3$ nuclei interactions are likely to be reduced with desorption of the polymer chains from the surface of the growing CaCO$_3$ crystal being more prevalent. This resulted in CaCO$_3$ crystal morphologies obtained at 80 ^{o}C being different from those found at 25 ^{o}C.

The thermal degradation of the CaCO$_3$ crystals synthesized in the presence of PAM and PAA modified cellulose are shown in Fig 4.10. The TGA curves (Fig. 4.10) show two stages of degradation. The initial weight loss around 50 ^{o}C is due to water. The first degradation step is due to the grafted polysaccharide and the second degradation step is due to calcium carbonate. Since the mass of the polymeric additives was similar, the amount of CaCO$_3$ formed is found to be different. The polysaccharide content is lower in PAA grafted cellulose, which means more crystals were formed in the PAA grafted cellulose system compared to the PAM grafted cellulose and cellulose systems. SEM showed more crystals to be on the surface of PAA grafted cellulose than on surface of PAM grafted cellulose and cellulose. Since the morphologies of CaCO$_3$ crystals synthesized in the presence of PAM, PAM grafted cellulose, PAA and PAA grafted cellulose were different; it shows that the nature of the crystal growth modifier has a significant effect on the nucleation and growth of CaCO$_3$.
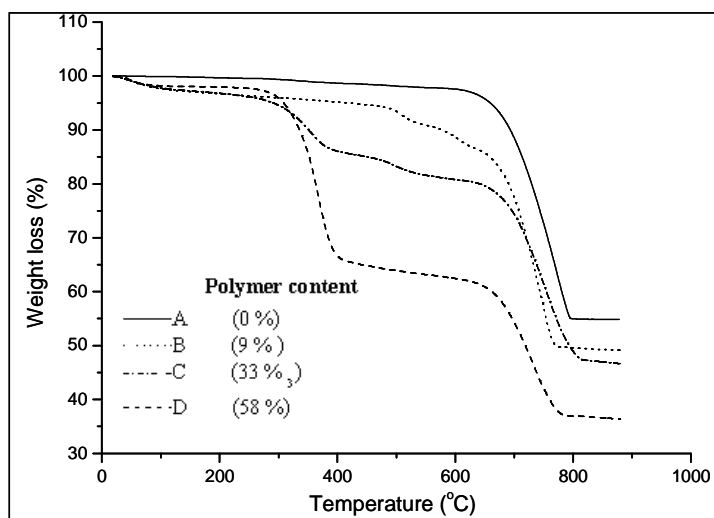
Fig. 4.10: TGA curves of (A) CaCO$_3$ and CaCO$_3$ synthesized in the presence of (B) acrylic acid grafted cellulose (HM 31$^{3.6}$), (C) acrylamide grafted cellulose (HM 29$^{3.6}$) and (D) cellulose. ([Ca^{2+}] = [CO$_3$$^{2-}$] = 0.025 M, pH = 8.5 and [polymeric additive] = 0.77g/L.)

4.3.4: Crystallization in the presence of starch and PAA modified starch

The crystal morphologies of $CaCO_3$ crystals synthesized in the presence of starch and PAA grafted starch are shown in Fig 4.11. Calcium carbonate crystals synthesized at 25 ^{o}C in the presence of unmodified starch were platelets that were stacked together forming cube-like particles with uneven edges (Fig. 4.11A). Only calcite crystals were detected by XRD (Fig. 4.12A(i)). At a crystallization temperature of 80 ^{o}C only calcite crystals were present (image not shown) and the crystal morphology was rhombohedral, with smaller crystallites of irregular shape, as shown in Fig. 4.11B.

(A) & (B) starch at 25 ^{o}C and 80 ^{o}C, respectively with $[Ca^{2+}]$ = $[CO_3^{2-}]$ = 0.025 M; (C) & (D) PAA grafted starch (HM 1$^{3.2}$) at 25 ^{o}C and 80 ^{o}C, respectively, with $[Ca^{2+}]$ = $[CaCO_3^{2-}]$ = 0.025 M; (E) & (D) PAA grafted starch (HM 1$^{3.2}$) with $[Ca^{2+}]$ = $[CaCO_3^{2-}]$ = 0.025 M and 0.050 M, respectively. (pH 8.5 and [polymeric additives] =0.77 g/L .)

Fig. 4.11: SEM images of $CaCO_3$ crystals obtained in the presence of starch and PAA grafted starch.

However, CaCO$_3$ crystals synthesized in the presence of the PAA grafted starch under the same conditions were spherical in shape (Fig. 4.11C) and calcite with traces of vaterite crystals were obtained, as shown in Fig. 4.12A(ii). It should be mentioned that the mechanism of nucleation and crystal growth in PAA and PAA grafted polysaccharides was likely to be the same since spherical morphologies were observed in all three systems at 25 ^{o}C and [Ca^{2+}] 0.025 M. Thus the morphology observed was attributed to the effect of the PAA polymer chains on stabilization, nucleation and crystal growth of CaCO$_3$.

When the temperature of the reaction was increased to 80 ^{o}C needle-shaped crystals were obtained and the polymorphs present were calcite and aragonite (Fig. 4.12A(iii)). The evolutions of CaCO$_3$ polymorphs as well as the crystal morphologies in PAA grafted starch were similar to that of PAA grafted cellulose at both 25 ^{o}C and 80 ^{o}C. Generally, crystal morphologies obtained at 80 ^{o}C in the absence or presence of a polymeric additives/crystal growth modifiers were less defined and secondary crystallites were a common characteristic. It is possible that the irregularity in crystal shapes may be due to dissolution of the preformed crystals, which then re-crystallized as secondary crystallites. However, for PAA grafted polysaccharides, the crystal morphologies were mainly needle-shaped or flake-like and of irregular shapes, and these crystals are likely to have been formed from the beginning of the reactions rather than through a dissolution and re-crystallization process.

The effect of the Ca^{2+} concentration (1:1 molar ratio with CO$_3^{2-}$) was also studied for PAA grafted starch. It was found that spherical crystals were obtained when the [Ca^{2+}] was 0.0125M (Fig. 4.11E), and for [Ca^{2+}] 0.05 M the crystal morphology was a mixture of rhombohedral, irregular crystals and very small crystallites, as shown in Fig. 4.11F. The average sizes of CaCO$_3$ crystals were o from the SEM images. The average particle size obtained for [Ca^{2+}] 0.0125 M was estimated to be 2.9 μm and for [Ca^{2+}] 0.025M 3.5 μm. Low [Ca^{2+}] means that the polymeric additive concentration is high enough to control crystal growth through adsorption, hence smaller particles emerged. As the [Ca^{2+}] was increased to 0.05 M the majority of the crystals grew independent of the polymeric additive and the small crystallites observed could be due to termination of crystal growth by the polymeric additive. The XRD spectra of crystals (Fig. 4.12B(i) and (ii)) show that vaterite crystals coexisted with calcite crystals and, from the intensity ratios, more vaterite crystals were formed at [Ca^{2+}] 0.0125 M than at [Ca^{2+}] 0.025 M. When the [Ca^{2+}] was increased to 0.05 M no vaterite peaks were detected in the XRD spectrum (Fig. 4.13B(iii)). The existence of vaterite crystals is due to the stabilization effect of the polymeric additives and, as the concentration of the [Ca^{2+}] increases, the presence of the polymeric additive becomes insufficient or inefficient to stabilize less thermodynamically stable polymorphs. Although the small crystallites may contain

vaterite the amount of this polymorph is likely to be very low compared to the calcite and hence below the detection limit of the instrument.

Fig. 4.12: (A) XRD spectra of $CaCO_3$ crystals obtained in the presence of: (i) starch at 25 °C, (ii) PAA grafted starch (HM $1^{3.2}$) at 25 °C, (iii) PAA grafted starch (HM $1^{3.2}$) at 80 °C and (B) XRD spectra of $CaCO_3$ crystals obtained in the presence of PAA grafted starch (HM $1^{3.2}$) at 25 °C and $[Ca^{2+}]$ (i) 0.0125 M, (ii) 0.025 M and (iii) 0.05 M. ($[Ca^{2+}]$ = $[CO_3^{2-}]$, pH 8.5 and [polymeric additives] = 0.77 g/L.)

Fig. 4.13, shows that increasing the $[Ca^{2+}]$ and $[CO_3^{2-}]$ in the system resulted in more crystals being formed, as evidenced by the decreasing grafted starch content. Thus the $CaCO_3$ to polymeric additive ratio was expected to increase when increasing the concentration of $CaCO_3$ precursors. A comparison between the grafted and ungrafted materials showed that there was less ungrafted starch than grafted starch found in the $CaCO_3$ crystals synthesized in the respective systems. This is explained by the fact that the carboxylate functional group interacts strongly with the growing nuclei so that the incorporation of the polysaccharide into the $CaCO_3$ crystals is highly probably. Therefore, the rinsing of the $CaCO_3$ crystals after crystallization resulted in less retention of the ungrafted starch (it was rinsed off) than PAA grafted starch (bonded).

When the $CaCO_3$ crystals crystallized at 25 °C in the presence of PAA and PAA grafted starch were left stirring for 6 days the crystals aggregated together (Fig. D2(B), Appendix D) and the polymorph that evolved was calcite. Spherical crystals were obtained when PAA grafted partially dissolved starch was used as crystal growth modifier as (Fig. D3, Appendix D). Large swollen starch granules were also observed.

Fig. 4.13: TGA curves of CaCO$_3$ synthesized in the presence of starch. (A) [Ca^{2+}] = 0.025 M and PAA grafted starch (HM 1$^{3.2}$); (B) [Ca^{2+}] = 0.0500 M; (C) [Ca^{2+}] = 0.0250 M and (D) [Ca^{2+}] = 0.0125 M at 25 ^{o}C. The polymer content in composites B, C, D was 11, 8 and 6% respectively. ([Ca^{2+}] = [CO$_3^{2-}$], pH = 8.5 and [polymeric additive] = 0.77 g/L.)

4.4: Implications of results of this study in the paper industry

In situ CaCO$_3$ crystallization in the presence of modified fiber during paper production could lead to improved filler retention. The crystallized CaCO$_3$ was found to be nucleated on the surface of the fiber and, thus, filler loss during drainage can be reduced. Also the fiber-filler bond could be improved; however, the fiber-fiber bonding strength is likely to be reduced if the surface of the fiber is completely covered by the filler. Hence there is need to balance all the factors that affect paper strength. From Fig. 4.10 it can be approximated that the filler content in PAM and PAA grafted cellulose was 66 and 78%, respectively. Paper currently has 20% filler hence there is room to reduce fiber surface coverage in these experiments. Reduction in surface coverage can be achieved by reducing the nucleation points (i.e. % G or the concentration of modified fiber), which would also pave the way for more fiber-fiber bonding. Thus the challenge will be to optimize the filler content in order to promote the fiber-fiber bonding whilst more filler is incorporated into the paper. This may introduce another novel way of adding filler to paper, which involves performing *in situ* CaCO$_3$ crystallization in the presence of modified fiber. There are two alternatives for *in situ* CaCO$_3$ crystallization, it can be done in the presence of i) a blend of modified fiber and unmodified fiber or ii) modified fiber that can later be blended with the rest of the pulp fiber to give the appropriate filler loading in paper.

The use of soluble modified polysaccharides such as starch in $CaCO_3$ crystallization could be another way of improving filler retention. The size of $CaCO_3$ filler can be optimized to give the best retention and the filler surface can be modified to promote filler retention. The crystallized $CaCO_3$ surface studies and the possible influence in filler retention are discussed in Chapter 5.

4.5: Conclusions

The crystal morphology and polymorph selectivity can be controlled by using different polymeric additives, the temperature and concentration of reactants. PAA and PAM grafted cellulose gave different types of morphologies but the dominant polymorph was the most thermodynamically stable, namely calcite, whereas PAA and PAM grafted polysaccharides gave similar polymorphs, namely calcite and traces of vaterite, at 25 ^{o}C. However, for crystallization reactions done at 80 ^{o}C calcite and aragonite were the dominant polymorphs obtained in PAA grafted polysaccharides reactions, whereas calcite and vaterite were still the polymorphs present when PAA was used. The fact that there were more crystals on the surface of the modified fiber in crystallization reactions done at 25 ^{o}C means that the grafted polymer effectively played a role in both nucleation and stabilization of the crystal nuclei. Crystallization of $CaCO_3$ in the presence of modified fibers can be applied in the paper industry in order to improve fiber-filler bonding, which may allow more filler to be incorporated in paper. However, the fiber surface coverage should be optimized to allow fiber-fiber bonding required for maintaining the strength of paper.

4.6: References

(1)   Guo, J., Stevertson S. J. *Industrial and Engineering Chemistry Research* **2003**, *42*, 3480-3486.

(2)   Wang, T., Antonietti M., Zhao X., Colfen H. *Chemistry - A European Journal* **2006**, *12*, 5722-5730.

(3)   Manoli, F., Koutsopoulos S., Dalas E. *Journal of Crystal Growth* **1997**, *182*, 116-124.

(4)   Pai, R. K., Hild S., Ziegler A., Marti O. *Langmuir* **2004**, 3123-3128.

(5)   Ulcinas, A., Butler M. F., Heppenstal-Butler M., Singleton S., Miles M. J. *Journal of Crystal Growth* **2007**, *307*, 378-385.

(6)   Han, T. Y., Aizenberg J. *Chemistry of Materials* **2008**, *20*, 1064-1068.

(7)   Gorna, K., Munoz-Espi R., Grohn F., Wegner G. *Macromolecular Bioscience* **2007**, *7*, 163-173.

(8)   Kulak, A. N., Iddon P., Li Y., Armes S. P., Colfen H., Paris O., Wilson R. M. Meldrum F. C. *Journal of the American Chemical Society* **2007**, *129*, 3729-3736.

(9)   Colfen, H., Qi L. *Chemistry - A European Journal* **2001**, *7*, 106-116.

(10)   Kim, I. W., Robertson R. E., Zand R. *Crystal Growth and Design* **2005**, *5*, 513-522.

(11)   Yu, Q., Ou H-D., Song R-Q., Xu A-W. *Journal of Crystal Growth* **2006**, *286*, 178-183.

(12)   Naka, K., Huang S-C ., Chuyo Y. *Langmuir* **2006**, *22*, 7760-7767.

(13)   Wei, H., Shen Q., Zhao Y., Zhou Y., Wang D., Xu D. *Journal of Crystal Growth* **2005**, *279*, 439-446.

(14)   Cheng, B., Lei M., Yu J., Zhao X. *Material Letters* **2004**, *58*, 1565-1570.

(15)   Yu, H., Lei M., Cheng B., Zhao X. *Journal of Solid State Chemistry* **2004**, *177*, 681-689.

(16)   Meng, Q., Chen D., Yue L., Fang J., Zhao H., Wang L. *Macromolecular Chemistry and Physics* **2007**, *208*, 474-484.

(17)   Dickinson, S. R., Henderson G. E., McGrath K. M. *Journal of Crystal Growth* **2002**, *244*, 369-378.

(18)   Qiao, L., Feng Q-L., Li Z. *Crystal Growth and Design* **2007**, *7*, 275-279.

(19)   Pan, Y., Zhao X., Sheng Y., Wang C., Deng Y., Ma X., Liu X., Wang Z. *Colloids and Surfaces, A: Physicochemical Engineering Aspects* **2007**, *297*, 198-202.

(20)   Chakraborty, D., Agarwal V. K., Bhatia S. K., Bellare J. *Industrial and Engineering Chemistry Research* **1994**, *33*, 2187-2197.

(21)   Liu, D., Yates M. Z. *Langmuir* **2006**, *22*, 5566-5569.

(22)   Wang, C., Zhao J., Zhao X., Bala H., Wang Z. *Powder Technology* **2006**, *163*, 134-138.

(23)   Wada, N., Kanamura K., Umegaki T. *Journal of Colloid and Interface Science* **2001**, *233*, 65-72.

(24)   Tamura, K., Tsuge H. *Chemical Engineering Science* **2006**, *61*, 5818-5826.

Chapter 5: Determination of surface properties and statistical evaluation

of crystallized $CaCO_3$

5.1: Introduction

In the crystallization experiments, described in Chapter 4, it was shown that the nature of the crystal growth modifier and temperature affect the morphology of crystallized $CaCO_3$. The surface properties of filler materials are also critical to matrix-filler bonding (e.g. fiber-filler bonding in filled paper).[1] The presence of polysaccharide polymer chains on the surface of the filler results in improved hydrogen bonding between the fiber and filler. This could result in improved fiber-filler bonding strength as well as filler retention. The filler surface charge is equally important to both filler retention as well as colloidal stability. According to thermodynamics, colloidal dispersions are inherently unstable and tend to coalesce in order to reduce their free energy.[2] The PCC used in papermaking is normally stabilized by dispersion agents such as the alkali metal and ammonium salts of polyacrylic acid.[3] Polysalt solutions of sodium polyacrylate of molecular weight in the range of 400000–500000 g/mol are also used to stabilize PCC for papermaking.[2] The additions of positive or negatively charged dispersing agents result in charge accumulation on the surface of the colloidal particles.[4] An electric double layer at the solid/liquid interface of particles is formed, which result in repulsive forces between particles (electrostatic forces) thereby inducing colloidal stability.[5] Thus, the crystal morphology, size and surface properties of $CaCO_3$ filler are important for the fiber-filler bonding as well as for filler retention.

5.1.1: Fluorescence

Fluorescence is a process that is distinct from emission of light due to high temperatures. When light is directed on a molecule that absorbs rather than transmits, one or more of the electrons of the molecule jumps to a higher energy level. These excited electronic states are unstable and eventually the electrons lose their excess energy and return to the lower energy states. This will result in the emission of a photon with a longer wavelength than the initially absorbed photon. The excess energy can then be dissipated as light (fluorescence) or by simply increasing atomic vibrations within the molecule. Thus, modification or labeling of materials with fluorescence molecules may help to determine mechanisms of reactions or processes.[6] The advantage of fluorescence measurements is that they can be carried out at very low concentrations or degrees of substitution of tagged materials.[7] In this part of the study, fluorescence was used to see whether the modified starch moieties were on the surface of crystallized $CaCO_3$. The $CaCO_3$ crystals when exposed to ultraviolet (UV) light should fluoresce if the fluorescence tagged modified starch molecules are on the surface of the $CaCO_3$ crystals.

5.1.2: Zeta potential

Zeta potential is defined as the electrical potential that exists at the shear plane of a particle that is a small distance from the surface. The ionic characteristics and dipolar attributes of colloidal particles, suspended in solution, result in particles that are electrically charged.

Fig. 5.1: Schematic representation of: A) electric double layer B) variation of the potential with distance from the electric double layer.

Once a particle carries a net charge on its surface the distribution of ions in the interfacial region is such that an increased concentration of counter ions (ions of charge opposite to that of the particles) is close to the surface.[8,9] Thus, an individual dispersed particle is surrounded by oppositely charged ions, called a Stern layer (Fig. 5.1A). Outside the fixed layer there are varying compositions of ions of opposite polarities. Thus, an electrical double layer is formed in the region of the particle-liquid interface.[9] This double layer may be considered to consist of two parts: an inner region, which includes ions bound relatively strongly to the surface, and an outer or diffuse region, in which the ion distribution is determined by a balance of electrostatic forces and random thermal motion. The potential in this region, therefore, decreases with the distance from the surface, until at a certain distance it becomes zero (Fig. 5.1B). Zeta potential can be calculated using the following Henry equation:[10,11]

$$\zeta = \frac{\mu_E 6\pi\pi}{\varepsilon f(ka)} \qquad\qquad 5.1$$
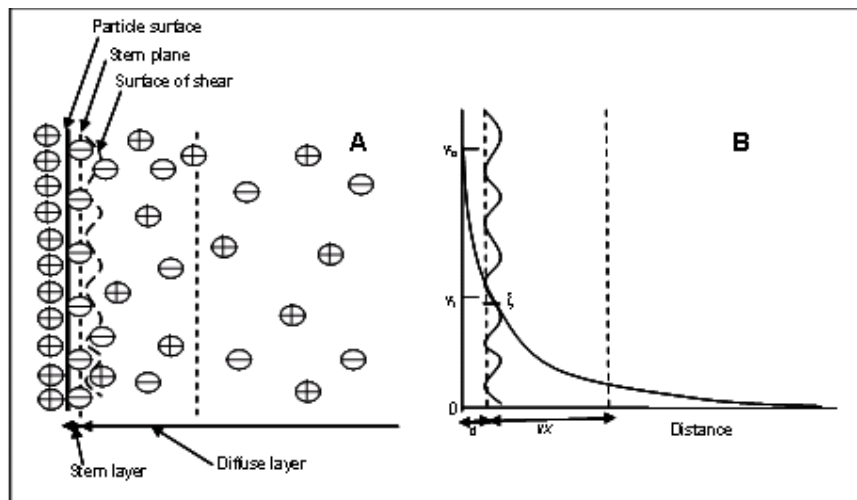
Where μ_E is the electrophoretic mobility, ζ is the zeta potential, ε is the dielectric constant of the medium, η is the viscosity of the medium and $f(ka)$ is the correction factor that takes in to account the thickness of the double layer and particle diameter.

The potential at the above-mentioned shear plane between the particle with its ion atmosphere and the surrounding medium is the zeta potential. Zeta potential is a function of the surface charge of a particle, any adsorbed layer at the interface, and the nature and composition of the surrounding medium in which the particle is suspended.

An investigation of the surface charge of crystallized $CaCO_3$ was carried out. The polymeric additives can be incorporated into the crystal or adsorbed on the surface of the crystals. The extent of both incorporation and adsorption depends on the functional groups of the polymer. The use of a charged crystal growth modifier can result in charged $CaCO_3$ crystals. Highly surface active anionic polymers interact more with the metal ions as well as the growing crystal than uncharged polymers, hence there is a greater chance of the polymer of being firmly bound onto crystal. Similarly, surface active polymers can be adsorbed onto the surface more readily than polymers whose surface activity is low. The zeta potential measurements provide data on the overall charge on the $CaCO_3$ crystals.

5.2: Experimental

Materials

Starch from potato (Acros) was used as received. Acrylic acid (Fluka) was purified by vacuum distillation at 30 ^{o}C. Sodium acrylate (Fluka), fluorescein isothiocyanate (Fine Chemicals), rhodamine B isothiocyanate (Fine Chemicals), cationic starch (Mondi Business Paper), dibutyltin dilaurate (Sigma-Aldrich), dimethylsulfoxide (DMSO, Acros), $CaCl_2$ (Associated Chemical Enterprises) and Na_2CO_3 (Saarchem) were used as received.

5.2.1: Synthesis of fluorescein-tagged anionic and cationic starch

The anionic and cationic starches were tagged with a green dye and a red dye, respectively. The anionic starch was used as crystal growth modifier and the cationic starch was deposited onto the surface of the $CaCO_3$ crystals.

5.2.3.1: Fluorescein-tagged anionic starch

Starch was modified using the functionalized fluorescein dye according to a procedure described in the literature,[7] followed by grafting of polyacrylic acid. In a typical reaction potato starch (3 g) was dissolved in DMSO (40 mL) at room temperature, and a few drops of pyridine were added. Then fluorescein isothiocyanate (0.15 g) was added to the solution followed by dibutyltin dilaurate (30 mg). The reaction was run for 2 h at 95 ^{o}C. The product was precipitated from ethanol several times

in order to remove the unreacted dye, and then dried at 60 ^{o}C. The degree of substitution was determined spectrophotometrically using a calibration curve and was 0.047%. The fluorescein-modified starch was conventionally grafted with acrylic acid, as in Section 3.2.2.2, using the Ce^{4+}-KPS initiator system. The percentage grafting obtained was 43%. A low percentage grafting was targeted in order to use a high concentration of the fluorescein-modified starch grafted with PAA (crystal growth modifier) during CaCO$_3$ crystallization, and therefore the fluorescence of the resulting CaCO$_3$ crystals is increased whilst the concentration of PAA remains optimum. The effect of the grafted PAA concentration on crystal nucleation and growth were easily regulated by varying the concentration of fluorescein modified starch grafted with PAA.

5.2.3.1: Rhodamine B-tagged cationic starch

Cationic starch (3 g) was dissolved in DMSO (40 mL) at room temperature. A few drops of pyridine and rhodamine B isothiocyanate (0.15 g) were added. The tin catalyst (dibutyltin dilaurate) was added and the reaction was run for 2 h at 95 ^{o}C, with stirring. The product was precipitated in ethanol several times to remove the unreacted dye, and then dried at 60 ^{o}C. The degree of substitution obtained was 0.026% from spectrophotometry. The structures of the dyes used to modify potato starch and cationic starch a shown in Scheme 5.1.
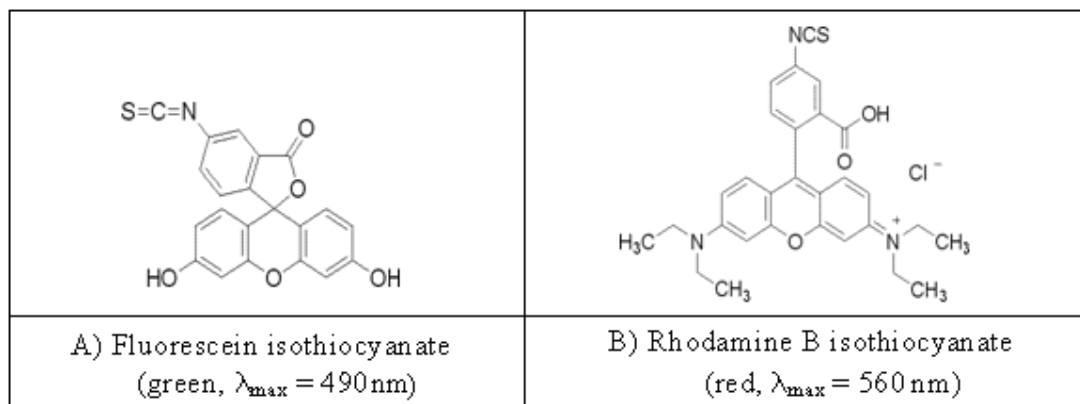
Scheme 5.1: Structures of green and red dyes used to tag anionic and cationic starch, respectively.

5.2.2: Crystallization experiments

Crystallization of calcium carbonate was carried out according to the procedure given in Section 4.2.1. The only differences here were that the crystal growth modifier was now tagged with a fluorescent dye and crystal growth modifier concentration was varied (1.4 g/L, 1.0 g/L 0.65 g/L). In a typical CaCO$_3$ crystallization reaction (synthesis of CaCO$_3$ (1)), modified polysaccharide (10 mL, 1.4 g/L), dissolved in de-ionized water, was stirred under N$_2$ and then Na$_2$CO$_3$ solution (15 mL,

0.025 M) was added at 25 °C after which $CaCl_2$ solution (15 mL, 0.025 M) was added slowly whilst stirring. The reactions were carried out at 25 ± 2 °C for 24 h. The crystals in half of the reaction mixture were filtered through a 0.22 micron membrane filter paper to collect the $CaCO_3$ microcrystals, which were then rinsed and centrifuged three times using deionized water, and resuspended in deionized water.

The crystallized calcium carbonate crystals (anionic) were coated with cationic starch tagged with a red dye (rhodamine B). In a typical procedure, 10 mL of 1 % solution of rhodamine tagged cationic starch was added to 0.3 g of anionic $CaCO_3$ crystals. The mixture was then stirred for two hours followed by a series of washing (3 xs) via the centrifugation process. The crystals were then dried and characterized.

A similar procedure was used for the zeta potential measurements. A typical sample preparation was as follows: Cationic starch (not fluorescence tagged) (1 mL, 1%) was added to a solution of crystallized $CaCO_3$ (10 mL, 0.1 g/L) and stirred for 15 min. This was followed by washing (3x) via centrifugation process to remove unattached cationic starch. The particles were then resuspended in distilled deionized water for zeta potential measurements. Thus the effect of the cationic starch on the zeta potentials was determined by addition of more cationic starch for each subsequent measurement.

5.3: Analysis

5.3.1: Fluorescence

Fluorescence images were acquired using an Olympus Cell^R system attached to an IX-81 inverted fluorescence microscope equipped with a F-view-II cooled CCD camera (Soft Imaging Systems). For the image frames, an Olympus Plan Apo N 60x/1.4 Oil objective and the Cell^R imaging software were used for the image acquisition and analysis.

Fluorescence statistical data was acquired using a BD FACSAria flow cytometer. Samples were suspended in distilled water and acquired with an event rate of 500–1000 events/second. In total, 50 000 events were acquired and analyzed using the BD FACSDiva software and Flowjo. Flow cytometry is technique used for counting, examining, and sorting microscopic biological cells suspended in a stream of fluid. The technique gives simultaneous multiparametric analysis of physical and/or chemical characteristics of particles. The instrument is equipped with multiple light scattering detectors and a fluorescence detector. The size and granularity of cells data is obtained

from the light scattering detector. Data for individual particles is obtained and then plotted in a scatter plot. In order to separate cells of different properties, the sorter is set according to predetermined sort criteria. Particles within the criteria are charged and deflected by charged metal plates into the collector whereas particles outside the set parameters are left to pass.

5.3.2: Zeta potentials

Zeta potentials were measured using a Zetasizer Mano-ZS90 instrument.

5.4: Results and discussion

5.4.1: Fluorescence and morphology of CaCO$_3$ crystals

The concentration of the fluorescein tagged anionic starch was varied to see the effect of polymer concentration of the morphology of the crystals. The CaCO$_3$ crystals synthesized in the presence of a fluorescein tagged anionic starch are referred to as CaCO$_3$ (1), CaCO$_3$ (2) and CaCO$_3$ (3) and the concentration of the crystal growth modifier were 1.4 g/L, 1.0 g/L and 0.65 g/L, respectively. CaCO$_3$ crystals synthesized in the presence of starch grafted with polyacrylic acid (non fluorescein tagged) were used as the control for images and the flow cytometry. Figures 5.3 to 5.5 show the effect of polymeric additive concentration on the fluorescence and morphology of CaCO$_3$ crystals. The fluorescence and SEM images in Fig. 5.2 were obtained from crystals that were grown using non tagged anionic starch and serve as controls. The fluorescence image (Fig. 5.2B) shows no glowing of the crystals and the transmission image (Fig. 5.2A) and SEM image (Fig. 5.2D) show spherical crystal morphology. When fluorescence-tagged anionic starch was used the crystals fluoresced (Figs. 5.3–5.5) indicating the presence of the polysaccharide on the surface of the crystals. The presence of polysaccharide on the surface can be due to absorption occurring during the crystal growth. The polymer-nuclei interaction was found to be prevalent (from the beginning of crystallization) for the carboxyl functional group of polyacrylic acid.[12] The crystal morphology of the synthesized CaCO$_3$ (1) was predominantly spherical (Fig. 5.3). CaCO$_3$ (2) crystal morphology was mostly granular spherical crystals (Fig. 5.4) whereas crystal morphology of CaCO$_3$ (3) was a mixture of irregular shaped and cubical crystals (Fig. 5.5). The cubical and irregular crystal morphology obtained for CaCO$_3$ (3) was expected since the crystal growth modifier had been reduced to a fraction of the optimum for effective crystal nucleation and growth control. In Fig. 5.5 it can be seen that not all the crystals possessed the polysaccharide on the surface as some of the

crystals did not fluoresce. Specifically, the cubical crystal in Fig. 5.5A can hardly be seen in the fluorescence image Fig. 5.5B, but in the overlay image (transmission and fluorescence) in Fig. 5.5C the crystal is visible. However, some of the irregular shaped and cubical crystals fluoresced and this could be due to either adsorption/absorption of the crystal growth modifier on the surface of the crystals after crystal growth or aggregation of non-fluorescing and fluorescing crystals. In Section 4.3.1 it was found that the crystal morphology was cubic for crystallization performed in the absence of anionic polymer additive.
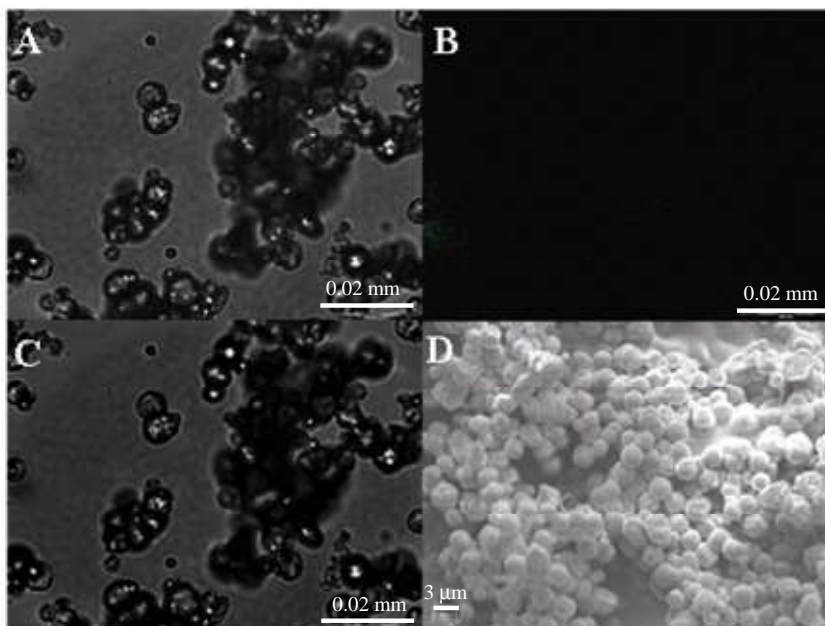
[Polymeric additive] = 1.4 g/L, [Ca2+] = [CO32-] = 0.025 M, pH = 7.5, the reaction temperature 25 ^{o}C

Fig. 5.2: Fluorescence images of CaCO$_3$ (control): (A) transmission, (B) fluorescence mode, (C) overlay of A and B, and (D) SEM image of the crystals.
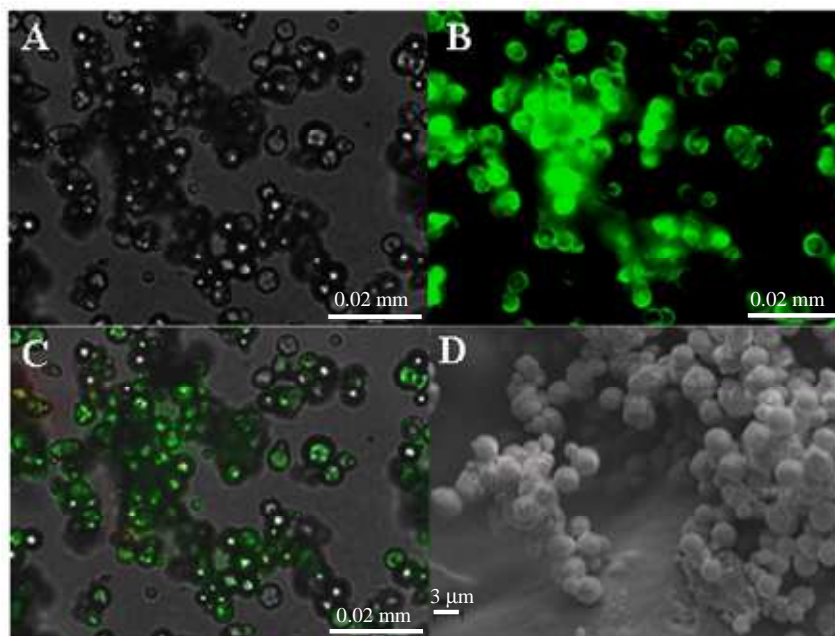
[Polymeric additive] = 1.4 g/L, [Ca2+] = [CO32-] = 0.025 M, pH = 7.5, the reaction temperature 25 $^{\circ}$C

Fig. 5.3: Fluorescence images of CaCO$_3$ (1): (A) transmission, (B) fluorescence mode, (C) overlay of A and B, and (D) SEM image of the crystals.
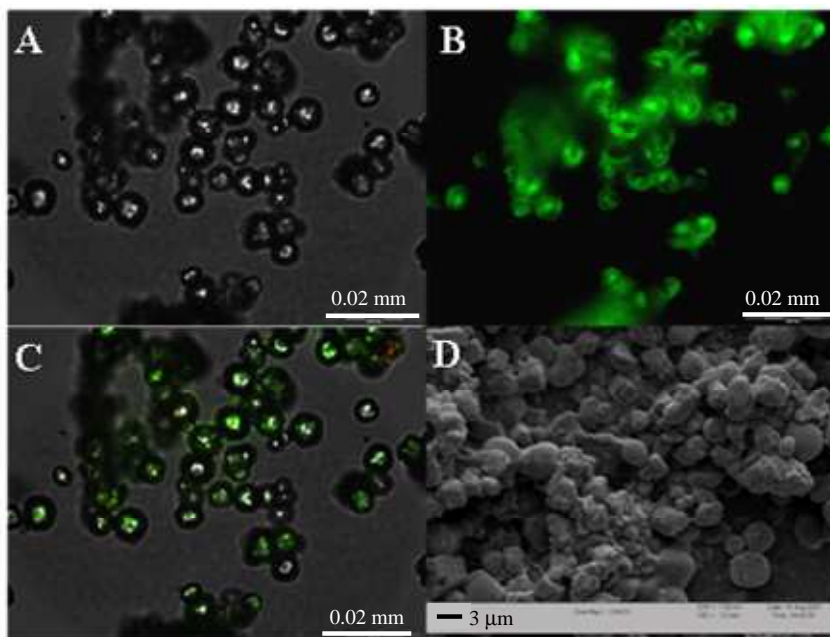
[Polymeric additive] = 1.0 g/L, [Ca2+] = [CO32-] = 0.025 M, pH = 7.5, the reaction temperature 25 $^{\circ}$C

Fig. 5.4: Fluorescence images of CaCO$_3$ (2): (A) transmission, (B) fluorescence mode, (C) overlay of A and B, and (D) SEM image of the crystals.
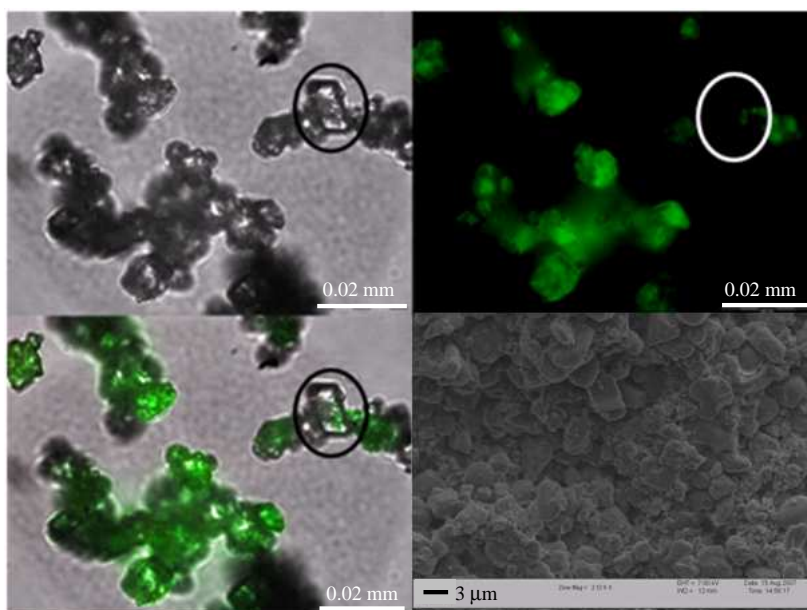
[Polymeric additive] = 0.65 g/L, [Ca2+] = [CO32-] = 0.025 M, pH = 7.5, the reaction temperature 25 °C

Fig. 5.5: Fluorescence images of CaCO$_3$ (3): (A) transmission, (B) fluorescence mode, (C) overlay of A and B, and (D) SEM image of the crystals.

The response of CaCO$_3$ crystals to cationic starch addition is of paramount importance as not only does it prove that the crystals carry the negative charge but it is important for further filler surface modification. However, when the pulp, filler and other additives are mixed or blended together during papermaking, the additive to be added just before papermaking is a solution of cationic starch. The cationic starch flocculates the pulp and has little effect on the PCC since PCC is partially positive (see Section 3.4.3.1). The use of negatively charged filler could improve its dispersion during the blending with pulp. Furthermore, the addition of cationic starch during papermaking will result in co-flocculation of both the anionic pulp and the anionic filler. The coating of fluorescing (green) anionic CaCO$_3$ crystals with fluorescing (red) cationic starch allowed the visualization of the deposition of the cationic starch. By using different fluorescence wavelengths both the green and red colors can be viewed separately. Figs 5.6, 5.7 and 5.8 show the separate green and red colors are observed on the surface of the crystals. The overlay of the green and red images (Fig. 5.6D) showed the red and green areas with some areas showing some yellowing (red plus green gives a yellow color, but subject to the concentrations of the dyes). Fig. 5.7D shows mostly the yellow color and thus the concentrations of the two dyes were in the proportion that was able to give the yellow color. In the case of CaCO$_3$ (3), the yellow color was more intense and red spots were observed, as shown in Fig. 5.8D. This also indicates that the

amount of polysaccharides on the surface of the CaCO$_3$ (1, 2 and 3) crystals were different since different colors emerged when equal concentration of rhodamine B tagged cationic starch was used.
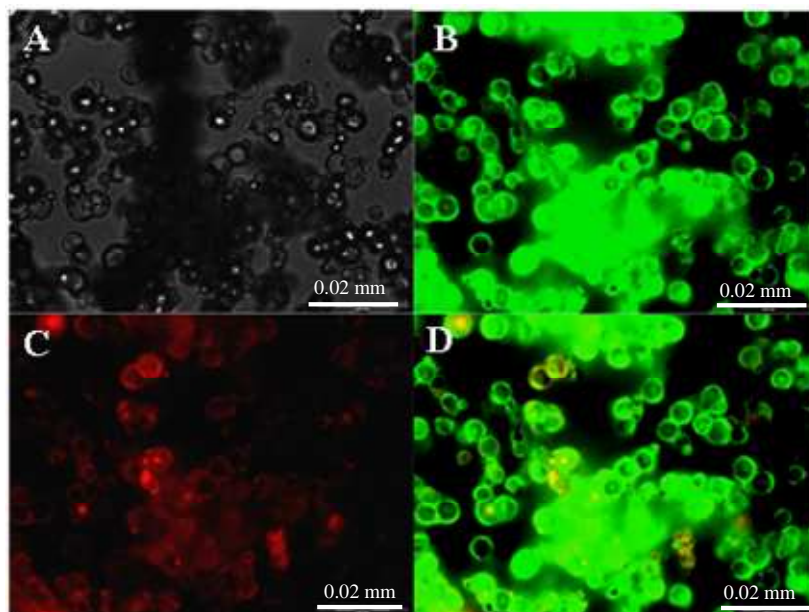
Fig. 5.6: Fluorescence images of CaCO$_3$ (1) with rhodamine modified cationic starch deposited on the surface: (A) transmission mode, (B) fluorescence mode (fluorescein), (C) fluorescence mode (rhodamine) and (D) overlay of A, B and C.
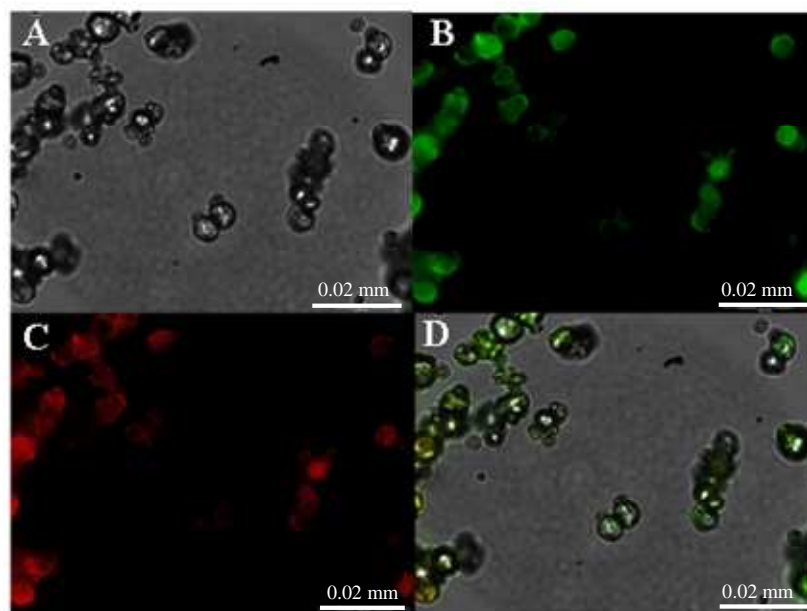
Fig. 5.7: Fluorescence images of CaCO$_3$ (2) with rhodamine modified cationic starch deposited on the surface: (A) transmission mode, (B) fluorescence mode (fluorescein), (C) fluorescence mode (rhodamine), (D) overlay of A, B and C.
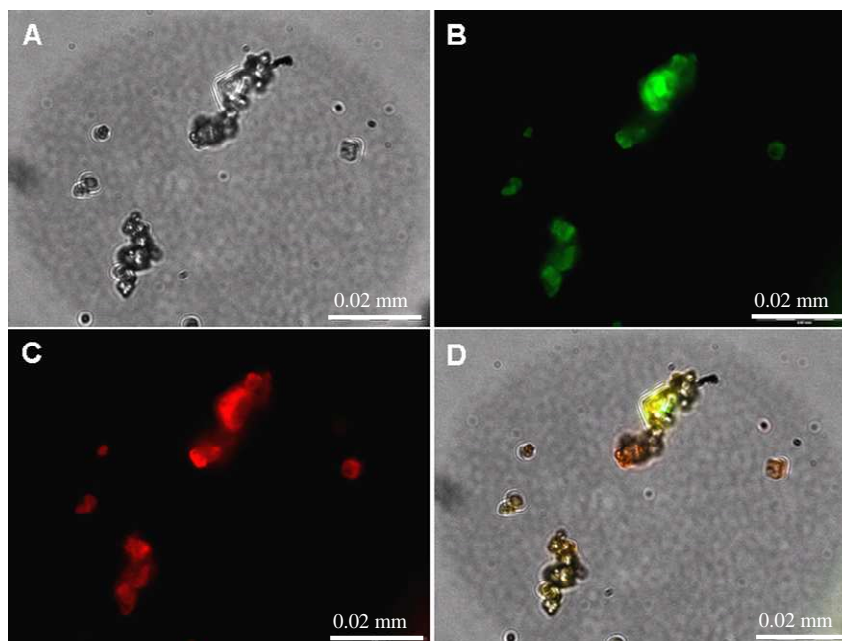
Fig. 5.8: Fluorescence images of CaCO$_3$ (3) with rhodamine modified cationic starch deposited on the surface: (A) transmission mode, B) fluorescence mode (fluorescein), (C) fluorescence mode (rhodamine), (D) overlay of A, B and C.

The synthesized CaCO$_3$ (1) consisted of calcite and vaterite polymorphs (Fig. 5.9). The presence of vaterite (the least thermodynamically stable polymorph of the three) is due to the anionic polymer used to synthesize CaCO$_3$ (1), which is capable of effecting the nucleation and stabilization of the vaterite phase. CaCO$_3$ (2) was dominated by the calcite peaks, with vaterite peaks of low intensity appearing (Fig. 5.9). The amount of the crystal growth modifier is important especially for crystal phase stabilization as the least thermodynamically stable polymorph can easily be transformed into calcite.[13] CaCO$_3$ (3) consists of calcite crystals only (Fig. 5.9) and since the lowest concentration of the anionic polymer was used in CaCO$_3$ crystallization, it was not capable of stabilizing the vaterite. Thus, nucleation of vaterite may occur but its crystal phase will not be stable, and therefore it will be transformed into calcite. The peaks due to calcite and vaterite were confirmed by FT-IR spectroscopy (Fig. 5.10). The additional peaks due to the anionic starch additive were also observed showing that the polysaccharide was present in or on the CaCO$_3$ crystals.
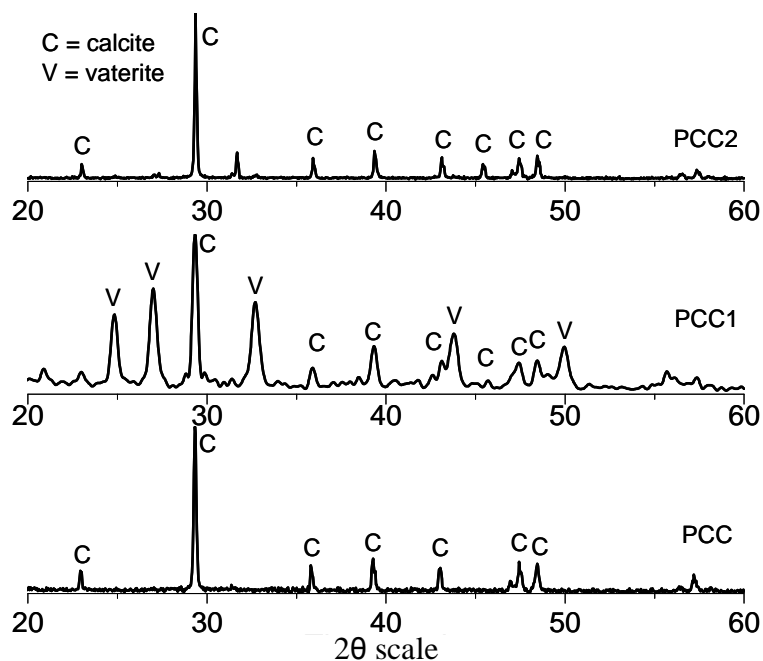
Fig. 5.9: XRD spectra of PCC, CaCO$_3$ (1), CaCO$_3$ (2) and CaCO$_3$ (3) showing the polymorph present. Polymeric additive concentrations for the synthesis of CaCO$_3$ (1), CaCO$_3$ (2), CaCO$_3$ (3) were 1.4, 1.0, and 0.65 g/L, respectively.
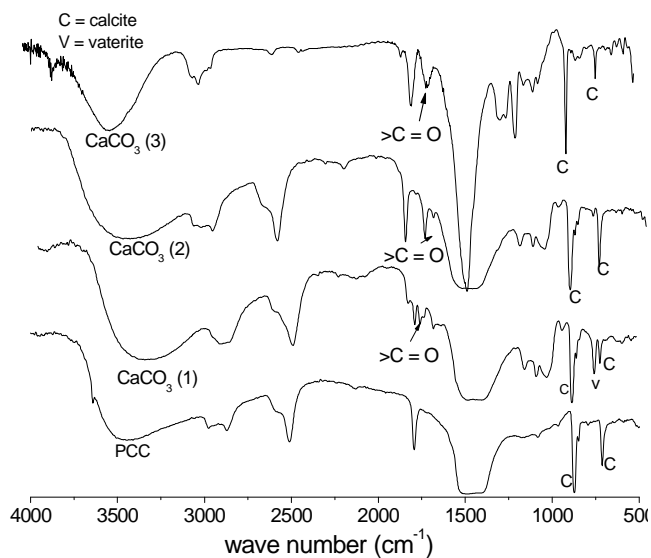
Fig. 5.10: FT-IR spectra of PCC, CaCO$_3$ (1) and CaCO$_3$ (2) and CaCO$_3$ (3). (Concentrations of polymeric additives for the synthesis of CaCO$_3$ (1), CaCO$_3$ (2), CaCO$_3$ (3) were 1.4, 1.0, and 0.65 g/L respectively.)

98

5.4.2: TGA and zeta potential measurements

TGA analysis of $CaCO_3$ crystals synthesized in the presence of fluorescein tagged anionic starch (Fig. 5.11) was done to determine the percentage of anionic starch polymer/organic content in the crystals. The synthesized $CaCO_3$ (1 and 2) has a first weight loss (~1.6%) in the temperature range 40–100 ^{o}C, due to loss of moisture. $CaCO_3$ (1) had more polymer content followed by $CaCO_3$ (2) and $CaCO_3$ (3), with PCC having the lowest organic content. This was expected, since more anionic starch was used in the synthesis of $CaCO_3$ (1) followed by $CaCO_3$ (2) and lastly $CaCO_3$ (3). The retention of polysaccharides in the crystals after rinsing and centrifugation shows that the polysaccharides were firmly bound to the crystals. Increasing the concentration of the crystal growth modifier had an effect on the size and morphology of both the primary and secondary crystals. The amount of the crystal growth modifier incorporated or bound onto the crystals were according to the concentrations of crystal growth modifier used during crystallization.
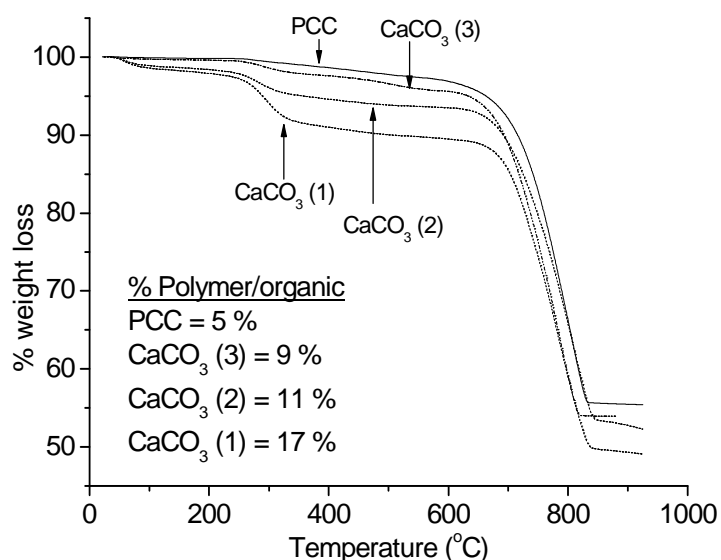
Fig. 5.11: TGA curves of PCC, CaCO₃ (1), CaCO₃ (2) and CaCO₃ (3).

Fig. 5.12 shows the zeta potentials of PCC and that of fluorescing $CaCO_3$ crystals. The synthesized fluorescing $CaCO_3$ (1), $CaCO_3$ (2) and $CaCO_3$ (3) crystals carried a net negative charge on the surface whilst PCC had a positive charge (Fig 5.12). The initial zeta potential values depended on the amount of crystal growth modifier used to crystallize $CaCO_3$. The addition of cationic starch to $CaCO_3$ crystals resulted in the zeta potentials becoming increasingly more positive, signaling the surface charge inversion. Thus, cationic starch is adsorbed on the surface of the crystals through either ionic interactions or van der Waals forces. For the negatively charged crystals, neutralization of the charge occurs and as more cationic starch is deposited on the surface the crystals surface

becomes positive. However, further adsorption of the cationic starch is limited by steric hindrances due to the polymer deposited on the crystal surface. Thus, the surface charge of the crystallized calcium carbonate can be easily manipulated, and the effect of filler surface charge on filler retention during papermaking can be investigated.
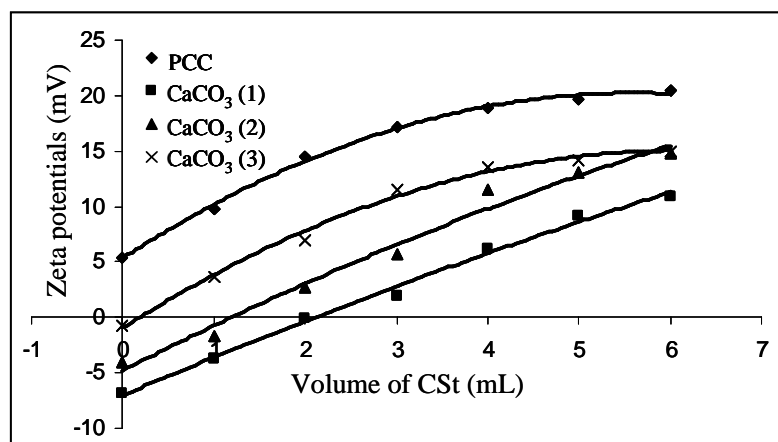
Fig. 5.12: The effect of increasing the concentration of cationic starch on the zeta potentials of PCC and the synthesized CaCO$_3$ (1), CaCO$_3$ (2) and CaCO$_3$ (3) particles. (A 1% (w/v) solution of cationic starch was used.)

5.4.3: CaCO$_3$ crystal size in aqueous solution

Fig 5.13 shows the aqueous particle size of PCC and the fluorescing CaCO$_3$ crystals. The synthesized CaCO$_3$ (1, 2 and 3) had larger flocculant sizes compared to PCC (Fig 5.13). The particle size analysis was done in aqueous phase using 20% solid content solutions of CaCO$_3$.
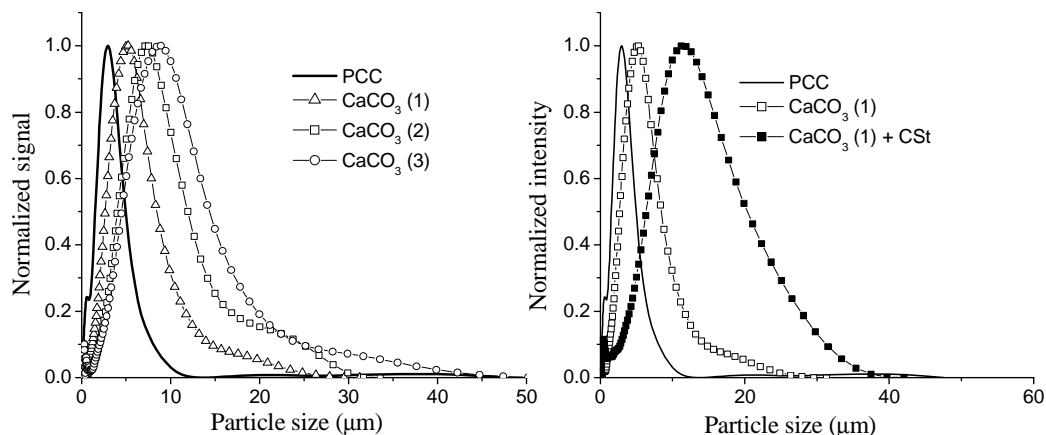
Fig. 5.13: A) Aqueous particle size distribution for PCC and the synthesized CaCO$_3$ (1) and CaCO$_3$ (2), and B) the effect of cationic starch on the synthesized CaCO$_3$ (1) particles.

Addition of cationic starch solution (10 mL, 2%) to a solution of CaCO$_3$ (1) (10 mL, 20%) resulted in an increase in the average flocculant size (see Fig. 5.13). Since the particles have a negative

surface charge (from zeta potential measurements), flocculation of these particles by cationic starch is facile. Thus, during papermaking the addition of cationic starch to a solution of pulp and negatively charged $CaCO_3$ may result in bonding the filler and fiber together, leading to improved filler retention.

5.4.4: Statistical analysis of $CaCO_3$ crystals

Flow cytometry was used to obtain data relating both the size and granularity of the $CaCO_3$ crystals to the chromophore distribution. Also, different populations of $CaCO_3$ crystals were separated according to their size and granularity and the crystals were imaged to see the different crystal morphologies in selected populations.

In order to get size and granularity limits as well as conditions to separate different $CaCO_3$ crystals granularity versus size scatter plots were obtained. Figs 5.14, 5.16 and 5.18 (A1 and B1) are granularity versus size scatter plots for the $CaCO_3$ reference sample and $CaCO_3$ crystals ($CaCO_3$ (1), $CaCO_3$ (2) and $CaCO_3$ (3)) synthesized in the presence of a fluorescence-tagged crystal growth modifier, respectively. The x axis represents the size dimension of the particles whereas the y axis represents the granularity of the particles. The granularity of the crystals is also referred to as the complexity. It must be mentioned that both the y and x axes have arbitrary units and the scatter plots are a relative indication of how crystals are scattered relative to their size and granularity. Therefore, a reference sample was required for qualitative analysis of the fluorescing crystals. Each dot in the scatter point represents a $CaCO_3$ crystal.

The relationship between the granularity and the amount of chromophore on the $CaCO_3$ crystals was also plotted as scatter plots for both the $CaCO_3$ control sample and the fluorescing $CaCO_3$ crystals. Thus, scatter plots in Figs. 5.14, 5.16 and 5.18 (A2 and B2) show the relationship between the granularity of the crystals and fluorescence whereas those in Figs. 5.14, 5.16 and 5.18 (A3 and B3) show the relationship between the crystal size and fluorescence for all the populations. From these scatter plots it can be concluded that the fluorescence of crystals increased with increasing both the size and the granularity of the $CaCO_3$ crystals. This is explained by the fact that particles of higher granularity or sizes are due to aggregation of smaller crystals forming either mesocrystals (big and low granularity particles) or polycrystalline crystals (large and high granularity crystals). Thus the fluorescence of these crystals can be a contribution of several smaller crystals constituting the large crystal. The scatter plots for the control clearly show that there was no relationship between either the size or granularity with fluorescence since the $CaCO_3$ crystals do not have a fluorescein-tagged crystal growth modifier.

A statistical evaluation was also obtained from various points of the scatter plots along the pattern, as shown in Figs. 5.15, 5.17 and 5.19 (A1 and B1). Scatter plots in Figs. 5.15, 5.17 and 5.19 (A2 and B2) also show the relationship between the granularity of selected populations of the CaCO$_3$ crystals and fluorescence. Figs. 5.15, 5.17 and 5.19 (A3 and B3) show the relationship between the crystal size for selected populations of the CaCO$_3$ and fluorescence. It should be noted that selected populations are distinguished from each other by color.
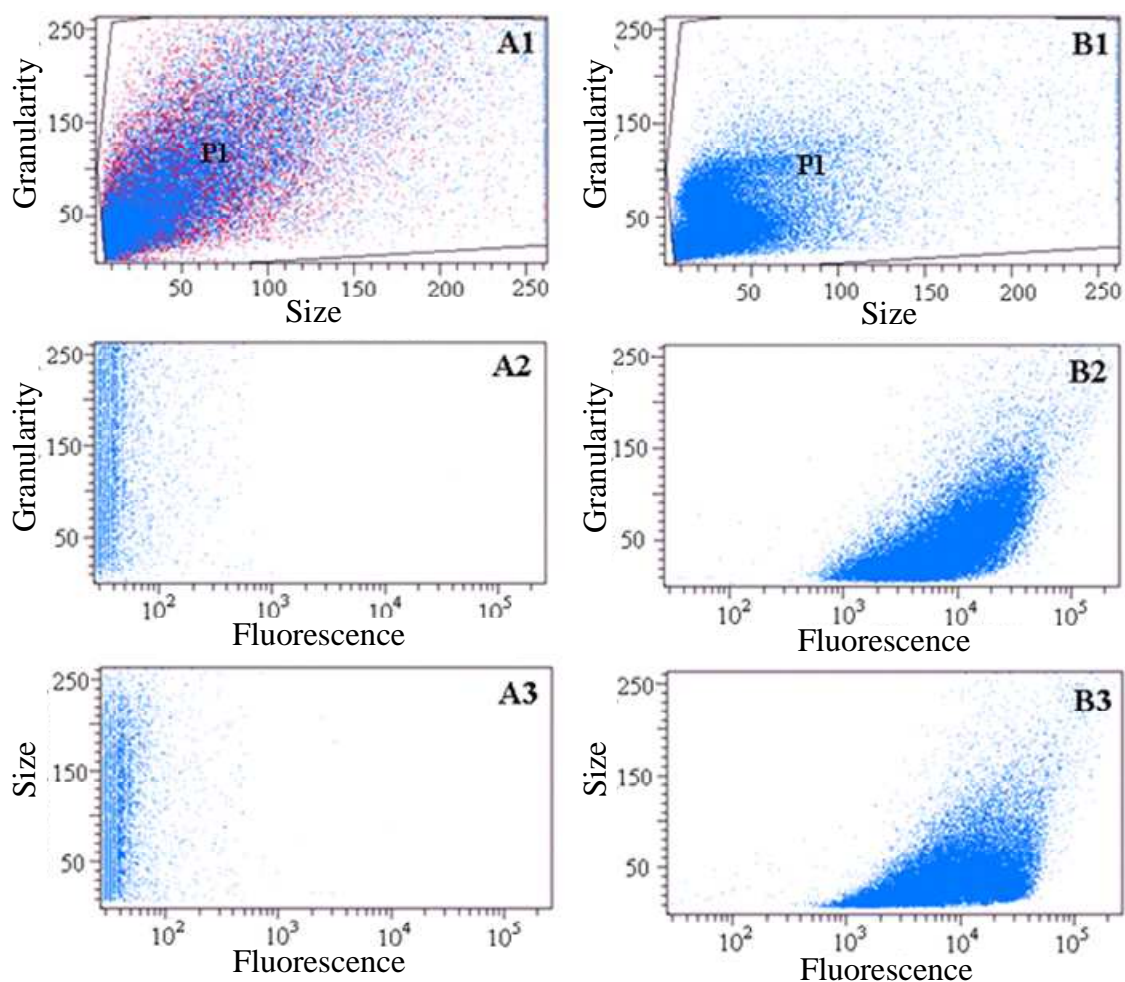
[Polymeric additive] = 1.4 g/L, [Ca^{2+}] = [CO$_3^{2-}$] = 0.025 M, pH = 7.5, reaction temperature was 25 °C

Fig. 5.14: Fluorescence scatter graphs for the control sample and CaCO$_3$ (1): A1, A2 and A3 show the population, granularity vs fluorescence, and size vs fluorescence curves for the control, respectively; B1, B2 and B3 show the selected population, granularity vs fluorescence, and size vs fluorescence curves for the CaCO$_3$ (1), respectively.

It was generally found that the fluorescence increased with increasing granularity and size. (i.e. crystals of low granularity and smaller size had the least fluorescence). However, the majority of the CaCO$_3$ particles in the population labeled P4 had fluorescence values that overlapped

significantly with the fluorescence values of CaCO$_3$ crystals in the population labeled P5. Thus, crystals in P4 had a broader fluorescence distribution than those in P5 and P3.
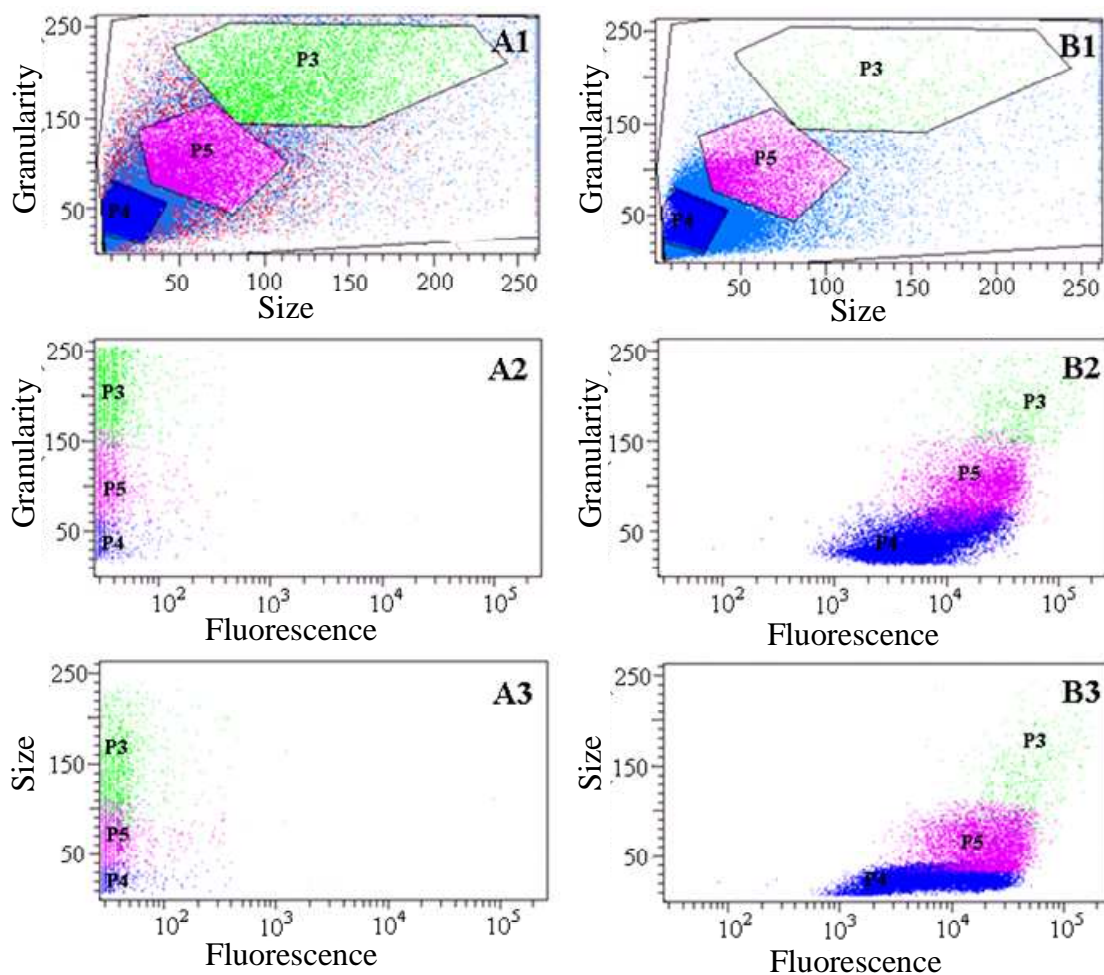
[Polymeric additive] = 1.4 g/L, [Ca^{2+}] = [CO$_3^{2-}$] = 0.025 M, pH = 7.5, reaction temperature was 25 $^\circ$C

Fig. 5.15: Fluorescence scatter graphs for the control sample and CaCO$_3$ (1): A1, A2 and A3 show the selected population, granularity vs fluorescence, and size vs fluorescence curves for the control, respectively; B1, B2 and B3 show the selected population, granularity vs fluorescence, and size vs fluorescence curves for the CaCO$_3$ (1), respectively
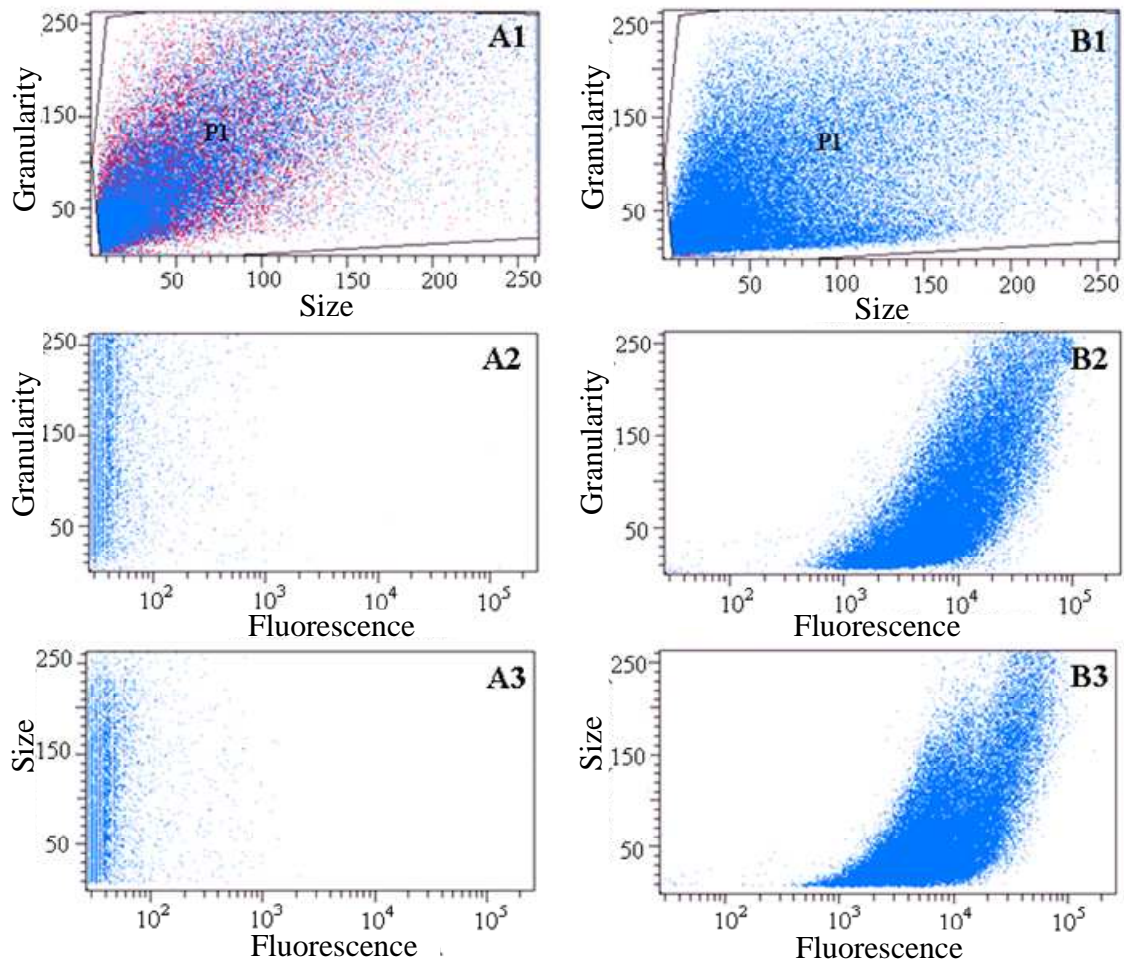
[Polymeric additive] = 1.0 g/L, $[Ca^{2+}] = [CO_3^{2-}] = 0.025$ M, pH = 7.5, reaction temperature was 25 °C

Fig. 5.16: Fluorescence scatter graphs for the control sample and CaCO₃ (2): A1, A2 and A3 show the population, granularity vs fluorescence, and size vs fluorescence curves for the control, respectively; B1, B2 and B3 show the selected population, granularity vs fluorescence, and size vs fluorescence curves for the CaCO₃ (2), respectively.
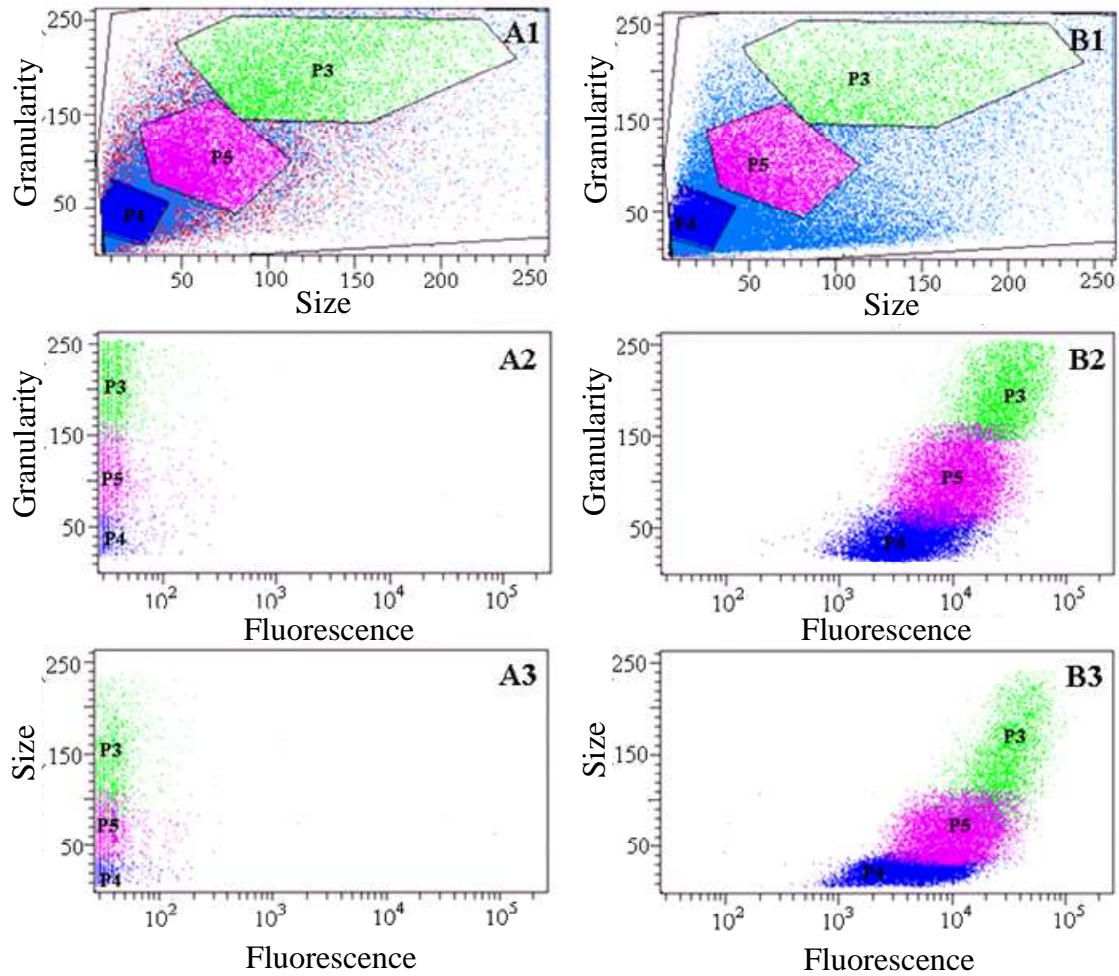
[Polymeric additive] = 1.0 g/L, $[Ca^{2+}] = [CO_3^{2-}] = 0.025$ M, pH = 7.5, reaction temperature was 25 °C

Fig. 5.17: Fluorescence scatter graphs for the control sample and CaCO₃ (2): A1, A2 and A3 show the selected population, granularity vs fluorescence, and size vs fluorescence curves for the control, respectively; B1, B2 and B3 shows the selected population, granularity vs fluorescence, and size vs fluorescence curves for the CaCO₃ (2) ,respectively.
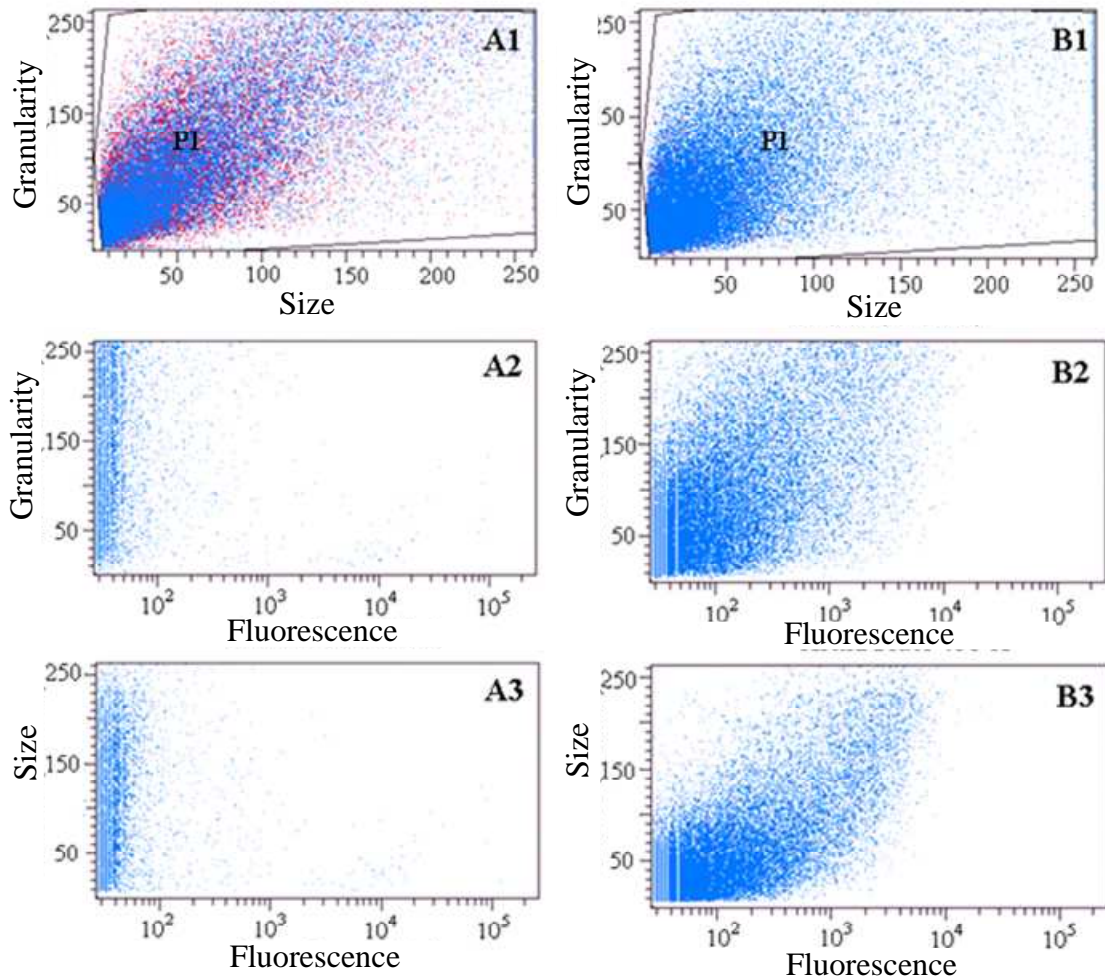
[Polymeric additive] = 0.65 g/L, $[Ca^{2+}] = [CO_3^{2-}] = 0.025$ M, pH = 7.5, reaction temperature was 25 °C

Fig. 5.18: Fluorescence scatter graphs for the control sample and CaCO$_3$ (3): A1, A2 and A3 show the population, granularity vs fluorescence, and size vs fluorescence curves for the control, respectively; B1, B2 and B3 show the selected population, granularity vs fluorescence, and size vs fluorescence curves for the CaCO$_3$ (3), respectively.
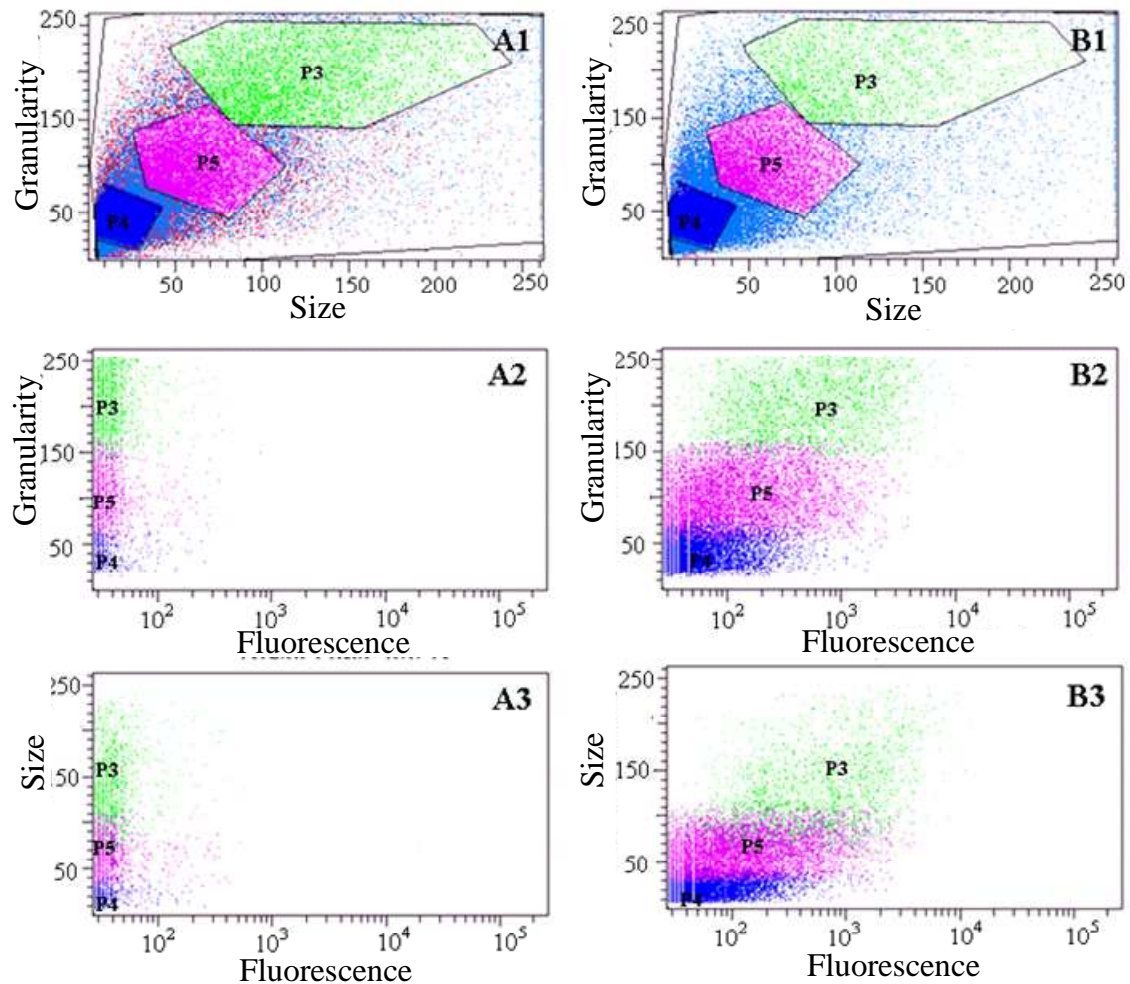
Fig. 5.19: Fluorescence scatter graphs for the control sample and CaCO₃ (3): A1, A2 and A3 show the selected population, granularity vs fluorescence, and size vs fluorescence curves for the control, respectively; B1, B2 and B3 shows the selected population, granularity vs fluorescence, and size vs fluorescence curves for the CaCO₃ (3), respectively.

The populations were fractionated first then imaged. The population region of low granularity and smaller crystal size (P4) in Fig. 5.20 had smaller homogeneous spherical particles. Population region P5 (Fig. 5.20) had larger spherical and irregular shaped crystals, and crystal aggregation was also observed. The crystal irregularity and aggregation was more pronounced in population region P3, where large and high granularity crystals were observed. The images of different populations are in good agreement with the granularity versus size scatter plots. The high fluorescence observed in the case of high granularity as well as large crystals was therefore due to the contribution of individual particles that formed the aggregates. Aggregation was less in CaCO₃ (1) compared to

CaCO$_3$ (2) (Figs. 5.15 and 5.17). This is due to the different colloidal stability of the crystals. The colloidal stability thus decreased with decreasing crystal growth modifier concentration.
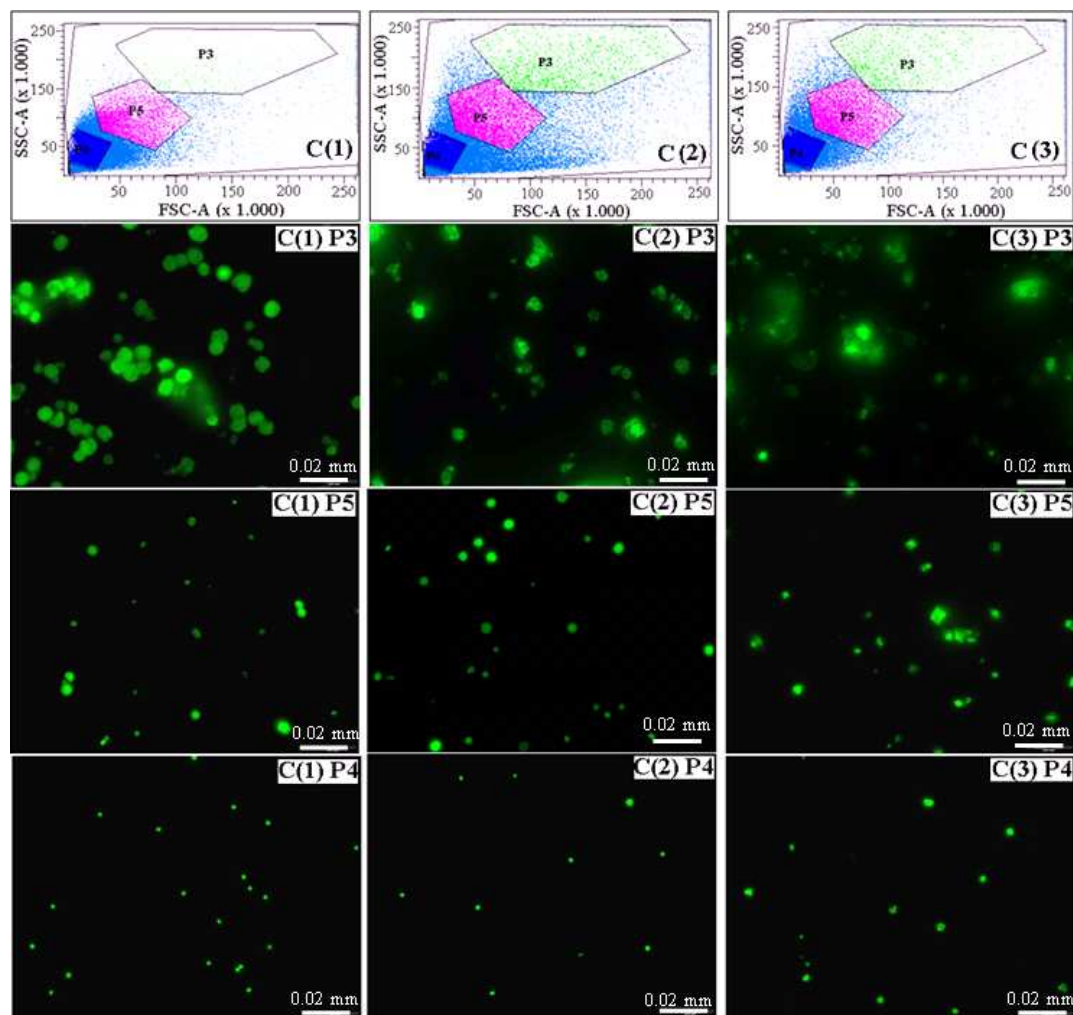
Fig. 5.20: Images for fluorescence scatter populations P3, P4, and P5 for CaCO$_3$ (2)–(3)

Table 5.1 shows the average fluorescence values for the entire distribution P1, and the average florescence values for the selected areas (see Figs. 5.15, 5.17, 5.19(A1 and B1)) P3, P4 and P5. The crystals synthesized in the presence of 1.4, 1.0 and 0.65 g/L crystal growth modifier gave different fluorescence distribution curves and scatter plots in terms of their position in the fluorescence scale. The order of increasing fluorescence in crystals was from the highest to the least concentration of crystal growth modifier, as shown in Fig. 5.21. The fluorescence results were in good correlation with results obtained from TGA and zeta potential measurements (Section 5.4.2), which showed that the retention of the polysaccharide in the crystals increased when the concentration of the crystal growth modifier in the system was increased.

Table 5.1: The average fluorescence values (no units) for selected areas in the scatter plot and their standard deviation for the control and synthesized CaCO₃

	Population	Mean fluorescence				Standard deviation			
		Control	$CaCO_3$ (1)	$CaCO_3$ (2)	$CaCO_3$ (3)	Control	$CaCO_3$ (1)	$CaCO_3$ (2)	$CaCO_3$ (3)
	P2	26	12064	11632	6371	101	13905	13052	7549
	P3	18	52663	30771	748	15	35307	15736	579
	P5	33	23120	12609	560	27	12204	7213	390
	P4	11	9088	5173	220	9	7052	3482	190

P2 denotes the overall fluorescence distribution of all the CaCO₃ crystals analyzed. The fluorescence distributions curves of all the CaCO₃ crystals are shown in Fig. 5.21.
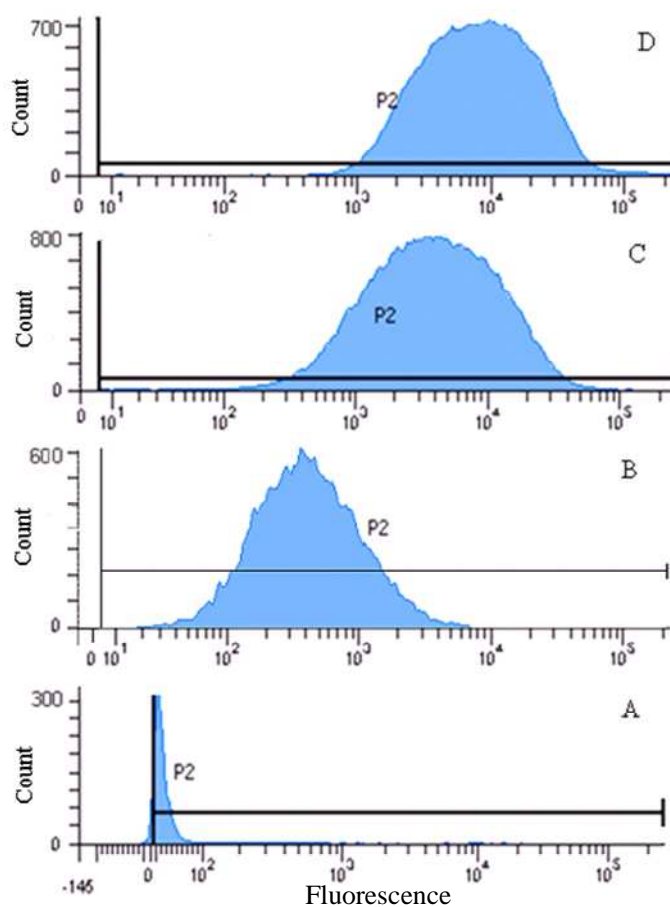
Fig. 5.21: Fluorescence distribution curves of (A) control sample and CaCO₃ crystals synthesized in the presence of fluorescence tagged anionic starch, (B) CaCO₃ (3), (C) CaCO₃ (2) and (D) CaCO₃ (1). (P2 denotes events in population P1.)

Statistical evaluation of $CaCO_3$ crystals also revealed the following: (i) large crystals of low granularity, (ii) smaller crystals of high granularity, (iii) large crystals of high granularity and (iv) the majority of the crystals were small and of low granularity. It can be concluded therefore that (i) large crystals of low granularity followed either the classical crystal growth mechanism or the non-classic crystal growth mechanism, leading to mesocrystals, which results in crystals low of granularity, (ii) smaller crystals of high granularity followed the non-classical crystal growth mechanism, leading to polycrystalline crystals due to aggregation of primary crystals, (iii) large crystals of high granularity followed a non-classical crystal growth mechanism, with aggregation of primary crystals larger than the primary crystals that formed crystals in (ii) and, lastly (iv) smaller to medium crystals of low-medium granularity followed either a single crystal growth mechanism or a non-classical crystal growth mechanism, with even smaller primary ions than those that formed crystals in (ii). This conclusion is based on the fact that different morphologies were obtained in one system, meaning that the nucleation and crystal growth mechanisms were different. It was also noted that the $CaCO_3$ crystals formed in the presence of the highest concentration of crystal growth modifier had the least number of crystals in both the high granularity and large crystal size region, which indicates that most crystals grew via a similar mechanism of crystal nucleation and growth. Previous studies showed that the higher the concentration of the crystal growth modifier the better is the control of crystal nucleation.[14]

5.4.5: Crystal nucleation and growth mechanisms

It is widely accepted in literature that the formation of ACC is the initial step in the crystallization of $CaCO_3$ and it can be formed in the absence of polymeric additives under high supersaturation conditions.[15] The polymeric additives such as PAA was found to stabilize the ACC and an ACC-PAA gel was observed in which the nucleation of the crystals occurred, resulting in the spherulitic growth of the nucleus.[12] A single crystal nucleus can be formed with or without the aid of additives. The crystalline nucleus will then grow at the expense of ACC via a dissolution and recrystallization process.[16] The inclusion of crystal growth modifiers alters the growth mechanism of the nuclei and is also subject to the relative concentrations of both the polymeric additive and precursor ions. The polymeric additive is capable of increasing the number of primary ions, which leads to smaller and possibly unstable primary crystals. The polymeric additives also have another role to play during crystal growth i.e. they are selectively adsorbed on to the surface of growing $CaCO_3$ crystal faces (depending on their functionality).[14,15] Their adsorption on crystal faces results in retardation or termination of crystal growth on those crystal faces. Thus, crystals are forced to grow in certain

dimensions. For PAM and PAM modified cellulose, where flat rhombohedrical crystals were observed (see Sections 4.3.1 and 4.3.3), the crystals were allowed to grow in 2-dimensions, and cubical crystals grew without the influence of PAM, as was observed for the control (no polymeric additive) run. For PAA and PAA grafted polysaccharides where spherical morphology was obtained the crystal growth of a nucleus is likely to follow the spherulitic mechanism derived from the ACC-PAA gel. The size and morphology of these primary crystals depends on the nature and concentration of the crystal growth modifier. The last step in the crystallization process is the growth of crystals to their ultimate size. Crystal growth can be via a classical or a non-classical mechanism. Non-classical crystal growth mechanisms occur via Oswald ripening and the driving force is the reduction of the interfacial energy.[12] Thus, for non-classical crystal growth mechanisms that leads to mesocrystals, secondary crystals retains the morphology of their primary crystals. The non-classical crystallization mechanism allows smaller crystals to aggregate to form large particles. These primary crystals have a natural tendency to aggregate, thereby reducing their surface energy. Theoretically, each primary crystal should have polymer chain(s) attached to it. The aggregation of these particles could lead to two possibilities, namely (i) incorporation of some polysaccharide inside the secondary crystals and (ii) polysaccharide residing on the surface of the secondary crystals caused by an initial or a primary absorption mechanism. Orientation of these particles during crystal growth could be similar to that of surface active agents in water, where aggregation occurs in a manner such that the surface energy of particles in the system is minimized. The classical crystal growth model is more prevalent in systems without crystal growth modifiers at low $CaCO_3$ precursor concentration or where the interaction of the crystal growth modifier and the growing crystal are at a minimum,[14] i.e. crystal growth will be independent of the polymeric additives but dependent on the concentration of $CaCO_3$ precursor ions' concentration. In the classical crystal growth mechanism, incorporation of the polymeric additive is possible especially when the polymer is involved in the stabilization of AAC initially formed. Thus, in the case of spherulitic crystal growth mechanism proposed for PAA system, crystallization will lead to incorporation of the PAA chains (that are responsible of stabilization of spherical ACC-gel) as the crystals grow. Crystals that have uniform morphology such as those shown in Fig. 5.2 and Fig. 5.3 are likely to be nucleated and grow via a similar mechanism. However, it is difficult to differentiate between crystals that followed classical and non-classic mechanism (that result in mesocrystals) if the size of their primary ions were small enough that with the current tools used to image the crystals, the crystals appear to be single crystals. The crystals with mixed morphologies are likely to be nucleated via different mechanisms and the crystal growth mechanism is also different.

Statistical analysis and imaging of fractionated crystals showed that large crystals of high granularity were due to aggregation of primary crystals. The extent of aggregation depended on the initial concentration of the polymeric additive used. It was also shown by other authors that the amount of polymeric additive on the surface of the crystals help in crystal stabilization.[15] In this study, it was found hat the crystal growth modifier was not homogeneously distributed in the crystals since the crystals of the same size or granularity were found to have different amounts of fluorescence. Although it is reported in literature that monodispersed crystal size would mean that crystal nucleation and growth was homogenous,[17,18] the actual crystal growth process can be complex. The amount of polymeric additive inside the crystal can be related to the initial amount of polymeric additive responsible for the stabilization of the ACC and the rest of the polymeric additive is absorbed (PAA) or adsorbed (starch). Adsorption and/or absorption of polymeric additive may occur during and after the crystal growth process. The spherical crystal morphology and size can be close to 1:1 copy of the ACC-PAA gel domains. The ACC is the least stable form of $CaCO_3$, and it was found to adapt any shape as directed by the polymeric additives.[15] Stabilized spherical nanometer-sized ACC particles were synthesized by Gorna *et al.*[15] The secondary inclusion of the polymeric additive that occurs during crystallization (after ACC stabilization) may not change the crystal morphology but have an effect on the stability of the less thermodynamic stable $CaCO_3$ polymorphs. The polymeric additive can prevent the dissolution (of the least stable polymorphs) and the recrystallization process (that results in a stable polymorph). When 0.65 g/L PAA grafted starch concentration was used, the morphology of the ACC was not dictated by the polymeric additive but by the concentration of the ACC precursor ions. Furthermore, if the ACC was formed initially, its stability would be low and, could easily dissolve and recrystallize forming thermodynamically stable polymorphs. Thus, the process of recrystallization occurred under little or no influence of the polymeric additive resulting in mixed crystal morphologies. Rates of crystallization are faster when crystal growth is independent of the crystal growth modifier as found in Section 4.3.1. Thus, fluorescence observed for $CaCO_3$ (3) was due to absorption/adsorption of the polymeric additive on the surface of the crystals.

5.4: Conclusions

The $CaCO_3$ crystals synthesized in the presence of fluorescence-tagged crystal growth modifier fluoresced under UV irradiation showing the presence of the polysaccharide on the surface of the crystals. Fluorescence allowed a study of agglomeration and growth habits of the crystals. A novel approach for characterization of $CaCO_3$ crystals using flow cytometry was successful. Statistical

analysis showed that most of the crystals fluoresced, with crystals of high granularity and large size fluorescing more than crystals of low granularity and small size. Thus, the fluorescence in crystals increased with increasing size and granularity of $CaCO_3$ crystals. The non-classical mechanism of crystal growth leading to polycrystalline crystals was proposed for large crystals with high granularity as well as smaller crystals with high granularity. Reducing the concentration of the polymeric additive resulted in an increase in the number of crystals of high granularity and large in size. The zeta potential measurements showed that the use of anionic starch in $CaCO_3$ crystallization resulted in anionically charged crystals, due to the presence of anionic polysaccharide. Coating of the crystals with cationic starch inverted the surface charge on the $CaCO_3$ crystals. TGA and FT-IR results corroborated the presence of polysaccharide in the $CaCO_3$ crystals. The average flocculant size of crystallized calcium carbonate increased when cationic starch was added. The fluorescing $CaCO_3$ can be used as tagging material for paper products. The inclusion of these fluorescing filler materials during papermaking will result in their retention leading to a paper that fluoresces under UV light.

5.6: References

(1)   Suty, S., Luzakova V. *Colloids and Surfaces A: Physicochemical Engineering Aspects* **1998**, *139*, 271-278.

(2)   Knez, S., Klinar D., Golob J. *Chemical Engineering Science* **2006**, *61*, 5867-5880.

(3)   Rogan, K. R., Bentham A. C., George I. A., Skuse P. R. *Colloid and Polymer Science* **1994**, *272(10)*, 1175-1189.

(4)   Jada, A., Verraes A. *Colloids Surf., A: Physicochem. Eng. Aspects* **2003**, *219(1-3)*, 7-15.

(5)   Attard, P. *Current Opinion in Colloid and Interface Science* **2001**, *6*, 366-371.

(6)   Dudman, W. F., Bishop C. T. *Canadian Journal of Chemistry* **1968**, *46*, 3079-3081.

(7)   Horton, D., Philips K. D. *Carbohydrate Research* **1973**, *30*, 375-378.

(8)   Cai, K., Frant M., Bossert J., Hildebrand G., Liefeith K., Jandt K.D. *Colloid and Surfaces B: Biointerface* **2006**, *50*, 1-8.

(9)   Werner, C., Korber H., Zimmermann R., Dukhin S., Jacobasch H-J. *Journal of Colloid and Interface Science* **1998**, *208*, 329-346.

(10)   Valdivieso, A. L., Bahena J. L. R., Song S., Urbina R. H. *Journal of Colloid and Interface Science* **2006**, *298*, 1-5.

(11)   El-Sadi, H., Carreau P., Esmail N. *Journal of Colloid and Interface Science* **2004**, *271*, 496-503.

(12)   Ulcinas, A., Butler M. F., Heppenstal-Butler M., Singleton S., Miles M. J. *Journal of Crystal Growth* **2007**, *307*, 378-385.

(13)   Naka, K., Huang S-C ., Chuyo Y. *Langmuir* **2006**, *22*, 7760-7767.

(14)   Wang, T., Antonietti M., Zhao X., Colfen H. *Chemistry - A European Journal* **2006**, *12*, 5722-5730.

(15)   Gorna, K., Munoz-Espi R., Grohn F., Wegner G. *Macromolecular Bioscience* **2007**, *7*, 163-173.

(16)   Han, T. Y., Aizenberg J. *Chemistry of Materials* **2008**, *20*, 1064-1068.

(17)   Cheng, B., Lei M., Yu J., Zhao X. *Material Letters* **2004**, *58*, 1565-1570.

(18)   Yu, H., Lei M., Cheng B., Zhao X. *Journal of solid state chemistry* **2004**, *177*, 681-689.

Chapter 6: Testing modified polysaccharides in paper production

6.1: Introduction

The focus of this part of the study was to test the modified polymers for their efficiency in increasing the PCC loading in paper without having any adverse effects on the paper properties. The efficiency of the modified polymers was tested on their ability to promote the following types of bonding (see also Fig. 6.1):

    i)   fiber-fiber bonding

    ii) fiber-filler bonding

    iii) filler-filler bonding
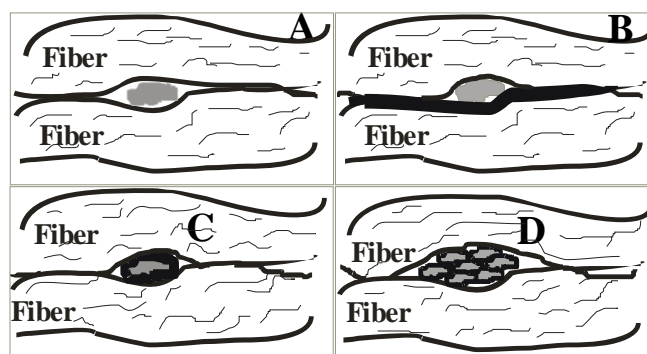
Fig. 6.1: Schematic representation of different types of bonding: (A) no bonding, (B) fiber-fiber bonding, (C) fiber-filler bonding and (D) filler-filler bonding.[1]

There is need to balance the quantity of filler added to paper and the overall properties of the paper. Increasing the filler content generally results in disruption of the fiber-fiber bonding strength and ultimately the strength of the paper is reduced.[1,2] The size and morphology of the filler is also of paramount importance and should be considered when selecting fillers. It has been shown that the smallest fillers have the most negative effects on paper strength, and lamellar type fillers have less detrimental effects than bulky fillers.[1,2] On the other hand, polymeric additives have a positive effect on fiber-fiber bonding/adhesion.[3-7] Furthermore polymers with carboxyl functionality have a binding affinity for PCC filler.

The paper industry use different additives to promote fiber-fiber bonding (hemi cellulose, cationic starch) and filler retention materials (polyacrylamide and short chain polyacrylic acid. Therefore chemically bonding the current additives by grafting techniques may also promote fiber-filler bonding as well as filler retention. Thus, in this section, polymeric additives that have binding affinity for both cellulose fiber and PCC are used to promote both the fiber-fiber and the fiber-filler bonding, to increase high PCC loading in paper without changing the paper strength.

6.2: Addition of PCC retention aids

There are several ways in which the polymers can be added to the paper (at stage A or B, as shown in Scheme 6.1). Generally, PCC for papermaking is formed from a sub plant and then channeled to a mixer where it is blended with treated pulp. The resulting slurry is then used for papermaking. The additives are introduced at different points along the papermaking plant. Thus, addition of the modified polysaccharides should be strategized in order to confer optimum performance towards their intended function.
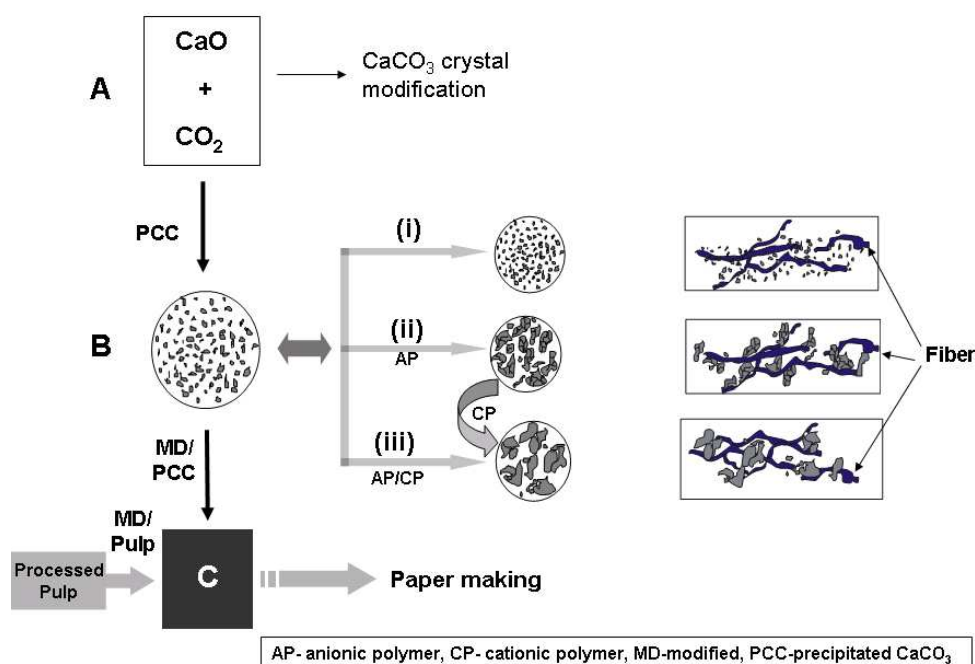
Scheme 6.1: Possible ways of introducing polymers to paper during paper production.

The different ways of introducing polymeric additives (as shown in Scheme 6.1) are described as follows:

Stage A

PCC is produced via the reaction of CaO and CO_2 resulting in calcium carbonate crystals with an average size of 3 µm. Addition of polymers at this stage would result in calcium carbonate crystal modification. More importantly, the filler formed would have its surface modified with the polysaccharide (as described in Section 5.4) when a soluble starch derived polymeric additive is used. Filler surface modification can be done during or after the precipitation process, whereby a second polysaccharide of opposite charge to that of the $CaCO_3$ particles is deposited onto the

surface of the filler. Thus, polysaccharide coated filler could result in increased filler retention and better fiber-filler bonding strength. If an insoluble modified polysaccharide such as modified cellulose fiber is added at stage A, then crystallization of the filler would occur on the surface of the fiber, as was described in Section 4.3.3. Ultimately this could lead to improved filler retention. The drawback of implementing this process in industry is the need for major plant modification.

Stage B

Stage B is easy to implement as it is compatible with the existing plant. However, there are various ways of adding the modified polymers, denoted as method (i)–(iii). The methods differ in the order of addition of polymers to both PCC and fiber.

Method (i)

Method (i) involves treating the fiber with anionic modified polysaccharides. The effective net charge of the fiber should be negative after treatment to allow the binding of PCC through the carboxylate groups. It is also necessary to optimize the net charge of the paper components to have a good performance of the paper additives. Then addition of cationic starch will be done to promote fiber-fiber bonding as well as fiber-filler bonding (according to the current procedures for hand sheet making, shown later in Scheme 6.4).

Method (ii)

In method (ii), PCC is treated with anionic polymer (AP) and this leads to flocculation of PCC forming relatively large particles, as described in Section 3.4.3. The flocculated particles would therefore carry a negative charge and the surface is likely to have adsorbed polysaccharides. On the other hand, the fiber is separately treated with the cationic polymer (CP) and therefore will carry a positive charge. The PCC/AP is then mixed with the fiber/CP and retention of PCC is expected via ionic interaction as well as hydrogen bonding between the polysaccharides and the fiber. The particle size of flocculated PCC should be optimum to prevent adverse effects on paper such as loss in paper strength, burst strength, etc. and the size of PCC flocculants depends on the concentration of the AP used (see Section 3.4.3.1).

Method (iii)

Method (iii) can be carried out in two ways, by either flocculating PCC using a mixture of CP and AP in different ratios, or in a sequential addition, starting with AP followed by CP (see Section 3.4.3.4). In either case, large particle sizes are obtained. However, the sequential method is expected to give particles with a net positive charge on the surface. The modified PCC will then be mixed with the fiber. It is important to note that the size of flocculants can be easily manipulated by varying the modified polymer concentration. Thus there is a need to find the critical size of

flocculants that gives the best paper properties. The ratio of anionic to cationic species needs to be balanced as an excess of either species may lead to detrimental effects such as the printability of the paper.

6.3: Experimental

Materials

Pulp cellulose (Mondi), cationic starch (Mondi), anionic starch (as described in Section 3.2.2), PCC (Mondi) and bentonite (Mondi Business Paper)

6.3.1: Preparation of anionic-starch-coated starch particles

Starch materials (swollen or fully dissolved) are mainly used to improve paper strength[5] and as such anionic starch coated starch particles were prepared. The swollen starch particles are capable of filling the flaws and binding the fiber and filler together, resulting in superior paper properties. An example of a SEM image of swollen anionic starch coated starch particles is shown in Fig. F1, in Appendix F. The size of the starch granules increases when swollen, depending on the level of swelling. An extreme swelling result in the particles bursting and distortion of the particle morphology occurs. The anionic-starch-coated starch particles were synthesized as described in Scheme 6.2.
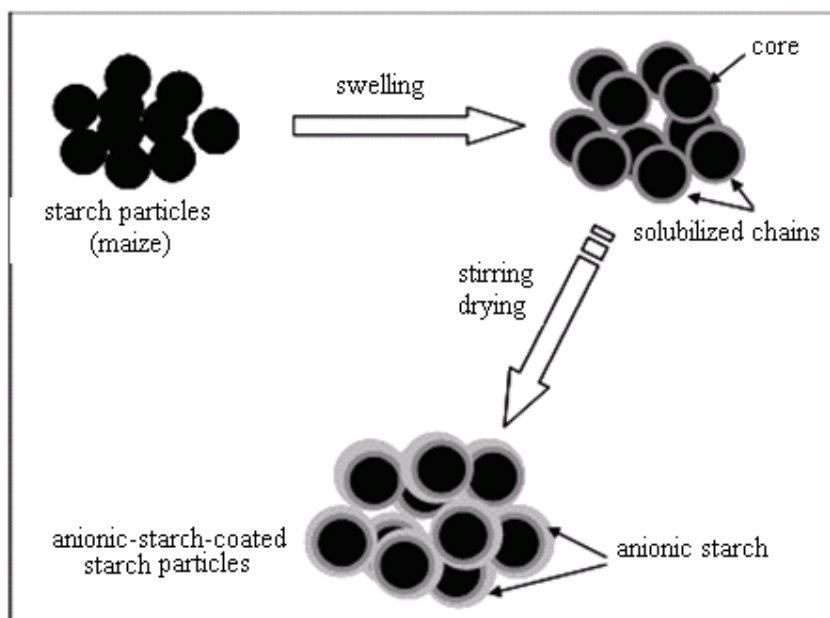
Scheme 6.2: Preparation of charged starch particles

119

Procedure. The anionic starch materials prepared as described in Section 3.2.2 were used to prepare anionic-starch-coated starch particles. In a typical preparation, the anionic starch was dissolved in deionized water to form a slurry of 10–30% solids. The maize starch particles were then added in their semi-swollen form to the slurry of anionically modified starch in different ratios of dry grafted material to starch particles w/w (1:1 to 1:3) followed by swelling the mixture at high stirring. The temperature was kept at 50 ^{o}C to avoid dissolving the starch particles. Thus, the change in particles morphology was minimized. The thick slurry was placed in ethanol for solvent exchange to allow the material to be ground into powder. The starch particles were then dried at ambient temperature and ground to powder. Application of these particles to papermaking was done in the swollen state.
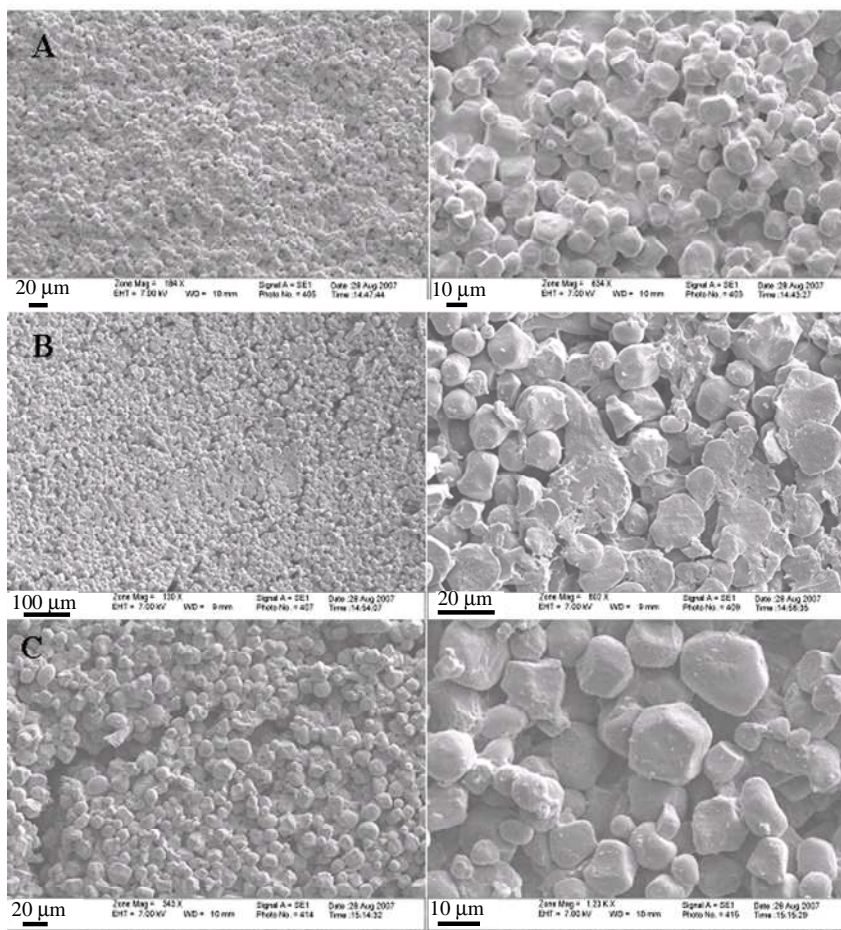
Fig. 6.2: SEM images of anionic-starch-coated starch particles in the ratios (A) 1:1, labeled HM 36, (B) 1:2, labeled HM 37 and (C) 1:3, labeled HM 38.

The anionic-starch-coated starch particles showed some flocculation properties (Fig. 6.3). However the particle size of the flocculants decreased with decreasing anionic starch to maize starch particles ratio. This was expected as addition of starch particles result in a decrease in the concentration of the flocculating agent. The broadness of the particle size distribution also decreased with decreasing anionic starch to maize starch particles ratio. It must also be mentioned that the particle size of the flocculants is also a function of stirring rate, concentration of the flocculating agent, pH of solution and time of stirring. However, all these parameters were kept constant, unless mentioned. One of the key points in using swollen starch particles is that they can easily be retained during papermaking via size exclusion during drainage.
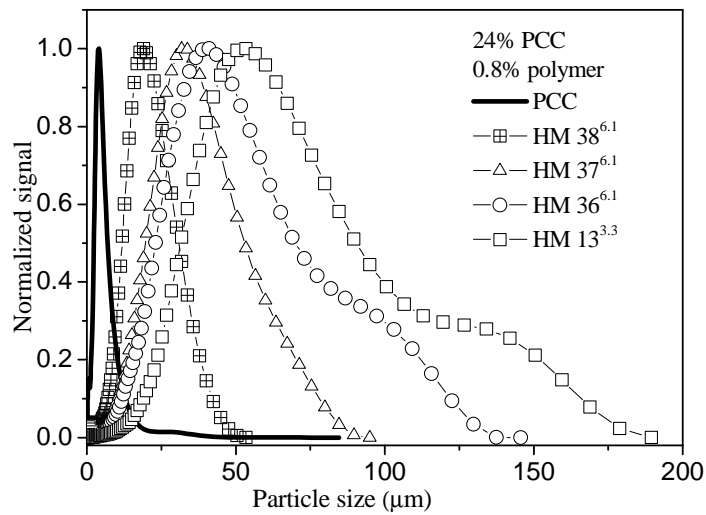
Fig. 6.3: The flocculation properties of modified starch coated starch particles.
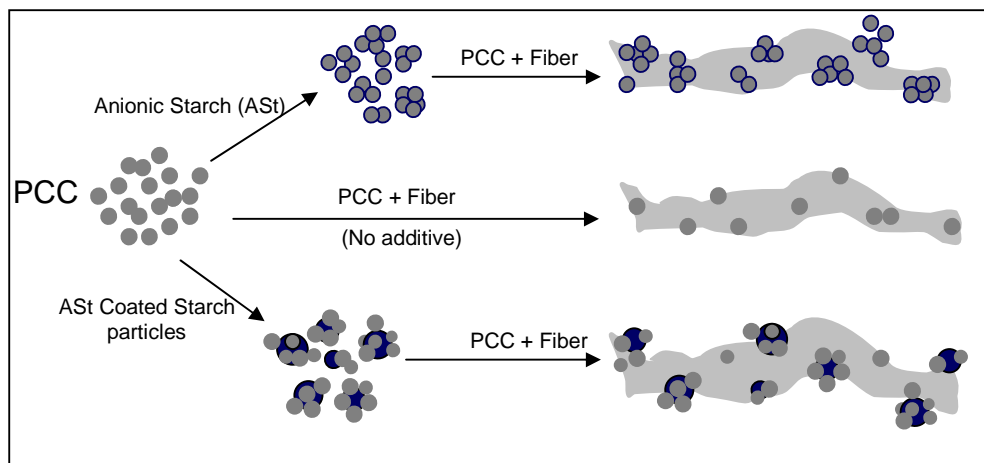
Scheme 6.3: Proposed interactions between PCC, polymer additives and the fiber

The size of swollen starch granules is larger than that of PCC particles. Thus, although the anionic starch and anionic-starch-coated starch particles are both PCC flocculants, the latter is expected to eliminate filler-filler bonding (by acting as a spacer as shown in Scheme 6.3). The result would be an increase in PCC retention and tensile properties induced by the starch particles.

Table 6.1: The code of anionic-starch-coated starch particles and the anionic starch graft copolymers used to make them

Code	Description
HM $6^{3.2}$	Anionic starch
HM $13^{3.3}$	Anionic starch
HM 36	HM $2^{3.2}$ + Maize starch particles (1:1)
HM 37	HM $2^{3.2}$ + Maize starch particles (1:2)
HM 38	HM $14^{3.3}$ + Maize starch particles (1:3)
HM 39	HM $6^{3.2}$ + Cationic starch particles (1:1)
HM 40	HM $6^{3.2}$ + Cationic starch particles (2:1)

The superscripts represent the table number where the material was described.

The anionic-starch-coated starch particles in Table 6.2 were made as described in Section 6.3.1. The SEM images as well as the flocculation properties are reported in the Appendix E, Figs E1–E4. The flocculation experiments took into consideration the ratio of PCC to anionic polymer additive in papermaking. All materials were PCC flocculants.

Table 6.2: The codes of the anionic-starch-coated starch particles and the anionic starch graft copolymers used to make them

Code	Description
HM 41	HM $14^{3.3}$ + maize starch (1:1)
HM 42	HM $14^{3.3}$ + maize starch (1:2)
HM 43	HM $14^{3.3}$ + maize starch (1:3)
HM 44	HM $8^{3.2}$ + maize starch (1:1)
HM 45	HM $8^{3.2}$ + maize starch (1:2)
HM 46	HM $8^{3.2}$ + maize starch (1:3)
HM 47	HM $16^{3.4}$ + maize starch (1:1)
HM 48	HM $16^{3.4}$ + maize starch (1:2)
HM 49	HM $16^{3.4}$ + maize starch (1:3)

The numbers in superscripts represent the table numbers in Chapter 3

6.3.2: Hand sheet making procedure

A general procedure for the fabrication of hand sheets was provided by Mondi Business Paper (Austria) with some minor alterations. In all experiments, unless mentioned otherwise, the anionic starch additive was 2% of the PCC, the cationic starch was 0.8% of the pulp per sheet, and the bentonite was 0.1% of the pulp per sheet. The anionic starch polymer was added either to PCC or pulp fiber. The hand sheets were made according to Scheme 6.2.
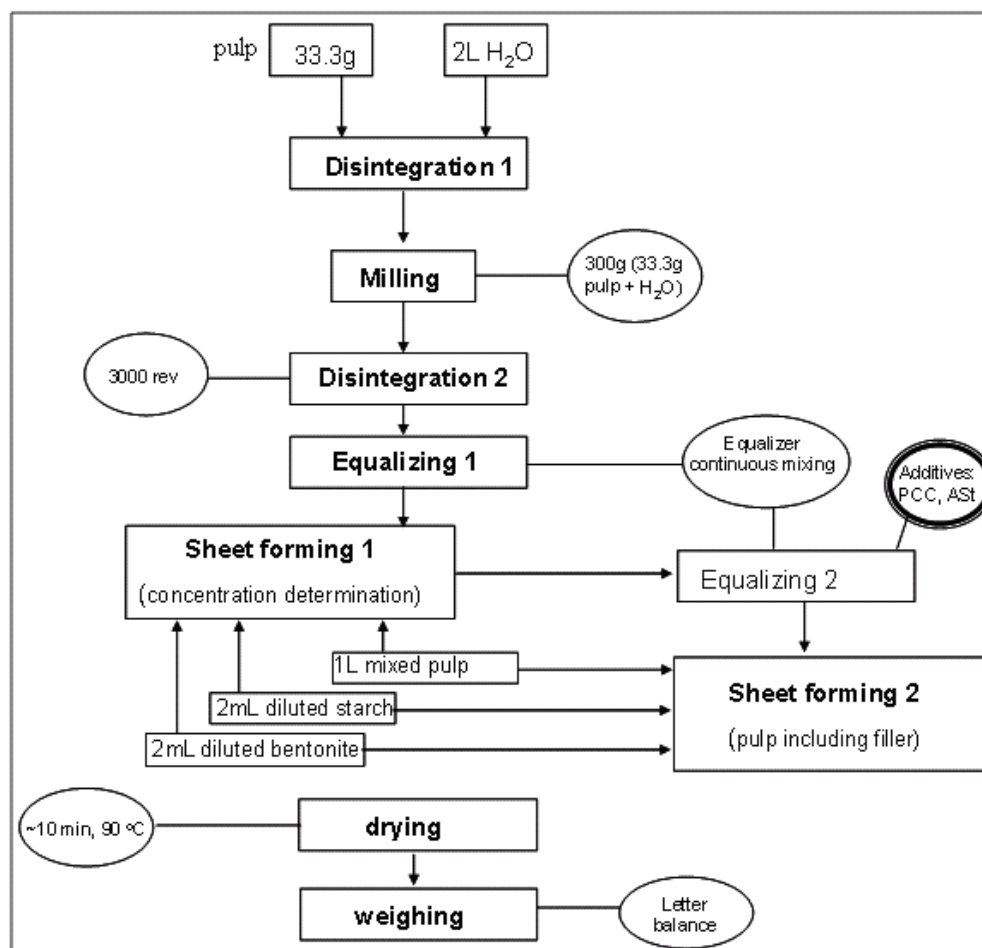
Scheme 6.4: The papermaking flow chart used in this study

6.3.3: Instrumentation

All instruments and testing procedures were provided by Mondi Business Paper (Austria)

L & W Gurley air resistance tester

In the Gurley air permeance tester, the air is forced through a sheet of paper by the fall of an inverted cylinder floating freely in an outside cylinder which is partly filled with oil. It measures the air permeance, i.e. air resistance.

"Canadian Standard" freeness tester

The tester is designed to provide a measure of the rate at which a dilute pulp suspension may be dewatered. The Canadian Standard Freeness (CSF) is related to the surface condition and swelling of fibers. The CSF gives a useful index of the amount of mechanical treatment to which the pulp was subjected to. Increasing fiber refining level results in a decrease in the CSF. The CSF is also referred to as 'drainability' and is designed to provide a measure of the rate at which a dilute suspension of pulp can be dewatered.

Bendtsen porosity tester

This instrument measures air permeability (i.e. the flow rate of air through a sheet of paper) at $23 \pm 3\ ^{o}C$.

Bursting strength tester

A test piece is placed over a circular diaphragm and rigidly clamped at the periphery but is free to bulge with the diaphragm. Hydraulic fluid is then pumped at a constant rate, bulging the diaphragm until the test piece ruptures. Thus the bursting strength of the test piece is the maximum value of the applied hydraulic pressure at rupture (KPa).

Micrometer (L & W)

The micrometer was used to measure the thickness of the hand sheets.

L & W stiffness tester

This instrument measures the force required to bend a test piece at one end through a given angle. The force is applied at a constant distance from the time of clamping. Stiffness is the degree of resistance offered by paper when it is bending under specified conditions.

Alwetron TH1 (computerized) tensile strength tester

For this test the test pieces are cut using a sample cutter D054. The instrument measures the tensile strength, stretch and tensile energy absorption.

Tensile strength is the maximum tensile force per unit width that a test piece of paper will withstand before breaking (KN/m).

Stretch is the ratio of the increase in length of the test piece of paper at the moment when maximum tensile force is reached to its original length before test, expressed as a percentage.

Tensile energy absorption is the total work done per unit area of the paper when stretching it to rupture (J/m^2).

Drainage is the time taken by water to pass through the sieve during papermaking and depends on the fiber refining and flocculation, as well as filler content (s).

6.4: Results and discussion

6.4.1: Effect of fiber refining on paper properties

A study on the effect of fiber refining on the properties of both unfilled (no filler) and filled (filler added) paper properties was carried out. The results thereof are reported in Sections 6.4.1.1–6.4.1.3 and all the figures are in Appendix H.

6.4.1.1: Fiber refining

The fiber was refined at various revolutions (rev) from 0 rev. (no refining) up to 6000 rev. Fiber refining changes the morphology of the fiber. As the refining revolutions are increased, the fibers collapse and fibrillation occurs. At high revolutions total collapsing of the fiber with more fibrillation will occur. Fig. H1 (Appendix H) shows that the fibrillation (fiber damage) and collapsing increases with increasing revolutions. Fiber fibrillation and collapsing is essential as it affects most of the properties of paper. Thus, the fiber refining process results in an increase in surface area for fiber-fiber and fiber filler interactions.

6.4.1.2: The effect of fiber refining on unfilled paper properties

Fig. H2 (Appendix H) shows the effect of fiber refining on the CSF and the drainage during hand sheet making. The CSF decreases whilst the drainage increases with increasing fiber refining. The apparent sheet density of unfilled hand sheets increased with increasing fiber refining (Fig. H2B), indicating that the sheet became thinner with increasing fiber refining. Thus, the unfilled paper loses its bulkiness with increasing refining, which is not desired. Fig. H2C shows that there was an increase in the burst index, stretch and tensile stiffness with increasing refining, which is desired in most paper grades. The tensile energy absorption also increased with increasing fiber refining, meaning that the paper strength also increased with increasing fiber refining. The Gurley porosity and Bendtsen smoothness also improved with increasing fiber refining (Fig. H2D). However, the trend obtained for bending stiffness was different from the other properties. Maximum bending stiffness was obtained at 500 rev., after which it decreased and leveled out. Since fiber refining results in fibers collapsing and fibrillation, ultimately, due to these effects, the surface area for fiber-fiber interaction increases. An increase in the surface area for interactions favors most of the desired paper properties except the bending stiffness. This is partially because the thickness of the paper decreases with increasing refining, as shown in Fig. H3. The results of this study show that the

intrinsic properties of fiber have less effect on the bending stiffness of the paper but on the other properties.

6.4.1.3: The effect of fiber refining on filled paper properties

There was no anionic starch polymer added in these hand sheets and the curves serve as controls/references. The grammage of the hand sheets are shown in Fig. G1 in Appendix G. The effect of fiber refining was studied at three different PCC loadings. The drainage (not shown) decreased with increasing PCC loading and increased with increasing fiber refining. Fig. H4 (Appendix H) shows the effect of increasing the fiber refining level on the thickness of hand sheets. In the case of unfilled hand sheets, increasing fiber refining resulted in a decrease in the thickness of the hand sheets. The plot of retention versus PCC loading for hand sheets made with fiber refined at 3000 rev. and 0 rev. have PCC retention values in the expected range for no retention aids. The hand sheets made with fiber refined at 1000 rev. however had unexpected better retention. The thickness of the hand sheets was mainly a function of fiber refining rather than the PCC loading.

Fig. H5 shows that increasing fiber refining resulted in an increase in the apparent sheet density (i.e. reduction in the bulkiness of the hand sheets). The burst index and the apparent sheet density increased with increasing fiber refining, and slightly decreased with increasing filler loading, as shown in Fig. H5. The same trend was observed for the tensile index and stretch, as shown in Fig. H5. The Gurley air resistance and the Bendtsen smoothness improved with increasing refining and generally did not change much with increasing PCC loading, as shown in Fig. H5. The bending stiffness improved with increasing levels of fiber refining and decreased with increasing PCC loading (Fig. H5). An increase in the properties of paper with refining was attributed to the increased fiber-fiber as well as increased fiber-filler interactions, and a decrease in the properties with PCC loading was mainly due to disruption of fiber-fiber interactions caused by the presence of filler (PCC). The bending stiffness also increased with increasing fiber refining regardless of a decrease in the apparent sheet density. This was in contrast to what was observed for the unfilled paper (Fig. H2), where an increase in fiber refining did not lead to an increase in the bending stiffness throughout the entire refining range used. Another factor introduced for filled paper is the effect of fiber-filler interactions on the bending stiffness. In this case, increasing fiber-filler interaction (by increasing the level of fiber refining) resulted in an increase in bending stiffness.

6.4.2: The effect of anionically modified polysaccharides on filled paper properties

The modified starches were added to PCC and then the treated pulp was mixed with the pulp. In general, most of the properties of paper made with the flocculation aid were more or less the same as the control, as shown in Table 6.3. The polymeric additives HM $28^{3.6}$, HM $16^{3.4}$ and HM $17^{3.4}$ gave better retention at all PCC loadings compared to the control whereas the polymeric additives HM $1^{3.2}$, HM $15^{3.4}$ and HM $27^{3.6}$ gave PCC retention values that were lower than the control. The stiffness of paper to which anionic polymeric additives were added was better than the control, especially at 20% filler loading. Thus, although the materials HM $1^{3.2}$ HM $15^{3.4}$ and HM $27^{3.6}$ showed flocculation capability, their performance in papermaking was poor. The reason for low PCC retention for HM $15^{3.4}$ and HM $27^{3.6}$ was ineffective flocculation of PCC due to low % G. Polymeric additive HM $17^{3.4}$ gave good PCC retention at both 25 and 30% PCC loading. However, the porosity of the resulting paper was higher than that of the control paper. The bending stiffness of paper made with HM $17^{3.4}$ was better than that of the control paper with the other properties being more or less similar to that of the control paper as shown in Table 6.3. When HM $16^{3.4}$ (acrylic acid and acrylamide graft copolymerized on potato starch) was used as additive, the resulting paper had good PCC retention at 25 and 30% PCC loading. Furthermore, the bending stiffness was the best of all the additives used and the other properties were similar to the control paper. Factors that affect PCC retention include the size of PCC flocculants which decreases with an increase in the volume of water added to PCC, i.e. after the equalizing 1 stage (Scheme 6.4). The later tests were done by adding a constant volume of water (300 mL) to PCC to effectively flocculate PCC, and the rest of the water for equalization was added directly to pulp. Furthermore, the effect of fiber refining on the properties of paper is investigated in the later tests.

Table 6.3: Results of hand sheets made with anionic polysaccharides as retention aids (additives were added to pulp)

	Filler loading (%)	Filler Content (%)	Grammage (g/m²)	Thickness (µm)	Volume (cm^3)	Tear length	Tear resistance	Stiffness (mN)	Porosity (mL/min)	Opacity	Retention (%)
PCC	20	20.86	80.63	139	1.72	42	13	86	3786	86.85	85.3
PCC	25	25.85	80.50	137	1.7	36	10	92	4484	88.44	80.3
PCC	30	30.19	80.63	138	1.71	29	8	76	5106	88.64	76.1
HM 1$^{3.2}$	20	20.53	81.13	136	1.68	43	14	91	3609	87.12	84.6
HM 1$^{3.2}$	25	25.64	80.63	136	1.69	39	9	88	4019	88.45	79.7
HM 1$^{3.2}$	30	30.30	80.25	138	1.71	31	9	77	4342	88.75	76.1
HM 27$^{3.6}$	20	20.68	80.25	142	1.77	43	14	92	4077	86.30	84.2
HM 27$^{3.6}$	25	24.92	80.00	141	1.76	37	9	91	5000	87.19	77.0
HM 27$^{3.6}$	30	29.93	80.38	138	1.72	33	7	79	4168	88.59	75.3
HM 28$^{3.6}$	20	23.25	80.50	139	1.72	41	12	94	3969	87.24	94.9
HM 28$^{3.6}$	25	25.84	80.63	139	1.72	38	11	88	4536	87.73	80.3
HM 28$^{3.6}$	30	30.44	80.63	138	1.71	33	9	74	4174	88.78	76.7
HM 15$^{3.4}$	20	20.21	80.50	141	1.76	41	12	92	4339	86.71	82.4
HM 15$^{3.4}$	25	25.05	80.38	136	1.7	37	10	88	4395	87.73	77.5
HM 15$^{3.4}$	30	30.60	80.50	140	1.73	33	9	78	4014	89.01	77.0
HM 16$^{3.4}$	20	20.30	82.00	139	1.7	41	12	127	5000	87.48	89.5
HM 16$^{3.4}$	25	28.29	82.50	138	1.67	39	11	101	5000	88.64	90.4
HM 16$^{3.4}$	30	29.56	81.50	139	1.7	35	9	100	5000	89.14	80.3
HM 17$^{3.4}$	25	30.98	80.25	139	1.71	42	10	91	5000	88.84	90.2
HM 17$^{3.4}$	30	34.67	81.50	143	1.75	38	9	91	5000	88.72	90.8

6.4.3: The effect of modified starch coated starch particles

6.4.3.1: The effect of anionic starch particles HM 36[6.1]

Fig 6.4 shows the effect of polymer HM 36[6.1], fiber refining and filler content on the drainage and apparent sheet density. The drainage and apparent sheet density of the PCC filled hand sheets made with or without anionic polymer additive were similar at 1000 and 3000 rev., as shown in Fig. 6.4.
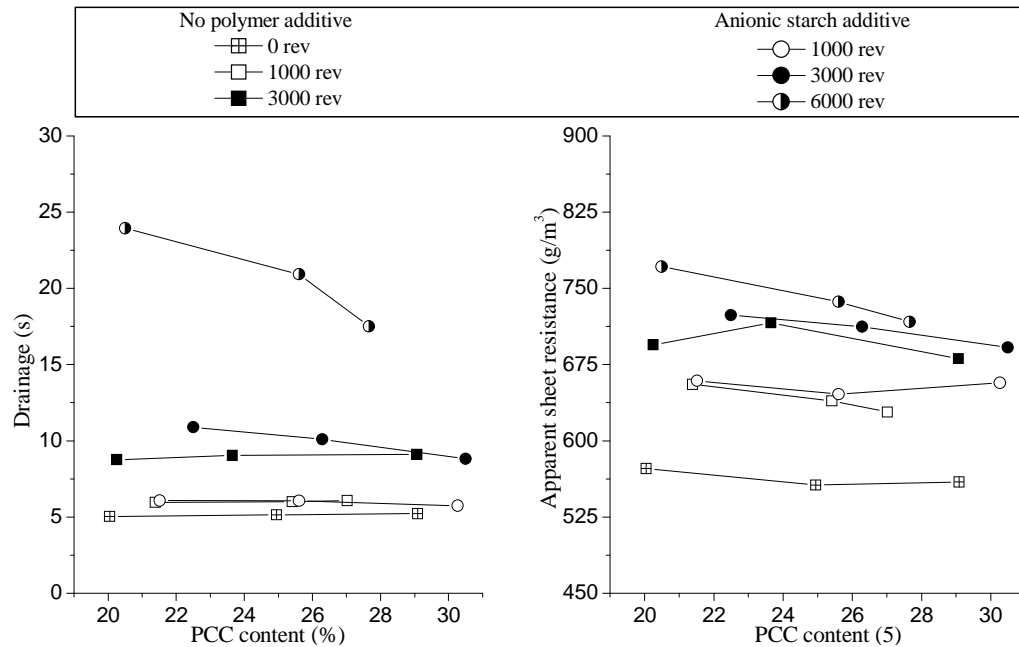

Fig. 6.4: Comparison of drainage and apparent sheet density between hand sheets made with and without anionic polymer additive (anionic-starch-coated starch particles HM 36[6.1] used).

Fig. 6.5 shows that PCC retention was higher for hand sheets made with anionic polymer additive HM 36[6.1] especially for the hand sheets made with fiber refined at 3000 rev. It was also observed that the retention was not, to a larger extent, a function of fiber refining but rather a contribution of a number of factors, which may include time of filler fiber interaction before making the hand sheet, effective particle size of the PCC, and the performance of the retention aids.

Fig. 6.6 compares the burst, tensile and stretch properties of the hand sheets made with or without anionic polymer additive were similar for fiber refining of 3000 rev. Generally minor differences were observed for fiber refining of 1000 rev. Hand sheets made with anionic polymer HM 36[6.1] showed better Gurley air resistance and Bendtsen smoothness. This is because the swollen starch particles fill the flows between the fiber and filler as well as between fibers. However, at fiber refining of 6000 rev., the hand sheets made with anionic starch polymer additive gave superior

properties compared to the ones at 1000 and 3000 rev refining. Although most of the properties were superior, the apparent sheet density increased, meaning that the paper was thinner. It can be seen that most of the properties were easily controlled by varying the level of fiber refining. However, the level of refining does not have much effect on the bending stiffness, as was found for unfilled paper (Fig. 6.5C).
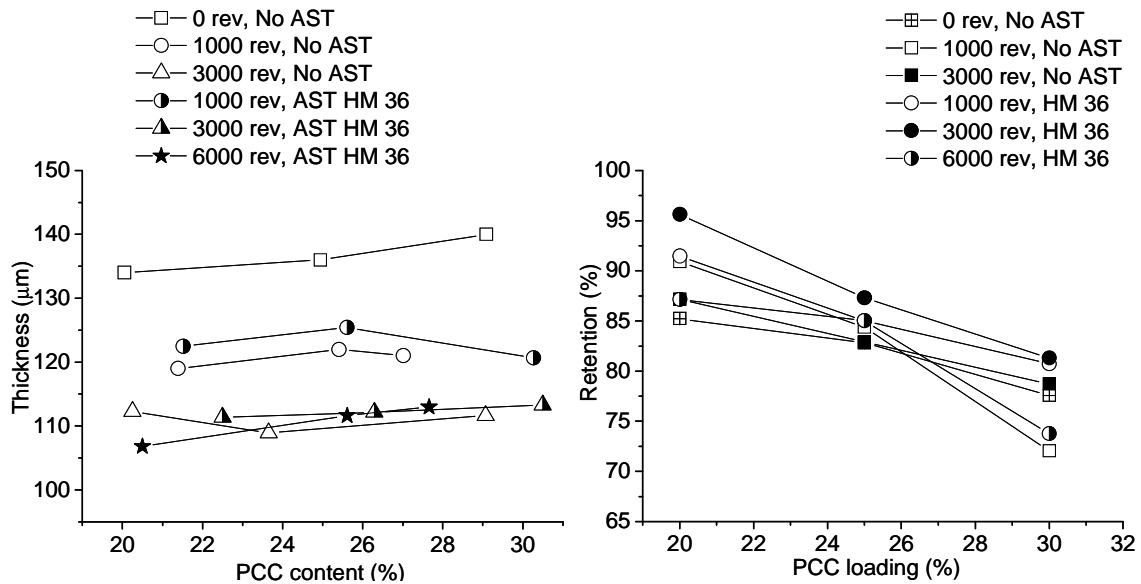

Fig. 6.5: A comparison in the thickness and PCC retention for hand sheets made without anionic starch additives and with anionic-starch-coated starch particles HM 36[6.1] at different fiber refining levels.

The difference between hand sheets made with and without anionic starch particles as additive is illustrated in graphs of property versus PCC loading (Fig. 6.6). There was a large improvement in the stiffness of paper for the hand sheets made with anionic starch polymer HM 36[6.1]. Even hand sheets made with a lower fiber refining had better stiffness compared to hand sheets made without anionic polymer but with a higher fiber refining level. It was also observed that the stiffness at the three different levels of fiber refining did not differ much. It is then evident that regardless of the level of fiber refining the stiffness of paper is affected by other factors, which may include the presence of crystalline starch particles and retention of PCC.
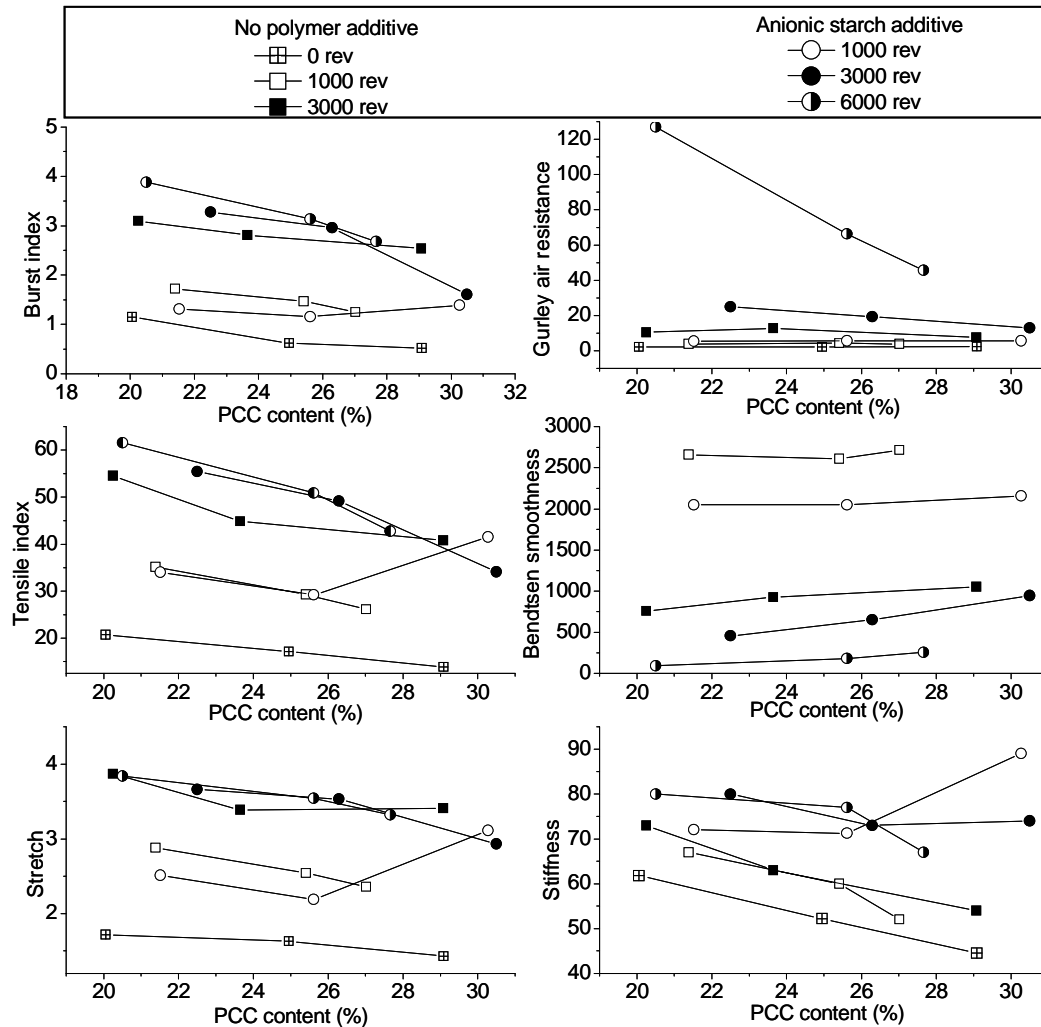
Fig. 6.6: Comparison between hand sheets made with and without anionic polymer additive (anionic-starch-coated starch particles HM 36[6.1]).

6.4.3.2: The effect of anionic starch particles HM 37[6.1]

The ratio of the grafted starch to maize starch particles was increased to 1:2 for polymer HM 37[6.1]. Fig. 6.7 compares the drainage and the apparent sheet density of the control hand sheets and hand sheets made with polymer HM 37[6.2]. The drainage was similar for the control and anionic starch particles HM 37[6.1] at 1000 and 3000 rev. However, apparent sheet densities were slightly different. Again it was noticed that increasing fiber refining resulted in an increase in the apparent sheet density of the filled paper. Similar behavior as was found for anionic polymer HM 36[6.1] was found for HM 37[6.1] (Fig. 6.8) where PCC retention was higher in hand sheets made with anionic polymer additives than without any retention aid. The thickness of hand sheets was influenced mainly by fiber refining and to a lesser degree by the extent of PCC retention.
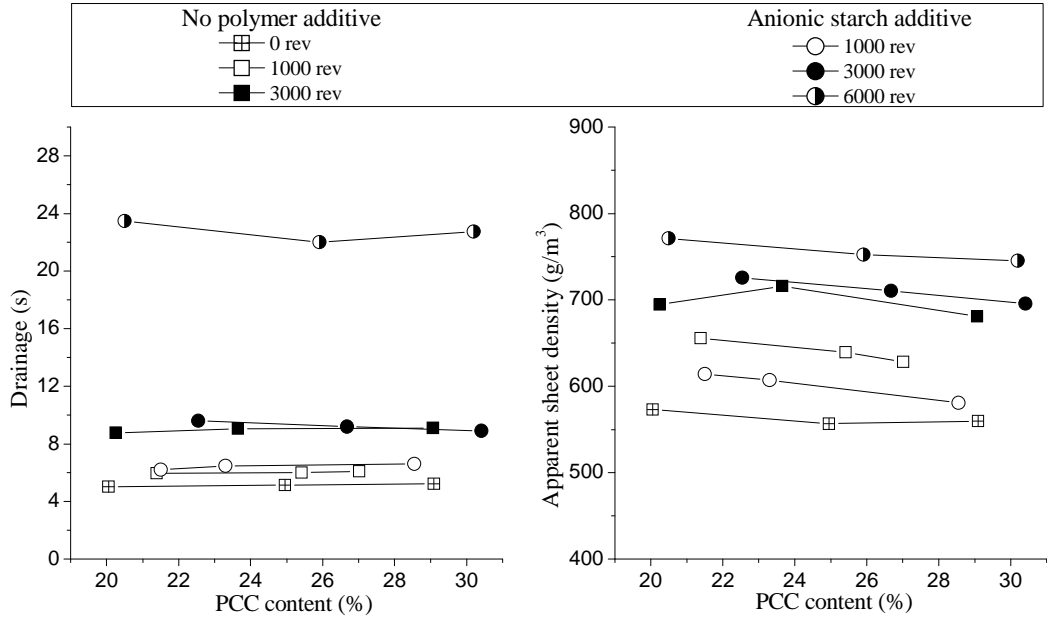
Fig. 6.7: Comparison between hand sheets made with and without anionic polymer additive (anionic-starch-coated starch particles HM 37[6.1] used).
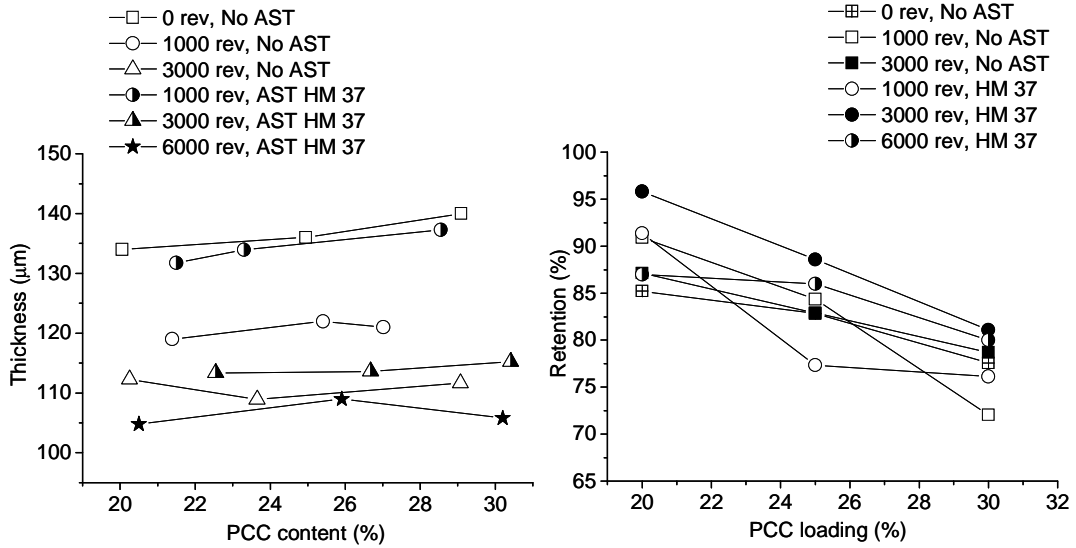

Fig. 6.8: Comparison of the thickness and PCC retention for hand sheets made without anionic starch additives and with anionic-starch-coated starch particles HM 37[6.1], at different fiber refining levels. (AST: anionic starch additive.)

The burst indices, tensile strength, and the stretch were relatively similar for the control (hand sheets made without any anionic polymer additive) and hand sheets for which anionic starch particles 37[6.1] was used at fiber refining levels of 1000 and 3000 rev. (Fig. 6.9). However, the hand sheets made with anionic polymer additive showed better Gurley air resistance, Bendtsen smoothness and bending stiffness. This was also found for anionic starch particles HM 37[6.1] and, in all cases, better properties were obtained with increasing fiber refining, for the reasons mentioned earlier (Section 6.4.2). Irrespective of the fiber refining level, the bending stiffness was better in hand sheets made with anionic starch additives than hand sheets made without anionic polymeric additives.
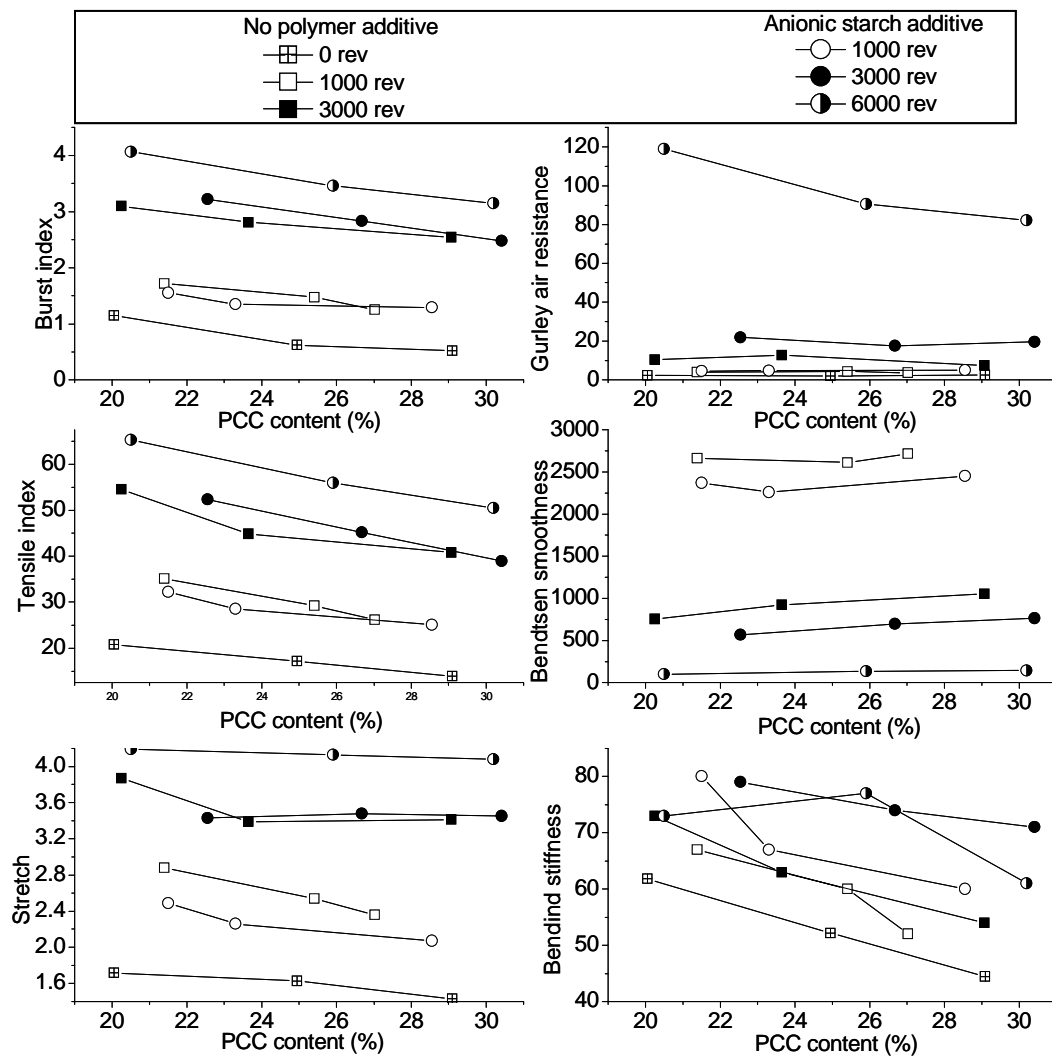

Fig. 6.9: Comparison between hand sheets made with and without anionic polymer additive (anionic-starch-coated starch particles HM 37[6.1] used).

6.4.3.3: Comparison between polymer HM 36[6.1] and HM 37[6.1]

HM 36[6.1] and HM 37[6.1] were different in the ratio of anionic starch to starch particles which were 1:1 and 1:2 for, respectively. The two polymers behaved in a similar manner in terms of the drainage and the apparent sheet density, except for the apparent sheet densities obtained at 1000 rev., as shown in Fig. 6.10. The thickness of hand sheets made with anionic polymers HM 36[6.1] and HM 37[6.1] were similar (Fig. 6.11) for fiber refining level of 3000 and 6000 rev. However, for fiber refining of 1000 rev., anionic polymer HM 37[6.1] gave thicker hand sheets. The PCC retentions were similar, particularly for fiber refined at 3000 rev., as shown in Fig. 6.11.
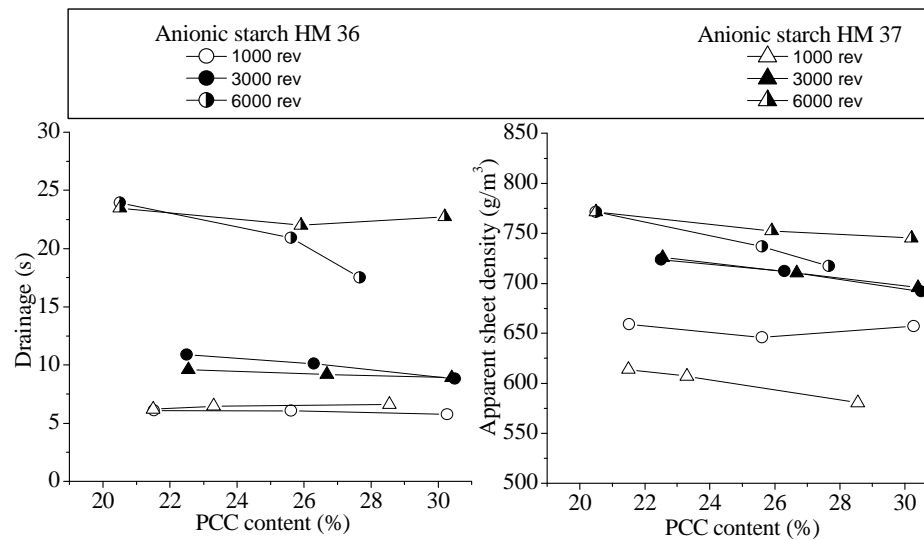

Fig. 6.10: Comparison between hand sheets made with different anionic-starch-coated starch particles (HM 36[6.1] and HM 37[6.1]) in terms of the drainage and sheet density.
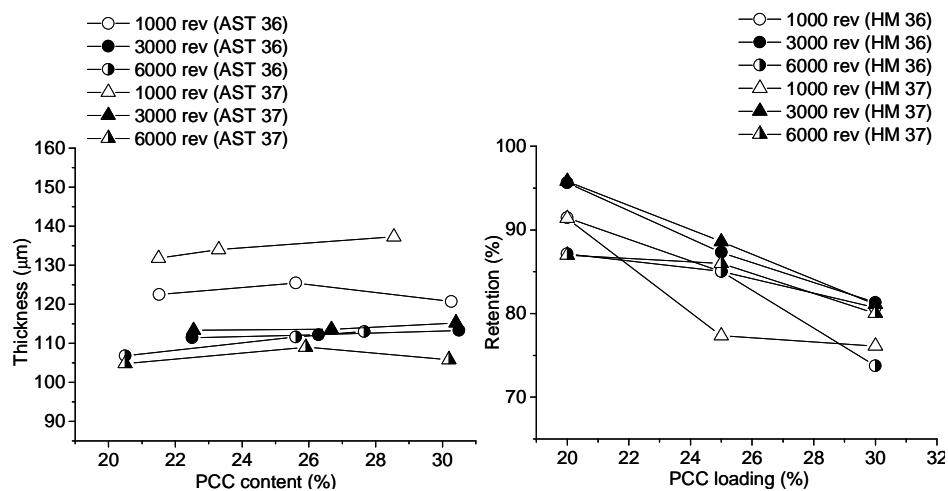
Fig. 6.11: Comparison in the thickness and PCC retention for hand sheets made with anionic-starch-coated starch particles HM 36[6.1] and HM 37[6.1], at different fiber refining levels.
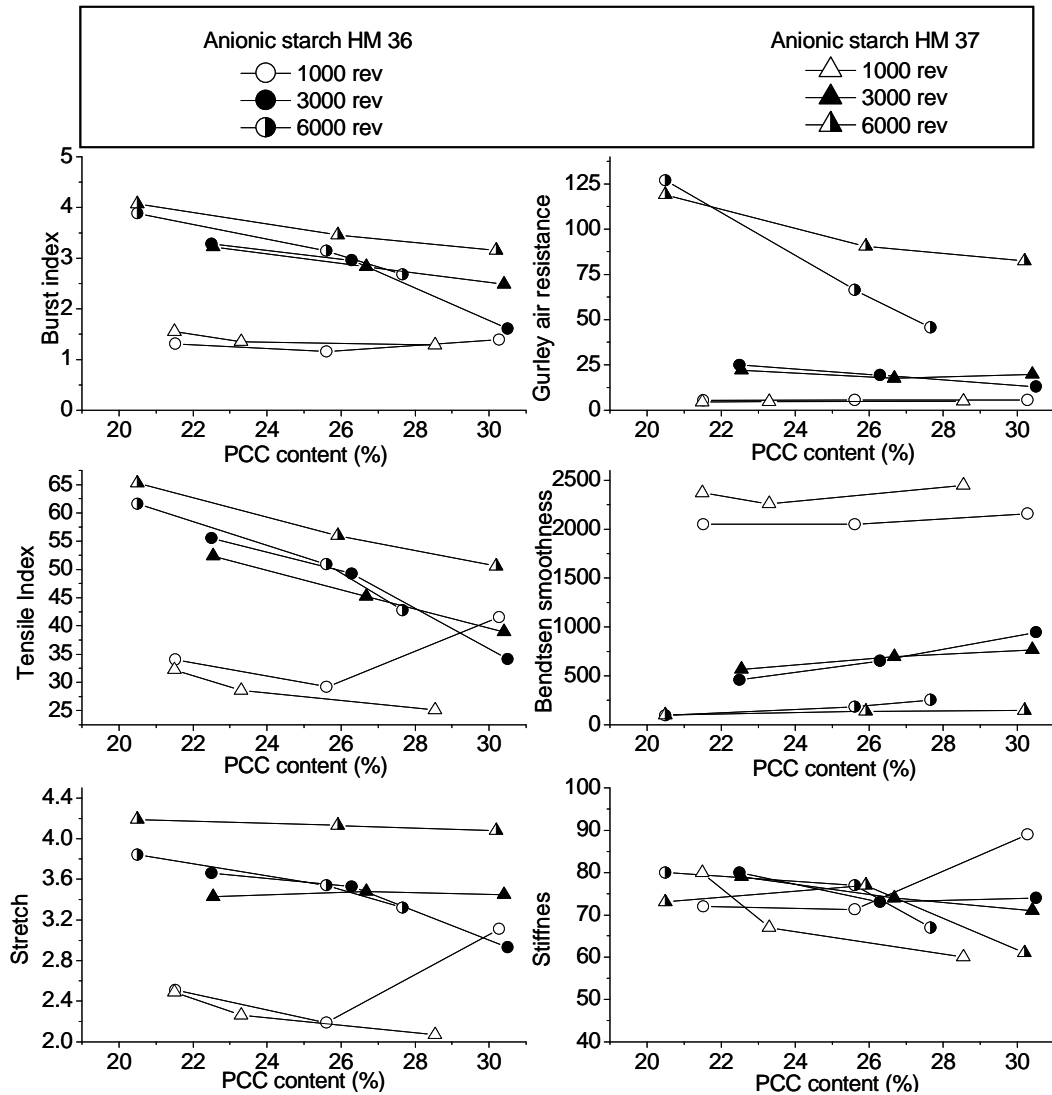
Fig. 6.12: Comparison between hand sheets made with different anionic-starch-coated starch particles (HM 36[6.1] and HM 37[6.1]).

6.4.3.4: Comparison plots of properties against apparent sheet density

The two polymeric additives HM 36[6.1] and HM 37[6.1] gave hand sheets with similar properties. However for fiber refining of 6000 rev., anionic polymer HM 37[6.1] gave better burst, tensile, stretch and Gurley air resistance (Fig. 6.12). Some minor differences in the properties of hand sheets (Fig. 6.12) can be attributed to small differences in the CSF values of the pulp used (i.e. differences in refining). The apparent sheet density was lower for polymers made with anionic polymer HM 37[6.1] at 1000 fiber refining, and this was irrespective of the fact that the drainage time was similar to that in the case of HM 36[6.1].
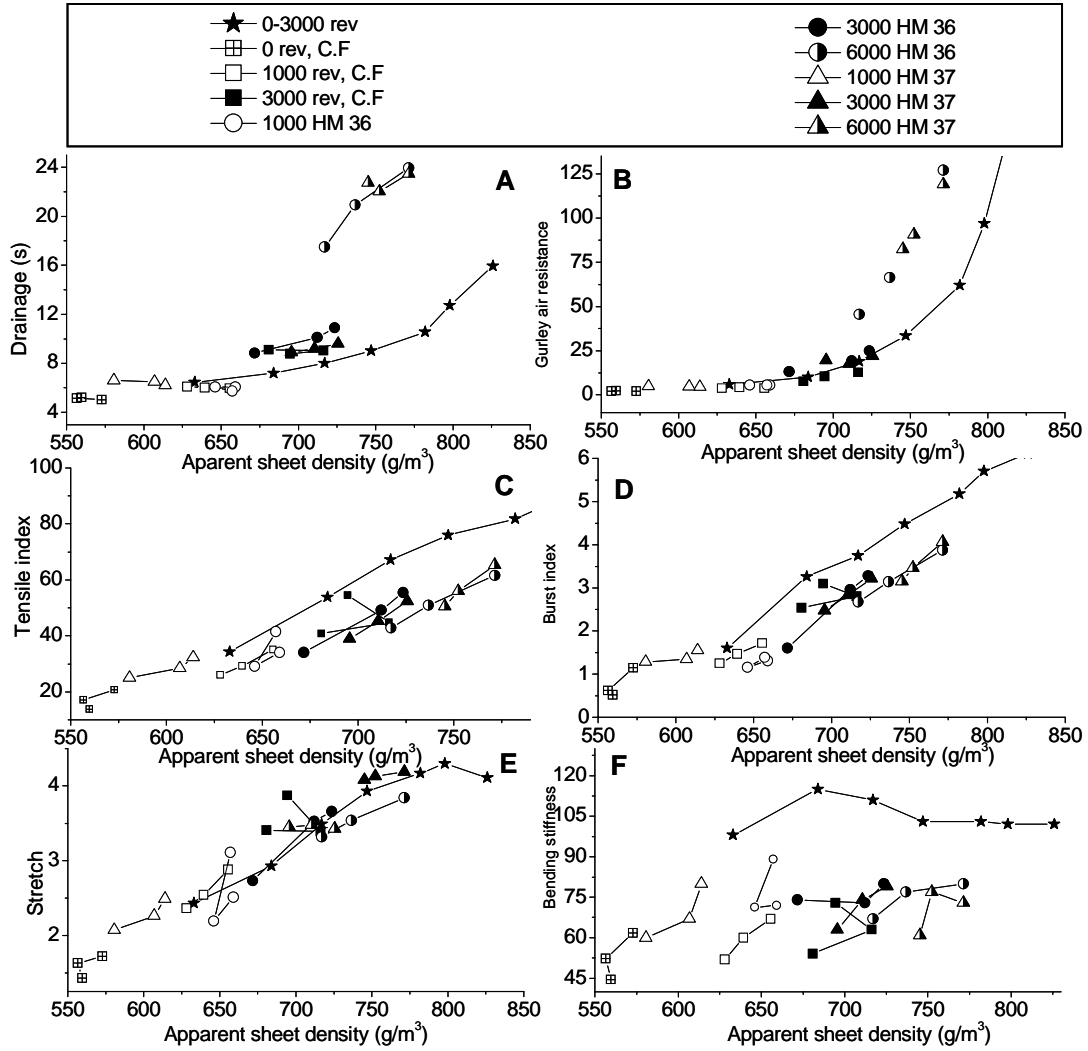
Fig. 6.13: Change in properties of paper with apparent sheet density and fiber refining. (C.F: control sheets for filled paper, i.e. paper made without anionic polymeric additive.)

The drainage increased with increasing fiber refining (Fig. 6.10A), however addition of PCC was shown to reduce the apparent sheet density, i.e. the paper became more bulky even for fiber refined at 6000 rev. when compared to the unfilled paper made with fiber refined at 6000 rev. At all levels of fiber refining the drainage was lower for hand sheets made with filler when compared to the drainage of hand sheets made without filler. The Gurley air resistance for PCC filled hand sheets was lower compared to the hand sheets made without PCC, thus the addition of PCC reduces the porosity of paper. From Fig. 6.13C, D, E and F it is evident that the addition of filler adversely affects the properties of unfilled paper (see curves with black stars that represent the properties of

136

hand sheets made without PCC at fiber refining of 0, 500, 1000, 1500, 2000, 2500 and 3000 rev. in the order of increasing apparent sheet density).

6.4.3.5: Comparison of anionic starch to anionic starch particles

The modified starch used to coat the maize starch granules was also used for papermaking on its own. The properties of the hand sheets formed were compared against the anionic starch coated starch particles as well as the control (see Figs 6.14 and 6.16). The fiber refining was done for 3000 rev. and the anionic starch content was kept constant.
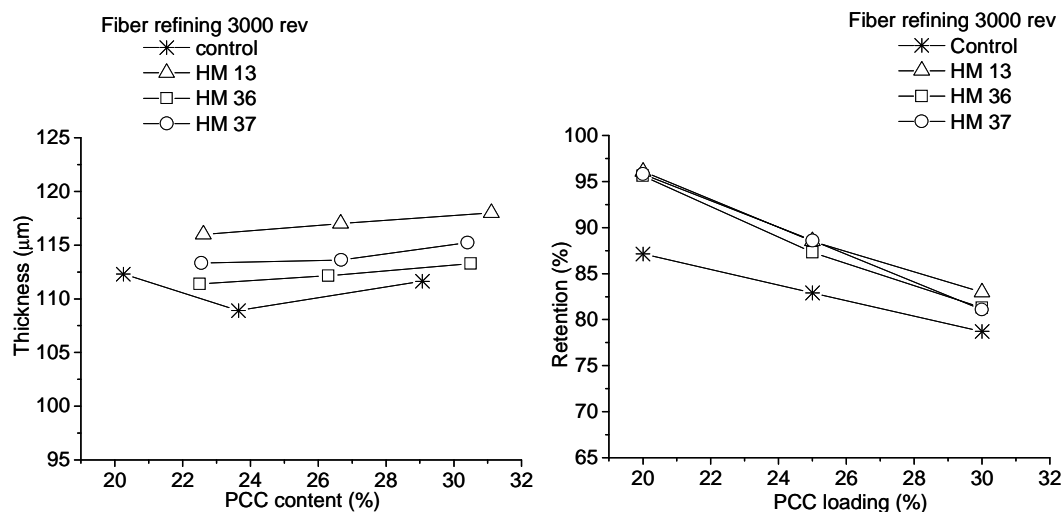
Fig. 6.14: Comparison of the thickness and PCC retention of hand sheets made without anionic starch additives, anionic starch (HM 13), and with anionic-starch-coated starch particles of different ratios of modified starch to starch particles (HM 36[6.1] and HM 37[6.1]).

The PCC retention for hand sheets made with anionic polymer additive HM 13 (no starch particles) was similar to that of HM 36[6.1] and HM 37[6.1] for fiber refined at 3000 rev. and at all three PCC loadings (Fig. 6.14). It was expected that addition of anionic polymers would result in different retentions due to different flocculation efficiencies. It must be mentioned that the ratios of anionic polymer additive to PCC used in flocculation experiments (Fig. 6.3) were much higher than the ratios used for hand sheet making. Thus, it is necessary to know effective particles sizes of PCC flocculants under hand sheet making conditions in order to be able to make conclusions regarding the effect of the anionic starch to starch particles ratio on the retention of PCC. Although the PCC retention values were similar, anionic polymer additive HM 13[3.3] gave thicker hand sheets compared to HM 36[6.1] and HM 37[6.1].

Fig. 6.15 shows the apparent sheet density for hand sheets made with anionic polymer HM 13[3.3] was lower (bulkier hand sheets obtained) than when the other three were used. These hand sheets had also inferior physical properties compared to the control except for the bending stiffness. It is possible that the size of the flocculants in these hand sheets was larger than those in the other hand sheets leading to bulkiness of the material and causing adverse effects on the other properties.
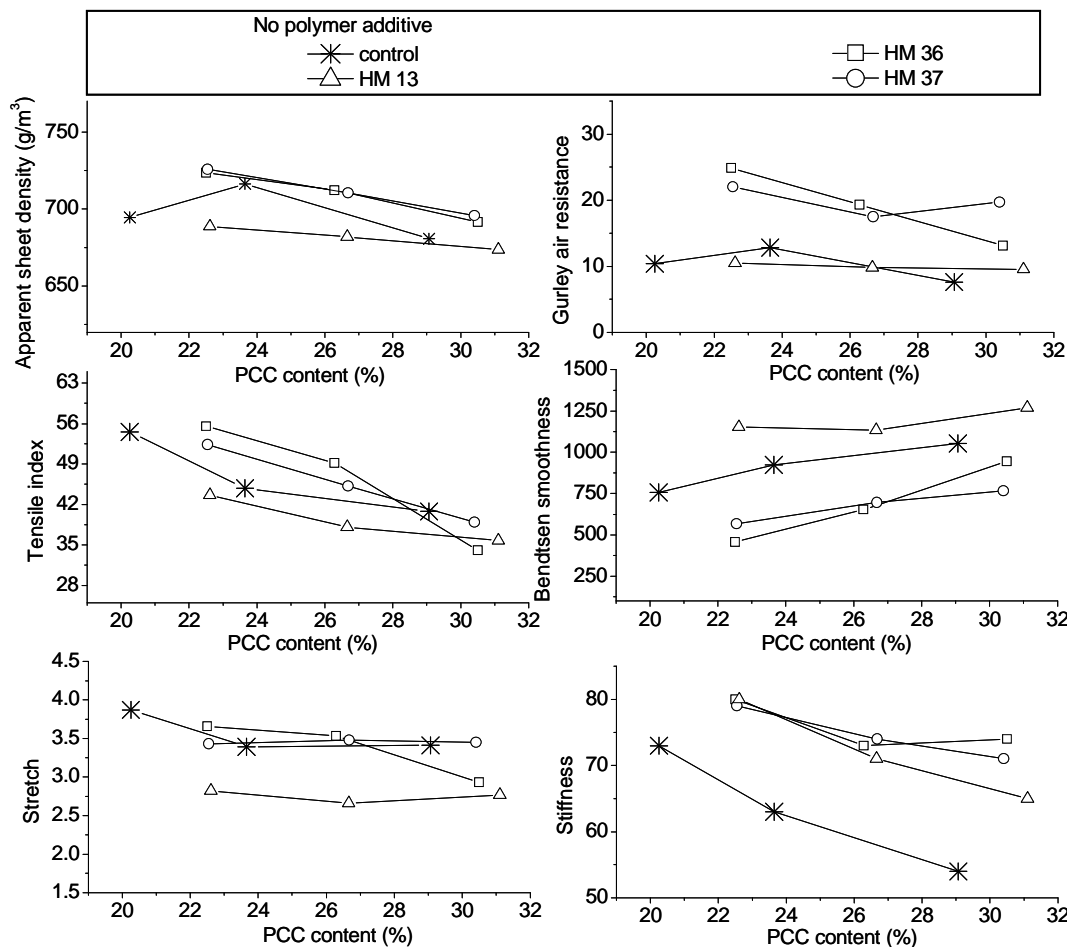

Fig. 6.15: Comparison of hand sheets made with different anionic polymer additives in terms of the ratio of modified starch to starch granules.

The resulting effect of superior flocculation caused a decrease in most of the properties (tensile index, tensile stretch, Bendtsen smoothness and the Gurley air resistance) compared to the control and the two blends HM 36[6.1] and HM 37[6.1]. It was also observed that most of the properties of hand sheets made with HM 13[3.3] as additive were also inferior to those obtained for control. Only the bending stiffness was better than in the case of the control. This can be attributed to the bulkiness of

the hand sheets made with anionic starch polymer HM $13^{3.3}$. It appears as if the HM $13^{3.3}$ acts mainly as a flocculant and not a good filler-fiber bonding agent.

6.4.3.6: Effect of anionic starch to starch maize particles ratio

A comparison based on the ratio of modified starch to starch maize particles was made for hand sheets prepared using fiber refined at 3000 rev. The curves also include the data obtained for the control at a similar fiber refining level. The hand sheets made with the anionic polymer HM $38^{6.1}$ (1:3, anionic starch to starch particles ratio) were thicker when compared to the hand sheets made with HM $36^{6.1}$ and HM $37^{6.1}$. However, the PCC retentions were similar at 20% filler loading but different at 25 and 30% filler loadings, as shown in Fig. 6.16.
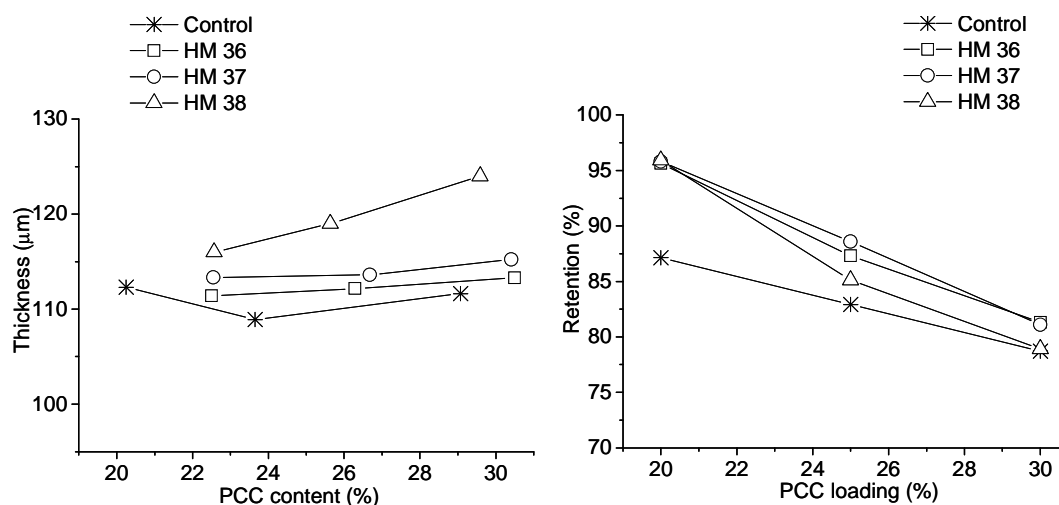
Fig. 6.16: Comparison in the thickness and PCC retention for hand sheets made without anionic starch additives and with anionic-starch-coated starch particles of different ratio of modified starch to starch granules, at 3000 rev. fiber refining level.

Fig. 6.17 shows a decrease in the ratio of modified starch to starch granules to 1:3 resulted in a loss of properties such as Gurley air resistance and a slight decrease in the burst. The drainage decreased with decreasing modified starch to starch granules ratio. The difference in the drainage in hand sheets made with HM $36^{6.1}$, HM $37^{6.1}$ and HM $38^{6.1}$ can be explained by the CSF factor and the degree of swelling.
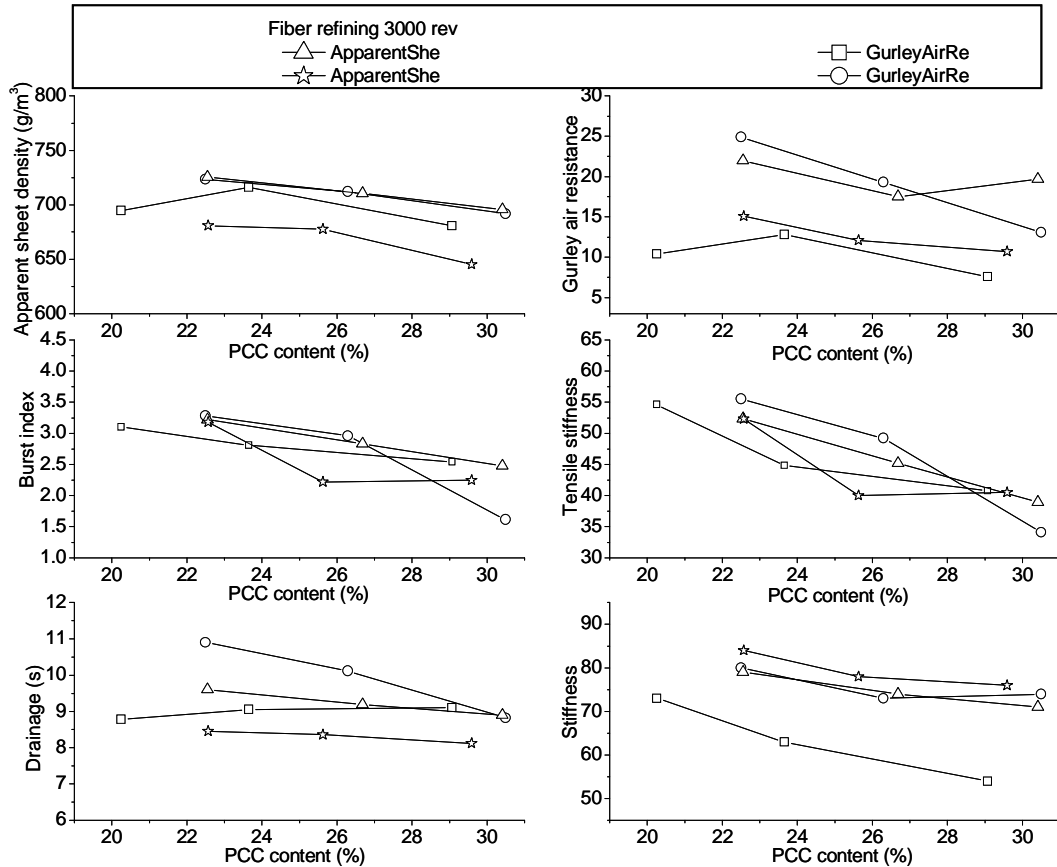
Fig. 6.17: Comparison between hand sheets made with different anionic-starch-coated starch particles in terms of the ratio of modified starch to starch granules.

Generally, drainage decreased with decreasing fiber refining level as well as with increasing filler loading. The decrease in drainage could not have been due to different PCC retentions since the retention values were similar. The bending stiffness was better in the case of the lower anionic starch to starch granules ratio (i.e. when anionic polymer HM 38[6.1] was used). Thus, clearly the presence of starch granules has a positive effect on the bending stiffness of paper. These granules contributed to the stiffness possibly due to their crystalline structure. *(See also the bar graphs in Appendix J showing the differences in the properties of hand sheets made with HM 13[3.3], HM 36[6.1], HM 37[6.1] and HM 38[6.1].)*

6.4.3.7: The effect of anionic and cationic polymer additive concentrations

Anionic polymer additive HM 38[6.1] was used and filler loadings of 25% and 30% were chosen. The fiber was refined at 3000 rev. and the CSF values were between 205 and 220. (The cationic starch was supplied by Mondi.) The fiber was mixed with the cationic starch and the filler was mixed with

the anionic starch. The cationic starch was added twice: first to the pulp and then a further 2% was added just before making the hand sheet (according to the general procedure used for papermaking). Increasing the concentration of the anionic starch from 2 to 4% resulted in a decrease in drainage (Fig. 6.18). This was expected, since by increasing the concentration of the anionic starch larger flocculants are obtained and packing efficiency is reduced, leading to a decrease in drainage. The opposite effect was observed when the cationic polymer concentration was increased from 2 to 4%.
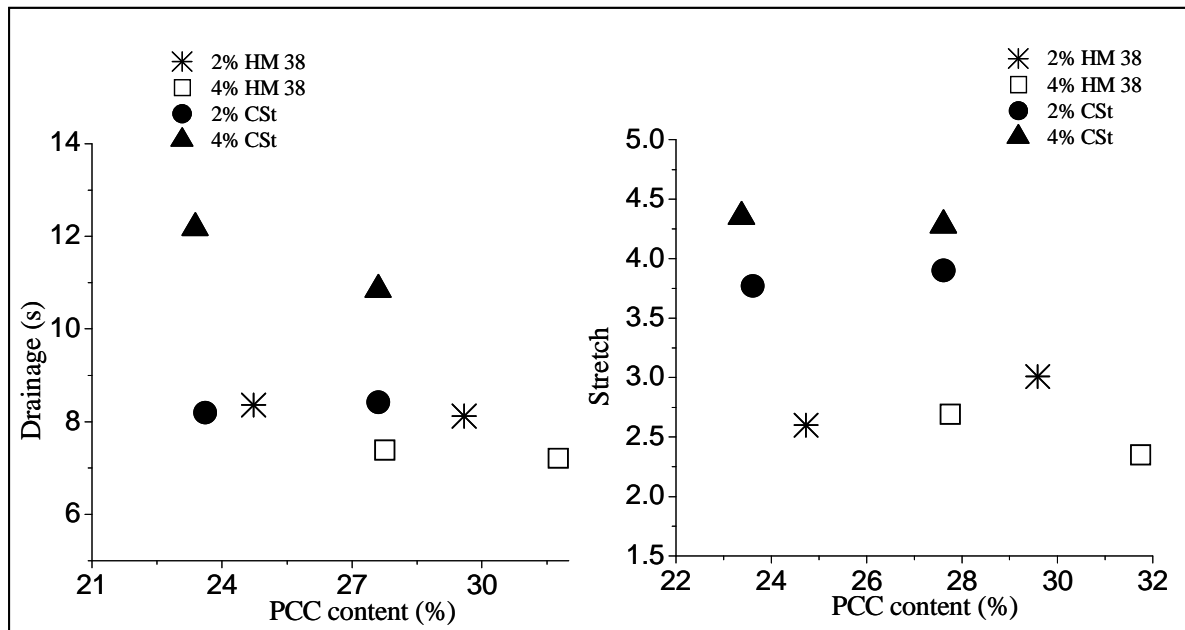
Fig. 6.18: Comparison between hand sheets made with different amounts of anionic-starch-coated starch particles HM 38[6.1] (expressed as a % relative to PCC) and the effect of cationic starch additive (expressed as % relative to the pulp mass).

Thus, cationic starch has a higher affinity towards the fiber than anionic starch, and it causes the fibers to bond together (a form of fiber flocculation) when added in the right concentration. However, as the concentration of cationic fiber is increased the 'flocculation' is decreased. This is due to the fact that most of the fiber surfaces carry a positive charge at high dosage of the cationic starch and the net effect is fiber-fiber repulsion when in solution, leading to the formation of a fine suspension. The addition of PCC with anionic starch to the fine fiber suspension resulted in a reduction of the size of PCC flocculants due to preferential binding of the cationic and anionic starch. When a further 2% cationic starch was added just before hand sheet making there was no flocculation of both fiber and PCC. The drainage was performed on a fine pulp–PCC suspension leading to low retention of PCC. The net effect was an increase in the drainage time. The resultant paper showed better fiber-fiber binding due to low PCC content. When 2% anionic polymer HM

$38^{6.1}$ was used the hand sheets were thicker compared to when 4% of the same anionic polymer was used regardless of higher retention in the latter (Fig. 6.19). This could be due to the fact that higher PCC retention means less fiber per hand sheet resulting in the loss of bulkiness. An increase in the cationic concentration from 2% to 4% resulted in a decrease in the thickness of hand sheets but the retention values were similar.


Fig. 6.19: **A comparison in the thickness and PCC retention for hand sheets made with different amounts of anionic-starch-coated starch particles HM 387$^{6.1}$ (expressed as a % relative to PCC) and the effect of cationic starch additive (expressed as % relative to the pulp mass).**

The stretch properties of the paper made with 2 and 4% anionic starch were similar at 25% filler loading (the star and unshaded square in Fig. 6.20) but at 30% filler loading the use of 2% anionic starch gave better tensile stretch. Thus the effect of flocculation was evident at 30% filler loading, since large flocculants have a negative effect on most paper properties as they disrupt the packing efficiency of the fiber during drainage creating flaws.

A large increase in the tensile index and stretch was obtained when additional cationic starch was mixed with pulp (Fig. 6.20). The cationic starch has a tendency to bind fiber together (in the dry end), leading to high tensile strength and stretch. The fact that PCC retention decreased with increasing cationic starch concentration shows that an excess of positive charges has detrimental effects on the filler retention. Increasing the cationic starch concentration resulted in paper with a high burst index compared to paper made using the standard papermaking procedure with anionic

starch. Increasing the concentration of cationic starch to 4% resulted in better burst, tensile index, tensile stretch, tensile stiffness and Gurley air resistance than when 2% cationic starch was used.


Fig. 6.20: Comparison between hand sheets made with different quantities of anionic-starch-coated starch particles HM 38[6.1] (expressed as a % relative to PCC) and the effect of cationic starch additive (expressed as % relative to the pulp mass).

However, the apparent sheet density also increased with increasing cationic starch content (i.e. the bulkiness of the paper decreased with increasing the cationic starch content) and the bending stiffness decreased with increasing the cationic starch content (Fig. 6.20). Thus, additional cationic starch resulted in the poorest bending stiffness values when compared to hand sheets that were made without additional cationic starch, with or without anionic starch. The filler retention also decreased with increasing cationic content resulting in better physical properties, especially those that are affected by the presence of filler. An increase in the anionic starch polymer content from 2 to 4% on the other hand resulted in a loss of properties such as Gurley air resistance, tensile stiffness and burst index. Moreover, the bending stiffness was better in the case of 2% than 4%

anionic starch content. The loss of properties with increasing anionic starch polymer content can be attributed to larger PCC flocculants at high anionic polymer content that decreased the fiber-filler bonding. It can be concluded form Fig. 6.21 that the filled hand sheets were bulkier than the unfilled hand sheets made at similar fiber refining. Furthermore, the drainage time was shorter for the filled hand sheets than for the unfilled hand sheets. However, the paper properties such as the bending stiffness, Gurley air resistance and tensile index were better in the unfilled hand sheets.
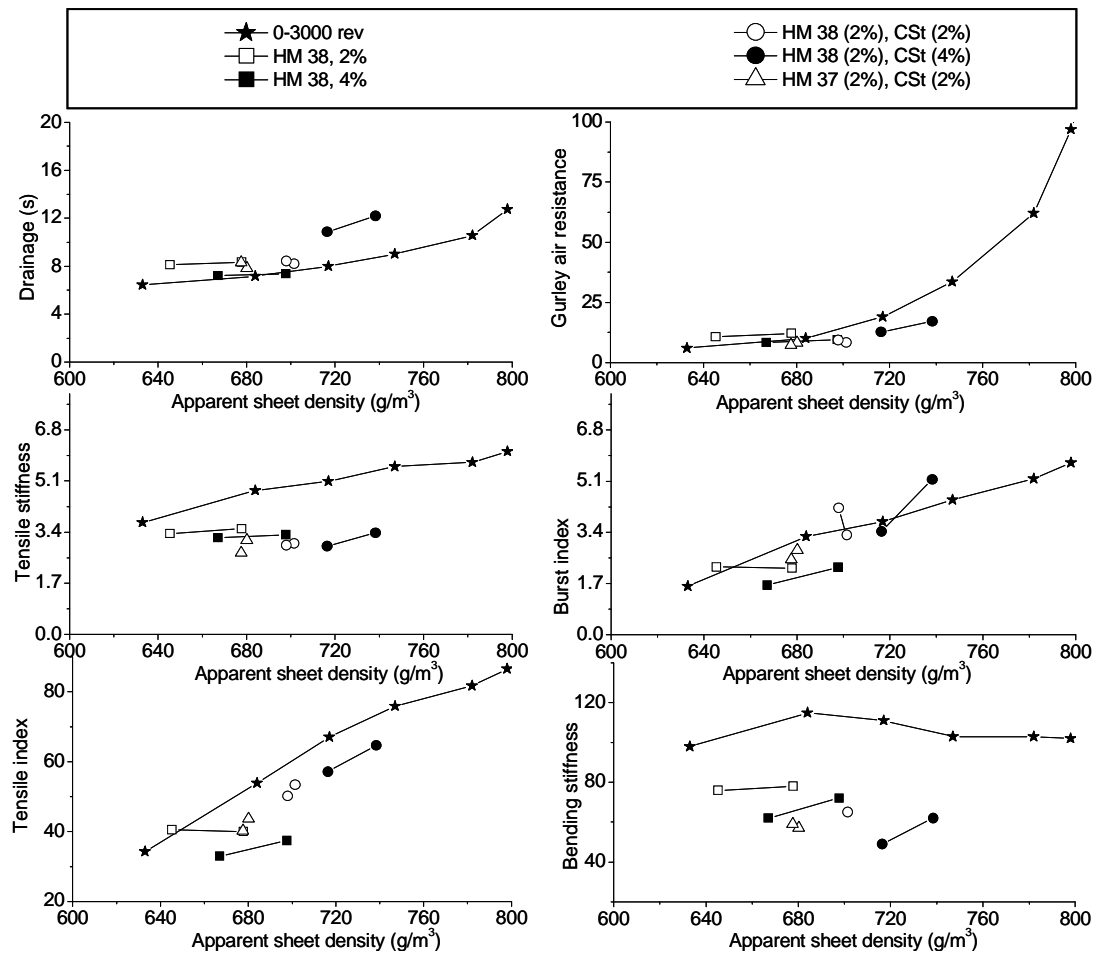
Fig. 6.21: Comparison of hand sheets made with different amounts of anionic-starch-coated starch particles HM 38[6.1] (expressed as a % relative to PCC) and the effect of cationic starch (CS) additive (expressed as % relative to the pulp mass) with 2% of HM 38[6.1] and HM 37[6.1].

6.4.3.8: Anionic-starch-coated cationic starch particles

Cationic starch particles were also coated with anionic starch and used as PCC flocculant (see Appendix E, Fig. E1). The anionic-starch-coated cationic starch particles were also tested for PCC retention and their effect on the paper properties. Fig. 6.2 shows that the drainage decreased with a decrease in the anionic starch to cationic starch particles ratio. Previous studies on the flocculation of PCC using a mixture of anionic and cationic starch showed that the blend flocculates better than either the anionic or the cationic starch polymer alone. Thus, the decrease in the drainage was a result of large flocculants. However the apparent sheet densities of the blends (HM $39^{6.1}$ and HM $40^{6.1}$) were similar to that of control and, conversely, the apparent sheet density of the anionic starch HM $40^{6.1}$ was lower (Fig. 6.22). This might be due to the effect of the cationic starch on the fiber whereby fiber-fiber bonding is promoted, resulting in high values of the apparent sheet density as previously observed (Fig. 6.20).
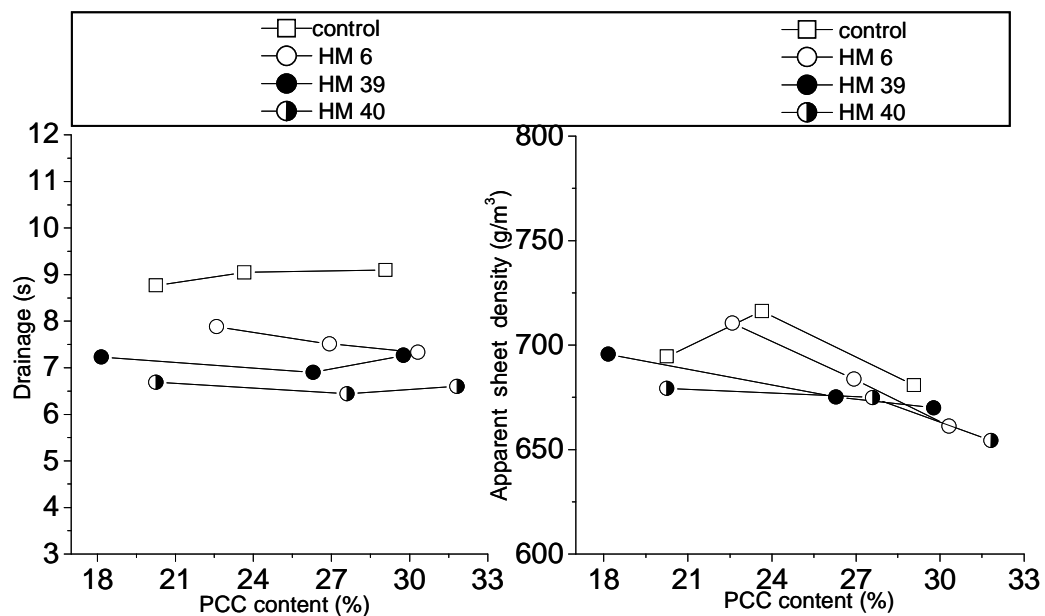
Fig. 6.22: Comparison of drainage and apparent sheet density between hand sheets made with different (in terms of modified starch to cationic starch granules ratio) anionic polymer additive blended with cationic particles.
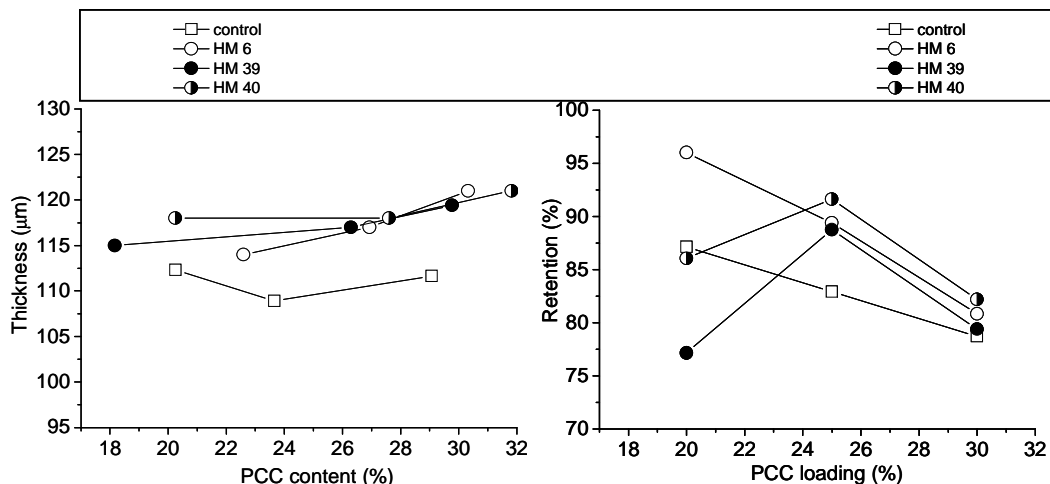
Fig. 6.23: A comparison in the thickness and PCC retention for hand sheets made without anionic starch additives and with different ratios (in terms of anionic starch to cationic starch granules ratio) of anionic-starch-coated cationic starch particles.

Fig. 6.24, it can be concluded that the inclusion of cationic starch particles into an anionic starch paste did not yield much in terms of the properties of the hand sheets. The tensile index and burst strength were lower than found for the control. The stiffness was however better at 30% filler loading than at 20 and 25%. Generally there should be a balance between the anionic and the cationic starch polymers, with an excess of either leading to detrimental effects. (Another important factor is the order and/or method of introducing the cationic and anionic starch polymers.) Thus the efficiency of each material can be reduced by the presence of the other (if not carefully introduced) due to the fact that the two materials carry opposite charges. In this study it is shown that increasing the concentration of anionic polymer has the opposite effect on the properties of hand sheets when compared to the effect of increasing the cationic polymer. Hence a balance of the two oppositely charged materials is required for optimum performance. As mentioned before, the properties of paper decrease with filler addition, as shown in the plots of properties against the apparent sheet density (see Fig. I1 in appendix I).
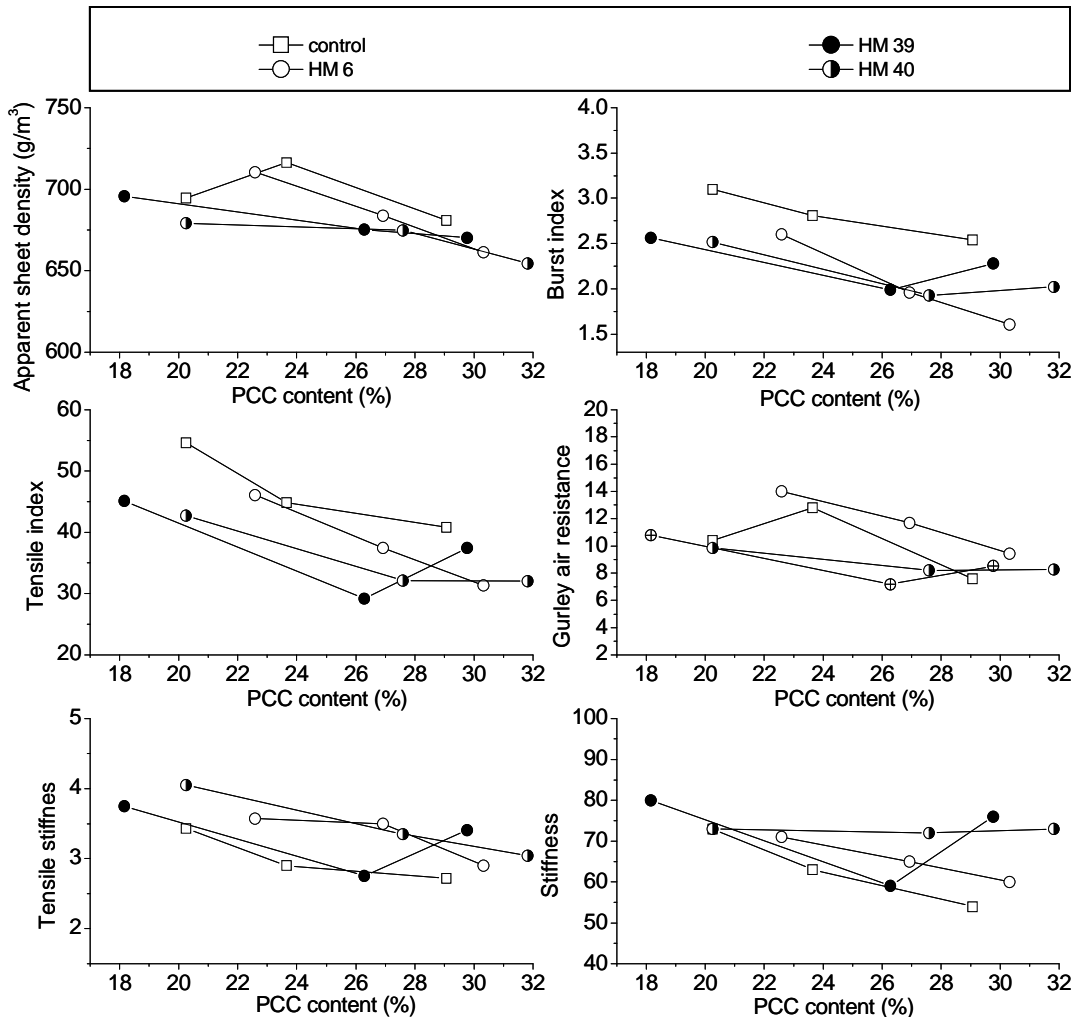
Fig. 6.24: Comparison of drainage and apparent sheet density between hand sheets made with different ratios (in terms of modified starch to cationic starch granules ratio) of anionic-starch-coated cationic starch particles.

6.4.4: Other modified starch particles

The anionic polymers used as paper additives are described in Table 6.2. The hand sheets were made as described in Scheme 6.4. The amount of anionic polymer additive was 2% of the filler in these experiments. Table 6.4 shows that the paper made with HM41-HM49[6.3] materials as additives gave superior tear strength, breaking length and folding endurance than the reference at all filler loadings and all blending ratios used. The increase in these properties was also attributed to the presence of the starch particles. However, the PCC retention and bending stiffness were in most cases, inferior to what was obtained for the control. This scenario can be compared to that described in Section 6.4.4, where a reduction in PCC retention resulted in an increase in some properties such

as the tensile strength. However, superior tear strength, breaking length and folding endurance was also obtained for sample HM 47-HM 49[6.3], which gave a slight increase in PCC retention. The PCC binding efficiency for sample HM 41-HM 43[6.3] was expected to be low since acrylamide was used as a comonomer during the graft copolymerization process. This could have contributed to inferior retention values. The material HM 41-HM 43[6.3] was expected to increase the hydrogen bonding to strengthen fiber filler bonding. The crosslinked material HM 44-HM 46[6.3] was used in a low anionic to starch particle ratio in order to reduce its flocculation efficiency but low retention values were also obtained. Although it was anticipated that the addition of polymeric additives would result in more PCC retention the results showed that other factors were influencing the PCC retention. These factors include the ineffective interaction between the additive and the PCC and ineffective size of flocculants due to dilution and time factors, resulting in a significant decrease in the size of flocculants.

Table 6.4: Results of hand sheets made with other anionic-starch-coated starch particles as retention aids

	PCC loading (%)	Volume (%)	Stiffness (%)	Tear resistance (%)	Breaking length (%)	Folding Endurance (%)	Opacity (%)	Retention (%)
HM 41[6.3]	20	0.06	-0.38	21.22	20.32	557	-1.20	-2.94
	25	2.44	-0.08	25.39	21.42	567	-1.35	-2.02
	30	4.73	0.31	31.22	22.93	597	-1.49	-1.04
HM 42[6.3]	20	-3.02	-3.06	35.91	31.28	764	-0.40	-6.25
	25	-3.13	2.53	36.78	25.89	649	-0.94	-4.40
	30	-3.23	9.71	38.01	18.51	321	-1.46	-2.45
HM 43[6.3]	25	-0.11	5.07	22.73	27.16	302	-0.76	-1.57
HM 44[6.3]	20	-4.73	3.17	13.61	29.28	960	-1.66	-4.96
	25	-4.23	3.73	18.26	25.74	802	-1.49	-4.54
	30	-3.76	4.46	24.77	20.91	354	-1.34	-4.09
HM 45[6.3]	25	0.32	-3.18	17.80	12.55	173	-1.26	4.49
HM 46[6.3]	25	3.43	2.82	16.67	3.50	193	-1.43	1.61
HM 47[6.3]	25	-0.09	-4.03	17.94	25.34	424	0.71	1.02
HM 48[6.3]	25	-1.95	-1.78	21.73	17.14	407	0.64	0.20
HM 49[6.3]	25	-1.80	-2.38	24.96	18.11	265	0.76	2.06

6.5: Conclusions

The use of anionic-starch-coated starch particles as retention aids resulted in hand sheets with better bending stiffness over hand sheets made with the anionic starch paste only and without any anionic starch additive. Moreover, the other properties remained superior to those obtained for the control. The use of anionic starch resulted in improvement in filler retention but poor paper properties (tensile strength, burst index and porosity) resulted. However, the use of the anionic-starch-coated cationic starch particles did not show much effect on the retention of filler and paper properties. (This is probably due to the unbalanced effect of the cationic and anionic polymers). Flocculation experiments showed that a mixture of the anionic and cationic starch resulted in more flocculation and broadness in the particle size distribution and some bimodal distribution were obtained. Thus, there is need to balance the effect of the cationic and anionic starch additives so as to control the final properties of hand sheets. It was also shown that the point of addition of the anionic additives is of paramount importance. The preferred route is to add the anionic additives to PCC rather than to the pulp. However, the size of PCC flocculants should be optimized in order to obtain the best properties.

6.6: References

(1)   Xu, Y., Chen X., Peltron R. *Tappi Journal* **2005**, *4(11)*, 8-12.

(2)   Li, L., Collis A., Pelton R. *Journal of Pulp and Paper Science* **2002**, *28(8)*, 267-273.

(3)   Alince, B., Lebreton R., St.-Amour S. *Tappi Journal* **1990**, *73(3)*, 191-193.

(4)   Formento, J. C., Maximino M. G., Mina L. R., Srayh M. I., Martinez M. J. *Appita* **1994**, *47(4)*, 305-308.

(5)   Laleg, M. *US Patent* **2006**, no. 7.074.845.

(6)   Johnson, K. A. *US Patent* **1988**, no. 4.750.974.

(7)   Ide, F., Kodama T., Kotake Y. *US Patent* **1974**, no.3.785.921.

Chapter 7: Conclusions and recommendations

7.1: Conclusions

The main aim of this study was to increase the PCC loading in paper without negatively impacting the properties of paper. This was achieved by using anionic-starch-coated starch particles which resulted in good PCC retention and improved paper properties even at high PCC loading. Several aspects of polysaccharide modification, their effects on $CaCO_3$ crystal growth modification and, their effect on PCC retention and paper strength were investigated.

The following conclusions can be made to the objectives as stated in Chapter 1:

1. Modification of polysaccharides was successfully carried out using various methods. The grafting techniques were found to yield starch based materials that are suitable for application in the retention of PCC.

2. Anionic starch materials were found to be good PCC flocculating agents. The concentration of the anionic starch critically affects the size of PCC flocculants. Moreover, use of a mixture of anionic and cationic starch, as well as the sequential treatment of PCC with the oppositely charged polymers, had a significant effect on the size of the PCC flocculants.

3. A study on *in situ* crystallization of $CaCO_3$ in the presence of chemically modified cellulose fiber showed that the filler particles were nucleated on the surface of the fiber. Modification of $CaCO_3$ crystal morphology and its surface properties can be achieved by carefully choosing the conditions and the crystal growth modifier. This study revealed new methods of filler synthesis and filler addition to paper via *in situ* crystallization of filler in the presence of the chemically modified fiber. (The use of this method in papermaking could result in improved filler retention although many factors such as fiber-fiber bonding strength should also be considered.)

Filler surface modification was achieved by using PAA grafted starch as the crystal growth modifier. This affected the shape polymorph and size of crystals, and resulted in crystals with functional chemical surfaces. Fluorescence studies revealed that the polysaccharide was also on the surface of the crystallized calcium carbonate. The surface charge was negative, and addition of cationic starch reversed the charge. A novel approach for the characterization of fluorescing $CaCO_3$ crystals using flow cytometry gave useful information on the distribution of the chromophore with granularity and size of the crystals. Surface properties of fillers are critical to fiber–filler interactions as well as interactions with other additives such as cationic starch that promote fiber–fiber bonding. The presence of starch and the negative charge on the surface of the crystals could

increase filler–fiber bonding when used in combination with cationic starch, and this can lead to good paper strength.

4. Hand sheets were made and the performance of the modified polysaccharides on paper properties was tested. The anionic-starch-coated starch particles were used as filler retention aids to produce paper with better filler loading. Soluble anionic starch gave improved PCC filler retention but the paper strength decreased when compared to the control paper. However, the use of anionic-starch-coated starch particles gave improved PCC filler retention and properties such as the bending stiffness, tensile strength and porosity were superior to those obtained for the control paper. Whilst addition of retention aids to PCC is easy to implement, it was also found that it is necessary to optimize the conditions in order to produce better quality paper. For an example, the effective particle size of the filler depends on a number of factors that require mechanical and chemical considerations. These variables include the rate of stirring of flocculants, stirring efficiency and reproducibility, volume water used, extent of modification and adjustment of modification from one sample to another, degree of swelling of the additives (which can vary from one run to another), degree of pulp refining, source of the pulp, time of interaction between filler, fiber and additives, etc. Nevertheless, the data obtained in this study indicates that positive attributes were induced by inclusion of anionic starch-coated-starch particles in paper. The designed anionic starch particles can be produced easily and quantitatively, paving the way to new retention aids.

7.2: Recommendations for future work

The following recommendations for future research are made:

1) Investigate the synthesis of PCC in the presence of soluble crystal growth modifiers to study the effect of size, shape and surface properties on the strength of paper and PCC filler retention. The present study showed that the surface of the crystallized filler can be easily modified in terms of both the surface charge as well as the amount of the starch polymer on the surface. Thus it will be interesting to see the effects of varying the charge and the amount of starch (absorbed or adsorbed) on the surface on the retention of PCC as well as on the paper strength.

2) Investigate the *in situ* formation of calcium carbonate filler in the presence of modified pulp fiber and then study the properties of the paper. *In situ* synthesis of filler in the presence of modified pulp and its use for the subsequent formation of hand sheets would also be of great

interest especially in terms of filler retention. The *in situ* crystallization process would result in filler being absorbed on the surface of the fiber, as was observed in this study. This may lead to improved filler retention, but measures do have to be taken in order to prevent the weakening of fiber–fiber bonding. Thus, it was necessary to do an onsite experiment or laboratory-designed process that includes all the aspects of *in situ* filler synthesis and hand sheet making which will indeed be a mammoth task.

Appendix A: FT-IR spectra of modified polysaccharides
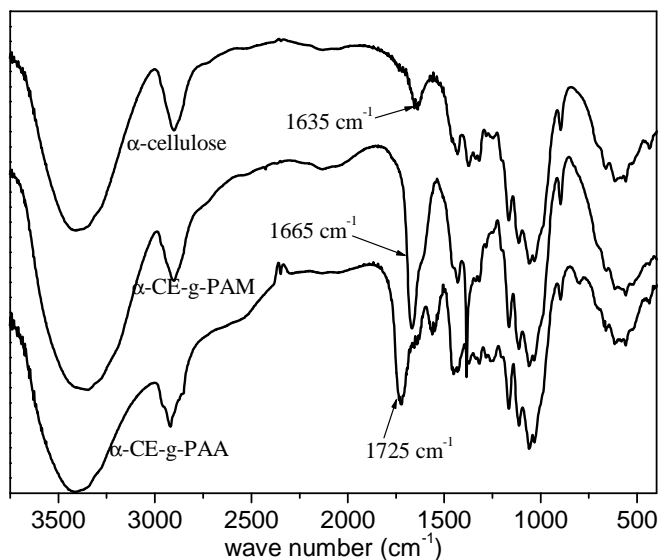
Fig. A1: Examples of FT-IR spectra of cellulose modified with polyacrylamide and polyacrylic acid polymers via the grafting reactions, showing the characteristic carbonyl carbon peak of the grafted polymers.
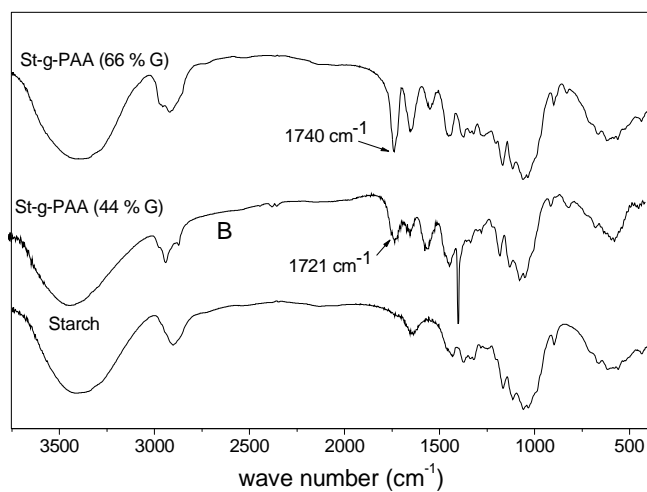
Fig. A2: Examples of FT-IR spectra of starch grafted with polyacrylic acid polymer, showing the characteristic carbonyl carbon peak of the grafted PAA.

Appendix B: TGA curves of modified polysaccharides and hand sheets
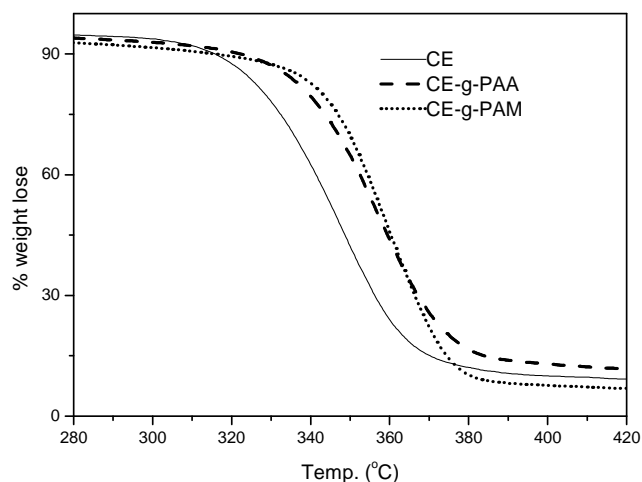
Fig. B1: Examples of TGA profiles of cellulose modified with polyacrylamide and polyacrylic acid polymers prepared via the grafting reactions.
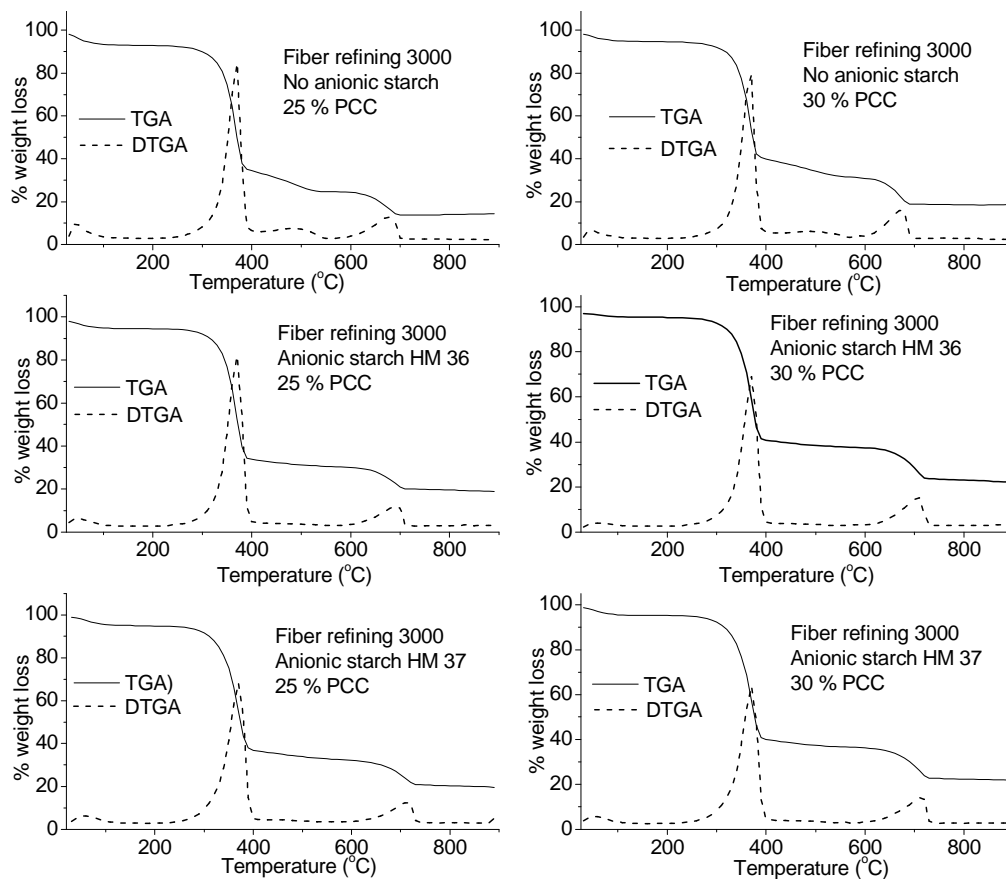
Fig. B2: Examples of TGA profiles of hand sheets made with and without polymeric additives (the PCC filler retention was calculated from these curves).

Appendix C: Absorption properties of crosslinked PAA grafted starch
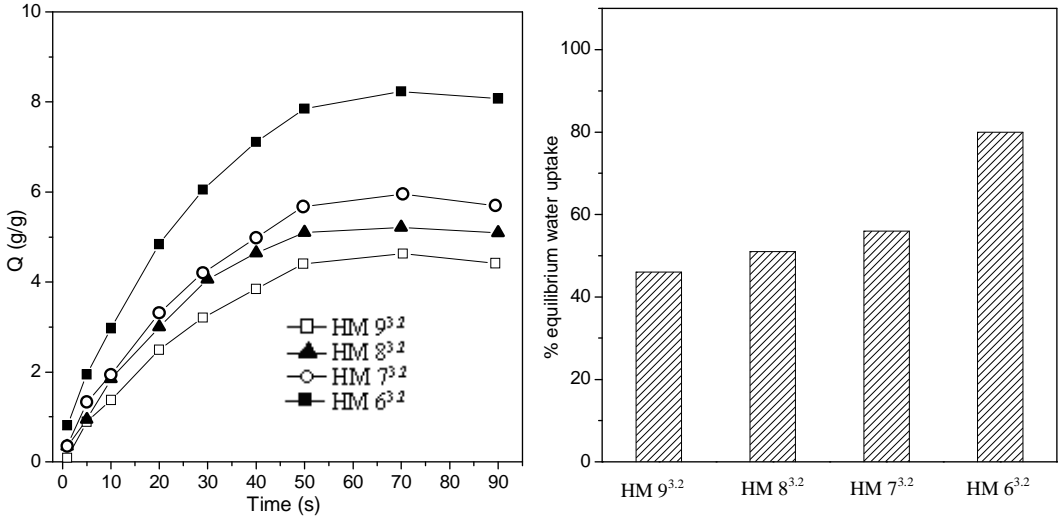
Fig. C1: Absorption of crosslinked PAA/PAANa grafted starch.

Appendix D: SEM images of crystallized $CaCO_3$
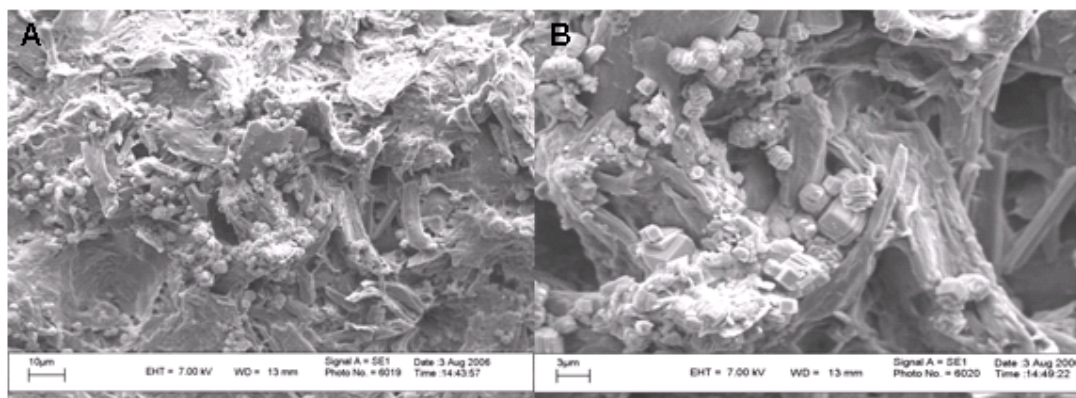
Fig. D1: SEM images of $CaCO_3$ crystals obtained in the presence of microcrystalline cellulose, at different magnifications (A & B) (Crystals were synthesized at 25 ^{o}C, [Ca^{2+}] = [CO_3^{2-}] = 0.025 M, pH 8.5 and [polymeric additives] = 0.77 g/L).
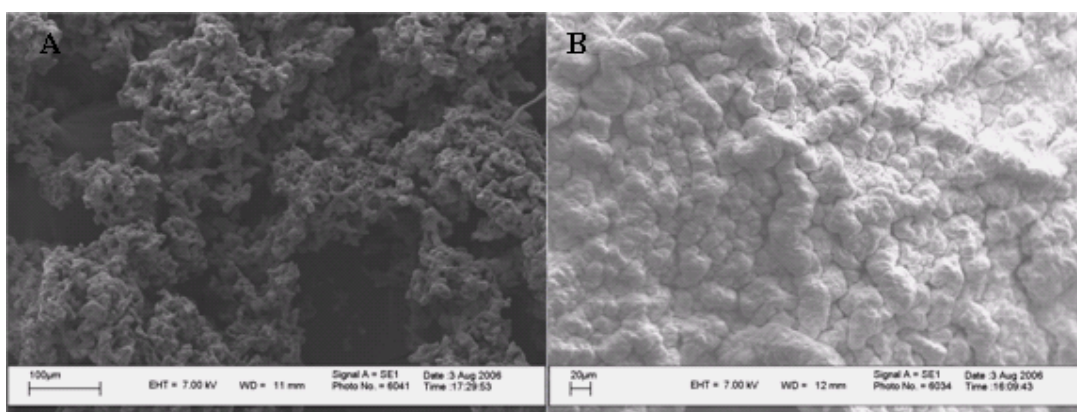
Fig. D2: SEM images of $CaCO_3$ crystals obtained in the presence of (A) PAA and (B) PAA grafted starch, after six days (Crystals were synthesized at 25 ^{o}C, [Ca^{2+}] = [CO_3^{2-}] = 0.025 M, pH 8.5 and [polymeric additives] = 0.77 g/L).
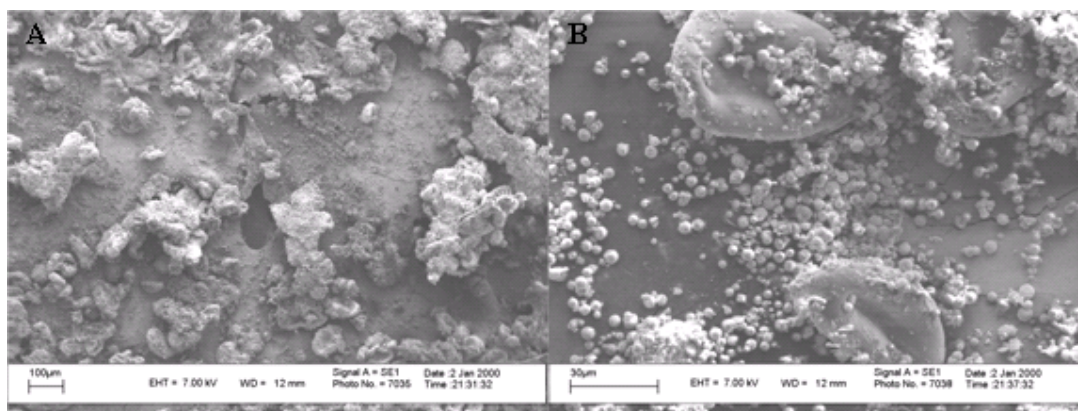
Fig. D3: SEM images of CaCO$_3$ crystals obtained in the presence PAA grafted partially-dissolved starch at different magnifications (A & B) (Crystals were synthesized at 25 ^{o}C, [Ca^{2+}] = [CO$_3^{2-}$] = 0.025 M, pH 8.5 and [polymeric additives] = 0.77 g/L).

Appendix E: SEM images and flocculation curves of anionic-starch-coated starch particles
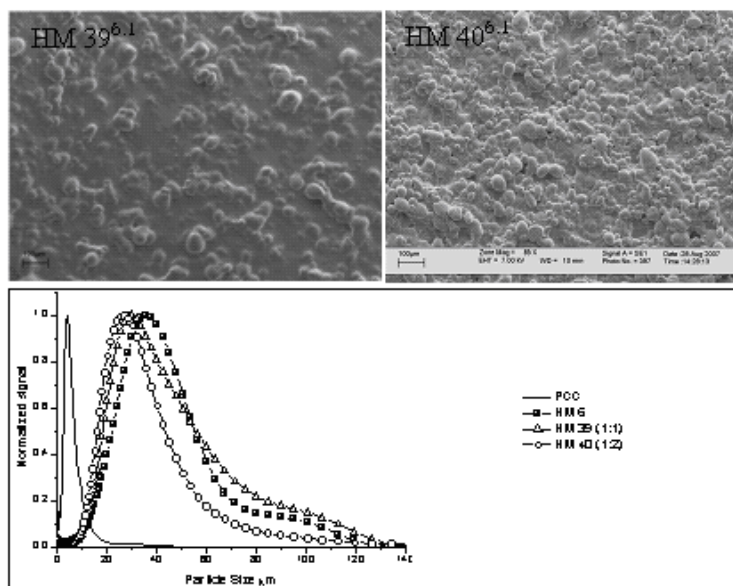
Fig. E1: SEM images of (A) anionic-starch-coated cationic starch particles (Mondi) in the ratio 1:1 (labeled HM 39[6.1]) and (B) Anionic starch coated cationic starch particles (Mondi) in the ratio 1:2 (labeled HM 40[6.1]). The graph shows the flocculation properties of HM6[6.1], HM 39[6.1] and HM 40[6.1]; 2 g PCC was flocculated using about 0.8% anionic starch polymer solution.
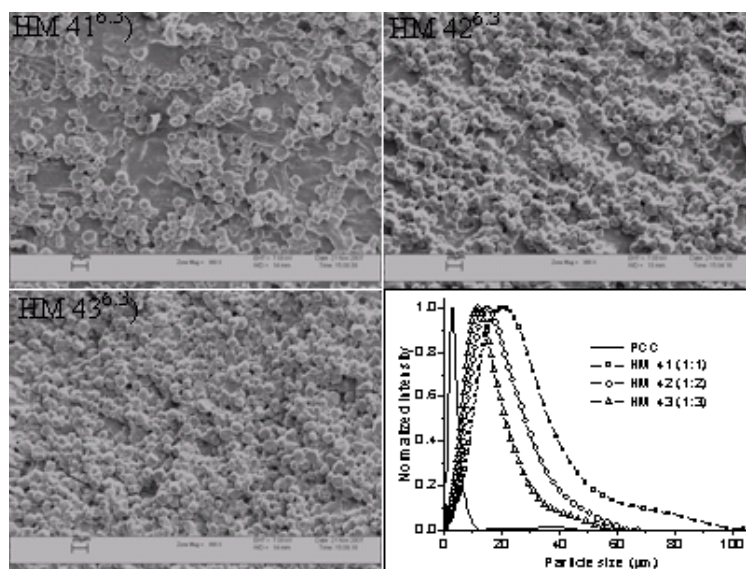
Fig. E2: SEM images of anionic-starch-coated starch particles at three different ratios: HM 41$^{6.3}$– HM 43$^{6.3}$. The graph shows the particle size distribution for flocculated PCC using the anionic starch particles; 2 g PCC was flocculated using about 0.8% anionic starch polymer solution.
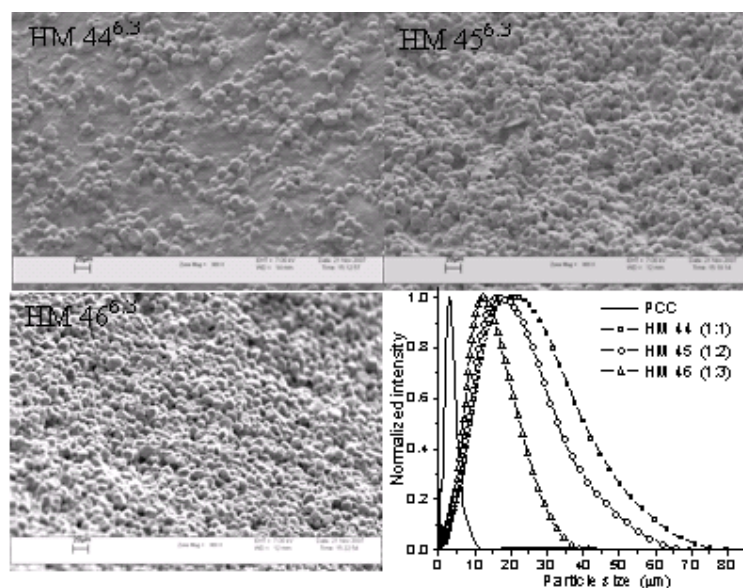
Fig. E3: SEM images of anionic starch particles at three different ratios (HM 44$^{6.3}$–HM 46$^{6.3}$. The graph shows the particle size distribution for flocculated PCC using the anionic starch particles; 2 g of PCC was flocculated using about 0.8% of anionic starch polymer solution.
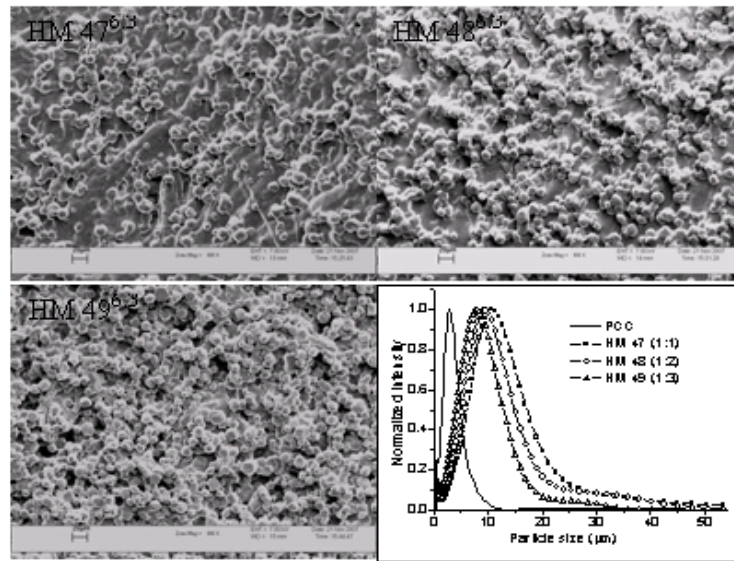
Fig. E4: SEM images of anionic-starch-coated starch particles at three different ratios HM 47$^{6.3}$–HM 49$^{6.3}$. The graph shows the particle size distribution for flocculated PCC using the anionic starch particles; 2 g of PCC was flocculated using about 0.8% of anionic starch polymer solution.

Appendix F: SEM images and flocculation curves of starch particles
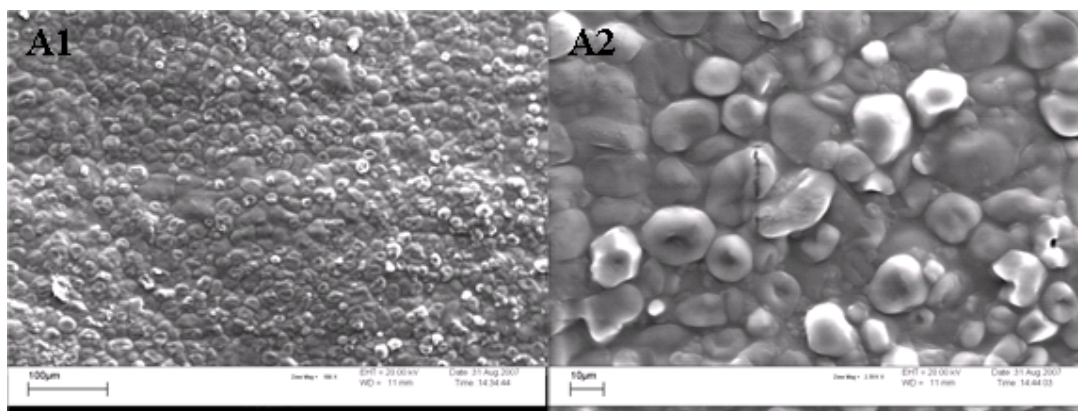
Fig. F1: SEM images of swollen anionic starch coated starch particles at different magnifications (A & B).
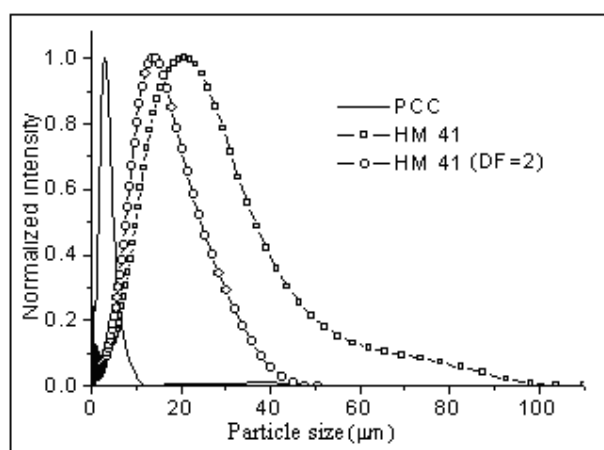
Fig. F2: The effect of dilution on particle size distribution of flocculated PCC prepared using anionic starch particles HM 41[6.3].

Appendix G: Grammage of all the hand sheets

Legend:
—■— No AST, 0 rev
—●— No AST, 1000 rev
—▲— No AST, 3000 rev
—□— HM 36, 1000 rev
—◇— HM 36, 3000 rev
—△— HM 36, 6000 rev
—■— HM 37, 1000 rev
—◆— HM 37, 3000 rev
—▲— HM 37, 6000 rev
—⊞— HM 38, 3000 rev
—◈— HM 41, 3000 rev
—⬠— HM 6, 3000 rev
—⊟— HM 39, 3000 rev
—✳— HM 40, 3000 rev
—✕— HM 13, 3000 rev
—■— HM 38, 3000 rev, 0.02 %
—◆— HM 38, 3000 rev, 0.04 %
—▲— HM 38, 3000 rev, CSt 0.02%
—★— HM 38, 3000 rev, CSt 0.04%
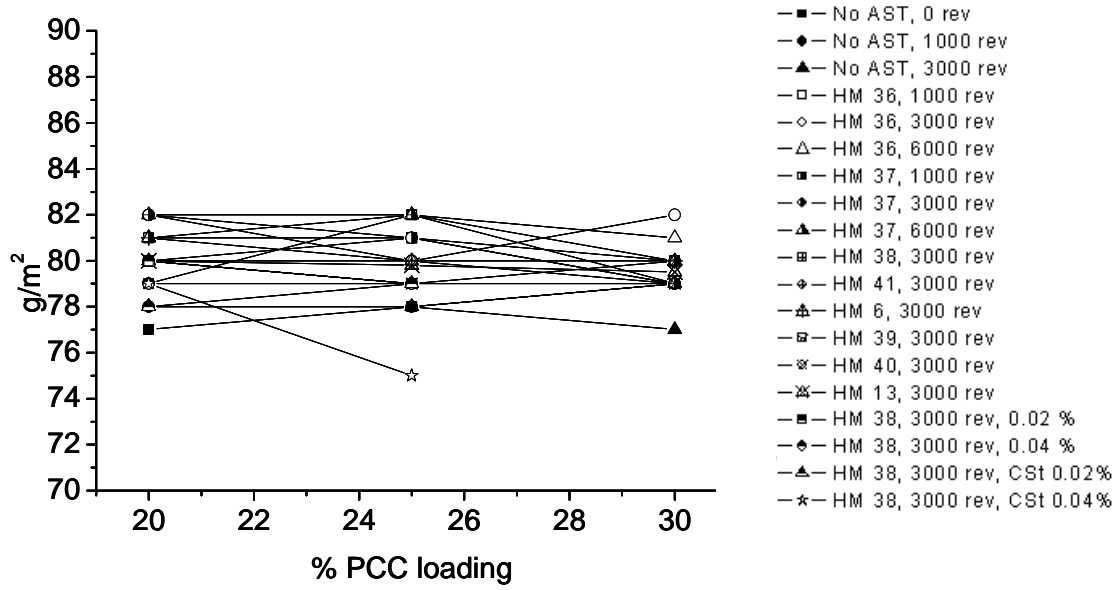
Fig. G1: Grammage of all the hand sheets made with PCC additions as well as with and without anionic or cationic polymer additions (the grammage of most of the hand sheets was in the range 80 ± 2 g/m^2).

Appendix H: Effect of fiber refining on properties of unfilled and filled paper
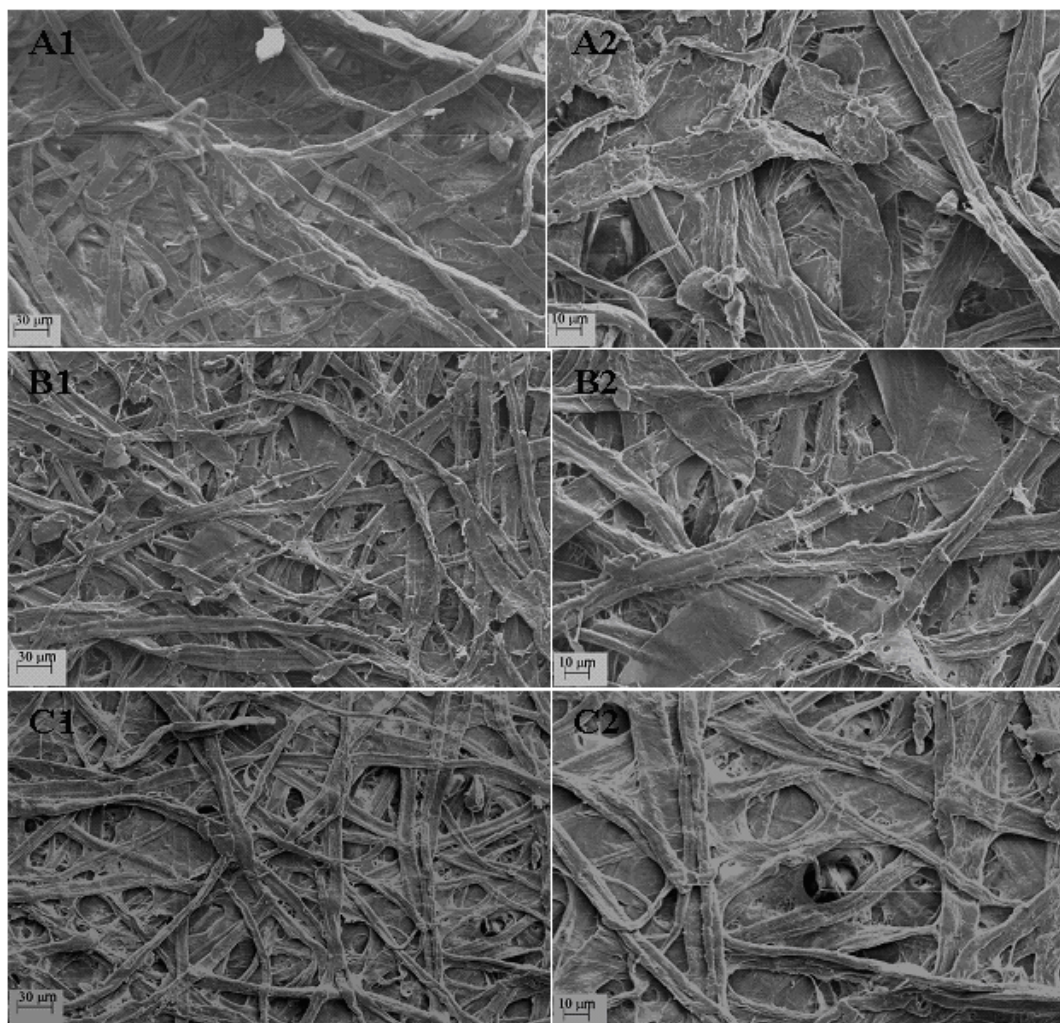
Fig. H1: SEM images showing the morphology of fibers refined at different revolutions (rev.); A) 0, B) 1500 and C) 3000, at different magnifications.
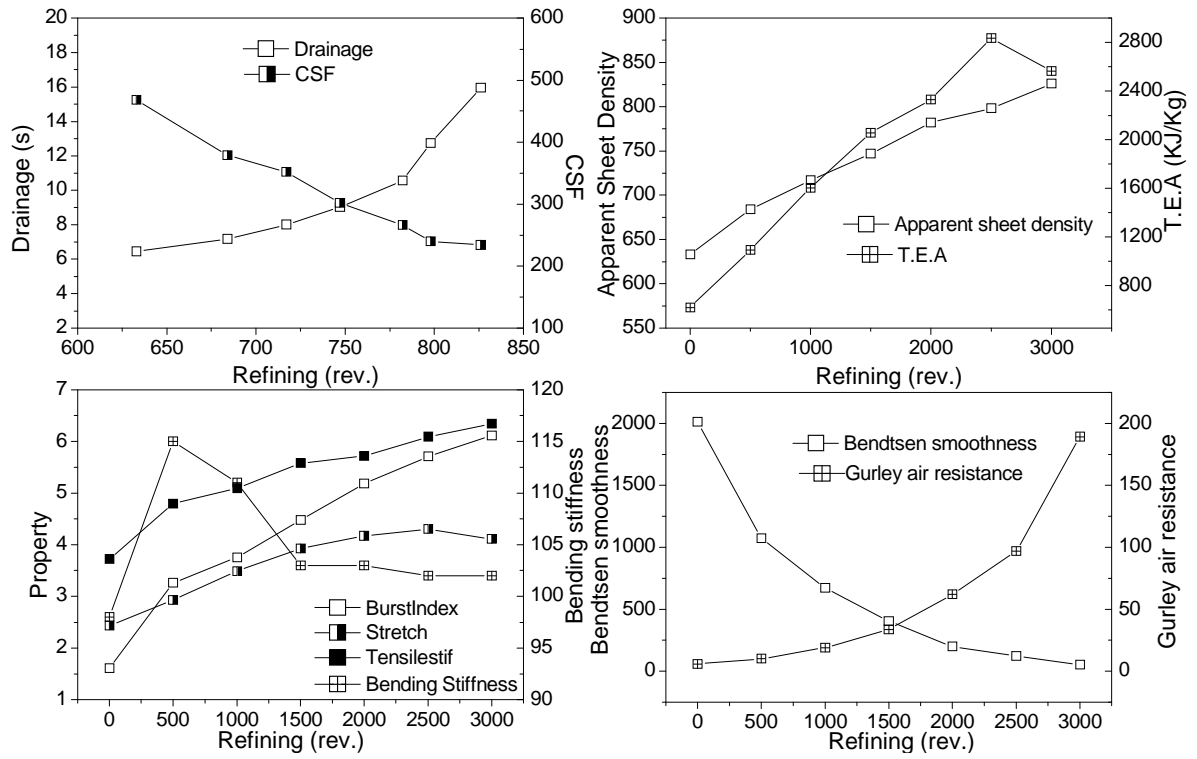
Fig. H2: Variation of paper properties with fiber refining for unfilled paper.
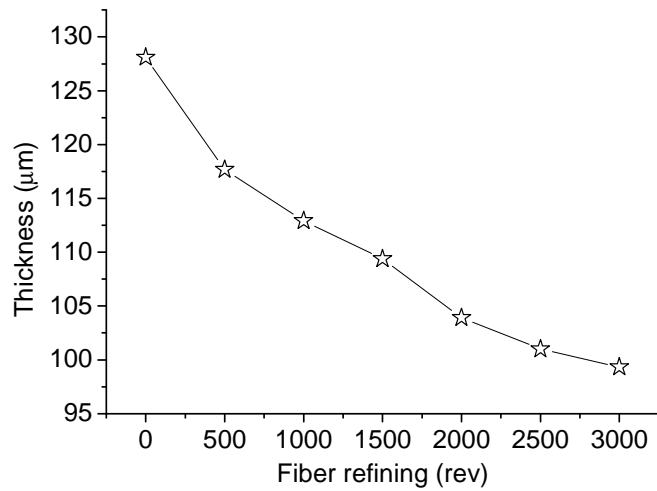
Fig. H3: Change in the thickness of paper with fiber refining (no PCC).
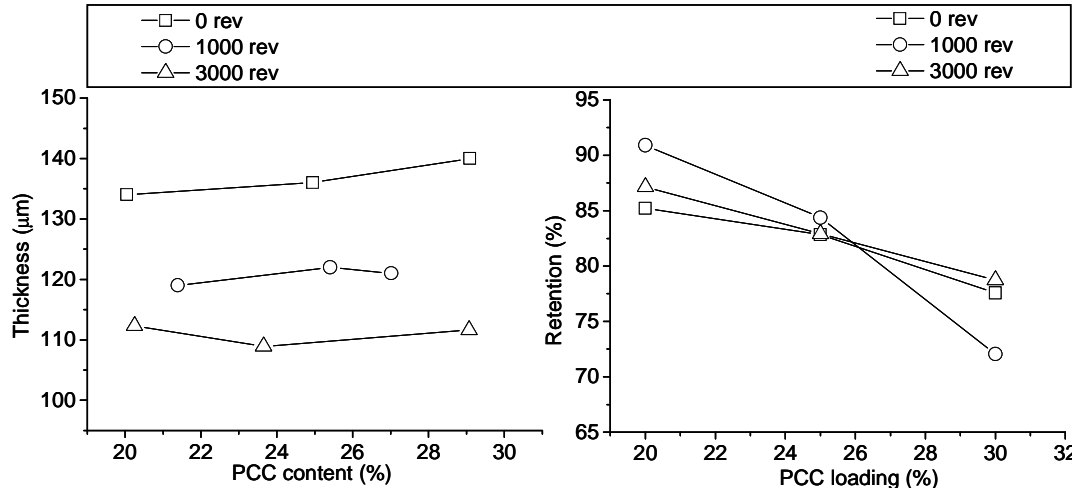
Fig. H3: **The thickness and PCC retention for hand sheets made without anionic starch additives at different fiber refining levels.**
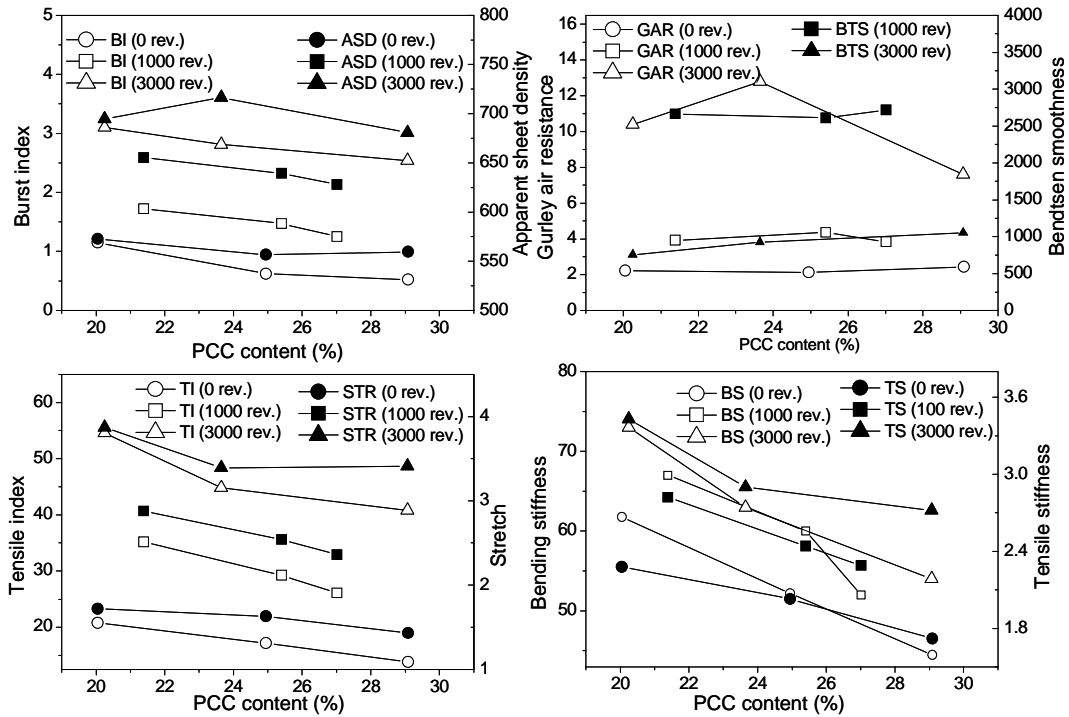
BI – burst index, ASD – apparent sheet density, GAR – Gurley air resistance, BTS – Bendtsen smoothness, TI – tensile index, BS – bending stiffness, TS – tensile stiffness

Fig. H4: Changes in paper properties with PCC loading and fiber refining.

Appendix I: Change in properties of hand sheets against the apparent sheet density of hand sheets
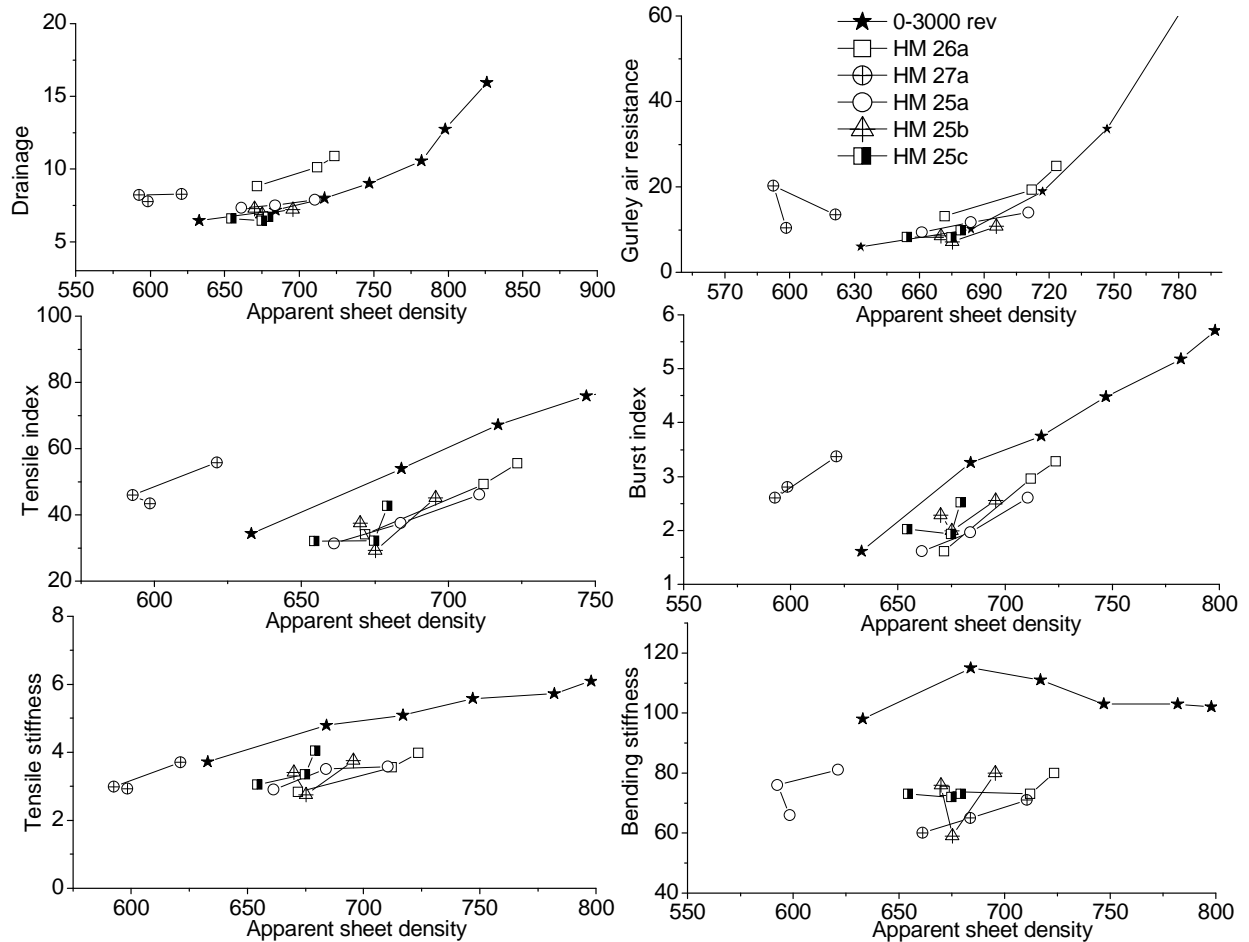
Fig. I1: Change in properties of paper against the apparent sheet density of hand sheets made with different (in terms of modified starch to cationic starch granules ratio) anionic polymer additives blended with cationic particles. The fiber refining of 3000 rev. was used. The shaded star represents hand sheet made without PCC and without anionic polymer additive at a fiber refining range of 0-3000 rev.

Appendix J: Bar graphs for hand sheets made with polymeric additives HM 13, HM 36, HM 37 and HM 38.

Fiber refining of 3000 rev. was used for the hand sheets results in Appendix I.
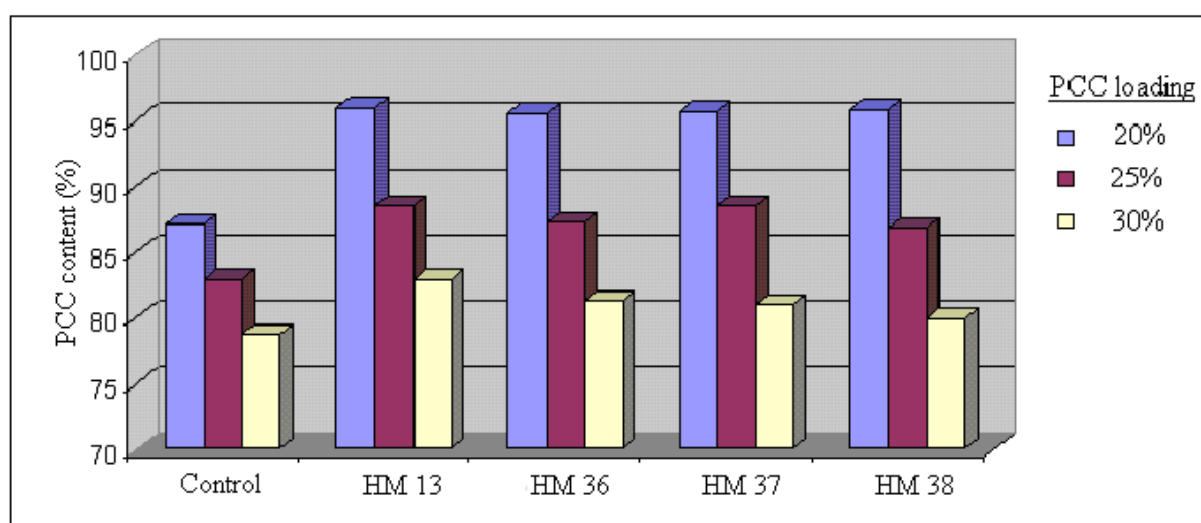
Fig. J1: Comparison in the PCC retention of hand sheets made with polymeric additives HM 13, HM 36, HM 37 and HM 38.
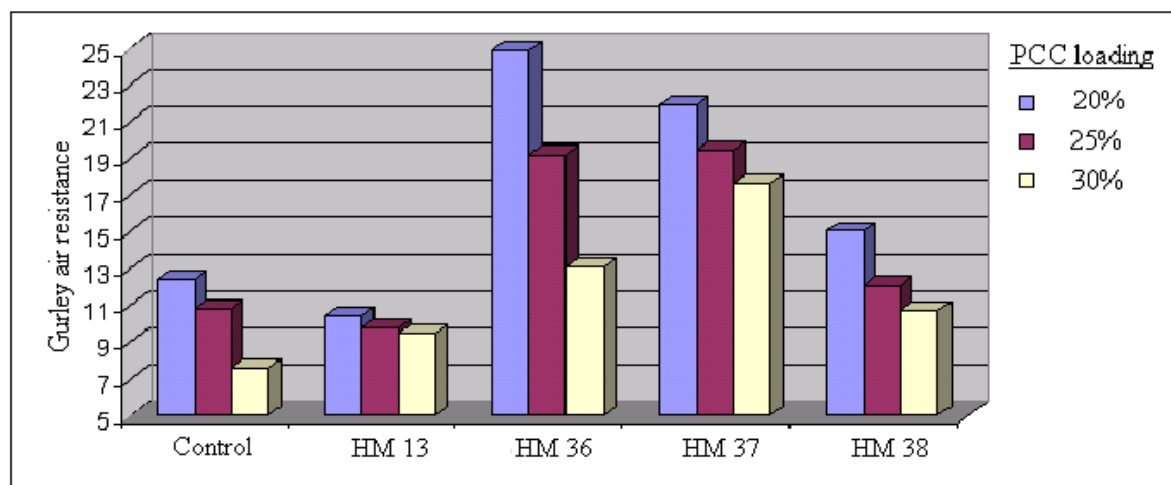
Fig. J2: Comparison in Gurley air resistance of hand sheets made with polymeric additives HM 13, HM 36, HM 37 and HM 38.
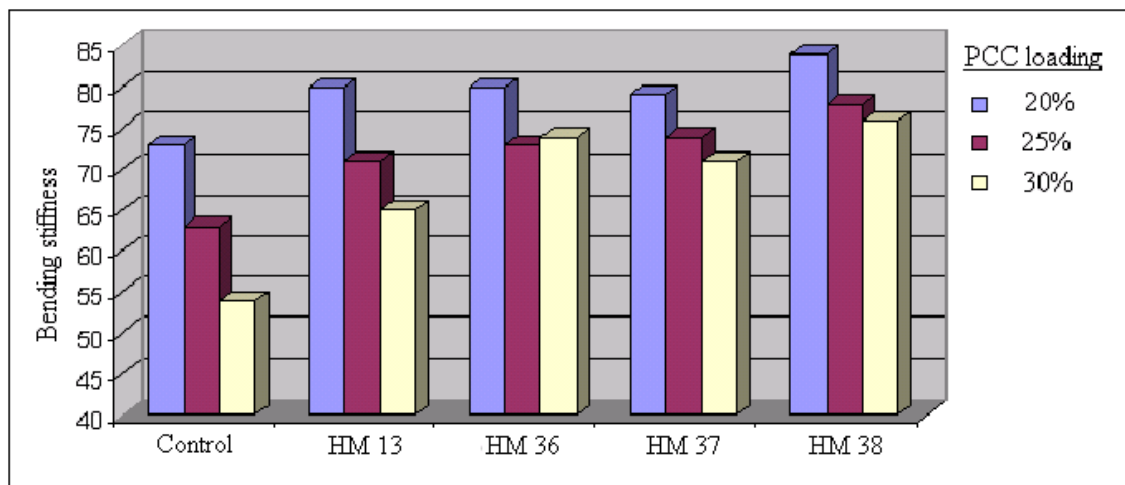
Fig. J3: Comparison in the bending stiffness of hand sheets made with polymeric additives HM 13, HM 36, HM 37 and HM 38.
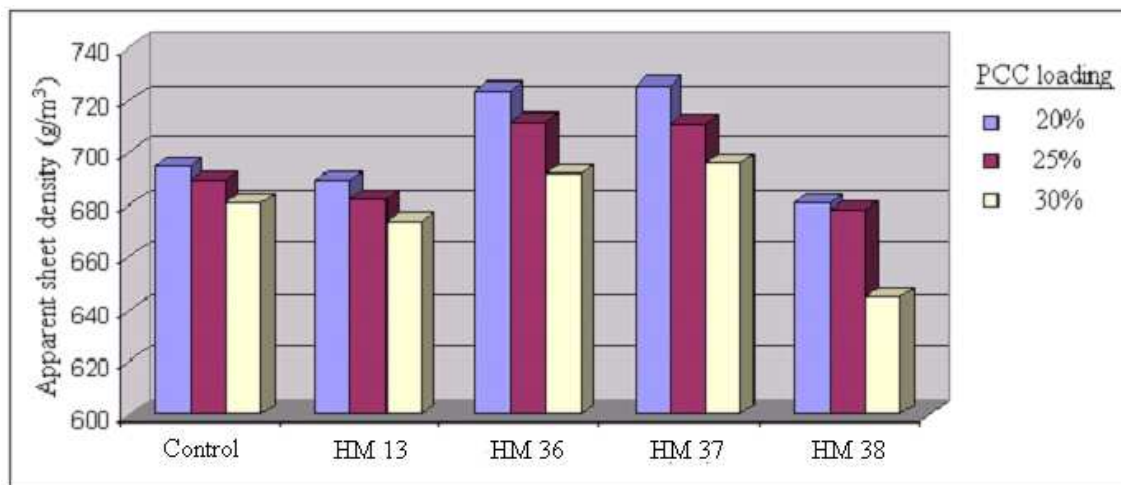
Fig. J4: Comparison in the apparent sheet density of hand sheets made with polymeric additives HM 13, HM 36, HM 37 and HM 38.
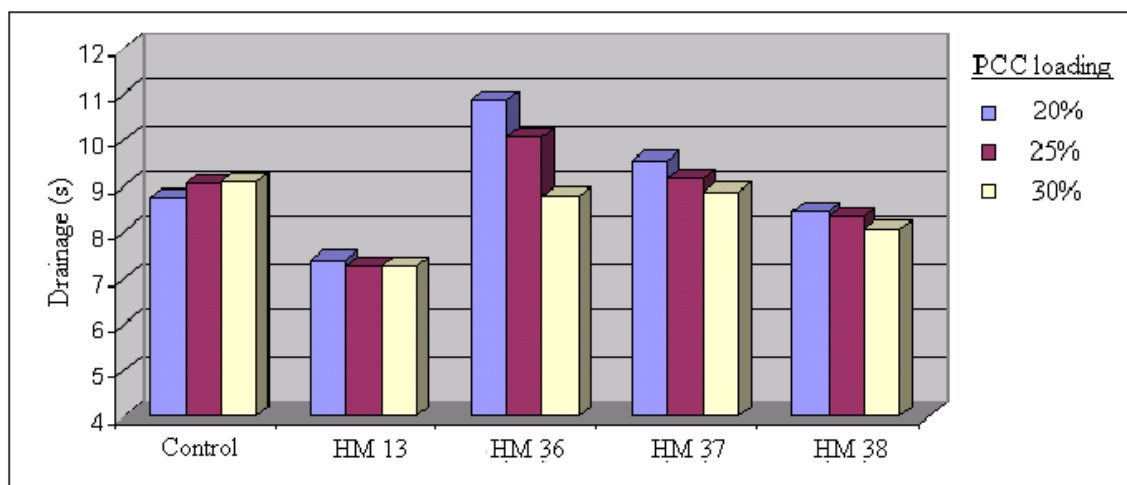
Fig. J5: Comparison in the drainage of hand sheets made with polymeric additives HM 13, HM 36, HM 37 and HM 38.
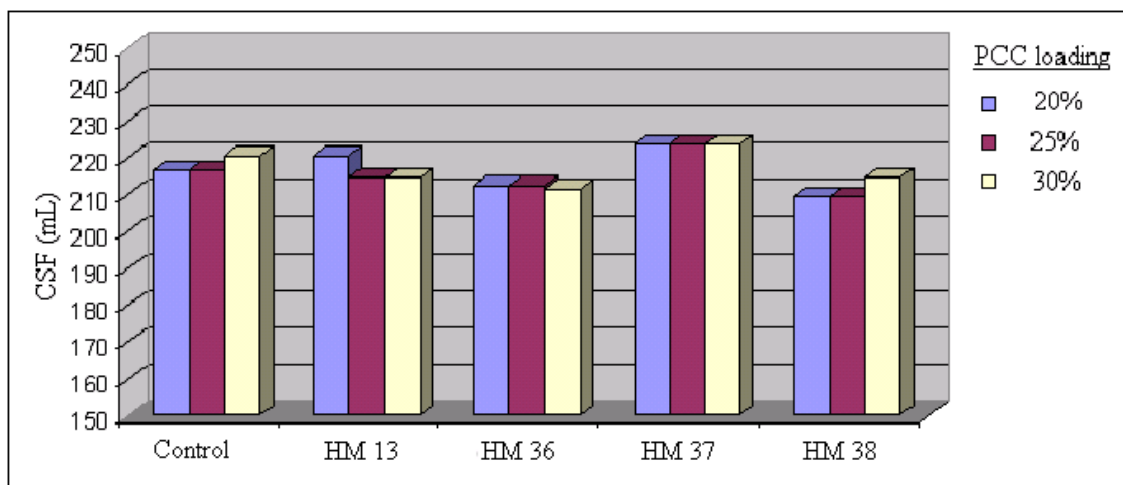

Fig. J6: Comparison in the CSF of hand sheets made with polymeric additives HM 13, HM 36, HM 37 and HM 38.
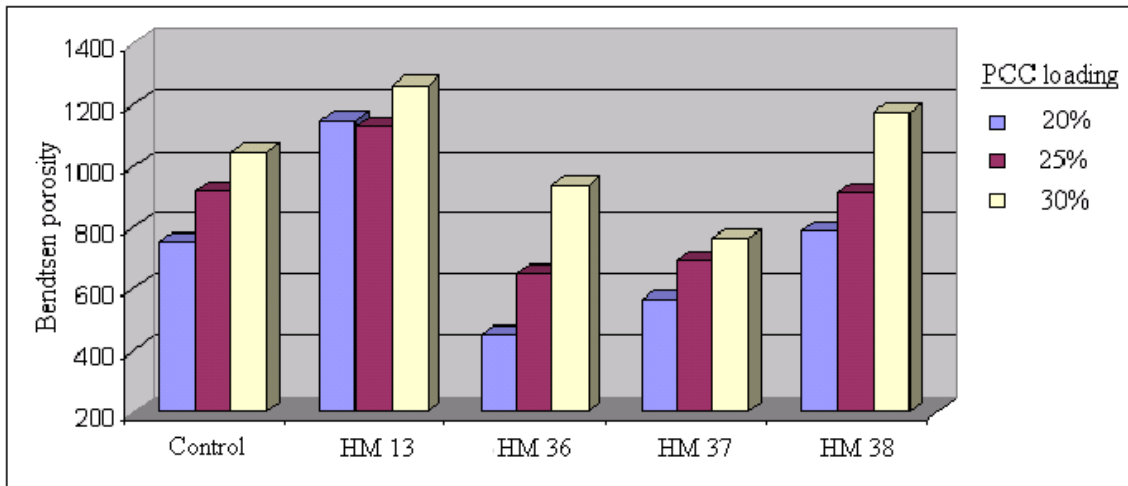
Fig. J7: Comparison in the Bendtsen porosity of hand sheets made with polymeric additives HM 13, HM 36, HM 37 and HM 38.
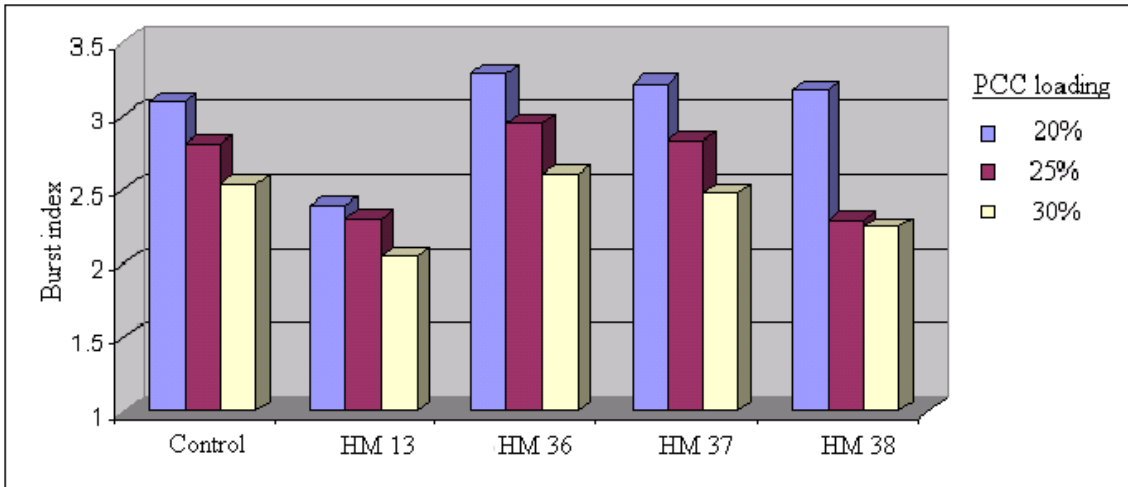

Fig. J8: Comparison in the burst index of hand sheets made with polymeric additives HM 13, HM 36, HM 37 and HM 38.
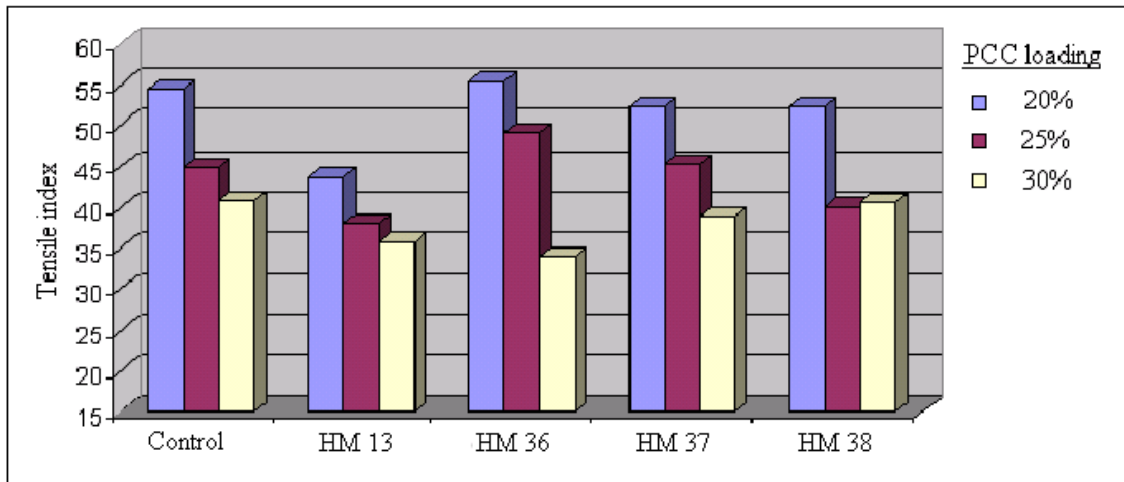
Fig. J9: Comparison in the tensile index of hand sheets made with polymeric additives HM 13, HM 36, HM 37 and HM 38.
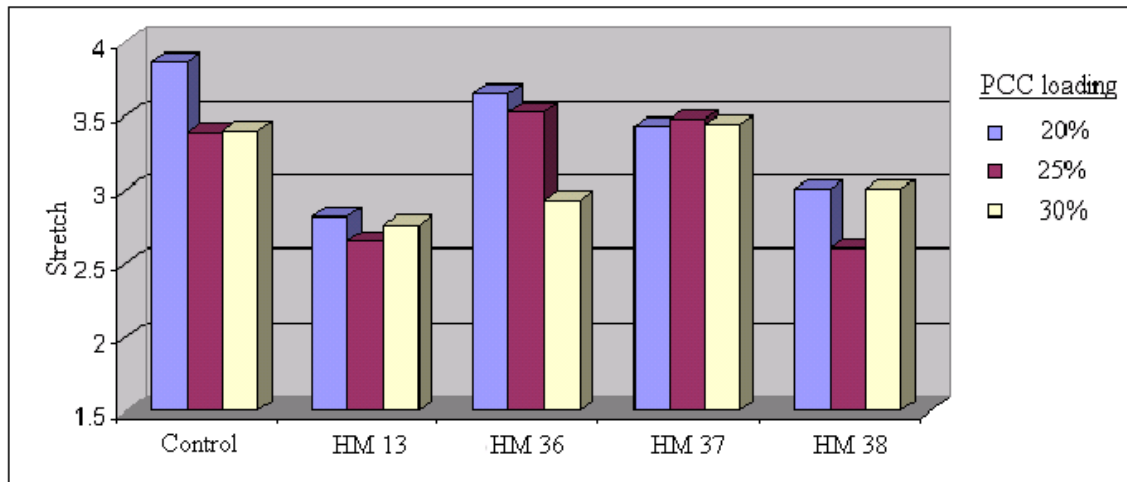

Fig. J10: Comparison in the stretch of hand sheets made with polymeric additives HM 13, HM 36, HM 37 and HM 38.
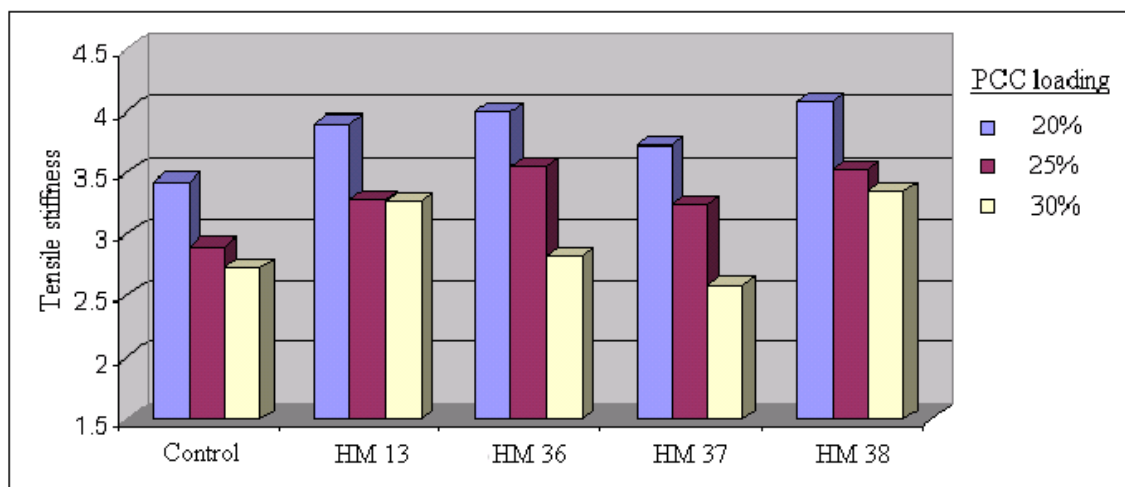
Fig. J11: Comparison in tensile stiffness of hand sheets made with polymeric additives HM 13, HM 36, HM 37 and HM 38.
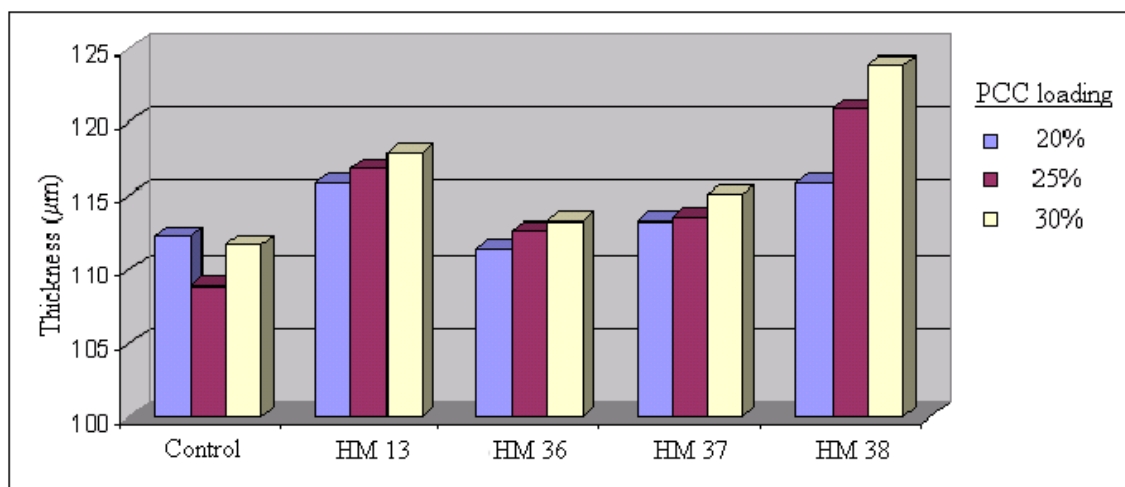

Fig. J12: Comparison in the thickness of hand sheets made with polymeric additives HM 13, HM 36, HM 37 and HM 38.